Journal of Immunology Research

Next Generation Vaccines for Infectious Diseases

Lead Guest Editor: Giuseppe A. Sautto
Guest Editors: Greg Kirchenbaum, Roberta A. Diotti, Elena Criscuolo, and Francesca Ferrara

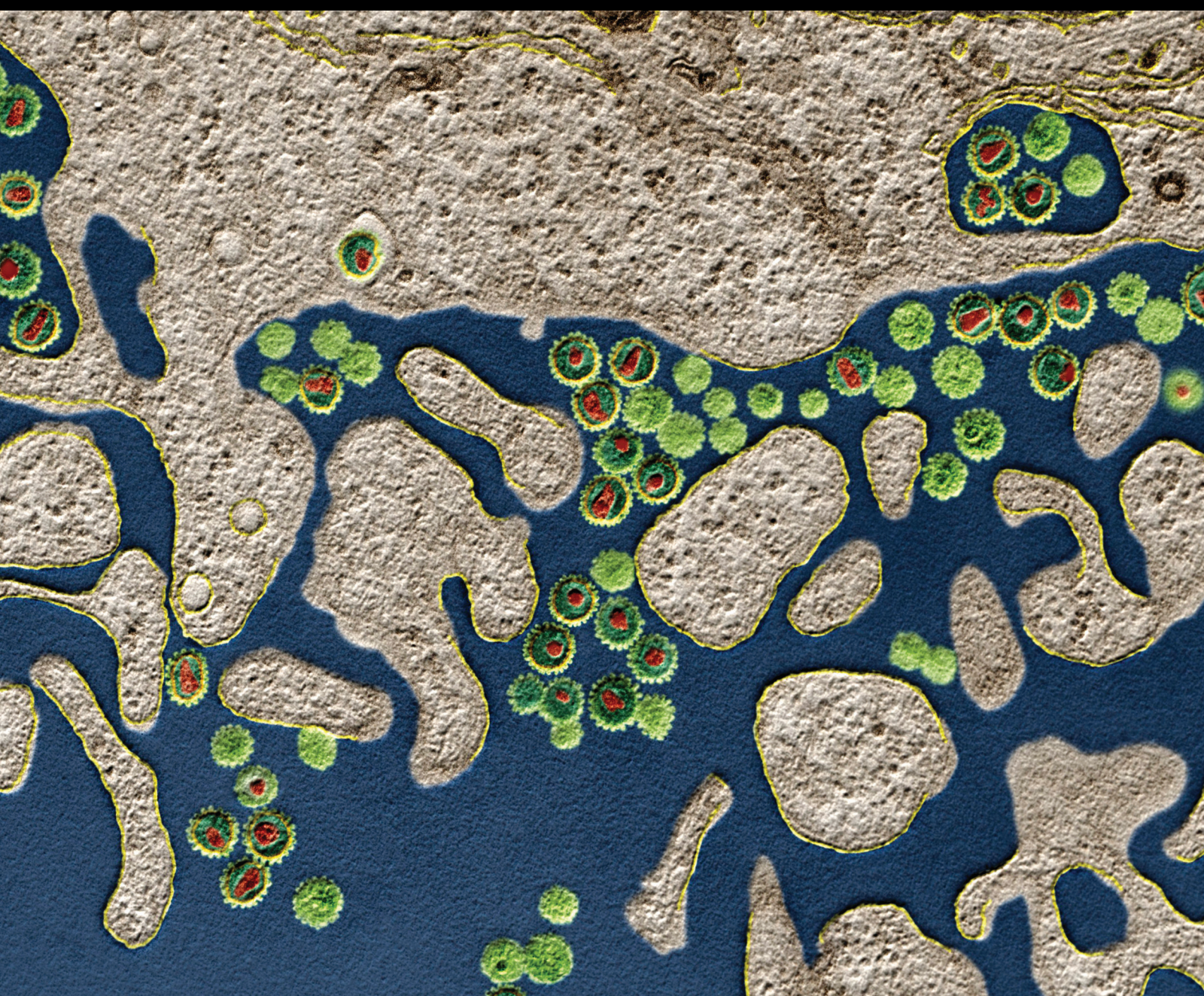

Next Generation Vaccines for Infectious Diseases

Journal of Immunology Research

Next Generation Vaccines for Infectious Diseases

Lead Guest Editor: Giuseppe A. Sautto
Guest Editors: Greg Kirchenbaum, Roberta A. Diotti, Elena Criscuolo, and Francesca Ferrara

Editorial Board

Contents

Hindawi
Journal of Immunology Research
Volume 2019, Article ID 5890962, 2 pages
https://doi.org/10.1155/2019/5890962

Editorial

Next Generation Vaccines for Infectious Diseases

Giuseppe A. Sautto,[1] **Greg A. Kirchenbaum**,[2] **Roberta A. Diotti**,[3,4] **Elena Criscuolo**,[3] **and Francesca Ferrara**[5]

[1]*Center for Vaccines and Immunology, University of Georgia, Athens, GA, USA*
[2]*Cellular Technology Ltd., Shaker Heights, OH, USA*
[3]*Microbiology and Virology Unit, "Vita-Salute San Raffaele" University, Milan, Italy*
[4]*Pomona Ricerca S.r.l., Turin, Italy*
[5]*Vector Development and Production Laboratory, St. Jude Children's Research Hospital, Memphis, TN, USA*

Correspondence should be addressed to Giuseppe A. Sautto; gasautto@uga.edu

Received 20 March 2019; Accepted 20 March 2019; Published 30 April 2019

Vaccines represent the most effective prophylactic strategy in our arsenal for controlling the spread of infectious diseases and have increased human life expectancy. As an example, the eradication of smallpox and the massive reduction of other infectious diseases such as polio, measles, and diphtheria represent major vaccination victories of the last century. Despite the important successes achieved through vaccination, ongoing efforts continue towards development of new and more protective vaccines. Namely, a number of challenges still remain in the context of vaccination. Specifically, many commercially available vaccines fail to elicit long-lasting immune responses and insufficiently trigger cell-mediated and mucosal immunity. Moreover, many vaccines remain dependent on a cold chain for maintenance of antigenicity and potency. Finally, vaccine compliance remains an issue in our society.

Most often, vaccines are composed of attenuated or inactivated pathogens and are capable of eliciting a protective immune response while avoiding the complications associated with an infection. In recent years, thanks to advances in biotechnology and improvements in the production of recombinant proteins, other vaccine strategies have been developed and approved for human use. Many other vaccines produced using recombinant technologies are currently under development and evaluation in clinical trials. As an example, the HBV, HPV, and serogroup B meningococcal vaccines currently in use are composed of subunits that focus the immune response towards specific components of the pathogen.

Moreover, to improve vaccine elicitation of a cell-mediated and mucosal immunity, new DNA-based, viral vector-based, and other novel vaccine delivery platforms, along with usage of adjuvants and chemotactic agents, have been developed. In this regard, N. Cotugno et al. describe the use of OMIC techniques to identify specific genomic profiles defining which vaccinal system might be used in nonresponder individuals. E. Criscuolo et al. review the most recent advances in edible vaccine systems and intradermal vaccine delivery. These new vaccination strategies represent significant advancements for vaccine stability considering the fact that they do not require a cold chain. E. N. Gary and M. A. Kutzler discuss the use of chemokines as adjuvant for inducing mucosal immunity. O. Koutsoni et al. describe how a new adjuvant, the Leishmania eukaryotic Initiation Factor, can be considered both as a natural adjuvant and as an antigen, highlighting its immunomodulatory properties *in vitro* and *in vivo*.

Additional challenges towards reducing the transmission of infectious diseases remain. As such, controlling the spread of these pathogenic microorganisms in animal reservoirs is another important step towards complete eradication. In this regard, vaccination of domestic poultry and livestock is an

important tool for maintaining animal health but is also essential for reducing spread of zoonotic pathogens. Nipah virus infection, severe acute respiratory syndrome, and Highly Pathogenic Avian Influenza (HPAI) are a few examples of infectious diseases originating with transmission from wild animal reservoirs to livestock and then to humans. The development of highly effective vaccines for livestock animals is therefore an essential block for transmission of zoonotic pathogens to humans. In an experimental challenge and transmission model, V. Palya et al. show that vector-based vaccines can efficiently protect commercial broilers and layer pullets from HPAI virus infection.

Especially in underdeveloped countries, affordability of new generation vaccines will be critically important for reducing disease transmission in both human and livestock species. As a necessary step in this direction, Y. Burakova et al. describe the development of cost-effective veterinary vaccine formulations.

In this open special issue, recent advances in the design, formulation, and delivery of vaccines against infectious diseases are covered by three review articles and nine research papers. As guest editors of this open special issue, we hope that readers find its content interesting and that these works inspire continuous efforts towards development and implementation of improved vaccines.

Conflicts of Interest

The authors declare that they have no conflicts of interest.

Giuseppe A. Sautto
Greg A. Kirchenbaum
Roberta A. Diotti
Elena Criscuolo
Francesca Ferrara

Hindawi
Journal of Immunology Research
Volume 2019, Article ID 9124326, 13 pages
https://doi.org/10.1155/2019/9124326

Research Article

New Insights on the Adjuvant Properties of the *Leishmania infantum* Eukaryotic Initiation Factor

Olga S. Koutsoni,[1,2] **Mourad Barhoumi**,[3] **Ikram Guizani**,[3] **and Eleni Dotsika**[1]

[1]*Laboratory of Cellular Immunology, Department of Microbiology, Hellenic Pasteur Institute, 127 Vass Sofias Av, 11521 Athens, Greece*
[2]*Department of Microbiology, Faculty of Medicine, National and Kapodistrian University of Athens, Athens, Greece*
[3]*Laboratory of Molecular Epidemiology and Experimental Pathology, Institut Pasteur de Tunis/Université de Tunis el Manar, 13 Place Pasteur, BP 74, 1002 Tunis-Belvédère, Tunisia*

Correspondence should be addressed to Eleni Dotsika; e.dotsika@pasteur.gr

Received 1 November 2018; Revised 16 January 2019; Accepted 19 February 2019; Published 30 April 2019

Guest Editor: Roberta A. Diotti

Vaccination is the most effective tool against infectious diseases. Subunit vaccines are safer compared to live-attenuated vaccines but are less immunogenic and need to be delivered with an adjuvant. Adjuvants are essential for enhancing vaccine potency by improving humoral and cell-mediated immune responses. Only a limited number of adjuvants are licensed for human vaccines, and their mode of action is still not clear. *Leishmania* eukaryotic initiation factor (LeIF) has been described having a dual role, as a natural adjuvant and as an antigen that possesses advantageous immunomodulatory properties. In this study, we assessed the adjuvant properties of recombinant *Leishmania infantum* eukaryotic initiation factor (LieIF) through *in vitro* and *in vivo* assays. LieIF was intraperitoneally administered in combination with the protein antigen ovalbumin (OVA), and the widely used alum was used as a reference adjuvant. Our *in vitro* studies using J774A.1 macrophages showed that LieIF induced stimulatory effects as demonstrated by the enhanced surface expression of CD80 and CD86 co-stimulatory molecules and the induced production of the immune mediators NO and MIP-1*α*. Additionally, LieIF co-administration with OVA in an *in vivo* murine model induced a proinflammatory environment as demonstrated by the elevated expression of *TNF-α*, *IL-1β*, and *NF-κB2* genes in peritoneal exudate cells (PEC). Furthermore, PEC derived from OVA-LieIF-immunized mice exhibited elevated expression of CD80 molecule and production of NO and MIP-1*α* in culture supernatants. Moreover, LieIF administration in the peritoneum of mice resulted in the recruitment of neutrophils and monocytes at 24 h post-injection. Also, we showed that this immunopotentiating effect of LieIF did not depend on the induction of uric acid danger signal. These findings suggest the potential use of LieIF as adjuvant in new vaccine formulations against different infectious diseases.

1. Introduction

Vaccines are an indisputable achievement of medical science since millions of lives have been saved from infectious diseases, while they also contribute significantly in reducing healthcare expenditure [1]. Nowadays, there are still several diseases that cause significant morbidity and mortality worldwide because either there is no access to vaccine market or the existing vaccines confer suboptimal protection. Another factor is the emergence of new pathogens or re-emergence of old ones [2]. New technologies divided into three major categories related to antigen discovery, adjuvants and vaccine vector delivery and deciphering human immune responses, have recently been developed providing a revolution in vaccine development [3].

The term adjuvant, derived from the Latin word adjuvare that means "to help" [4], comprises all compounds that have the ability to enhance and/or shape antigen-specific immune responses [5, 6]. Adjuvants are used in vaccine formulations in order to enhance the immunogenicity of highly purified native or recombinant antigens, to reduce the amount of antigen or the number of immunizations needed for the

establishment of a protective immunity, and generally to improve the efficacy of vaccine formulations. Therefore, identification and determination of mode of action of potent adjuvants are particularly important for vaccine discovery [7].

Vaccine adjuvants represent a diverse class of compounds, such as microbial products (e.g., pertussis toxin, cholera toxin, bacterial flagellin, and heat shock proteins), cytokines (e.g., IL-12, IFN-γ, and granulocyte-macrophage colony-stimulating factor (GM-CSF)), toll-like receptor agonists (e.g., LPS, poly(I:C), and CpG), mineral salts (e.g., alum), emulsions (e.g., MF59 and Freund's), microparticles, liposomes, and virosomes [8, 9]. So far, very few adjuvants are being used in licensed human and livestock vaccines, such as alum, MF59, monophosphoryl lipid A plus alum (AS04), and saponin (QS-21) [8, 10].

Various adjuvants exert their functions through different mechanisms of action including formation of antigen depot, induction of immune mediators such as cytokines and chemokines, activation of antigen-presenting cells (APCs) (e.g., dendritic cells (DCs)), enhancement of antigen uptake by APCs, and induction of local inflammation and cellular recruitment [11]. Delineation of adjuvants' mode of action provides valuable scientific knowledge for the induction of competent interplay among innate and adaptive immunity, while the deep understanding of the mechanism of action of adjuvants is indispensably important in expediting their development.

Until now, alum-based compounds still remain the predominant human adjuvants due to their safety, ease of preparation, and stability [2]. Thus, alum is found in numerous commercial vaccines including HAV, HBV, HPV, diphtheria and tetanus (DT), Haemophilus influenzae type B (HIB), and pneumococcal conjugate vaccines [12]. Alum's mechanism of action includes the depot effect even though there are reports demonstrating that depot formation is not required for alum adjuvanticity [13, 14], the induction of Th2-type immune responses, the stimulation of inflammation at the injection site like the production of proinflammatory cytokines, and the recruitment of innate immune cells [15, 16]. However, the use of alum presents several drawbacks: (a) is a poor inducer of T-cell mediated responses in humans, namely, Th1-type or cytotoxic T-cell responses which are essential in protective immunity against intracellular pathogens (such as *Leishmania*) and (b) vaccines containing alum cannot be sterilized by standard methods, e.g., filtration, be deep frozen, or be lyophilized [2]. Thus, the development of new effective vaccine formulations that require strong cellular-mediated immunity needs the use of appropriate adjuvants.

Leishmaniasis is a tropical and subtropical disease found in 98 countries, while the achievement of developing safe, effective, durable, and low-cost prophylactic vaccines against the disease is still a major challenge [17]. Several native and recombinant *Leishmania* proteins have been successfully tested as vaccine candidate antigens against leishmaniasis revealing a number of important immune compounds that determine the immune outcome towards protection or exacerbation of experimental infections [18]. Interestingly, among these *Leishmania* proteins, recombinant *Leishmania* eukaryotic initiation factor (LeIF) has been described as an antigen able to induce a protective Th1-type immune response against leishmaniasis [19, 20]. LeIF protein has 403 residues and is highly conserved among *Leishmania* species, also showing high sequence similarity to the mammalian translation initiation factor eIF4A [20, 21]. It has also advantageous immunomodulatory properties, like induction of the production of Th1-type cytokines, IL-12 and IFN-γ, by human peripheral mononuclear cells (PBMCs) from either leishmaniasis patients or normal individuals [19]. It is also able to induce the production of IL-12, IL-10, and TNF-α by monocytes, macrophages, and DCs derived from healthy volunteers [20, 22, 23]. Additionally, we have recently shown that recombinant *Leishmania infantum* eukaryotic initiation factor (LieIF) in the presence of IFN-γ inhibits *L. donovani* growth in murine macrophages [24] and is able to induce phenotypic maturation and functional differentiation of murine bone marrow-derived DCs (unpublished data). Moreover, the NH_2-terminal part (1-226) of LeIF, known to preserve its immunomodulatory properties [19, 20], has been incorporated in a trifusion recombinant protein vaccine, Leish-111f, which was shown to be protective in mice models, when administered in association with immune adjuvants [25–27]. Furthermore, the Leish-111f protein vaccine formulated with the monophosphoryl lipid A (MPL) adjuvant in an oil-in-water stable emulsion using synthetic squalene (MPL-SE) has been tested in clinical trials demonstrating its safety and immunogenicity, supporting the future plan for its clinical development in prophylaxis of human cutaneous and mucosal leishmaniasis (ClinicalTrials.gov Identifier: NCT00121862, NCT00121849, NCT00111553, NCT00111514, and NCT00486382) [28]. In addition, LeIF has been used as adjuvant to promote the induction of Th1-type immune response against the tumor-associated MUC1 tandem repeat peptide in a chimpanzee animal model [29]. It has been shown that the vaccination with tumor-associated MUC1 tandem repeat peptide in combination with LeIF induced proliferative T cell responses and expression of IFN-γ by CD4+ peripheral blood and lymph node T cells in immunized chimpanzees [29].

Until recently, adjuvant selection was empirical and despite the wide use of alum adjuvant in licensed human vaccines, their mode of action is not well characterized. In the present study, we present data showing the potential of LieIF to provide adjuvant properties in *in vitro* and *in vivo* assays. To achieve this objective, recombinant LieIF adjuvant was tested *in vitro* for its ability to potentiate antigen presentation properties of J774A.1 macrophages and *in vivo* for its capability to generate the requisite cellular environment favoring the development of adaptive immune responses.

2. Materials and Methods

2.1. Laboratory Animals. Six- to eight-week-old female BALB/c mice were obtained from the breeding unit of Hellenic Pasteur Institute (HPI; Athens, Greece). All experimental animals were housed in a specific pathogen-free animal facility, at a temperature of 22-25°C and a photoperiod of 12 h. They received a balanced diet of commercial food

pellets and water *ad libitum*. The reporting of the animal experiments in this study followed the ARRIVE guidelines. *In vivo* experimentation was approved by the Institutional Protocols Evaluation Committee according to PD 56/2013 as adoption of Directive 2010/63/EU. Protocol license was issued by the Official Veterinary Authorities of the Prefecture of Attiki in compliance with the above legislation in force.

2.2. Macrophage Culture. The immortalized J774A.1 macrophage cell line was purchased from the American Type Culture Collection (ATCC; Rockville, USA/ATCC No. TIB-67). The J774A.1 macrophage cells were cultured in complete RPMI-1640 medium (Biochrom AG, Berlin, Germany), i.e., RPMI-1640 supplemented with 2 mM L-glutamine, 10 mM Hepes, 24 mM $NaHCO_3$, 50 μM of 2-mercaptoethanol, 100 U/mL penicillin, 100 μg/mL streptomycin, and 10% *v*/*v* heat-inactivated fetal bovine serum (FBS; Gibco, Paisley, UK). Cells were maintained in 25 cm^2 cell culture flasks (CELLSTAR, Greiner Bio-one, Germany), at 37°C with 5% CO_2 environment. J774A.1 macrophage cells were cultured to 80% confluence, and monolayers of cells were routinely harvested by gentle scraping with a cell scraper and diluted 1 : 5 in fresh medium. Cells were counted in a Malassez hemocytometer, and the viability (>95%) of J774A.1 cells was determined by trypan blue exclusion dye.

2.3. Cloning, Expression, and Purification of LieIF Protein. The *LieIF* gene was amplified from *L. infantum* (MHOM/-TN/88/Aymen) genomic DNA by PCR, as previously described [24]. The LieIF construct was subcloned into the *NdeI* and *XhoI* sites of pET-22b expression vector (Novagen, San Diego, CA, USA). LieIF protein was expressed in Origami (DE3) *E. coli* strain (Novagen) and purified using Ni-affinity chromatography, as previously reported [22]. Protein concentration was determined using the Bio-Rad Protein Assay (Hercules, CA, USA) with the use of bovine serum albumin (BSA) as a standard while its purity was verified on a 12% Coomassie-stained SDS-PAGE gel (Figure 1). Recombinant LieIF was tested for the amount of endotoxin levels (≤5 EU/mg) using the *Limulus* amebocyte lysate (LAL) assay (Charles River, USA).

2.4. Antigens and Adjuvant. OVA antigen was purchased from Sigma-Aldrich Corp. (USA) and was also tested for bacterial endotoxin using the LAL assay. At the dose used in our experiments, the endotoxin level of OVA was ≤0.001 μg/mL. Imject Alum adjuvant (Pierce, Rockford, USA) is a mixture of aluminum hydroxide and magnesium hydroxide and was mixed at a 1 : 1 ratio with a solution of OVA antigen in phosphate-buffered saline (PBS) pH = 7.4, followed by stirring for at least 1 h to effectively absorb the antigen.

2.5. Immunization Protocols. Female BALB/c mice, $n = 20$/group, were injected intraperitoneally (i.p.) in the right lower quadrant using a 26-gauge needle, with 500 μL of LieIF suspension (10 μg/mouse) in sterile PBS containing equal quantity of OVA (10 μg/mouse) (OVA-LieIF), or with 10 μg of OVA alone in 500 μL PBS, while mice receiving only PBS were included as negative control (Figure 2(a)), as previously described [16]. In another set of experiments, BALB/c mice received the known adjuvant alum (10 mg/mouse) in combination with OVA (10 μg/mouse) (OVA-alum) (Figure 3(a)). Two, 6, and 24 h after injection, the peritoneal exudate cells (PEC) were harvested with 5 mL of ice-cold PBS. Cells were depleted from red blood cells with ammonium-chloride-potassium lysing buffer (ACK buffer), pH = 7.2 (0.15 M NH_4Cl, 10 mM $KHCO_3$, and 0.1 mM Na_2EDTA) and resuspended in complete RPMI-1640 medium.

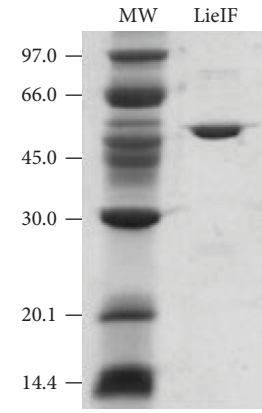

Figure 1: Expression and purification of the recombinant LieIF protein. Aliquots of purified protein were resolved by SDS-PAGE gel and stained with Coomassie Brilliant Blue. The positions of the Bio-Rad prestained markers (in kDa) are indicated at the left.

2.6. Flow Cytometry. For the detection of B7 co-stimulatory molecules (CD80 and CD86) in J774A.1 macrophages, cells were stimulated with LieIF (10 μg/mL) for 24 h, at 37°C with 5% CO_2 environment. The protein concentration was carefully selected after concentration kinetic experiments [24]. As a positive control for macrophage stimulation, J774A.1 cells were cultured with LPS (1 μg/mL) derived from *Escherichia coli* (Sigma-Aldrich, USA), as previously described in similar experimental conditions [30]. Accordingly, PEC were harvested in ice-cold PBS, as described in Section 2.5. At the end of the incubation period, cells were centrifuged at 600 × g for 10 min and then were resuspended in PBS at a density of 5×10^6 cells/mL. Cells were washed in FACS buffer (PBS-3% FBS) and were stained with anti-CD80 and anti-CD86 monoclonal antibodies conjugated with fluorescein (FITC) (BD Biosciences, Belgium), for 30 min.

For the detection of recruited cells at 6 and 24 h after intraperitoneal injections, cell suspensions of peritoneal lavage were centrifuged at 600 × g for 10 min. The cell pellets were resuspended in PBS and stained with anti-CD11b monoclonal antibody conjugated with FITC together with anti-F4/80 monoclonal antibody conjugated with phycoerythrin (PE) (AbD Serotec, UK) or anti-Ly6C or anti-Ly6G monoclonal antibodies conjugated with PE (BD Biosciences, Belgium), for 30 min.

Control unstained samples were similarly processed for all the above cases. 20,000 events were analyzed for each sample in a FACSCalibur cytometer (Becton-Dickinson, San Jose, CA, USA), and data were analyzed with FlowJo V.10.0.8 software (Tree Star Inc., Ashland, OR, USA).

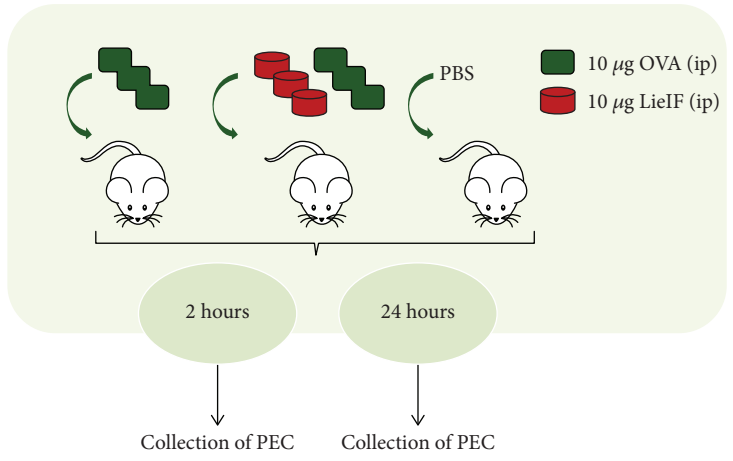

(a)

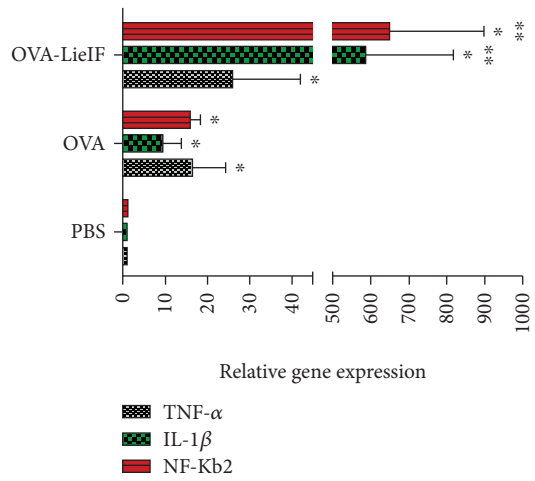

(b)

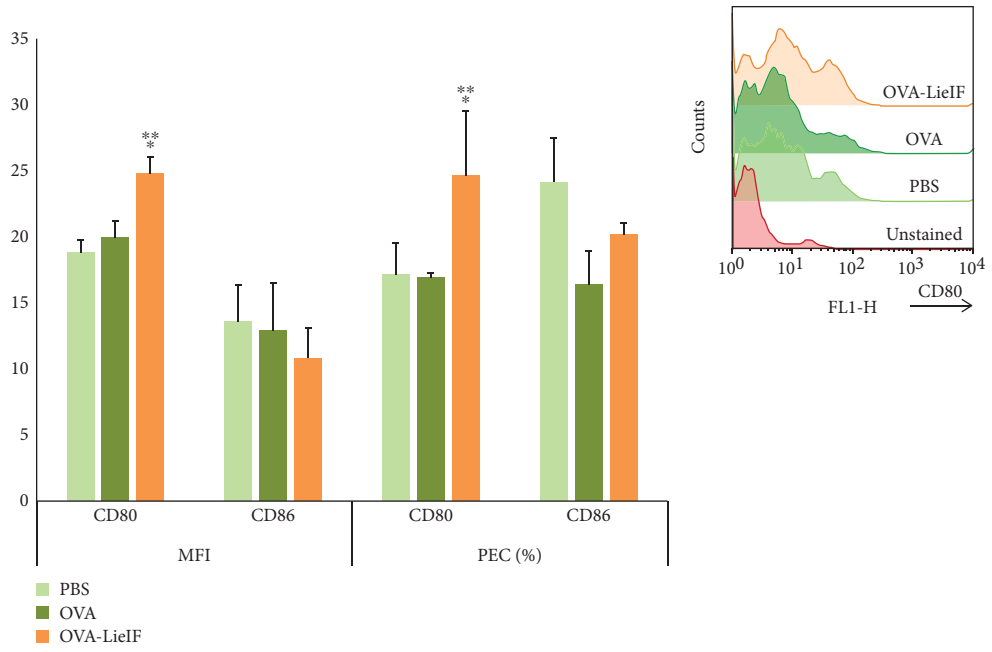

(c)

Figure 2: Continued.

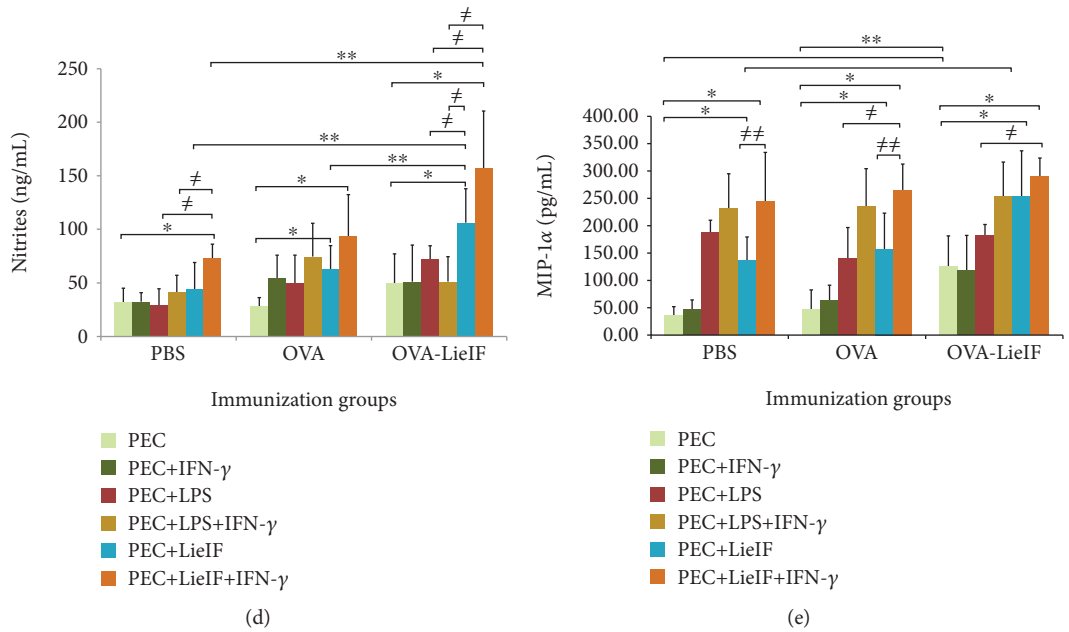

Figure 2: *In vivo* effect of recombinant LieIF protein on the peritoneal exudate cells. (a) Schematic representation of the experimental protocol. Female BALB/c mice were i.p. injected in the right quadrant with 500 μL of LieIF suspension (10 μg/mouse) in sterile PBS containing equal quantity of OVA protein (10 μg/mouse) or with 500 μL of OVA suspension (10 μg/mouse) in sterile PBS, while mice receiving only PBS were included. 2 and 24 h after injection, the peritoneal exudate cells (PEC) were harvested with 5 mL of ice-cold PBS. (b) Relative expression of *TNF-α*, *IL-1β*, and *NF-κB2* genes in PEC. 2 h post-immunization, PEC were derived from each experimental group and relative expression of *TNF-α*, *IL-1β*, and *NF-κB2* genes was determined by real-time PCR, performed with a SYBR Green PCR Master Mix. The expression of glyceraldehyde-3-phosphate dehydrogenase (GAPDH) gene was used for normalization, and all expression levels were computed via the ΔΔCt method. Results shown are representative of three independent experiments. ∗ indicates statistically significant differences compared to PBS-immunized mice while ∗∗ indicates significant differences compared to OVA-immunized group. (c) Recombinant LieIF protein induces the upregulated expression of CD80 co-stimulatory molecule in PEC. 24 h post-immunization, PEC were harvested from each experimental group and cell surface expression of CD80 and CD86 co-stimulatory molecules was assessed by FACS analysis. The results are expressed as median fluorescent intensity (MFI) and as percentage (%) of cells expressing CD80 and CD86 molecules. Data are presented as mean values ± SD of three independent experiments. The histogram overlay is representative of one experiment. ∗ and ∗∗ indicate statistically significant differences as compared to PBS- and OVA-immunized groups, respectively. (d) Recombinant LieIF protein promotes the production of NO by PEC. 24 h post-immunization, PEC were harvested from each experimental group and were further incubated *in vitro* with LieIF (10 μg/mL), IFN-γ (1 ng/mL), and LPS (1 μg/mL) or with LieIF+IFN-γ and LPS+IFN-γ, for 24 h at 37°C under 5% CO_2 environment. After the incubation period, NO production of each experimental group was determined in supernatants with the Griess reaction. Data are presented as mean values ± SD of three independent experiments. For each *in vivo* experimental group, comparisons with cultured PEC that received no stimulation *in vitro* (light green bars) are indicated with ∗ and comparisons with cultured PEC received LPS (red bars) or LPS+IFN-γ (yellow bars) are indicated with ≠. Comparisons among the *in vivo* experimental groups are indicated with ∗∗. (e) Recombinant LieIF protein elicits the secretion of MIP-1α by PEC. 24 h post-immunization, PEC were harvested from each experimental group and were further incubated *in vitro* with LieIF (10 μg/mL), IFN-γ (1 ng/mL), and LPS (1 μg/mL) or with LieIF+IFN-γ and LPS+IFN-γ, for 24 h at 37°C in the presence of 5% CO_2 environment. At the end of incubation period, culture supernatants were collected and MIP-1α levels were determined by ELISA. Data are presented as mean values ± SD of three independent experiments. For each *in vivo* experimental group, comparisons with cultured PEC that received no stimulation *in vitro* (light green bars) are indicated with ∗, comparisons with cultured PEC that received LPS (red bars) or LPS+IFN-γ (yellow bars) are indicated with ≠, and comparisons between cultured PEC that received LieIF (light blue bars) and LieIF+IFN-γ (orange bars) are indicated with ≠≠. Comparisons among the *in vivo* experimental groups are indicated with ∗∗.

2.7. Chemokine Production. J774A.1 macrophages were incubated with LieIF for 24 h, at 37°C in the presence of 5% CO_2. Macrophages cultured with LPS (1 μg/mL) or cultured only with complete RPMI-1640 medium were used as positive and negative controls, respectively. Accordingly, for the determination of MIP-1α in PEC derived from immunized mice as described in Section 2.5, cells (at a density of 1×10^6 cells/mL) were further incubated *in vitro* with the following antigens: LieIF (10 μg/mL), recombinant murine (rm) IFN-γ (1 ng/mL), LPS (1 μg/mL) [31], or with combinations of LieIF+IFN-γ or LPS+IFN-γ, for 24 h at 37°C under 5% CO_2 environment. At the end of the incubation periods, culture supernatants were collected to determine MIP-1α chemokine levels by ELISA. The ELISA kit (900-K125) was purchased from PeproTech Corp. (Rocky Hill, NJ), and the assay was performed according to the manufacturer's instructions. The concentration of MIP-1α was calculated by using a standard curve generated by recombinant MIP-1α starting at 0.5 ng/mL and serially diluted in duplicate. The detection threshold was at 8 pg/mL.

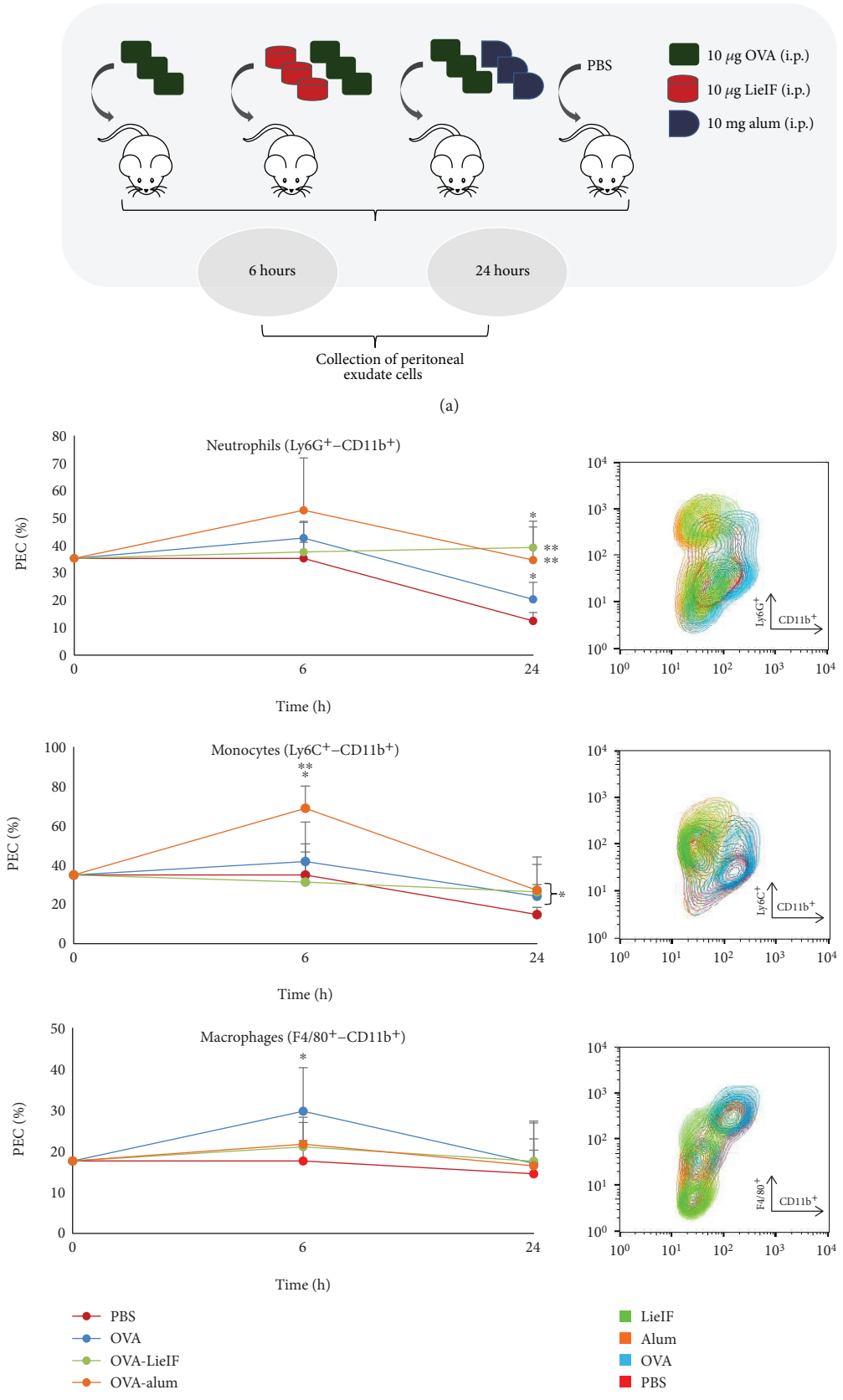

Figure 3: Continued.

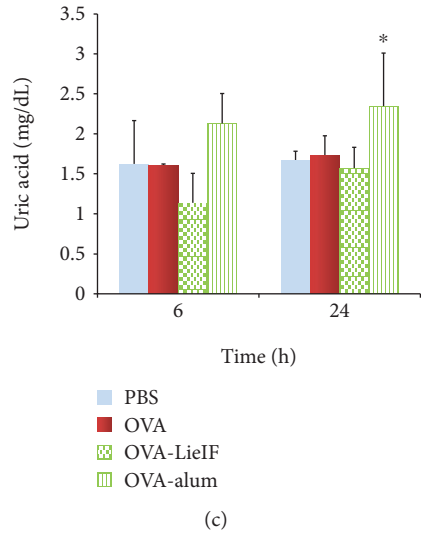

(c)

Figure 3: *In vivo* effect of recombinant LieIF protein on the response of innate immune cells. (a) Schematic representation of the experimental protocol. Female BALB/c mice were i.p. injected in the right quadrant with 500 μL of LieIF suspension (10 μg/mouse) in sterile PBS containing equal quantity of OVA protein (10 μg/mouse) (OVA-LieIF) or with 500 μL of OVA suspension (10 μg/mouse) in sterile PBS. Mice of the positive control received the known adjuvant alum (10 mg/mouse) in combination with OVA (10 μg/mouse) (OVA-alum). Mice receiving only PBS were also included. Six and 24 h after injection, the peritoneal exudate cells (PEC) were harvested with 5 mL of ice-cold PBS. (b) Recombinant LieIF protein recruits innate immune cells to the peritoneal cavity. Six and 24 h after immunization, the peritoneal lavage was harvested and the percentages of neutrophils ($Ly6G^+$-$CD11b^+$), monocytes ($Ly6C^+$-$CD11b^+$), and macrophages ($F4/80^+$-$CD11b^+$) were determined by FACS. Results are presented in 2D line charts and in representative contour plots. $*$ indicates statistical difference compared with the PBS-immunized mice (negative control group), and $**$ indicates statistical difference compared to OVA-immunized mice. (c) The immunopotentiating effect of LieIF does not depend on the production of uric acid. The levels of uric acid (mg/dL) were measured in serum of immunized mice using the enzymatic colorimetric uricase PAP method. The results are presented as the mean ± SD, and data shown are representative of three independent experiments. $*$ indicates statistically significant differences as compared to the negative control.

2.8. Quantification of Extracellular Nitric Oxide (NO). The NO synthesis was measured as the accumulation of nitrites in cell culture supernatants using the Griess reaction (Sigma-Aldrich, USA), according to manufacturer's protocol [32]. For the determination of NO in J774A.1 macrophages, cells were stimulated with LieIF for 24 h and then culture supernatants were collected. Macrophages cultured with LPS (1 μg/mL) were used as the positive control and cells cultured only with complete RPMI-1640 medium constituted the negative control. Accordingly, for the determination of NO in PEC derived from immunized mice as described in Section 2.5, cells (at a density of 1×10^6 cells/mL) were further incubated *in vitro* with the following antigens: LieIF (10 μg/mL), IFN-γ (1 ng/mL), LPS (1 μg/mL), or with combinations of LieIF+IFN-γ or LPS+IFN-γ, for 24 h at 37°C under 5% CO_2 environment [33]. At the end of the incubation period, culture supernatants were collected.

50 μL of each sample supernatant was mixed with 100 μL of Griess reagent (1 : 1 solution A : solution B; 1% w/v sulfanilamide in 5% w/v phosphoric acid (solution A) and 0.1% v/v naphthylethylenediamine dihydrochloride in distilled water (solution B)) [34]. The relative NO concentrations were calculated using a standard curve generated with known amounts of $NaNO_2$, and the absorbance was measured at 570 nm with a Dynatech Laboratories MRX spectrophotometer (Germany).

2.9. Gene Expression Analysis. PEC were derived from immunized and non-immunized BALB/c mice (Section 2.5) at 2 h post-immunization, and RNA was extracted using an RNeasy Mini Kit (Qiagen, Germany) according to manufacturer's instructions. The quantity and purity of extracted RNA were determined with the spectrophotometer NanoDrop® 2000 (Thermo Scientific, USA). RNA (1 μg) was used as a template for cDNA synthesis using a SuperScript II kit (Invitrogen Molecular Probes™) and oligo-dTs (Promega, WI, USA), and all reactions included the recombinant ribonuclease inhibitor, RNaseOUT™ (Invitrogen).

Real-time polymerase chain reaction (real-time PCR) was performed using an Exicycler 96 (Bioneer, Daejeon, Korea) with a SYBR Green PCR Master Mix (Kapa Biosystems, Boston, USA). The expression of the *glyceraldehyde-3-phosphate dehydrogenase* (*GAPDH*) gene was used for normalization. Specific primers for genes of interest: interleukin-1β (IL-1β), tumor necrosis factor-α (TNF-α), subunit 1 and subunit 2 of nuclear factor kappa-B (NF-κB1 and NF-κB2), and *GAPDH* were designed by Qiagen (QuantiTect Primer Assays; Qiagen, Netherlands) and were run in triplicate. The PCR was conducted according to Qiagen's PCR protocol for the QuantiTect Primer Assays. The cycling conditions were 94°C for 10 min, followed by 40 cycles at 94°C for 10 s and 60°C for 30 s. All expression levels were computed via the $\Delta\Delta$Ct method [35].

2.10. Serum Uric Acid Determination. Serum samples were collected from immunized mice, described in Section 2.5, at 6 and 24 h post-immunization. Serum uric acid (SUA) levels in (mg/dL) were determined by the enzymatic colorimetric uricase PAP method [36], according to manufacturer's instructions and using a Cobas Mira autoanalyzer (Roche, Switzerland), kindly accessed by V. Sideris, MD, at Diagnostiki Athinon, Clinical and Research Laboratory (Athens, Greece).

2.11. Statistical Analysis. The data shown are representative of at least three independent experiments and are presented as mean values ± standard deviation (SD). In the *in vivo* procedures, we used six to seven animals per group and the experiments were repeated three times. Statistical analysis was performed by the two-sided Mann-Whitney test using the IBM SPSS Statistics software (v.24). P values less than 0.05 were considered to indicate statistical significance.

3. Results

3.1. Recombinant LieIF Induces the Upregulation of CD80 and CD86 Co-stimulatory Molecules in J774A.1 Macrophages. LieIF was expressed and purified by Ni-affinity chromatography and its purity was more than 90% (Figure 1). Firstly, the phenotypic changes of murine macrophages in response to LieIF were analyzed; since the expression of co-stimulatory molecules (e.g., CD80, CD86) on APCs, macrophages, and DCs is critical in shaping the extent and nature of immune responses [37]. LieIF-stimulated macrophages were labeled with antibodies directed against the B7 surface markers (CD80 and CD86). FACS analysis showed that stimulation of J774A.1 macrophages with LieIF induced a significant increase in the expression of CD80 and CD86 co-stimulatory molecules in terms of MFI (Figures 4(a) and 4(c)) along with the percentage (%) of J774A.1 cells (Figures 4(b) and 4(c)). Specifically, LieIF-stimulated macrophages exhibited a 1.3-fold increase of MFI of cells expressing both CD80 and CD86 molecules (Figures 4(a) and 4(c)) along with a 1.3- and a 2.2-fold increase of % of J774A.1 cells expressing CD80 ($62.1 \pm 2.5\%$ vs. $49.4 \pm 4.8\%$) and CD86 ($41.8 \pm 4.8\%$ vs. $19.2 \pm 1.05\%$), respectively, as compared with unstimulated cells (Figures 4(b) and 4(c)). It is also noteworthy that LieIF-stimulated macrophages exhibited similar expression of CD80 and CD86 molecules as compared to the expression caused by LPS-stimulated cells ($p = 0.386$ and 0.657, respectively) (Figure 4).

3.2. Recombinant LieIF Induces the Production of Nitric Oxide and MIP-1α Chemokine by J774A.1 Macrophages. NO production is a marker for macrophage activation and one of the major antimicrobial mechanisms of macrophages. Indeed, sustained production of NO endows macrophages with cytotoxic activity against viruses, bacteria, fungi, protozoa, helminths, and tumor cells [38]. NO levels were measured in culture supernatants of J774A.1 macrophages after their *in vitro* stimulation with LieIF and the amount of the released NO is given in Figure 5. The obtained data indicated that NO production in LieIF-stimulated cells was significantly higher (141.89 ± 44.63 ng/mL) as compared to unstimulated cells (47.77 ± 6.9 ng/mL, $p = 0.004$) and the amount of produced NO was almost equal to the levels produced by the LPS-stimulated J774A.1 cells (113.15 ± 25.33 ng/mL, $p = 0.327$) (Figure 5).

On the other hand, chemokines play an important role in the selective movement of leucocytes into areas of inflammation [39]. Macrophage inflammatory protein-1 alpha (MIP-1α) is a member of the CC chemokine family and is a chemotactic attractant for lymphocytes, monocytes, and eosinophils [40]. MIP-1α levels were also measured in culture supernatants of J774A.1 macrophages after their *in vitro* stimulation with LieIF, and the amount of the produced MIP-1α is also shown in Figure 5. Clearly, LieIF induced the secretion of statistically significant amounts of MIP-1α chemokine by J774A.1 macrophages *in vitro* as compared to unstimulated cells (402.76 ± 42.6 pg/mL vs. 337.15 ± 34.5 pg/mL, $p = 0.045$) while these amounts were similar to those produced by LPS-stimulated J774A.1 macrophages (391.47 ± 32.78 pg/mL, $p = 0.855$).

3.3. Effect of Recombinant LieIF Co-administered with OVA Antigen on the Innate Immune Response Elicited after Intraperitoneal Injection. BALB/c mice were intraperitoneally immunized either with OVA antigen alone or with LieIF protein together with OVA antigen dissolved in PBS, or PBS alone as negative control, as it is shown in Figure 2(a). At 2 and 24 h after injection, PEC were harvested in order to determine the primary response induced. The expression of proinflammatory immune genes and immune mediators that may indicate the capacity of LieIF to trigger locally *in vivo* an immunological profile describing an adjuvant activity was measured.

3.3.1. Recombinant LieIF Induces a Proinflammatory Environment at the Injection Site. Most of the times, adjuvants are associated with the transient secretion of cytokines and chemokines which mediates the formation of a local proinflammatory environment composed of various immune cells recruited to the injection site [41]. Production of IL-1β, IL-6, and TNF-α cytokines is one of the hallmarks of the inflammatory response and plays an important role in the initiation of innate immunity [42, 43]. The relative expression of *TNF-α*, *IL-1β*, and *NF-κB2* genes was determined by real-time PCR at 2 h post-immunization. Obtained data demonstrated that co-administration of OVA-LieIF is able to induce a proinflammatory environment at the injection site as illustrated by the elevated gene expressions. More specifically, *TNF-α* gene expression in PEC from OVA-LieIF-immunized mice was 25.8- and 1.6-fold upregulated compared to the corresponding expression level in PEC from PBS- and OVA-immunized mice ($p = 0.037$ and 0.456, respectively; Figure 2(b)). Furthermore, the *IL-1β* gene expression in mice that received OVA-LieIF was 585- and 61.5-fold upregulated as compared to that in PBS- and OVA-immunized mice ($p \leq 0.050$; Figure 2(b)). At last, we determined the expression of two members of the NF-κB family *NF-κB1* and *NF-κB2* genes that play an important role in the regulation of immune and inflammatory responses. We observed an upregulation of 648- and 40.6-fold of *NF-*

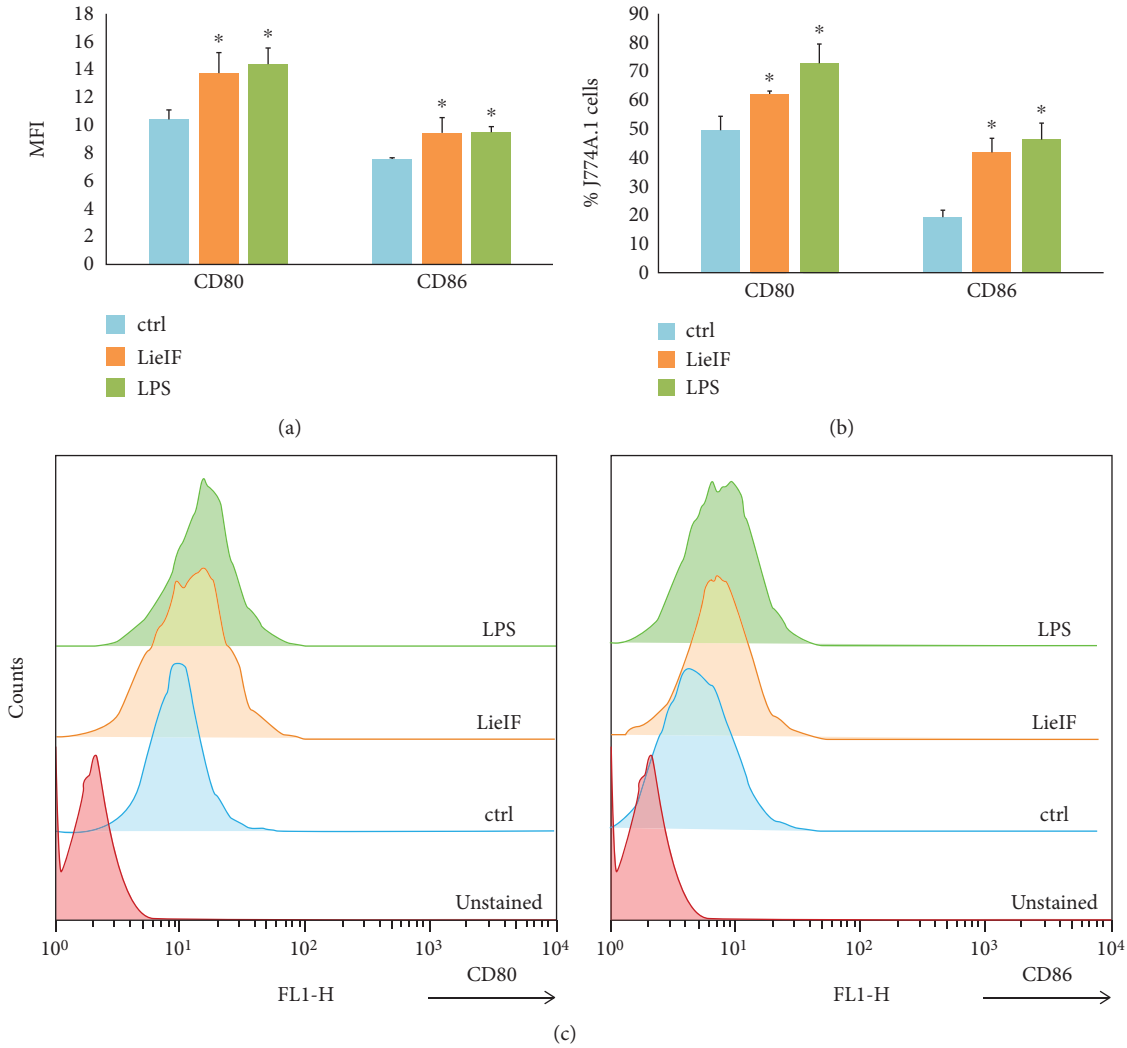

Figure 4: Effect of recombinant LieIF protein on the expression of co-stimulatory molecules by J774A.1 macrophages. Macrophages were stimulated with recombinant LieIF (10 μg/mL) for 24 h, and the expression of CD80 and CD86 molecules was measured using FACS with the use of specific monoclonal fluorochrome-labeled antibodies. Macrophages stimulated with LPS (1 μg/mL) were used as the positive control while unstimulated cells were used as the negative control. The results are expressed as (a) median fluorescent intensity (MFI) and (b) percentage (%) of macrophages expressing CD80 and CD86 molecules. Data are presented as mean values ± SD of three independent experiments. (c) Histogram overlays are representative of one experiment. ∗ indicates statistically significant differences as compared to the negative control.

κB2 gene expression in PEC from OVA-LieIF-immunized mice versus the control groups of PBS- and OVA-immunized mice, respectively ($p \leq 0.050$; Figure 2(b)). The *NF-κB1* gene expression was equal in mice of both immunized groups (data not shown).

3.3.2. Effect of Recombinant LieIF on the Functional Maturation of PEC. At first, changes in the expression of co-stimulatory molecules in PEC, elicited by OVA-LieIF intraperitoneal co-administration, were analyzed and it was found that PEC derived from OVA-LieIF-immunized mice exhibited elevated expression of CD80 molecule in terms of MFI along with the percentage (%) of cells (Figure 2(c)). Specifically, PEC from OVA-LieIF-immunized mice exhibited a 1.3-fold increase of MFI as compared with both PBS- and OVA-immunized mice ($p \leq 0.050$) at 24 h post-injection. Moreover, OVA-LieIF-immunized mice exhibited an elevated number of cells expressing CD80 (24.6 ± 4.9%) as compared with PBS- (17.1 ± 2.4%) and OVA- (16.9 ± 0.4%) immunized mice ($p = 0.023$ and 0.004, respectively), at 24 h post-injection (Figure 2(c)). No upregulated expression of CD86 was induced by OVA-LieIF or OVA administration (Figure 2(c)).

Moreover, the NO levels in culture supernatants of PEC obtained from immunized mice of each experimental group were also determined. *In vitro* restimulation of PEC with LieIF alone or LieIF+IFN-γ led to increased NO production in all experimental groups as compared with the NO produced from unstimulated cells (p values ranging from 0.009 to 0.034) (Figure 2(d)). Likewise, stimulation with LieIF +IFN-γ resulted also in equal or higher amounts of NO production in all experimental groups, as stimulation with LPS

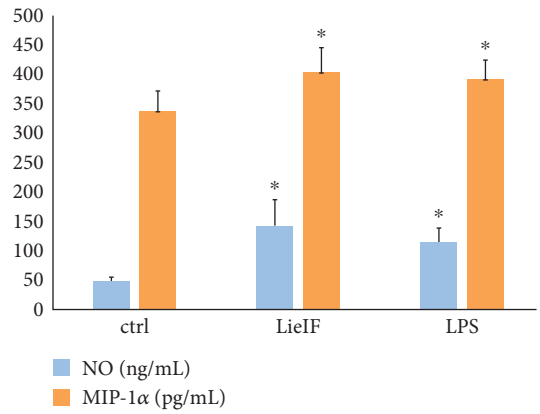

FIGURE 5: Effect of recombinant LieIF protein on nitric oxide (ng/mL) and MIP-1α (pg/mL) production by J774A.1 macrophages. Macrophages were stimulated with recombinant LieIF (10 μg/mL) and LPS (1 μg/mL). Unstimulated cells were used as the negative control. After 24 h, the cell supernatants were collected and NO and MIP-1α secretion were measured by Griess reaction and ELISA, respectively. The results are presented as the mean ± SD and data shown are representative of three independent experiments. $*$ indicates statistically significant differences as compared to the negative control.

or LPS+IFN-γ, respectively (recorded p values 0.046, 0.050, 0.275, and 0.289) (Figure 2(d)). Unstimulated cells derived from OVA-LieIF-immunized mice demonstrated a moderate increase of NO production when compared to the PBS- or OVA-immunized mice ($p = 0.091$). Of note, the immunization with OVA-LieIF promoted noticeably increased NO levels upon stimulation with LieIF or LieIF+IFN-γ as compared with PBS- and OVA-immunized mice also restimulated with LieIF±IFN-γ (p values 0.046 and 0.009) (Figure 2(d)). Overall, the data on NO production indicated that LieIF promoted macrophage activation when administered *in vivo*.

Next, it was determined whether coadministration of OVA-LieIF elicited the production of MIP-1α, the known chemotactic attractant for lymphocytes. MIP-1α was measured in PEC culture supernatants after *in vitro* restimulation with LieIF±IFN-γ and LPS±IFN-γ for 24 h. The obtained data showed that the secreted levels of MIP-1α were significantly higher in supernatants of PEC restimulated *in vitro* with recombinant LieIF±IFN-γ than those of unstimulated cells (p values ranging from 0.009 to 0.018), for all the experimental groups (Figure 2(e)). It was also noticed that stimulation with LieIF+IFN-γ resulted in equal or higher levels of secreted MIP-1α in all experimental groups, as compared to those induced by stimulation with LPS or LPS+IFN-γ, respectively (recorded p values 0.018, 0.237, and 1.000) (Figure 2(e)). It is noteworthy that the induction of MIP-1α secretion was significantly enhanced in unstimulated PEC derived from OVA-LieIF-immunized mice than that of corresponding secretion from the PBS- or OVA-immunized mice ($p = 0.018$). Moreover, OVA-LieIF-immunized mice had an enhanced MIP-1α production upon stimulation with LieIF±IFN-γ (Figure 2(e)), as compared to PBS- and OVA-immunized mice (recorded p values 0.009, 0.083, and 0.237).

3.4. Assessment of the Effect of Recombinant LieIF on the Response of Innate Immune Cells. BALB/c mice were either immunized with LieIF protein together with an equal amount of OVA antigen (OVA-LieIF), or with alum plus OVA (OVA-alum), while other mice received OVA antigen alone. Mice of the negative control group received sterile PBS (Figure 3(a)). The innate immune response to LieIF in the peritoneum, 6 and 24 h after immunization, was investigated.

Within 24 h after injection, OVA-LieIF administration induced a marked increase of $Ly6G^+$-$CD11b^+$ neutrophils, as compared to PBS- and OVA- immunized mice ($p = 0.034$ and 0.025, respectively; Figure 3(b)). The effect of LieIF on the recruitment of neutrophils was similar to alum ($p = 0.456$; Figure 3(b)). Furthermore, at the same time point, as compared to PBS-immunized mice, OVA-LieIF led to a significant recruitment of inflammatory $Ly6C^+$-$CD11b^+$ monocytes ($p = 0.023$; Figure 3(b)), previously shown to be immediate precursors for DCs [44, 45]. As it is shown here, LieIF leads to the recruitment of cells that coincide to key players of the inflammatory reaction such as neutrophils and monocytes. The results reported here revealed that the alterations in peritoneal cell populations elicited by co-administration of OVA-LieIF almost mimicked the alterations elicited by alum.

It has been demonstrated that alum induces a strong neutrophilic influx accompanied by the production of IL-1β, akin to the response seen when the endogenous danger signal, uric acid, is injected into the peritoneal cavity [46, 47]. Kool et al. demonstrated that the immunopotentiating effect of alum depends on the induction of uric acid. In the present study, we checked if the immunopotentiating effect described above and attributed to LieIF was mediated by the presence of uric acid acting as a danger signal. Our results indicated that the administration of LieIF did not reveal an increase in uric acid levels (Figure 3(c)), suggesting the induction of a different mechanism of attraction of cells to the peritoneal cavity as compared to that induced by alum.

4. Discussion

Only a handful of adjuvants are approved for prophylactic vaccination of humans, despite their obvious benefits, decades of research, and hundreds of preclinical candidates [11]. Failures of adjuvants during the development phase are related to the manufacturing process (e.g., lack of a reproducible formulation, negative impact on antigen stability) or to local or systemic adverse events [12]. Recent advances in the immune pathways involved in the modulation of the host-protective immune response have opened new avenues to design improved vaccine adjuvants [12].

In this study, we have demonstrated that the recombinant *Leishmania infantum* eukaryotic initiation factor (LieIF) acts as a prostimulatory agent on monocytic cell types in *in vitro* and *in vivo* assays by inducing innate immune responses and could be considered as a potential molecular adjuvant. Initially, LeIF had been proven as a potent inducer of immunity exhibiting advantageous immunomodulatory properties such as the induction of production of IL-12,

IL-10, and TNF-α by monocytes, macrophages, and DCs derived from healthy volunteers [20, 22, 23]. Moreover, we have recently demonstrated using reverse vaccinology approaches that selected parts of LieIF can be used to develop innovative subunit protective vaccine candidates able to induce effective immunity mediated by MHC class I-restricted as well as class II-restricted T cell responses [48, 49]. Additionally, LeIF has been harnessed as a vaccine adjuvant targeted to cancer [29]. Collectively, these data suggested the potential of LeIF as a vaccine adjuvant that deserves further investigation. Our study features a number of important strengths towards the assessment of its adjuvant properties in *in vitro* and *in vivo* assays. To our knowledge, this is the first study that evaluated the ability of LieIF protein to induce the upregulation of both CD80 and CD86 macrophage surface molecules which is indispensable for the activation of T cells by APCs [50]. Also, we have demonstrated that LieIF induced increased expression of co-stimulatory molecules CD86, CD80, and CD40 in murine BMDCs (unpublished data), in consistence with another study where *L. braziliensis* eIF protein (LbeIF), having 98% identity with LieIF, was reported to induce upregulation of CD80 on human monocyte-derived macrophages [20]. Moreover, in the present study, we explored the ability of LieIF to activate host macrophages as demonstrated by the production of NO and MIP-1α chemokine in the supernatants of LieIF-stimulated J774A.1 macrophages [22]. These immune mediators are regulators of inflammatory responses since NO is an effector molecule in macrophage-mediated cytotoxicity [51] and MIP-1α is a chemoattractant mediator to a variety of cells including monocytes, eosinophils, and T and B cells to sites of infection, leading to the clearance of the microorganisms [52].

The introduction of an adjuvant in new vaccine formulation or in already licensed vaccine is still a challenge and may take several years of intensive research [15]. Thus, the understanding of their mechanism(s) of action would facilitate the acceleration of the development of effective adjuvants. In this regard, we further evaluated the potential of LieIF to provide adjuvant properties in an *in vivo* murine experimental model. Although, as mentioned above, some reports have indicated that LeIF is a natural Th1-type adjuvant [21], this is the first study documenting the adjuvant properties of LieIF using a murine model. In the present study, noticeable side effects such as abnormal behavior were not observed after intraperitoneal administration of LieIF. Analysis of immune parameters, such as phenotypic and functional differentiation of the cells locally recruited in the peritoneum after LieIF administration, revealed that LieIF protein is able to confer adjuvant properties to OVA, a soluble protein antigen, when both were intraperitoneally administered, as illustrated by the upregulated expression of the CD80 molecule and the increased production of NO and MIP-1α in PEC. Macrophage activation induced by the immunization of mice with OVA-LieIF was demonstrated by induction of NO synthesis in response to *in vitro* restimulation with recombinant LieIF protein. Immunization with OVA antigen alone did not enhance NO production by PEC even after stimulation with LPS or LPS+IFN-γ. Furthermore, a significant MIP-1α release was observed in culture supernatants of PEC derived from OVA-LieIF-immunized mice compared to other experimental groups after different potent *in vitro* stimulations. Moreover, a number of observations support that a cluster of genes encoding cytokines, innate immune receptors, interferon-induced genes, and gene encoding adhesion molecules are defined as "adjuvant core response genes" since they have been found to be modulated by adjuvants such as alum, MF59, and CpG-ODN at the injection site [53]. To this end, we determined the relative expression of two prototypic proinflammatory cytokines, IL-1β and TNF-α, and demonstrated that LieIF induced significant higher levels of *IL-1β* and *TNF-α* gene expression in PEC as early as 2 h post-immunization. Collectively, the above data demonstrate that proinflammatory signals elicited by LieIF result to a proinflammatory environment at the injection site and this is indeed a mechanism common to various known adjuvants [41].

To more critically address the adjuvant properties of LieIF, we used a similar approach which had been used for alum, a widely used adjuvant in humans [16]. Mice were immunized with LieIF in combination with the poorly immunogenic OVA antigen in order to assess the cellular recruitment into the peritoneal lavage fluid. We found that LieIF was effective to provoke similar recruitment of immune cells at the injection site as compared to alum, namely, increased frequencies of neutrophils and monocytes at 24 h post-immunization, even though, in contrast with alum, the immunopotentiating effect of LieIF was not mediated by uric acid danger signal.

In conclusion, the present study provides evidence that LieIF acts as an immune potentiator by inducing a proinflammatory environment at the injection site that enables the recruitment of innate immune cells, induces cytokine expression, activates macrophages, and exhibits stimulatory effects for antigen presentation.

5. Conclusions

In this study, we demonstrate the adjuvant properties of LieIF that collectively suggest its potential use for novel vaccine formulations. LieIF induces the upregulation of CD80 and CD86 co-stimulatory molecules, as well as the production of the NO and MIP-1α immune mediators *in vitro*, by J774A.1 macrophages. Moreover, LieIF is able to promote macrophage activation and to induce a proinflammatory environment at the injection site after its intraperitoneal co-administration with OVA antigen in a murine model. Additionally, LieIF leads to the recruitment of neutrophils and monocytes at the injection site, similar to alum's effect.

Abbreviations

APCs: Antigen-presenting cells
DCs: Dendritic cells
FACS: Fluorescence-activated cell sorter
IFN-γ: Interferon gamma
IL-10: Interleukin 10
IL-12: Interleukin 12

LieIF: *Leishmania infantum* eukaryotic initiation factor
LPS: Lipopolysaccharide
MIP-1α: Macrophage inflammatory protein-1 alpha
NO: Nitric oxide
PEC: Peritoneal exudate cells
r: Recombinant
TNF-α: Tumor necrosis factor alpha.

Data Availability

All data related to this study have been provided within the manuscript and are also available from the corresponding author based on a reasonable request.

Conflicts of Interest

The authors declare no conflict of interest.

Acknowledgments

This study was supported by the project entitled "Infectious and Neurodegenerative Diseases in the 21st Century: Study of Basic Mechanisms for the Development of the Translational Research and Cutting Edge Technologies Aiming to Effective Diagnosis Prevention and Therapy" which was cofunded by the European Regional Development Fund and National Resources, in the framework of the action: "KRIPIS: Development Proposals of Research Institutions," issued by the Greek General Secretariat for Research and Technology, Ministry of Education (Award number: MIS450598). MB was supported through a Calmette and Yersin fellowship of the Institut Pasteur. IG's and MB's activities are supported by the Ministry of Higher Education and Scientific Research in Tunisia (LR16IPT04).

References

[1] S. Rauch, E. Jasny, K. E. Schmidt, and B. Petsch, "New vaccine technologies to combat outbreak situations," *Frontiers in Immunology*, vol. 9, article 1963, 2018.

[2] S. Lee and M. T. Nguyen, "Recent advances of vaccine adjuvants for infectious diseases," *Immune Network*, vol. 15, no. 2, pp. 51–57, 2015.

[3] W. C. Koff, D. R. Burton, P. R. Johnson et al., "Accelerating next-generation vaccine development for global disease prevention," *Science*, vol. 340, no. 6136, article 1232910, 2013.

[4] F. R. Vogel, "Adjuvants in perspective," *Developments in Biological Standardization*, vol. 92, pp. 241–248, 1998.

[5] S. G. Reed, M. T. Orr, and C. B. Fox, "Key roles of adjuvants in modern vaccines," *Nature Medicine*, vol. 19, no. 12, pp. 1597–1608, 2013.

[6] S. Calabro, M. Tortoli, B. C. Baudner et al., "Vaccine adjuvants alum and MF59 induce rapid recruitment of neutrophils and monocytes that participate in antigen transport to draining lymph nodes," *Vaccine*, vol. 29, no. 9, pp. 1812–1823, 2011.

[7] N. Petrovsky and J. C. Aguilar, "Vaccine adjuvants: current state and future trends," *Immunology and Cell Biology*, vol. 82, no. 5, pp. 488–496, 2004.

[8] J. H. Wilson-Welder, M. P. Torres, M. J. Kipper, S. K. Mallapragada, M. J. Wannemuehler, and B. Narasimhan, "Vaccine adjuvants: current challenges and future approaches," *Journal of Pharmaceutical Sciences*, vol. 98, no. 4, pp. 1278–1316, 2009.

[9] M. V. Sanchez, R. J. Eliçabe, M. S. di Genaro et al., "Total *Leishmania* antigens with Poly(I:C) induce Th1 protective response," *Parasite Immunology*, vol. 39, no. 11, 2017.

[10] H. F. J. Savelkoul, V. A. Ferro, M. M. Strioga, and V. E. J. C. Schijns, "Choice and design of adjuvants for parenteral and mucosal vaccines," *Vaccines*, vol. 3, no. 1, pp. 148–171, 2015.

[11] J. de Souza Apostólico, V. A. S. Lunardelli, F. C. Coirada, S. B. Boscardin, and D. S. Rosa, "Adjuvants: classification, modus operandi, and licensing," *Journal of Immunology Research*, vol. 2016, Article ID 1459394, 16 pages, 2016.

[12] M. L. Mbow, E. de Gregorio, N. M. Valiante, and R. Rappuoli, "New adjuvants for human vaccines," *Current Opinion in Immunology*, vol. 22, no. 3, pp. 411–416, 2010.

[13] S. Hutchison, R. A. Benson, V. B. Gibson, A. H. Pollock, P. Garside, and J. M. Brewer, "Antigen depot is not required for alum adjuvanticity," *The FASEB Journal*, vol. 26, no. 3, pp. 1272–1279, 2012.

[14] P. Marrack, A. S. McKee, and M. W. Munks, "Towards an understanding of the adjuvant action of aluminium," *Nature Reviews Immunology*, vol. 9, no. 4, pp. 287–293, 2009.

[15] G. Del Giudice, R. Rappuoli, and A. M. Didierlaurent, "Correlates of adjuvanticity: a review on adjuvants in licensed vaccines," *Seminars in Immunology*, vol. 39, pp. 14–21, 2018.

[16] M. Kool, T. Soullié, M. van Nimwegen et al., "Alum adjuvant boosts adaptive immunity by inducing uric acid and activating inflammatory dendritic cells," *The Journal of Experimental Medicine*, vol. 205, no. 4, pp. 869–882, 2008.

[17] S. Iborra, J. C. Solana, J. M. Requena, and M. Soto, "Vaccine candidates against Leishmania under current research," *Expert Review of Vaccines*, vol. 17, no. 4, pp. 323–334, 2018.

[18] J. M. Mutiso, J. C. Macharia, and M. M. Gicheru, "A review of adjuvants for Leishmania vaccine candidates," *Journal of Biomedical Research*, vol. 24, no. 1, pp. 16–25, 2010.

[19] Y. A. W. Skeiky, M. Kennedy, D. Kaufman et al., "LeIF: a recombinant *Leishmania* protein that induces an IL-12-mediated Th1 cytokine profile," *The Journal of Immunology*, vol. 161, no. 11, pp. 6171–6179, 1998.

[20] P. Probst, Y. A. W. Skeiky, M. Steeves, A. Gervassi, K. H. Grabstein, and S. G. Reed, "A *Leishmania* protein that modulates interleukin (IL)-12, IL-10 and tumor necrosis factor-α production and expression of B7-1 in human monocyte-derived antigen-presenting cells," *European Journal of Immunology*, vol. 27, no. 10, pp. 2634–2642, 1997.

[21] Y. A. Skeiky, J. A. Guderian, D. R. Benson et al., "A recombinant *Leishmania* antigen that stimulates human peripheral blood mononuclear cells to express a Th1-type cytokine profile and to produce interleukin 12," *The Journal of Experimental Medicine*, vol. 181, no. 4, pp. 1527–1537, 1995.

[22] M. Barhoumi, A. Garnaoui, B. Kaabi, N. K. Tanner, and I. Guizani, "*Leishmania infantum* LeIF and its recombinant polypeptides modulate interleukin IL-12p70, IL-10 and tumour necrosis factor-α production by human monocytes," *Parasite Immunology*, vol. 33, no. 10, pp. 583–588, 2011.

[23] M. Barhoumi, A. Meddeb-Garnaoui, N. K. Tanner, J. Banroques, B. Kaabi, and I. Guizani, "DEAD-box proteins, like *Leishmania* eIF4A, modulate interleukin (IL)-12, IL-10 and tumour necrosis factor-alpha production by human monocytes," *Parasite Immunology*, vol. 35, no. 5-6, pp. 194–199, 2013.

[24] O. Koutsoni, M. Barhoumi, I. Guizani, and E. Dotsika, "Leishmania eukaryotic initiation factor (LeIF) inhibits parasite growth in murine macrophages," *PLoS One*, vol. 9, no. 5, article e97319, 2014.

[25] Y. A. W. Skeiky, R. N. Coler, M. Brannon et al., "Protective efficacy of a tandemly linked, multi-subunit recombinant leishmanial vaccine (Leish-111f) formulated in MPL® adjuvant [vol 20, pg 3292, 2002]," *Vaccine*, vol. 20, no. 31-32, pp. 3783–3783, 2002.

[26] R. N. Coler, Y. Goto, L. Bogatzki, V. Raman, and S. G. Reed, "Leish-111f, a recombinant polyprotein vaccine that protects against visceral leishmaniasis by elicitation of $CD4^+$ T cells," *Infection and Immunity*, vol. 75, no. 9, pp. 4648–4654, 2007.

[27] S. Sakai, Y. Takashima, Y. Matsumoto, S. G. Reed, Y. Hayashi, and Y. Matsumoto, "Intranasal immunization with Leish-111f induces IFN-γ production and protects mice from *Leishmania major* infection," *Vaccine*, vol. 28, no. 10, pp. 2207–2213, 2010.

[28] I. D. Vélez, K. Gilchrist, S. Martínez et al., "Safety and immunogenicity of a defined vaccine for the prevention of cutaneous leishmaniasis," *Vaccine*, vol. 28, no. 2, pp. 329–337, 2009.

[29] S. M. Barratt-Boyes, A. Vlad, and O. J. Finn, "Immunization of chimpanzees with tumor antigen MUC1 mucin tandem repeat peptide elicits both helper and cytotoxic T-cell responses," *Clinical Cancer Research*, vol. 5, no. 7, pp. 1918–1924, 1999.

[30] F. D'Acquisto, T. Iuvone, L. Rombolà, L. Sautebin, M. di Rosa, and R. Carnuccio, "Involvement of NF-κB in the regulation of cyclooxygenase-2 protein expression in LPS-stimulated J774 macrophages," *FEBS Letters*, vol. 418, no. 1-2, pp. 175–178, 1997.

[31] E. E. B. Ghosn, A. A. Cassado, G. R. Govoni et al., "Two physically, functionally, and developmentally distinct peritoneal macrophage subsets," *Proceedings of the National Academy of Sciences of the United States of America*, vol. 107, no. 6, pp. 2568–2573, 2010.

[32] D. Tsikas, "Analysis of nitrite and nitrate in biological fluids by assays based on the Griess reaction: appraisal of the Griess reaction in the L-arginine/nitric oxide area of research," *Journal of Chromatography B*, vol. 851, no. 1-2, pp. 51–70, 2007.

[33] I. D. Kyriazis, O. S. Koutsoni, N. Aligiannis, K. Karampetsou, A. L. Skaltsounis, and E. Dotsika, "The leishmanicidal activity of oleuropein is selectively regulated through inflammation- and oxidative stress-related genes," *Parasites & Vectors*, vol. 9, no. 1, p. 441, 2016.

[34] B. B. Aggarwal and K. Mehta, "[15] Determination and regulation of nitric oxide production from macrophages by lipopolysaccharides, cytokines, and retinoids," *Methods in Enzymology*, vol. 269, pp. 166–171, 1996.

[35] K. J. Livak and T. D. Schmittgen, "Analysis of relative gene expression data using real-time quantitative PCR and the $2^{-\Delta\Delta C}{}_T$ method," *Methods*, vol. 25, no. 4, pp. 402–408, 2001.

[36] N. Kageyama, "A direct colorimetric determination of uric acid in serum and urine with uricase-catalase system," *Clinica Chimica Acta*, vol. 31, no. 2, pp. 421–426, 1971.

[37] N. Khan, U. Gowthaman, S. Pahari, and J. N. Agrewala, "Manipulation of costimulatory molecules by intracellular pathogens: veni, vidi, vici!!," *PLoS Pathogens*, vol. 8, no. 6, article e1002676, 2012.

[38] J. MacMicking, Q. W. Xie, and C. Nathan, "Nitric oxide and macrophage function," *Annual Review of Immunology*, vol. 15, no. 1, pp. 323–350, 1997.

[39] A. Zlotnik and O. Yoshie, "Chemokines: a new classification system and their role in immunity," *Immunity*, vol. 12, no. 2, pp. 121–127, 2000.

[40] Y. Hatano, K. Katagiri, and S. Takayasu, "Increased levels in vivo of mRNAs for IL-8 and macrophage inflammatory protein-1 alpha (MIP-1α), but not of RANTES mRNA in peripheral blood mononuclear cells of patients with atopic dermatitis (AD)," *Clinical and Experimental Immunology*, vol. 117, no. 2, pp. 237–243, 1999.

[41] S. Awate, L. A. Babiuk, and G. Mutwiri, "Mechanisms of action of adjuvants," *Frontiers in Immunology*, vol. 4, p. 114, 2013.

[42] B. Su, J. Wang, X. Wang et al., "The effects of IL-6 and TNF-α as molecular adjuvants on immune responses to FMDV and maturation of dendritic cells by DNA vaccination," *Vaccine*, vol. 26, no. 40, pp. 5111–5122, 2008.

[43] M. Akdis, A. Aab, C. Altunbulakli et al., "Interleukins (from IL-1 to IL-38), interferons, transforming growth factor β, and TNF-α: receptors, functions, and roles in diseases," *The Journal of Allergy and Clinical Immunology*, vol. 138, no. 4, pp. 984–1010, 2016.

[44] G. J. Randolph, K. Inaba, D. F. Robbiani, R. M. Steinman, and W. A. Muller, "Differentiation of phagocytic monocytes into lymph node dendritic cells in vivo," *Immunity*, vol. 11, no. 6, pp. 753–761, 1999.

[45] F. Geissmann, S. Jung, and D. R. Littman, "Blood monocytes consist of two principal subsets with distinct migratory properties," *Immunity*, vol. 19, no. 1, pp. 71–82, 2003.

[46] C. J. Chen, Y. Shi, A. Hearn et al., "MyD88-dependent IL-1 receptor signaling is essential for gouty inflammation stimulated by monosodium urate crystals," *Journal of Clinical Investigation*, vol. 116, no. 8, pp. 2262–2271, 2006.

[47] F. Martinon, V. Pétrilli, A. Mayor, A. Tardivel, and J. Tschopp, "Gout-associated uric acid crystals activate the NALP3 inflammasome," *Nature*, vol. 440, no. 7081, pp. 237–241, 2006.

[48] O. S. Koutsoni, J. G. Routsias, I. D. Kyriazis et al., "*In silico* analysis and *in vitro* evaluation of immunogenic and immunomodulatory properties of promiscuous peptides derived from *Leishmania infantum* eukaryotic initiation factor," *Bioorganic & Medicinal Chemistry*, vol. 25, no. 21, pp. 5904–5916, 2017.

[49] M. Agallou, E. Athanasiou, O. Koutsoni, E. Dotsika, and E. Karagouni, "Experimental validation of multi-epitope peptides including promising MHC class I- and II-restricted epitopes of four known *Leishmania infantum* proteins," *Frontiers in Immunology*, vol. 5, p. 268, 2014.

[50] D. J. Lenschow, T. L. Walunas, and J. A. Bluestone, "CD28/B7 system of T cell costimulation," *Annual Review of Immunology*, vol. 14, no. 1, pp. 233–258, 1996.

[51] R. Korhonen, A. Lahti, H. Kankaanranta, and E. Moilanen, "Nitric oxide production and signaling in inflammation," *Current Drug Targets Inflammation and Allergy*, vol. 4, no. 4, pp. 471–479, 2005.

[52] P. Menten, A. Wuyts, and J. Van Damme, "Macrophage inflammatory protein-1," *Cytokine & Growth Factor Reviews*, vol. 13, no. 6, pp. 455–481, 2002.

[53] F. Mosca, E. Tritto, A. Muzzi et al., "Molecular and cellular signatures of human vaccine adjuvants," *Proceedings of the National Academy of Sciences of the United States of America*, vol. 105, no. 30, pp. 10501–10506, 2008.

Hindawi
Journal of Immunology Research
Volume 2019, Article ID 8732191, 10 pages
https://doi.org/10.1155/2019/8732191

Review Article

OMIC Technologies and Vaccine Development: From the Identification of Vulnerable Individuals to the Formulation of Invulnerable Vaccines

Nicola Cotugno,[1] **Alessandra Ruggiero**,[1] **Veronica Santilli**,[1] **Emma Concetta Manno**,[1] **Salvatore Rocca**,[1] **Sonia Zicari**,[1] **Donato Amodio**,[1] **Manuela Colucci**,[2] **Paolo Rossi**,[1] **Ofer Levy**,[3,4] **Federico Martinon-Torres**,[5,6] **Andrew J. Pollard**,[7] **and Paolo Palma**[1]

[1]*Academic Department of Pediatrics, Research Unit of Congenital and Perinatal Infection, Children's Hospital Bambino Gesù, Rome, Italy*
[2]*Laboratory of Nephrology, Department of Rare Diseases, Children's Hospital Bambino Gesù, Rome, Italy*
[3]*Precision Vaccines Program, Division of Infectious Diseases, Department of Medicine, Boston Children's Hospital, Boston, MA, USA*
[4]*Broad Institute of MIT & Harvard, Cambridge, MA, USA*
[5]*Translational Pediatrics and Infectious Diseases, Department of Pediatrics, Hospital Clínico Universitario de Santiago, Santiago de Compostela, Galicia, Spain*
[6]*Grupo de Investigación en Genética, Vacunas, Infecciones y Pediatría (GENVIP), Instituto de Investigación Sanitaria de Santiago and Universidade de Santiago de Compostela (USC), Galicia, Spain*
[7]*Oxford Vaccine Group, Department of Paediatrics, University of Oxford and the NIHR Oxford Biomedical Research Centre, Oxford, UK*

Correspondence should be addressed to Paolo Palma; paolo.palma@opbg.net

Received 26 November 2018; Revised 1 March 2019; Accepted 6 March 2019; Published 28 April 2019

Guest Editor: Roberta A. Diotti

Routine vaccination is among the most effective clinical interventions to prevent diseases as it is estimated to save over 3 million lives every year. However, the full potential of global immunization programs is not realised because population coverage is still suboptimal. This is also due to the inadequate immune response and paucity of informative correlates of protection upon immunization of vulnerable individuals such as newborns, preterm infants, pregnant women, and elderly individuals as well as those patients affected by chronic and immune compromising medical conditions. In addition, these groups are undervaccinated for a number of reasons, including lack of awareness of vaccine-preventable diseases and uncertainty or misconceptions about the safety and efficacy of vaccination by parents and healthcare providers. The presence of these nonresponders/undervaccinated individuals represents a major health and economic burden to society, which will become particularly difficult to address in settings with limited public resources. This review describes innovative and experimental approaches that can help identify specific genomic profiles defining nonresponder individuals for whom specific interventions might be needed. We will provide examples that show how such information can be useful to identify novel biomarkers of safety and immunogenicity for future vaccine trials. Finally, we will discuss how system biology "OMICs" data can be used to design bioinformatic tools to predict the vaccination outcome providing genetic and molecular "signatures" of protective immune response. This strategy may soon enable identification of signatures highly predictive of vaccine safety, immunogenicity, and efficacy/protection thereby informing personalized vaccine interventions in vulnerable populations.

1. Introduction

Vaccine-preventable disease (VPDs) pose an ongoing threat to health worldwide which can be avoided by protective and long-lasting vaccination coverage. Vaccines already prevent 3 million deaths every year by providing immunity against relevant pathogens. Nonetheless, current coverage rates are suboptimal especially in the so-called "vulnerable populations" (VPs) which include newborns, preterm infants, pregnant women, and elderly individuals as well as those patients affected by chronic and immune compromising medical conditions [1]. There are various reasons for this undervaccination, including lack of awareness of vaccine-preventable diseases and uncertainty or misconceptions about the safety and efficacy of vaccination among vulnerable patients, parents, and healthcare providers. Furthermore, in these VPs, the immune responses obtained with currently available vaccines and schedules can be inadequate leading to lower protection compared with healthy individuals [1, 2]. This situation represents a major health and economic burden to society, which will become particularly difficult to address in settings with limited public resources. As a consequence, renewed attention and innovative strategies are required to overcome the many challenges faced by public health authorities to improving the efficacy of immunization programs [3]. Two strategies are needed: (1) improve current vaccination approaches by addressing education and management of vaccine hesitancy and (2) develop innovative tools that enable explanation of mechanisms behind low or no responsiveness to current vaccine regimens in these groups and design specific interventions accordingly (i.e., booster doses of vaccines and/or tailoring adjuvantation systems for vaccine formulations targeted to specific subpopulations). In this review, we will mainly focus on innovative genomic and transcriptomic tools that can identify specific host characteristics defining nonresponder individuals for whom specific interventions might be needed.

1.1. Low Vaccination Coverage in Vulnerable Populations: Some Concerning Data. Low vaccination coverage in vulnerable groups increases the risk of developing vaccine-preventable diseases with higher morbidity and mortality [1]. The fact that vaccination rates among at-risk populations remain low despite national and international recommendations indicates a continuing failure to provide appropriate standards of care. One example is represented by maternal immunization against influenza, pertussis, and tetanus, which has the untapped potential of protecting the infant, which remains low in European pregnant women (38-50%) [4]. As a consequence, pertussis cases and outbreaks have increased over the last few decades with ~1400 cases of whooping cough documented in children < 6 months of age in the US that lead to hospitalization in 44.3% of cases in 2016 CDC [5]. Additionally, infants < 6 months who experience influenza virus infection have the highest rates of hospitalization and death of all children especially if born preterm [6]. Indeed, as current influenza vaccines are licensed for use in those from 6 months of age, those less than 6 months of age are too young to receive routine influenza vaccination with protection relying on that conferred by a vaccinated mother. Another example of low vaccination coverage is represented by elderly populations: in developing countries, the need for better vaccination coverage of aging populations is well recognised (reviewed in [1]). In the US, coverage among people aged ≥65 years was 67% for the influenza vaccine in the 2014–2015 and 55–60% for tetanus and pneumococcal vaccines in 2013, while the coverage rate for herpes zoster vaccination among those aged ≥60 years was only 24%. In most other countries, rates are far lower (reviewed in [1]). Furthermore, patients who are immunocompromised are also undervaccinated [1, 7]. This diverse group of patients includes patients with primary immunodeficiency, human immunodeficiency virus (HIV) infection, transplantation, cancer, asplenia, and autoimmune inflammatory diseases treated with immunosuppressive medications (corticosteroid therapy, immunomodulatory medications, or biological agents) [8–11].

Vaccine hesitancy, access to immunization, and inadequate response to vaccination are three distinct and equally concerning contributors to poor vaccination coverage in the global population as well as in the vulnerable population. For these and other reasons, personalized vaccine strategies could be considered to improve vaccination coverage and outcome as discussed below.

1.2. Reasons to Personalize Vaccine Intervention in Vulnerable Populations. High vaccination coverage is paramount to ensure global health, and it can be achieved by promotion of vaccination and by the design of effective vaccine. However, vulnerable populations consistently generate vaccine-specific immune responses that are considerably weaker than those of the healthy immunocompetent population [1, 2, 12–15]. We previously demonstrated that patients with chronic granulomatous disease (CGD) present a significantly reduced measles-specific antibody levels and antibody-secreting cell number indicating poor ability to maintain long-term memory in these patients [16]. Similarly, we demonstrated that 19% of kidney transplanted patients (TPs) on immunosuppressive therapy experienced loss of vaccine-induced immunity against measles after two doses of live attenuated measles vaccine at 13 months and 6 years of age [17]. Furthermore, we found a positive correlation between the antibody titres and the time elapsed between vaccination and transplant, demonstrating that patients transplanted close to vaccination had lower measles antibody titre than patients vaccinated earlier before transplantation. Reversing this situation is likely to require a broad range of interventions. For example, financial incentives, patient reminders, and patient recall systems can improve vaccination rates and are more readily implemented in high-income country settings [18]. Nonetheless, there is lack of harmonized research data that can provide meaningful evidence on the efficacy and safety of vaccination in this group. Indeed, most vaccine indications in special and vulnerable groups derive from extrapolations, assumptions, or postlicensure studies in healthy populations.

Generating and analysing clinical, laboratory, system biology "OMICs," and computational data are needed to

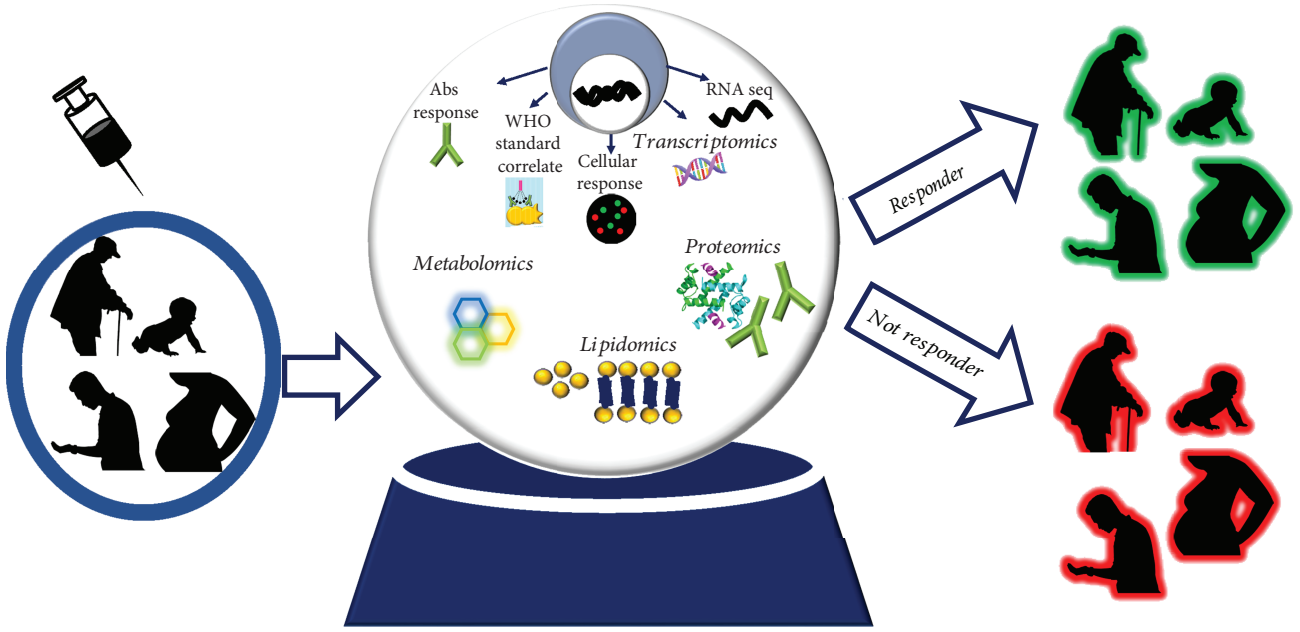

Figure 1: Conventional and system biology "OMICs" technologies [35] currently available to predict vaccine-induced immune response.

inform selection of patients at risk for vaccine failure and specifically tailor vaccination approaches in these groups. The number of patients who are immunocompromised is increasing [19], and the suboptimal vaccination coverage in this growing number of people represents a substantial health and economic burden to society, as discussed above. Furthermore, vaccine-preventable infectious diseases have been reported in these groups despite a history of vaccination [19–24]. Such cases are often the first demonstrable sign of inefficacy of the current vaccination strategies in specific populations within a community. This situation has generated major concern in the World Health Organization (WHO) that is promoting strategies (The Guide to Tailoring Immunization Programmes (TIP)) [3] to enhance efficient vaccination in newborns and children, with a plan to extend this action to individuals within other vulnerable populations. Although they are useful, such recommendations are based on expert opinions and extrapolated from data produced in healthy people and not developed based on vaccine immunity data in vulnerable populations.

2. Modern System Biology Tools to Characterize Immune Responses to Vaccination

Despite the fact that conventional immunological assays, such as ELISA, ELISpot, flow cytometry, and neutralization assays, have supported all previous researches [25–33], the toolkit of the modern immunologists now includes a broad range of "OMICs" technologies [34–37], such as high-throughput sequencing of DNA (DNA-seq), RNA (RNA-seq), transcriptomic assays, microarrays, epigenetics, and high-resolution mass spectrometry proteomics and metabolomics [22, 38–43]. Data produced by these different approaches will enable prediction of patients likely to have a poor outcome from vaccination with respect to safety and/or immunogenicity (Figure 1). The amount of information provided by these experimental approaches represent considerable experimental data analysis challenges [44]; therefore, sophisticated bioinformatic tools are under development for data integration [45].

2.1. High-Throughput Sequencing of DNA and RNA (Transcriptomic Assays). High-Throughput Sequencing of DNA and RNA (Transcriptomic Assays) has helped to identify specific mechanisms that regulate gene expression and associated with differentiation and functionality of different cell lineages including immune cells [39, 46]. For example, Reif et al. identified and validated three SNPs associated with adverse events to smallpox vaccine in healthy vaccinia virus-naïve individuals [47]. The study demonstrated how common genetic variants can be related to a complex clinical phenotype, and prescreening is needed to predict adverse events. Poland and colleagues identified genetic variations in HLA and non-HLA genes associated with non- or hyper-immune phenotypes after measles, mumps, rubella, and smallpox, proposed as "genetic blueprints to guide personalized vaccination regimens" [48, 49]. Other studies have characterized the sequences of heavy and light chains of the antibody following vaccination against pathogens such as influenza and tetanus, with the ultimate aim of engineering responsive antibodies that could be administered to support immunization [50, 51].

Furthermore, DNA sequencing has helped to identify and describe stimulus-induced epigenetic events, paving the way to a new research area: epigenomics. In particular, *DNA methylation* [52, 53] events are associated with (a) differential expression of proinflammatory (IL12p70, IL-1β, IL-6, and TNF-α) and regulatory (IL-10) cytokines and costimulatory molecules (CD80, CD86, and CD40) in antigen-presenting cells (APCs); (b) regulation of macrophage

functional responses and polarization, influencing the innate immune system through macrophage tolerance and training [54]; and (c) modulation of T and B cell differentiation and maturation [54]. Accordingly, recent studies have explored the effect of epigenetic regulation in response to vaccination. For example, individuals showing antimycobacterial activity following BCG vaccination had reduced the presence of methylation events in promoters associated with immune responses in PBMC [55]. In particular, at 3 weeks after vaccination, 540 promoters displayed a more than 5-fold loss of methylation in the responders, whereas only 20 promoters were losing methylation in the nonresponders. Furthermore, at 4 and 8 months, after vaccination, a substantial gain of methylation was observed in the nonresponders. On the contrary, a group of hypomethylated CpGs has been associated with lower humoral immune response to influenza vaccination [56]. Similarly, another study by Marsit et al. [57] demonstrated a small but statistically significant reduction in the methylation of peripheral blood repetitive elements in an HIV-exposed and antiretroviral therapy- (ART-) exposed pediatric cohort when compared with an HIV-exposed and combined ART-unexposed cohort. However, data are still scarce and often contradictory, and efforts are needed to define the power of specific methylation marks in predicting vaccine responses.

The combination of flow-based sorting and microfluidic *transcriptomic assays* (Fluidigm) has enabled dissection of transcriptional signatures of immune cell subsets particularly involved in the memory response upon vaccinations. The low number of cells needed for these assays has made such studies feasible in pediatric cohorts and provides the possibility to investigate gene expression on purified memory subsets rather than in the highly variable pool of PBMCs allowing the analysis of low abundance transcripts. Such methodology increases the specificity of transcriptional characteristics found in peculiar cell subsets which are involved in the immune memory response but are quantitatively rare in the pool of PBMCs [58]. With such strategy, Cotugno et al. have recently investigated the prevaccination gene expression signatures of lymphocyte subsets in groups of HIV-1-infected children differentially responding to trivalent influenza vaccination (TIV). A 25-gene signature in resting memory (RM) B cells ($CD27^+CD21^+$) distinguished vaccine responders from nonresponders (NR). In fact, prevaccination RM B cells of responders demonstrated a higher expression of gene sets involved in B cell adaptive immune responses (*APRIL, BTK, BLIMP1*) and BCR signalling (*MTOR, FYN, CD86*) when compared with NR. We further investigated the variation of gene expression of peripheral T follicular helper (pTfH) cells after *in vitro* stimulation with H1N1 peptides. In line with previous FACS and ELISA results [59], our analysis revealed that the ability to upregulate the gene expression of interleukin-21 (IL-21) within pTfH after *in vitro* stimulation was strongly associated with H1N1-specific B cell responses postvaccination [60]. These results suggest that the targeted transcriptional evaluation of B and T cell subsets at the time of vaccination may identify predictive correlates of vaccine responses in this population. Other advantages of this analytical tool account for containment of costs when compared to RNA-seq (approximately 1/25) and to DNA microarray (approximately 1/10). In addition, the integration and the analysis of targeted multiplexed RT-PCR (e.g., Fluidigm) rather than "big data" deriving from RNA-seq need less sophisticated bioinformatic expertise which may enhance clinical applicability of such analysis.

On the other hand, the selection of specific gene sets for analysis also represents a limitation. Indeed, whole transcriptome or genome analysis may provide more specific and unbiased information on molecular mechanisms underlying vaccine-induced reactogenicity and immunogenicity. In the context of vulnerable populations, such information may provide important input into discovery of specific pathways, inadequately engaged by current vaccines, which may inform future targeted adjuvant strategies. In this context, the interindividual variability in vaccine responses or reaction upon vaccinations has been investigated, and several polymorphisms of genes, including *HLA*, *KIR*, *MICA*, and *BTN* genes, were identified that impact immune responses to immunization against hepatitis B [61–63], influenza [61], and smallpox [64, 65]. Possible mechanisms underlying such correlation presumably refer to the selectivity of specific HLA types to naturally process particular vaccine peptides and present to T and B cells. Such peptides are enriched by specific particles and adjuvants and are now being utilized in a reverse-engineering strategy to develop peptide-based candidates for measles and mumps vaccines [66]. Ovsyannikova et al. recently reported how specific coding polymorphisms in Toll-like receptor (TLR) genes are associated with immunogenicity of measles vaccine [67, 68]. Although these findings represent great steps towards the design of personalized peptides and adjuvants in the immunization schedule for NR, most of these studies have been conducted in healthy individuals (reviewed in [69]). Indeed, such approaches have only rarely investigated vaccine-related immunogenicity and adverse events in vulnerable populations (especially in the elderly) showing how signatures of NR found in healthy individuals are only partially applicable to such populations [70]. However, the few studies conducted on vulnerable populations showed that the genetic signatures associated with lack of vaccine immunogenicity in healthy individuals were not fully powerful when applied to vulnerable populations. Thus, there is an urgent need for more vaccinology studies in these vulnerable populations.

To improve robustness and power of transcriptomic data, gene set enrichment analyses (GSEA) have been developed in order to analyse genes within their functional group or as being part of the same signalling pathway. In line with this approach, increasing numbers of functional annotation tools available online free of charge can identify enriched biological themes—Gene Ontology (http://geneontology.org), DAVID (http://david.abcc.ncifcrf.gov), http://www.pathjam.org, and http://genemania.org—and functionally related gene groups.

In a different approach, the *whole transcriptome* was implemented to describe factors correlated to vaccination immunogenicity in the blood cells of humans few days after yellow fever vaccination [42]. In particular, the authors found enrichment of genes promoting apoptosis including GSTP1, STAT4 inhibitor, IL17D, and ZNF-148 (also known as

ZBP-89) (reviewed in [71]). This approach was further explored to define possible correlates of adaptive and innate immunity able to predict immunogenicity of influenza vaccination (live attenuated influenza vaccine and TIV) [37]. Both Nakaya et al. [40] and Tsang et al. [43] found that the calcium/calmodulin-dependent kinase IV (Camk4) gene expression modules could be used as a predictor of low antibody titres upon influenza vaccination. In order to define the vaccine specificity, Li et al. [36] compared five 5different vaccinations and found three different signatures of immune response according to the type of vaccinations used. It is still unclear however, whether gene signatures of vaccine immunity should be investigated in selected lymphocyte subsets or in antigen- (Ag-) specific cells. Technological advances in single-cell analysis allow for deeper interrogation of cellular signatures in cell population with diverse functions, such as Ag-specific cells in memory cell compartments.

Among these, single-cell RNA sequencing (scRNA-seq) [72–74] has provided insights on key processes in immune cell development and differentiation [73, 74], on haematopoietic pathways [75], and on gene regulatory networks that predict immune function [76]. There are multiple scRNA-seq approaches, the most current version being massively parallel RNA single-cell sequencing (MARS-seq), Fluidigm C1 single-cell full length messenger RNA (mRNA) sequencing, switching mechanisms at the $5'$ end of RNA template (SMART-seq2), and 10x genomic chromium single-cell DNA sequencing (herein referred to as 10x cell sequencing (reviewed in detail by [74])). Among those, the most promising at the moment is the 10x cell sequencing (described in [77]). This cutting-edge technology performs rapid droplet-basedencapsulation of single cells using a gel bead in emulsion (GEM) approach. Each gel bead is labelled with oligonucleotides that consist of a unique barcode, a 10 bp unique molecular identified and an anchored 30 bp oligo-dT. The high-throughput system is designed to enable analysis of rare cell types in a sufficient heterogeneous biological space avoiding the cell sorting step with reduced waste of the precious clinical sample. Similar to other droplet-based methods, clinical samples must be handled with caution in order to minimize perturbation of existing cellular characteristics [78]. Importantly, this method also enables cellular indexing of transcriptomes and epitopes using DNA-barcoded antibodies by Cellular Indexing of Transcriptomes and Epitopes by sequencing (CITE-seq) of thousands of single cells [79]. Accordingly, CITE-seq could find major applicability in immunology for sequencing of antigen-specific cells by multiplexing specific antigenic protein markers.

2.2. Proteomics and Metabolomics. Although high-throughput technologies can provide a valuable "snapshot" of the transcriptional levels of genes inside the cells, the interactions among those genes cannot be fully captured if the above described tools are uniquely used to generate lists of genes or pathways associated to a specific cellular activity. Indeed, it is the functional relationships between genes, proteins, and metabolites that may help us to better understand biological processes involved in cellular responses.

In this optic, the identification of the subset of proteins and peptides involved in the immune response could be pivotal to unravel mechanisms supporting a successful vaccination outcome [80]. Targeted protein analysis assays (e.g., ELISA and WB) only allow for quantification of a certain list of protein candidates limiting the proteomic discoveries. To overcome this hurdle, different high-throughput methods have recently been developed. Mass spectrometry- (MS-) based proteomics is the most widely used approach, and it has been essential to define the major histocompatibility complex (MHC) in the context of T cell profiling [81] as well as the antigenic determinants triggering B cell activity [82–84]. As the MS method is not limited to the use of predefined proteins, it has become the method of choice for protein discoveries across different fields as already been extensively described somewhere else [80]. More recently, Bennike et al. [85] have optimized use of as little as 1 μl of blood plasma for a high-throughput MS approach with bioinformatic analysis employing Spectronaut. This innovative, cost-effective high-throughput technology has, for example, supported the discovery of 16 serum proteins predicting chronic pancreatitis. Indeed, low sample input, high throughput, and robust proteomic depth render this method attractive for large diagnostic studies aiming at the identification of protein biomarkers in different clinical and scientific settings.

Evaluation of metabolomic signatures can be an additional mass spectrometery-based tool to capture perturbation of the immune system after a vaccination and translate such information as potential new biomarkers of vaccine immunogenicity. McClenathan et al. [86] used the nuclear magnetic resonance metabolomic approach to characterize specific metabolites predicting adverse reaction following vaccination. These studies provided a set of metabolites associated with the vaccine outcome that can be used in the clinical practice for identification of vaccine nonresponder individuals. Furthermore, Li et al. applied a multidisciplinary approach to define immunological response to herpes zoster (shingles) by studying transcriptomics, metabolomics, plasma cytokines, and cell phonotypes in blood samples.

2.3. Data Integration. OMIC approaches have changed perspectives and dimension of data to be handled and interpreted. Indeed, most of these sophisticated approaches often require big sample volume, which may hurdle the large-scale applicability of the methods. The Human Immunology Project Consortium (HIPC, https://www.immuneprofiling.org [87]) program has developed novel analytic tools to integrate the information derived from OMICs, *in vitro* assays, and functional assays to define vaccine responsiveness.

The overwhelming amount of data represents both a precious source and a hurdle towards the design of rule-driven precision medicine [34]. Indeed, there is the need for more complex algorithms capable of integrating data from different system biology approaches that will consequentially be implemented, tested, and validated in order to generate a clinical tool that can support the personalization of vaccination strategy. Accordingly, novel research approaches in the last two decades have led to partnerships of basic scientists,

bioinformaticians, and physicians to appropriately interpret data. With this aim, specific tools have been developed to enable gene set enrichment analyses (GSEA) in order to improve robustness, power, and readability of transcriptomic data, as mentioned above. Furthermore, there are various modelling frameworks that can be applied which range from simple linear regression models to advanced and computationally expensive feature selection methods for identifying predictive signatures (reviewed in [88]). For example, network modelling provides a powerful way to uncover the organizing principles and regulatory elements of cellular networks and how these networks modulate immunological responses to vaccination (reviewed in [88]). Additional tools such as Network Analyst and DIABLO (Data Integration Analysis for Biomarker discovery using Latent variable approaches for 'Omics studies) have been employed to understand multidimensional data across multiple assay platforms [45].

3. Ebola and Influenza Vaccines: Two Successful OMIC Examples of Applied System Vaccinology

3.1. Ebola. Rechtien et al. applied a system vaccinology approach to unravel if the early immune response towards Ebola vaccine rVSV-Zaire Ebola virus (ZEBOV) predicts the generation of anti-Ebola virus (EBOV) glycoprotein-(GP-) specific antibody responses [89]. The study employed blood samples from days 0, 1, 3, 7, and 14 postvaccination to investigate changes in cytokine levels, innate immune cell subsets, and gene expression. Integrative statistical analyses with cross-validation identified a signature of 5 early innate markers correlating with antibody titres on day 28. Among those, interferon-γ-inducible protein 10 (IP-10) on day 3 and MFI of CXCR6 on NK cells on day 1 were independent correlates. Consistently, they found an early gene expression signature linked to IP-10. This comprehensive characterization of early innate immune responses to the rVSV-ZEBOV vaccine in humans revealed immune signatures linked to IP-10. These results suggested correlates of vaccine-induced antibody induction and provide a rationale to explore strategies for augmenting the effectiveness of vaccines through manipulation of IP-10.

3.2. Influenza. In line with our data on influenza previously discussed [22, 60, 90], Franco and colleagues studied a homogenous population of 199 healthy male volunteers with trivalent influenza vaccines [38]. They performed an integrative genomic analysis of the human immune response to influenza vaccination exploring association of genotype to gene expression, gene expression to antibody titre, and genotype to antibody titre. They identified 20 genes associated with a transcriptional response to vaccination, significant genotype effects on gene expression, and correlation between the transcriptional and antibody responses. The following loci were found to have the strongest evidence of genetic variation influencing the immune response to the vaccine: *TAP2*, *SNX29*, *FGD2*, *NAPSA*, *NAPSB*, *GM2A*, *C1orf85*, *JUP*, *FBLN5*, *CHST13*, *DIP2A*, *PAM*, *D4S234E*, *C3AR1*, *HERC2*, *LST1*, *LRRC37A4*, *OAS1*, *RPL14*, and *DYNLT1*. The results showed that variation at the level of genes involved in membrane trafficking and antigen processing significantly influenced the human response to influenza vaccination. Overall, this study identified crucial genes in the humoral response to vaccination suggesting such marks as logical biomarkers predicting the vaccination outcome. Such examples show how OMICs can be used to predict vaccination outcome in order to identify nonresponders.

4. Rationalising the Development of Adjuvants as Possible Strategy to Personalize Vaccines

In order to improve the efficacy of the vaccine, adjuvants can be added to antigens in order to stimulate in a selective way the different routes of innate and adaptive immunity [34]. The use of optimized adjuvanted formulations may overcome host characteristics that limit vaccine response and possibly favour personalized vaccine interventions. Adjuvants can be crucial to enhance immune response in low-responder individuals. Reference [91] explored the potentiality of TLR8 agonist as adjuvant for BCG and pneumococcal vaccination in newborns. TLR8 agonist-encapsulating polymersome triggered dendritic cell (DC) responses enhancing vaccine immunogenicity, thus suggesting TLR8 potential for early-life immunization against intracellular pathogens. Adjuvants may be delivered as components of microorganisms. For example, *Neisseria meningitidis* lipopolysaccharide (LPS) is a good example. Mehta et al. demonstrated that LPS exhibited differential adjuvant properties when formulated as native outer membrane vesicles (nOMVs). nOMVs enhanced immunogenicity suggesting that they may be an effective adjuvantation approach for future meningococcal protein vaccines. [92].

By combining OMIC technologies, data on vaccine immunity in groups with special vaccination needs, and adjuvant screening and development, we can increase our knowledge on mechanisms of vaccine hyporesponsiveness and how to overcome it. In the near future, these efforts will enable a new generation of adjuvants designed to stimulate, in a selective way, the different routes of innate and adaptive immunity.

5. Future Perspectives: From Vulnerable One-Fits-All Vaccines towards Invulnerable One-Fits-One Vaccines

Vaccines have greatly improved life expectancy by containing and in some cases eradicating diseases causing pathogens. Preventing vaccine disease has great impact not only on global health but also on the economy of the society 5by reducing hospitalization costs. Originally, one single vaccine was developed to target the global population accounting for limited cases of vaccine failure, even though data on vaccine failure was scarce especially in vulnerable populations (Figure 2). However, this approach is becoming less successful with the expansion of a population of immunocompromised individuals that fail to

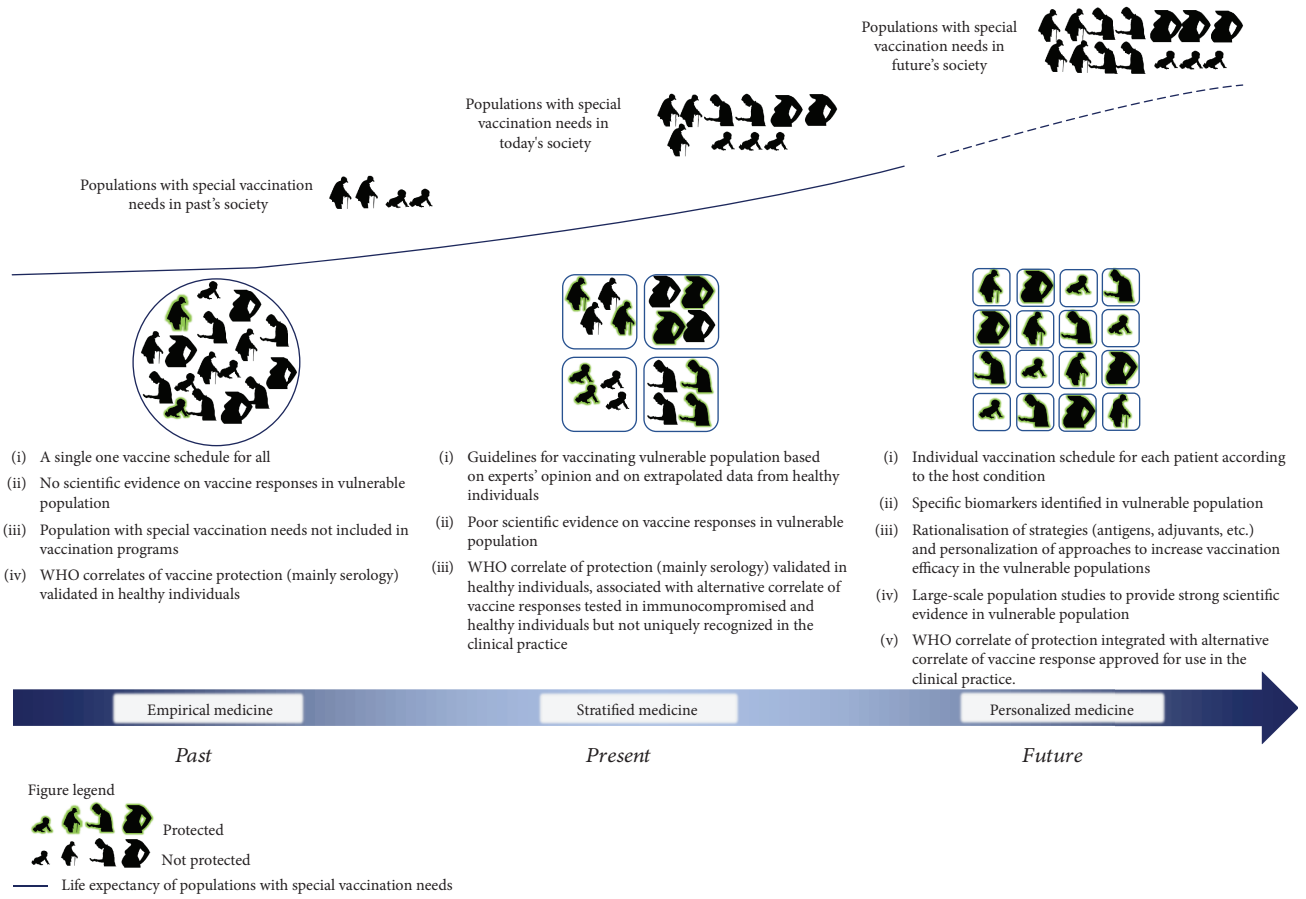

Figure 2: The figure shows changes in populations' composition with special vaccination needs over time. Traditionally, only elderly people and infants were considered vulnerable. During this time period, little scientific evidence regarding vaccine responses of different populations was available, and a single vaccination schedule was proposed for all (empirical medicine). Currently, an increasing number of people with special vaccination needs, such as immunocompromised patients and pregnant women, are considered in specific vaccine programs based on expert opinion and on extrapolated data from healthy individuals (stratified medicine). In the near future, the increased number and life expectancy of groups with special vaccination needs will lead to large-scale population studies. This approach will provide robust scientific evidence and new correlates of protection and safety. As a result, rationalisation of vaccine strategies (antigens, adjuvants, etc.) and personalization of approaches will increase vaccination efficacy and safety in these populations within a framework of personalized medicine.

respond to standard vaccination schedules and compositions. Therefore, vaccinology is in part focused on tailoring specific interventions for these vulnerable individuals in the near future.

At the moment, there are some indications on how to optimize vaccine strategies in vulnerable individuals. However, interventions are still decided upon evidence deriving from study of healthy individuals or upon expert's opinion. To improve on this current approach, current efforts aim to better characterize the vulnerable population, which can be integrated to generate predictive bioinformatic models for precise early identification of nonresponders. System biology studies are already revealing genetic and molecular "signatures" of protective immune response in healthy population [93]. In the near future, we trust that it will be possible to narrow such signatures to highly predictive assays of efficacy/effectiveness and identify precise correlates of protection in vulnerable groups (Figure 2).

Conflicts of Interest

The authors declare that no conflict of interest exists for the present work.

Authors' Contributions

Nicola Cotugno, Alessandra Ruggiero, and Veronica Santilli share first authorship.

Acknowledgments

We acknowledge Jennifer Faudella and Mattia Locatelli for administrative assistance. This work was supported by Associazione Volontari Bambino Gesù and Ricerca Corrente Ospedale Pediatrico Bambino Gesù 2017/2018. The *Precision Vaccines Program* is supported in part by NIH/NIAID Human Immunology Project Consortium U19 AI118608

and an internal award from the Boston Children's Hospital Department of Pediatrics.

References

[1] M. Doherty, R. Schmidt-Ott, J. I. Santos et al., "Vaccination of special populations: protecting the vulnerable," *Vaccine*, vol. 34, no. 52, pp. 6681–6690, 2016.

[2] D. O'Shea, L. A. Widmer, J. Stelling, and A. Egli, "Changing face of vaccination in immunocompromised hosts," *Current Infectious Disease Reports*, vol. 16, no. 9, p. 420, 2014.

[3] R. Butler, N. MacDonald, and SAGE Working Group on Vaccine Hesitancy, "Diagnosing the determinants of vaccine hesitancy in specific subgroups: The Guide to Tailoring Immunization Programmes (TIP)," *Vaccine*, vol. 33, no. 34, pp. 4176–4179, 2015.

[4] R. Baxter, J. Bartlett, B. Fireman, E. Lewis, and N. P. Klein, "Effectiveness of vaccination during pregnancy to prevent infant pertussis," *Pediatrics*, vol. 139, no. 5, article e20164091, 2017.

[5] CDC, "2016 Final Pertussis Surveillance Report," 2016, https://www.cdc.gov/pertussis/downloads/pertuss-surv-report-2016.pdf.

[6] S. A. Rasmussen, D. J. Jamieson, and T. M. Uyeki, "Effects of influenza on pregnant women and infants," *American Journal of Obstetrics and Gynecology*, vol. 207, no. 3, pp. S3–S8, 2012.

[7] E. Kuchar, K. Miskiewicz, and M. Karlikowska, "A review of guidance on immunization in persons with defective or deficient splenic function," *British Journal of Haematology*, vol. 171, no. 5, pp. 683–694, 2015.

[8] M. A. Friedman and K. Winthrop, "Vaccinations for rheumatoid arthritis," *Current Opinion in Rheumatology*, vol. 28, no. 3, pp. 330–336, 2016.

[9] L. G. Rubin, M. J. Levin, P. Ljungman et al., "2013 IDSA clinical practice guideline for vaccination of the immunocompromised host," *Clinical Infectious Diseases*, vol. 58, no. 3, pp. 309–318, 2014.

[10] M. J. Alcusky and J. Pawasauskas, "Adherence to guidelines for hepatitis B, pneumococcal, and influenza vaccination in patients with diabetes," *Clinical Diabetes*, vol. 33, no. 3, pp. 116–122, 2015.

[11] K. Chaudrey, M. Salvaggio, A. Ahmed, S. Mahmood, and T. Ali, "Updates in vaccination: recommendations for adult inflammatory bowel disease patients," *World Journal of Gastroenterology*, vol. 21, no. 11, pp. 3184–3196, 2015.

[12] A. Cagigi, N. Cotugno, C. Giaquinto et al., "Immune reconstitution and vaccination outcome in HIV-1 infected children," *Human Vaccines & Immunotherapeutics*, vol. 8, no. 12, pp. 1784–1794, 2012.

[13] A. Cagigi, S. Rinaldi, N. Cotugno et al., "Early highly active antiretroviral therapy enhances B-cell longevity: a 5 year follow up," *The Pediatric Infectious Disease Journal*, vol. 33, no. 5, pp. e126–e131, 2014.

[14] N. Cotugno, I. Douagi, P. Rossi, and P. Palma, "Suboptimal immune reconstitution in vertically HIV infected children: a view on how HIV replication and timing of HAART initiation can impact on T and B-cell compartment," *Clinical and Developmental Immunology*, vol. 2012, Article ID 805151, 11 pages, 2012.

[15] S. Rinaldi, A. Cagigi, V. Santilli et al., "B-sides serologic markers of immunogenicity in kidney transplanted patients: report from 2012-2013 flu vaccination experience," *Transplantation*, vol. 98, no. 3, pp. 259–266, 2014.

[16] N. Cotugno, A. Finocchi, A. Cagigi et al., "Defective B-cell proliferation and maintenance of long-term memory in patients with chronic granulomatous disease," *The Journal of Allergy and Clinical Immunology*, vol. 135, no. 3, pp. 753–761.e2, 2015.

[17] S. Rocca, V. Santilli, N. Cotugno et al., "Waning of vaccine-induced immunity to measles in kidney transplanted children," *Medicine*, vol. 95, no. 37, article e4738, 2016.

[18] J. C. Jacobson Vann and P. Szilagyi, "Patient reminder and recall systems to improve immunization rates," *Cochrane Database of Systematic Reviews*, no. 3, article CD003941, 2005.

[19] M. A. Miller and M. H. Rathore, "Immunization in special populations," *Advances in Pediatrics*, vol. 59, no. 1, pp. 95–136, 2012.

[20] A. Bamford, M. Hart, H. Lyall, D. Goldblatt, P. Kelleher, and B. Kampmann, "The influence of paediatric HIV infection on circulating B cell subsets and $CXCR5^+$ T helper cells," *Clinical & Experimental Immunology*, vol. 181, no. 1, pp. 110–117, 2015.

[21] A. Cagigi, S. Rinaldi, A. di Martino et al., "Premature immune senescence during HIV-1 vertical infection relates with response to influenza vaccination," *The Journal of Allergy and Clinical Immunology*, vol. 133, no. 2, pp. 592–594.e1, 2014.

[22] N. Cotugno, L. de Armas, S. Pallikkuth et al., "Perturbation of B cell gene expression persists in HIV-infected children despite effective antiretroviral therapy and predicts H1N1 response," *Frontiers in Immunology*, vol. 8, p. 1083, 2017.

[23] S. Pensieroso, A. Cagigi, P. Palma et al., "Timing of HAART defines the integrity of memory B cells and the longevity of humoral responses in HIV-1 vertically-infected children," *Proceedings of the National Academy of Sciences of the United States of America*, vol. 106, no. 19, pp. 7939–7944, 2009.

[24] K. Titanji, A. de Milito, A. Cagigi et al., "Loss of memory B cells impairs maintenance of long-term serologic memory during HIV-1 infection," *Blood*, vol. 108, no. 5, pp. 1580–1587, 2006.

[25] P. J. Ford, "Immunological techniques: ELISA, flow cytometry, and immunohistochemistry," *Methods in Molecular Biology*, vol. 666, pp. 327–343, 2010.

[26] R. Hanna-Wakim, L. L. Yasukawa, P. Sung, A. M. Arvin, and H. A. Gans, "Immune responses to mumps vaccine in adults who were vaccinated in childhood," *The Journal of Infectious Diseases*, vol. 197, no. 12, pp. 1669–1675, 2008.

[27] A. P. Ivanov and E. M. Dragunsky, "ELISA as a possible alternative to the neutralization test for evaluating the immune response to poliovirus vaccines," *Expert Review of Vaccines*, vol. 4, no. 2, pp. 167–172, 2005.

[28] N. R. Klatt, N. T. Funderburg, and J. M. Brenchley, "Microbial translocation, immune activation, and HIV disease," *Trends in Microbiology*, vol. 21, no. 1, pp. 6–13, 2013.

[29] F. Roodbari, M. H. Roustai, A. Mostafaie, H. Soleimanjdahi, R. S. Foroshani, and F. Sabahi, "Development of an enzyme-linked immunosorbent assay for immunoglobulin M antibodies against measles virus," *Clinical and Diagnostic Laboratory Immunology*, vol. 10, no. 3, pp. 439–442, 2003.

[30] A. Ruggiero, A. Cozzi-Lepri, A. Beloukas et al., "Factors associated with persistence of plasma HIV-1 RNA during long-term continuously suppressive firstline antiretroviral therapy," *Open Forum Infectious Diseases*, vol. 5, no. 2, 2018.

[31] A. Ruggiero, W. de Spiegelaere, A. Cozzi-Lepri et al., "During stably suppressive antiretroviral therapy integrated HIV-1

DNA load in peripheral blood is associated with the frequency of CD8 cells expressing HLA-DR/DP/DQ," *EBioMedicine*, vol. 2, no. 9, pp. 1153–1159, 2015.

[32] C. M. Wernette, C. E. Frasch, D. Madore et al., "Enzyme-linked immunosorbent assay for quantitation of human antibodies to pneumococcal polysaccharides," *Clinical and Diagnostic Laboratory Immunology*, vol. 10, no. 4, pp. 514–519, 2003.

[33] V. I. Zarnitsyna, A. H. Ellebedy, C. Davis, J. Jacob, R. Ahmed, and R. Antia, "Masking of antigenic epitopes by antibodies shapes the humoral immune response to influenza," *Philosophical Transactions of the Royal Society B: Biological Sciences*, vol. 370, no. 1676, article 20140248, 2015.

[34] F. Borriello, S. D. van Haren, and O. Levy, "First International Precision Vaccines Conference: multidisciplinary approaches to next-generation vaccines," *mSphere*, vol. 3, no. 4, 2018.

[35] D. Furman and M. M. Davis, "New approaches to understanding the immune response to vaccination and infection," *Vaccine*, vol. 33, no. 40, pp. 5271–5281, 2015.

[36] S. Li, N. Rouphael, S. Duraisingham et al., "Molecular signatures of antibody responses derived from a systems biology study of five human vaccines," *Nature Immunology*, vol. 15, no. 2, pp. 195–204, 2014.

[37] H. I. Nakaya, J. Wrammert, E. K. Lee et al., "Systems biology of vaccination for seasonal influenza in humans," *Nature Immunology*, vol. 12, no. 8, pp. 786–795, 2011.

[38] L. M. Franco, K. L. Bucasas, J. M. Wells et al., "Correction: integrative genomic analysis of the human immune response to influenza vaccination," *eLife*, vol. 5, 2016.

[39] J.-D. J. Han, "Understanding biological functions through molecular networks," *Cell Research*, vol. 18, no. 2, pp. 224–237, 2008.

[40] H. I. Nakaya, S. Li, and B. Pulendran, "Systems vaccinology: learning to compute the behavior of vaccine induced immunity," *Wiley Interdisciplinary Reviews: Systems Biology and Medicine*, vol. 4, no. 2, pp. 193–205, 2012.

[41] G. Obermoser, S. Presnell, K. Domico et al., "Systems scale interactive exploration reveals quantitative and qualitative differences in response to influenza and pneumococcal vaccines," *Immunity*, vol. 38, no. 4, pp. 831–844, 2013.

[42] T. D. Querec, R. S. Akondy, E. K. Lee et al., "Systems biology approach predicts immunogenicity of the yellow fever vaccine in humans," *Nature Immunology*, vol. 10, no. 1, pp. 116–125, 2009.

[43] J. S. Tsang, P. L. Schwartzberg, Y. Kotliarov et al., "Global analyses of human immune variation reveal baseline predictors of postvaccination responses," *Cell*, vol. 157, no. 2, pp. 499–513, 2014.

[44] B. R. Lanning and C. R. Vakoc, "Single-minded CRISPR screening," *Nature Biotechnology*, vol. 35, no. 4, pp. 339-340, 2017.

[45] A. H. Lee, C. P. Shannon, N. Amenyogbe et al., "Dynamic molecular changes during the first week of human life follow a robust developmental trajectory," *Nature Communications*, vol. 10, no. 1, p. 1092, 2019.

[46] N. Dhiman, D. I. Smith, and G. A. Poland, "Next-generation sequencing: a transformative tool for vaccinology," *Expert Review of Vaccines*, vol. 8, no. 8, pp. 963–967, 2009.

[47] D. M. Reif, B. A. McKinney, A. A. Motsinger et al., "Genetic basis for adverse events after smallpox vaccination," *The Journal of Infectious Diseases*, vol. 198, no. 1, pp. 16–22, 2008.

[48] G. A. Poland, I. G. Ovsyannikova, and R. M. Jacobson, "Vaccine immunogenetics: bedside to bench to population," *Vaccine*, vol. 26, no. 49, pp. 6183–6188, 2008.

[49] G. A. Poland, I. G. Ovsyannikova, R. M. Jacobson, and D. I. Smith, "Heterogeneity in vaccine immune response: the role of immunogenetics and the emerging field of vaccinomics," *Clinical Pharmacology & Therapeutics*, vol. 82, no. 6, pp. 653–664, 2007.

[50] B. J. DeKosky, G. C. Ippolito, R. P. Deschner et al., "High-throughput sequencing of the paired human immunoglobulin heavy and light chain repertoire," *Nature Biotechnology*, vol. 31, no. 2, pp. 166–169, 2013.

[51] Y. C. Tan, L. K. Blum, S. Kongpachith et al., "High-throughput sequencing of natively paired antibody chains provides evidence for original antigenic sin shaping the antibody response to influenza vaccination," *Clinical Immunology*, vol. 151, no. 1, pp. 55–65, 2014.

[52] B. Suárez-Álvarez, A. Baragaño Raneros, F. Ortega, and C. López-Larrea, "Epigenetic modulation of the immune function," *Epigenetics*, vol. 8, no. 7, pp. 694–702, 2014.

[53] B. Suarez-Alvarez, R. M. Rodriguez, M. F. Fraga, and C. Lopez-Larrea, "DNA methylation: a promising landscape for immune system-related diseases," *Trends in Genetics*, vol. 28, no. 10, pp. 506–514, 2012.

[54] J. Cole, P. Morris, M. J. Dickman, and D. H. Dockrell, "The therapeutic potential of epigenetic manipulation during infectious diseases," *Pharmacology & Therapeutics*, vol. 167, pp. 85–99, 2016.

[55] D. Verma, V. R. Parasa, J. Raffetseder et al., "Anti-mycobacterial activity correlates with altered DNA methylation pattern in immune cells from BCG-vaccinated subjects," *Scientific Reports*, vol. 7, no. 1, article 12305, 2017.

[56] M. T. Zimmermann, A. L. Oberg, D. E. Grill et al., "System-wide associations between DNA-methylation, gene expression, and humoral immune response to influenza vaccination," *PLoS One*, vol. 11, no. 3, article e0152034, 2016.

[57] C. J. Marsit, S. S. Brummel, D. Kacanek et al., "Infant peripheral blood repetitive element hypomethylation associated with antiretroviral therapy in utero," *Epigenetics*, vol. 10, no. 8, pp. 708–716, 2015.

[58] N. Cotugno, L. De Armas, S. Pallikkuth, P. Rossi, P. Palma, and S. Pahwa, "Paediatric HIV infection in the 'omics era: defining transcriptional signatures of viral control and vaccine responses," *Journal of Virus Eradication*, vol. 1, pp. 153–158, 2015.

[59] S. Pallikkuth and S. Pahwa, "Interleukin-21 and T follicular helper cells in HIV infection: research focus and future perspectives," *Immunologic Research*, vol. 57, no. 1-3, pp. 279–291, 2013.

[60] L. R. de Armas, N. Cotugno, S. Pallikkuth et al., "Induction of *IL21* in peripheral T follicular helper cells is an indicator of influenza vaccine response in a previously vaccinated HIV-infected pediatric cohort," *Journal of Immunology*, vol. 198, no. 5, pp. 1995–2005, 2017.

[61] N. D. Lambert, I. H. Haralambieva, R. B. Kennedy, I. G. Ovsyannikova, V. S. Pankratz, and G. A. Poland, "Polymorphisms in HLA-DPB1 are associated with differences in rubella virus–specific humoral immunity after vaccination," *The Journal of Infectious Diseases*, vol. 211, no. 6, pp. 898–905, 2015.

[62] L. Pan, L. Zhang, W. Zhang et al., "A genome-wide association study identifies polymorphisms in the HLA-DR region associated with non-response to hepatitis B vaccination in Chinese

Han populations," *Human Molecular Genetics*, vol. 23, no. 8, pp. 2210–2219, 2014.

[63] T. W. Wu, C. F. Chen, S. K. Lai, H. H. Lin, C. C. Chu, and L. Y. Wang, "SNP rs7770370 in *HLA-DPB1* loci as a major genetic determinant of response to booster hepatitis B vaccination: results of a genome-wide association study," *Journal of Gastroenterology and Hepatology*, vol. 30, no. 5, pp. 891–899, 2015.

[64] R. B. Kennedy, I. G. Ovsyannikova, V. S. Pankratz et al., "Genome-wide genetic associations with IFNγ response to smallpox vaccine," *Human Genetics*, vol. 131, no. 9, pp. 1433–1451, 2012.

[65] I. G. Ovsyannikova, R. B. Kennedy, M. O'Byrne, R. M. Jacobson, V. S. Pankratz, and G. A. Poland, "Genome-wide association study of antibody response to smallpox vaccine," *Vaccine*, vol. 30, no. 28, pp. 4182–4189, 2012.

[66] E. J. Homan and R. D. Bremel, "Are cases of mumps in vaccinated patients attributable to mismatches in both vaccine T-cell and B-cell epitopes?: an immunoinformatic analysis," *Human Vaccines & Immunotherapeutics*, vol. 10, no. 2, pp. 290–300, 2014.

[67] I. G. Ovsyannikova, N. Dhiman, I. H. Haralambieva et al., "Rubella vaccine-induced cellular immunity: evidence of associations with polymorphisms in the Toll-like, vitamin A and D receptors, and innate immune response genes," *Human Genetics*, vol. 127, no. 2, pp. 207–221, 2010.

[68] I. G. Ovsyannikova, I. H. Haralambieva, R. A. Vierkant, V. S. Pankratz, R. M. Jacobson, and G. A. Poland, "The role of polymorphisms in Toll-like receptors and their associated intracellular signaling genes in measles vaccine immunity," *Human Genetics*, vol. 130, no. 4, pp. 547–561, 2011.

[69] G. A. Poland, I. G. Ovsyannikova, and R. B. Kennedy, "Personalized vaccinology: a review," *Vaccine*, vol. 36, no. 36, pp. 5350–5357, 2018.

[70] A. L. Cunningham, H. Lal, M. Kovac et al., "Efficacy of the herpes zoster subunit vaccine in adults 70 years of age or older," *The New England Journal of Medicine*, vol. 375, no. 11, pp. 1019–1032, 2016.

[71] D. Furman, V. Jojic, B. Kidd et al., "Apoptosis and other immune biomarkers predict influenza vaccine responsiveness," *Molecular Systems Biology*, vol. 9, no. 1, p. 659, 2013.

[72] A. Giladi and I. Amit, "Single-cell genomics: a stepping stone for future immunology discoveries," *Cell*, vol. 172, no. 1-2, pp. 14–21, 2018.

[73] E. Papalexi and R. Satija, "Single-cell RNA sequencing to explore immune cell heterogeneity," *Nature Reviews Immunology*, vol. 18, no. 1, pp. 35–45, 2017.

[74] P. See, C. A. Dutertre, J. Chen et al., "Mapping the human DC lineage through the integration of high-dimensional techniques," *Science*, vol. 356, no. 6342, article eaag3009, 2017.

[75] E. Mass, I. Ballesteros, M. Farlik et al., "Specification of tissue-resident macrophages during organogenesis," *Science*, vol. 353, no. 6304, article aaf4238, 2016.

[76] A. Dixit, O. Parnas, B. Li et al., "Perturb-seq: dissecting molecular circuits with scalable single-cell RNA profiling of pooled genetic screens," *Cell*, vol. 167, no. 7, pp. 1853–1866.e17, 2016.

[77] G. X. Y. Zheng, J. M. Terry, P. Belgrader et al., "Massively parallel digital transcriptional profiling of single cells," *Nature Communications*, vol. 8, article 14049, 2017.

[78] B. Hwang, J. H. Lee, and D. Bang, "Single-cell RNA sequencing technologies and bioinformatics pipelines," *Experimental & Molecular Medicine*, vol. 50, no. 8, p. 96, 2018.

[79] M. Stoeckius, C. Hafemeister, W. Stephenson et al., "Simultaneous epitope and transcriptome measurement in single cells," *Nature Methods*, vol. 14, no. 9, pp. 865–868, 2017.

[80] R. H. M. Raeven, E. van Riet, H. D. Meiring, B. Metz, and G. F. A. Kersten, "Systems vaccinology and big data in the vaccine development chain," *Immunology*, vol. 156, no. 1, pp. 33–46, 2019.

[81] D. Hunt, R. Henderson, J. Shabanowitz et al., "Characterization of peptides bound to the class I MHC molecule HLA-A2.1 by mass spectrometry," *Science*, vol. 255, no. 5049, pp. 1261–1263, 1992.

[82] D. Donnarumma, A. Faleri, P. Costantino, R. Rappuoli, and N. Norais, "The role of structural proteomics in vaccine development: recent advances and future prospects," *Expert Review of Proteomics*, vol. 13, no. 1, pp. 55–68, 2016.

[83] A. C. Galassie and A. J. Link, "Proteomic contributions to our understanding of vaccine and immune responses," *PROTEOMICS - Clinical Applications*, vol. 9, no. 11-12, pp. 972–989, 2015.

[84] K. F. M. Opuni, M. Al-Majdoub, Y. Yefremova, R. F. El-Kased, C. Koy, and M. O. Glocker, "Mass spectrometric epitope mapping," *Mass Spectrometry Reviews*, vol. 37, no. 2, pp. 229–241, 2018.

[85] T. B. Bennike, M. D. Bellin, Y. Xuan et al., "A cost-effective high-throughput plasma and serum proteomics workflow enables mapping of the molecular impact of total pancreatectomy with islet autotransplantation," *Journal of Proteome Research*, vol. 17, no. 5, pp. 1983–1992, 2018.

[86] B. M. McClenathan, D. A. Stewart, C. E. Spooner et al., "Metabolites as biomarkers of adverse reactions following vaccination: a pilot study using nuclear magnetic resonance metabolomics," *Vaccine*, vol. 35, no. 9, pp. 1238–1245, 2017.

[87] HIPC-CHI Signatures Project Team and HIPC-I Consortium, "Multicohort analysis reveals baseline transcriptional predictors of influenza vaccination responses," *Science Immunology*, vol. 2, no. 14, 2017.

[88] H. I. Nakaya and B. Pulendran, "Vaccinology in the era of high-throughput biology," *Philosophical Transactions of the Royal Society B: Biological Sciences*, vol. 370, no. 1671, article 20140146, 2015.

[89] A. Rechtien, L. Richert, H. Lorenzo et al., "Systems vaccinology identifies an early innate immune signature as a correlate of antibody responses to the Ebola vaccine rVSV-ZEBOV," *Cell Reports*, vol. 20, no. 9, pp. 2251–2261, 2017.

[90] L. R. Armas, S. de Pallikkuth, L. Pan et al., "Single Cell Profiling Reveals PTEN Overexpression in Influenza-Specific B cells in Aging HIV-infected individuals on Anti-retroviral Therapy," *Scientific Reports*, vol. 9, no. 1, article 2482, 2019.

[91] D. J. Dowling, E. A. Scott, A. Scheid et al., "Toll-like receptor 8 agonist nanoparticles mimic immunomodulating effects of the live BCG vaccine and enhance neonatal innate and adaptive immune responses," *The Journal of Allergy and Clinical Immunology*, vol. 140, no. 5, pp. 1339–1350, 2017.

[92] O. H. Mehta, G. Norheim, J. C. Hoe et al., "Adjuvant effects elicited by novel oligosaccharide variants of detoxified meningococcal lipopolysaccharides on *Neisseria meningitidis* recombinant PorA protein: a comparison in mice," *PLoS One*, vol. 9, no. 12, article e115713, 2014.

[93] S. Li, N. L. Sullivan, N. Rouphael et al., "Metabolic phenotypes of response to vaccination in humans," *Cell*, vol. 169, no. 5, pp. 862–877.e17, 2017.

Hindawi
Journal of Immunology Research
Volume 2019, Article ID 9804584, 13 pages
https://doi.org/10.1155/2019/9804584

Research Article

Reverse Immunology Approach to Define a New HIV-gp41-Neutralizing Epitope

Karim Dorgham,[1] Nicolas Pietrancosta,[2] Amel Affoune,[1] Olivier Lucar,[1] Tahar Bouceba,[3] Solenne Chardonnet,[4] Cedric Pionneau,[4] Christophe Piesse,[3] Delphine Sterlin,[1,5] Pablo Guardado-Calvo,[6] Philippe Karoyan,[7] Patrice Debré,[1,5] Guy Gorochov,[1,5] and Vincent Vieillard[1]

[1]*Sorbonne Université, INSERM, CNRS, Centre d'Immunologie et des Maladies Infectieuses-Paris (CIMI-Paris), F-75013 Paris, France*
[2]*Université Sorbonne Paris Cité, CNRS, Laboratoire de Chimie et Biochimie Pharmacologiques et Toxicologiques, F-75006 Paris, France*
[3]*Sorbonne Université, CNRS, Institut de Biologie Paris-Seine (IBPS), Service de Synthèse Peptidique et d'Interactions Moléculaires, F-75005 Paris, France*
[4]*Sorbonne Université, INSERM, Plateforme Post-génomique de la Pitié Salpêtrière (P3S), F-75013 Paris, France*
[5]*Assistance Publique-Hôpitaux de Paris (AP-HP), Groupement Hospitalier Pitié Salpêtrière, Département d'Immunologie, F-75013 Paris, France*
[6]*Institut Pasteur, Unité de Virologie Structurale (VIST), F-75015 Paris, France*
[7]*Sorbonne Université, Ecole Normale Supérieure, PSL University, CNRS, Laboratoire des Biomolécules, LBM, F-75005 Paris, France*

Correspondence should be addressed to Karim Dorgham; karim.dorgham@inserm.fr

Received 2 November 2018; Revised 26 December 2018; Accepted 10 January 2019; Published 24 March 2019

Guest Editor: Greg Kirchenbaum

The design of immunogens susceptible to elicit potent and broadly neutralizing antibodies against the human immunodeficiency virus type 1 (HIV-1) remains a veritable challenge in the course of vaccine development. Viral envelope proteins adopt different conformational states during the entry process, allowing the presentation of transient neutralizing epitopes. We focused on the highly conserved 3S motif of gp41, which is exposed to the surface envelope in its trimeric prefusion state. Vaccination with a W614A-modified 3S peptide induces in animals neutralizing anti-HIV-1 antibodies among which we selected clone F8. We used F8 as bait to select for W614A-3S phage-peptide mimics. Binding and molecular docking studies revealed that F8 interacts similarly with W614A-3S and a Mim_F8-1 mimotope, despite their lack of sequence homology, suggesting structural mimicry. Finally, vaccination of mice with the purified Mim_F8-1 phage elicited HIV-1-neutralizing antibodies that bound to the cognate W614A-3S motif. Collectively, our findings provide new insights into the molecular design of immunogens to elicit antibodies with neutralizing properties.

1. Introduction

Despite the success of antiretroviral therapy, which has turned human immunodeficiency virus type 1 (HIV-1) infection into a chronic disease and has reduced the number of new infections worldwide, a vaccine against HIV-1 is still urgently needed. Due to its high mutability (1–10 mutations/genome/replication cycle), HIV-1 has evolved a unique arsenal of tricks to evade the immune system. Other mechanisms of immune evasion by HIV-1 are mediated by the nature of the native envelope (Env) spikes on the viral surface that mediate infection through receptor binding and fusion and that are the major targets for virus-neutralizing antibodies (Abs) [1]. Finally, the trimeric Env spike does not have a fixed conformation but is characterized by a tendency to breathe, resulting in tremendous flexibility with

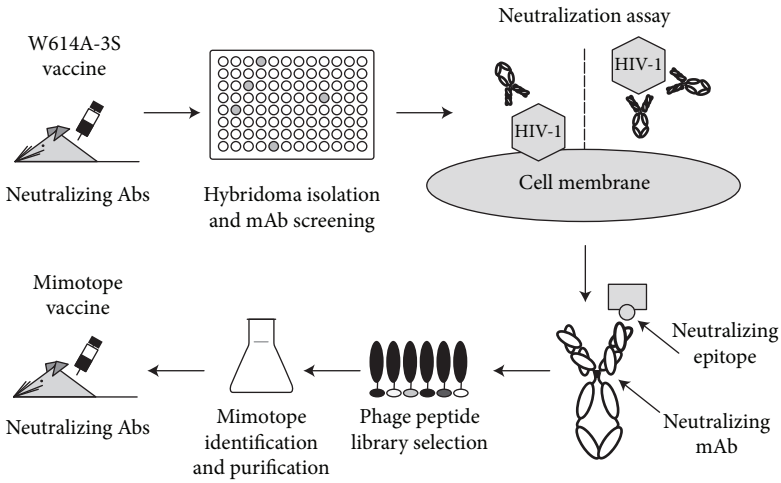

Figure 1: Reverse immunology applied to an epitope-based vaccination strategy. Mice immunized with the W614A-3S peptide were used to generate mAbs. Clones that reacted with the vaccine peptide were studied for their HIV-1-neutralizing properties. The neutralizing F8 mAb was then used to screen a phage peptide library for mimotopes of the F8 epitope. Finally, vaccination of mice with the selected mimotope induced neutralizing Abs in the serum.

a native closed form, shifting toward more open conformations. In agreement with this model, while breathing, some neutralizing epitopes that are not accessible in the native state become available in the relaxed conformation (e.g., the CD4 binding site epitope recognized by the IgG1b12), whereas other broadly neutralizing Abs, such as VRC01, lock down the spike in its native closed conformation suppressing further breathing [2].

Consistent with the difficulties encountered in attempts to induce broadly neutralizing Abs against HIV-1 in vaccination studies, most patients generate some level of neutralizing Abs, and after years of infection, these can mature into HIV-1 broadly neutralizing Abs in 10 to 25% of HIV-infected patients. These Abs are able to target more conserved regions of the Env and thus neutralize about 90% of circulating HIV-1 strains [3–9]. Several animal and human studies have highlighted their putative role in protective immunity after passive transfer, in which a major but transient effect on the viral load was observed, due to the rapid implementation of viral escape mechanisms [10–18].

Neutralizing Abs map to four major Env antigenic sites: the CD4 binding site, the V1-V2 glycopeptidic loop, glycan V3 structures, and some gp41 motifs. Although gp41 is more conserved than the gp120 subunit, neutralizing Abs targeting gp41 are rarely detected in patients [19]. Only peculiar conformations of gp41 might be prone to induce broadly neutralizing Abs [20–25]. In addition to the highly conserved gp41 membrane-proximal external region (MPER) [26] and the gp120/gp41 interface [27], a conserved and protective motif, called 3S, localized between the N-terminal heptad repeats (HR) 1 and HR2 has been described [28, 29]. Vaccination of SHIV-challenged macaques with the 3S motif leads to immune protection and restores immune homeostasis, although anti-3S Abs do not neutralize the virus [30, 31]. An alanine-scanning assay identified the W614 position into the 3S motif as crucial for the virus entry although the W614A-3S mutant peptide is nevertheless able to elicit cross-clade-neutralizing Abs (nAbs) in vaccinated mice [32] as well as in rabbit and macaque models (Vieillard et al., unpublished data). Accordingly, amino-acid changes into gp41 MPER induce viral neutralization sensitivity [33]. Interestingly, among HIV-1-infected patients, natural anti-W614A-3S Abs were detected in less than 5% of progressors [32], but up to 25% of long-term nonprogressors (LTNP) [34]. The neutralizing capacity of W614A-3S Abs was inversely correlated with viral load and viral DNA and was associated with the preservation of high CD4+ T-cell counts and T-cell responses in LTNP patients [34].

We postulated that W614A-3S-specific nAbs could play a role in the maintenance of the non-progressor status and that they could be used to select for anti-HIV immunogens with improved activity. Analysis of HIV-1-Env trimer structures [35, 36] highlighted the 3S area being part of a flexible loop, which ensures the junction between strand $\beta 27$ ($Leu602_{gp41}$-$Thr606_{gp41}$) and helix $\alpha 8$ ($Leu619_{gp41}$-$Trp623_{gp41}$) in the gp41-prefusion structure and between HR1 and HR2 helices in the postfusion state of gp41. Rearrangements between each conformational state require Cα-movements from either side of the linker in which the 3S motif is anchored. No structural data are presently available regarding the conformation of the neutralizing epitope recognized by anti-W614A-3S Abs, and we can only infer that this epitope could also be conformation dependent. The goal of this study was therefore to better characterize the molecular capability of the W614A-3S epitope using molecular modeling and reverse immunology approaches.

In this work, a murine anti-W614A-3S mAb with HIV-1-neutralizing properties was isolated and then used to screen a phage peptide library for W614A-3S mimotopes. Phage-mimotope vaccination led to the generation of antibodies that bind the cognate W614A-3S vaccine associated with neutralizing activity in mice (Figure 1).

2. Materials and Methods

2.1. Mouse Vaccination. All experiments were undertaken by experienced and authorized staff, following health and safety procedures established according to French legislation governing the use of animals in experiments. Mice were immunized with the W614A-3S peptide conjugated to KLH (KLH-W614A-3S) with MBS (m-maleimidobenzoyl-*N*-hydroxysuccinimidyl ester), and serum IgG titers were evaluated by ELISA, as previously reported [32]. Fusion and production of mAbs were performed by the HT-MAb platform (Sysdiag-UMR3145, Montpellier, France). Briefly, mice received a final i.v. boost injection two weeks after the previous immunization. Four days later, the animals were euthanized and B cells obtained from the spleen were fused with the SP2/0 cell line (ratio 5 : 1) using polyethylene glycol. Hybridoma cells were selected in HAT media supplement (Sigma), and culture supernatants were screened by indirect ELISA with BSA-W614A-3S as coating molecule. Finally, selected hybridomas were subcloned five times to obtain stable Ig-producing cells and maintained in culture in DMEM enriched with L-glutamine, pyruvate, and 4.5 g/L glucose, supplemented with 100 μg/mL gentamicin and with 10% inactivated fetal bovine serum. IgGs were purified from culture supernatant by protein G chromatography.

Immunization of mice with the Mim_F8-1 phagotope was realized by CovalAb (Villeurbanne, France). Six- to eight-week-old BalB/c mice were immunized four times at two weekly intervals subcutaneously with 10^{10} cfu of the inactivated Mim_F8-1 phagotope according to the protocol described in Supplemental Figure 1.

2.2. Enzyme-Linked Immunosorbent Assay (ELISA). Ninety-six-well Maxisorp immunoplates (NUNC) were coated overnight at 4°C with 0.2 μg/well of peptide conjugated with the carrier protein in PBS. After three washes in PBS, plates were incubated for 1 hour at 37°C with 4% PBS low-fat milk (PBSM). Dilutions of mAbs or serum from immunized mice were blocked with 1 vol. of PBSM and incubated in plates for 1 hour at 37°C. Plates were then washed three times with PBS 0.05% Tween 20 (PBST) followed by three more washings with PBS and wells incubated for 1 hour at 37°C with 100 μL of HRP-conjugated anti-mouse IgG (Sigma, #A9917).

2.3. Neutralization Assays. Neutralization of the purified Abs was tested at various concentrations, as described [32, 34] using the TZM-bl reporter cell line. At 48 hours after infection, luciferase activity in TZM-bl lysates was measured using the Bright-Glo™ Luciferase Assay Substrate (Promega). A cutoff value of 2.5 times background was applied to determine positive values. Total IgG from mouse sera were purified with the Melon Gel IgG Purification System (Thermo Scientific), and concentrations were determined by ELISA. Depletion of anti-W614A-3S Abs was done by incubating purified IgG with immobilized CRM-W614A-3S (10 μg/mL) for 2 hours. The IC_{50} values were calculated by nonlinear regression analysis using Prism 6 (GraphPad Software).

2.4. Biopanning of the Phage-Peptide Library. The phage-peptide library [37] was kindly provided by Igor Fisch and Greg Winter (MRC, Centre for Protein Engineering, Cambridge, UK). The phage library was selected using 50 μg of mAb, as previously reported [38]. After the third round of biopanning, isolated clones were picked randomly from LB agar plates and used in PCR for DNA insert amplification and sequencing. In parallel, colonies were grown overnight at 30°C in 200 μL of 2YT/tetracycline and the supernatant used directly for phage ELISA.

The selected F8 phagotope was PEG purified from 1 L culture supernatant, resuspended into 10 mL water, and filtered through a 0.45 μm filter. The suspension was then buffer exchanged with PBS by ultrafiltration using Amicon Ultra 2 mL centrifugal filters MWCO 100 kDa and concentrated 10 times. Phages were heat inactivated at 72°C for 4 hours and frozen in aliquot to be used subsequently for mice immunization.

2.5. Molecular Modeling. The crystal structure of the HIV-1 BG505 SOSIP.664 Env trimer ectodomain, comprising atomic-level definition of prefusion gp120 and gp41, in complex with human antibodies PGT122 and 35O22 was used as the template (pdb code 4TVP) [35]. The homology model of antibodies was built using the model full-length antibody protocol of discovery studio 4.5. The protocol requires the sequences for the light and heavy chains of the antibody to be modeled, which are duplicated to generate the sequence for the full-length antibody. The Immunoglobulin G based on templates for IgG (pdb code: 1igy) was used for the homology model [39]. The alignment was then used to build homology models using Modeler. The best model of the 50 generated was selected based on its Modeler PDF energy and DOPE Scores.

The 3D structures of mimotopes were designed using the de novo peptide structure prediction server PEP-FOLD [40]. The five most probable 3D structures were retained for docking experiments. Mimotopes were docked into the homology model using the ZDOCK protocol using discovery studio interface. ZDOCK is a rigid-body protein-protein docking algorithm based on the fast Fourier transform correlation technique that is used to explore the rotational and translational space of a protein-protein system. The poses were refined with RDOCK, a CHARMm-based energy minimization procedure for refining and scoring docked poses using energy scoring functions [41]. The best poses were selected to analyze the binding pattern of peptides.

3. Results

3.1. Molecular and Functional Characterization of Anti-W614A-3S mAbs. Serum from mice immunized with KLH-W614A-3S peptide showed a significant neutralizing activity on cross-clade HIV-1 strains, as reported in reference [32]. Monoclonal antibodies (mAbs) isolated from these mice were studied in this work. Two fusion experiments were realized, and 1152 supernatants of hybridoma were screened by indirect enzyme-linked immunosorbent assay (ELISA). Twelve wells showed a specific binding on the W614A-3S conjugated to BSA. After stabilization by repeated cell cloning, five hybridomas (B8, C9, F8, G6, and G9) were

analyzed to characterize the secreted mAbs at the molecular level. All mAbs were of the IgG1 isotype, and the sequence analysis of their variable domains revealed that the F8 and C9 clones secreted the same mAb (hereafter called F8), whereas B8 and G9 clones secreted identical mAbs (hereafter called B8), leading to the identification of three different mAbs (B8, F8, and G6; Supplemental Table I). It is of note that the B8 mAb shares the same variable light chain with the G6 mAb, using the IGKV1-117 and IGKJ5 genes to form the junction, while the Vk domain of the F8 mAb used GKV1-117 and IGKJ2 genes. Mass spectrometry analysis of the F8 mAb validated the sequence of the light chain (Supplemental Figure 2). Furthermore, the variable domains of the heavy chains of the three mAbs were very different in terms of the V/D/J gene family used in the junction and regarding the amino acid sequences of the CDR1, 2, and 3 (Supplemental Table I). The F8 CDR3 loop is consisting of only five residues (YGYGY), according to the IMGT unique numbering for V domain [42].

The three mAbs (B8, F8, and G6) were then tested for their HIV-1-neutralizing potential against tier 1 (NL4.3) and tier 2 (JR-CSF and YU-2) HIV-1 clade B strains (Figures 2(a)–2(c)). F8 only could neutralize NL4.3, JR-CSF, and YU-2 strains, with IC_{50} values of 0.4, 2.4, and 9.7 μg/mL, respectively. F8 was also capable to neutralize ADA, TRO.11, QHO692.44 HIV-1 clade B, and ZM249M.Pl1 HIV-1 clade C strains, with IC_{50} values of 1.7, 2.3, 3.1, and 4.7 μg/mL, respectively (Table 1). As a control, a chimeric Ab, connecting the variable murine domains of the F8 mAb with the constant domains of a human IgG1, was constructed (Supplemental methods and supplemental Figure 3.A). The F8 chimeric Ab preserved the neutralizing activity of the parent murine mAb (Supplemental Figure 3.B), thus demonstrating that the identified variable domains mediate neutralization, regardless of the context provided by constant Ig domains.

The different neutralizing properties of the mAbs suggest that they recognize different epitopes presented by the immunogenic peptide used for immunization. Thus, their binding capacities were further studied by ELISA. The G6 mAb interacts with both the unconjugated wild-type 3S and W614A-3S peptides, but not with the randomly scrambled control sequence peptide (3S-scr), while neither F8 nor B8 mAbs bind these three peptides (Figure 2(d)). As expected, all mAbs bind to the BSA-coupled W614A-3S peptide but not the control BSA-3S-scr peptide. It is of note that they also interact with the BSA-3S peptide (Figure 2(e)). These results indicate that G6 mAb binds a linear epitope, whereas B8 and F8 mAbs both recognize a conformational epitope. To investigate the contribution of the carrier protein in the peptide presentation, BSA was exchanged with KLH or CRM197, a detoxified form of diphtheria toxin. Both the B8 and F8 mAbs recognize W614A-3S peptide independently of the carrier protein, as shown in Figure 2(f). Interestingly, none of the isolated mAbs interacted with soluble recombinant gp160MN/LAI-2 [43] in ELISA (data not shown), suggesting that neither the linear nor the conformational epitopes, recognized by the W614A-3S mAbs, are accessible into the monomeric gp160.

Whereas immunization of mice with the wild-type 3S peptide of gp41 did not induce neutralizing Abs [30, 31], generation of the F8 mAb after vaccination with the W614A-3S peptide suggests that the neutralizing epitope is associated with the W614A-3S point mutation introduced in the 3S motif. Comparative kinetics and apparent affinity measurements of F8 mAb binding to 3S or W614A-3S were performed by surface plasmon resonance (SPR). While apparent rates of association were similar, the calculated affinity constant (KD) was higher for BSA-3S than for BSA-W614A-3S because of a more rapid F8 mAb dissociation rate from the former peptide (Supplemental Figure 4).

3.2. Characterization of the Neutralizing Epitope by Reverse Immunology. Phage display technology has proven to be an effective and practical technique for the identification of linear or conformational epitopes and has been widely used for mapping HIV-1 epitopes [44]. To characterize the neutralizing conformational epitope of the immunogenic W614A-3S peptide, a phage peptide library was screened with the F8 mAb. After four rounds of biopanning, DNA sequencing of the selected clones led to the identification of a single sequence (denoted Mim_F8-1). This major clone was also found in the third round of selection with 25% enrichment (6 of 24 clones). A new biopanning experiment was performed, using less drastic washing conditions, to select other mimotopes. Finally, after three rounds of selection, three supplemental mimotopes could be isolated and a preferentially selected clone (denoted Mim_F8-2) was found to have a 42% enrichment level (10 of 24 clones). It is noteworthy that the clone Mim_F8-1 was not recovered in the second biopanning experiment; however, its sequence shared a common five-residue motif "ECAGC" with that of Mim_F8-2 (Figure 3(a)), suggesting identification of the F8 mAb epitope, regardless of sequence homology with BSA-W614A-3S (supplemental Table II). Figure 3(b) shows that all selected mimotopes bound the F8 mAb, but not the non-neutralizing G6 and B8 mAbs. To evaluate the capacity to compete with W614A-3S for binding to the F8 mAb, the Mim_F8-1 phagotope (i.e., phage-bearing mimotope) was incubated with plate-immobilized Abs in the presence of various concentrations of the BSA-coupled W614A-3S peptide and phage binding was measured by ELISA. Figure 3(c) shows that the phagotope interaction with F8 is inhibited in a dose-dependent manner with BSA-W614A-3S but not with BSA-3S-scr (used as negative control), suggesting competition between the phagotope and BSA-W614A-3S for binding to the F8 mAb. The F8 mAb did not interact with the synthetic-free peptides corresponding to the sequence mimotopes, neither in direct ELISA nor in competition assay with the phagotopes (data not shown). Altogether, these results could suggest that peptide mimotopes adopt a constrained conformation at the phage surface, allowing binding to the F8 mAb.

In the context of the phage, the C-terminal extremity of the mimotope is fused to the pIII coat protein, leaving its N-terminal extremity free to move. A Mim_F8-1 peptide was therefore synthesized using a biotinylated resin to

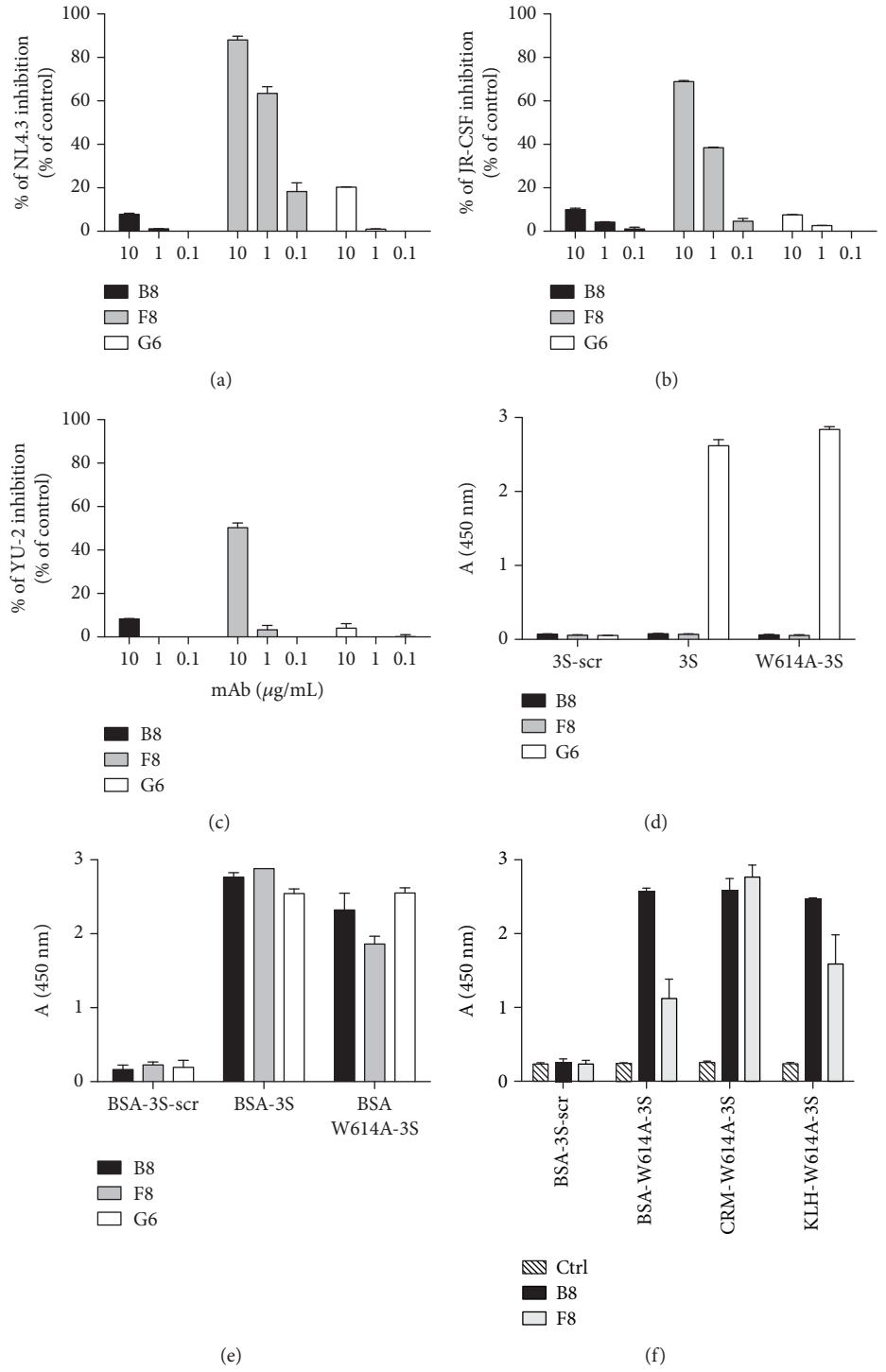

Figure 2: Functional characterization of the anti-W614A mAbs. Neutralization of HIV infection with anti-W614A-3S mAbs is shown in (a–c). Dose response of neutralizing activity was performed with a standard TZM-bl assay against tier 1 (NL4.3) and tier 2 (JR-CSF, YU-2) HIV-1 clade B strains, with the purified anti-W614A-3S mAbs. Data are presented as percent infection compared to the maximum signal (100%) into the positive control (infected cells in medium without mAb). Experiments were run in duplicates and bars indicate SD. Characterization of the binding properties of the anti-W614A-3S mAbs is shown in (d–f). Purified anti-W614A-3S mAbs were tested by ELISA at 1 μg/mL on immobilized free peptides (d) and immobilized BSA-conjugated peptides (e). The 3S-scrambled peptide (3S-scr) functioned as negative control for those experiments. (f) illustrates reactivity of the B8 and F8 mAbs in ELISA with immobilized W614A-3S conjugated to different carrier proteins (BSA: bovine serum albumin, CRM: CRM197, and KLH: keyhole limpet hemocyanin). The mouse IgG1 isotype mAb (Ctrl) functioned as negative control (hashed bars). Binding activity of mAbs is expressed as mean OD at 450 nm of duplicate wells, and bars indicate SD. These data are representative of three independent experiments. B8 activity and F8 activity are indicated as black and gray columns, respectively, in all panels. G6 activity is indicated as white columns in (a–e).

Table 1: Neutralizing activity of F8 mAb on tier 1 and tier 2 HIV-1 clade B and clade C strains.

Virus	TZM-bl assay						
	NL4.3	JRCSF	YU-2	ADA	TRO.11	QHO692.44	ZM249M.Pl1
Tier	1	2	2	2	2	2	2
Clade	B	B	B	B	B	B	C
IC_{50} (μg/mL)	0.4	2.4	9.7	1.7	2.3	3.1	4.7

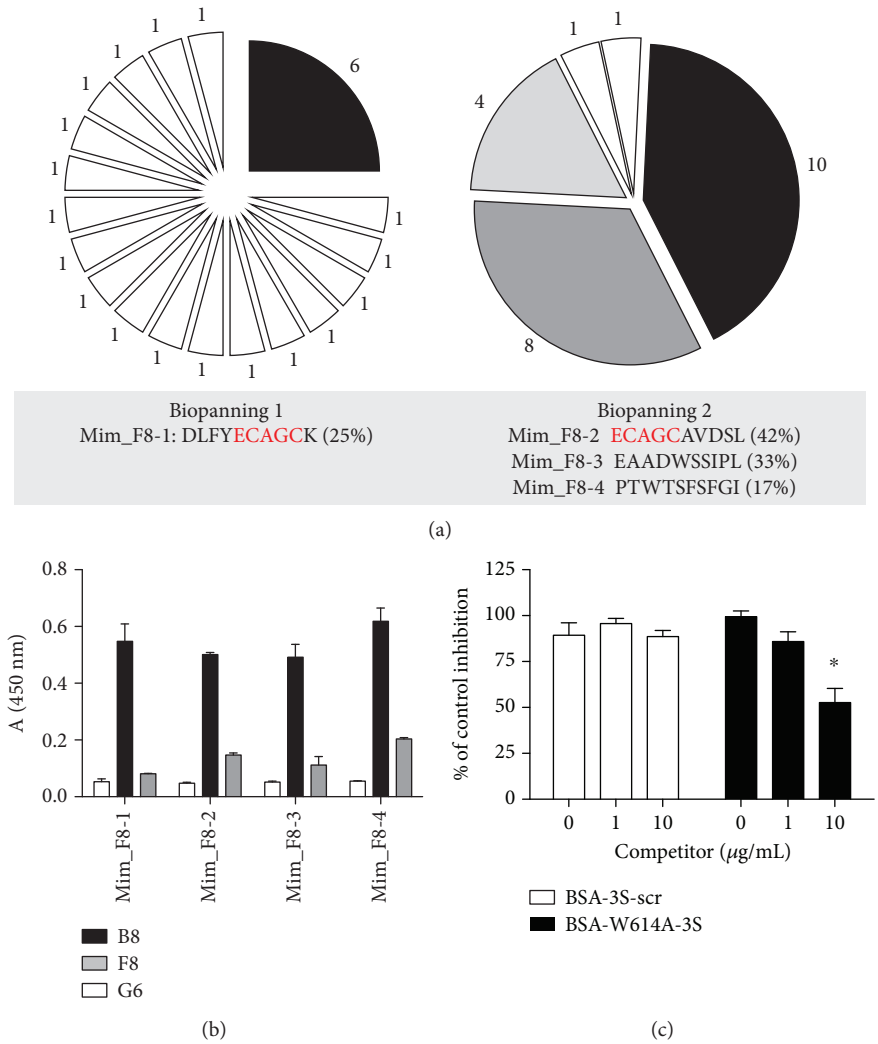

Figure 3: Phage-mimotope selection and reactivity of the anti-W614A-3S mAbs. A phage library of decapeptides was screened with the F8 mAb (a). After three rounds of selection in the first biopanning, the mim_F8-1 phagotope represented 25% of the selected clones. In a second experiment of biopanning, three phagotopes were identified at the third round of selection. Mim_F8-2 represented 42% of the selected clones and shared a five-residue motif with those of Mim_F8-1. (b) Binding properties of the selected phagotopes were tested by ELISA on immobilized anti-W614A-3S mAbs. Binding activity is expressed as mean OD at 450 nm of duplicate wells and bars indicate SD. These data are representative of three independent experiments. (c) Competitive binding ELISA of Mim_F8-1 on the immobilized F8 mAb with indicated concentrations of BSA-W614A-3S (black bars). BSA-3S-scr functioned as negative control (white bars). Results are expressed as percentage of binding of the Mim_F8-1 without competitor (100%). Values are the means of two different experiments with two replicated measurements, and bars indicate SEM. $^*p < 0.05$, according to Mann–Whitney U test.

produce a peptide biotinylated exclusively at the carboxy terminus in an attempt to mimic peptide phage display. Furthermore, a disulfide bridge was created by oxidation of the two Mim_F8-1 cysteines, to investigate the role of a potential loop between these amino acids. A study of interactions by biolayer interferometry (BLI), using a streptavidin biosensor to immobilize the biotinylated Mim_F8-1 peptide, showed that the F8 mAb was unable to bind either the linear or the cyclic Mim_F8-1 peptides, as compared to a control mAb (Supplemental methods and data not shown).

F8 VL domain residues implicated in interactions

```
W614A-3S   VLMTQTPLSLPVSLGDKVSISCRSSQSIVHSDGNIYLEWSLQKPGQSPKLLIY
Mim_F8-1   VLMTQTPLSLPVSLGDKVSISCRSSQSIVHSDGNIYLEWSLQKPGQSPKLLIY
Mim_F8-2   VLMTQTPLSLPVSLGDKVSISCRSSQSIVHSDGNIYLEWSLQKPGQSPKLLIY
3S         VLMTQTPLSLPVSLGDKVSISCRSSQSIVHSDGNIYLEWSLQKPGQSPKLLIY
IGKV1-117  ..............QA..............N..T....Y.............

W614A-3S   KVSNRFFGVPDRFSGSGSGTDFTLKISRVEAEDLGVYYCFQGSHFPYTFGGG
Mim_F8-1   KVSNRFFGVPDRFSGSGSGTDFTLKISRVEAEDLGVYYCFQGSHFPYTFGGG
Mim_F8-2   KVSNRFFGVPDRFSGSGSGTDFTLKISRVEAEDLGVYYCFQGSHFPYTFGGG
3S         KVSNRFFGVPDRFSGSGSGTDFTLKISRVEAEDLGVYYCFQGSHFPYTFGGG
IGKV1-117  S.......................................V..
```

F8 VH domain residues implicated in interactions

```
W614A-3S   EVQLEESGPGLVKPSQSLSLTCSVTGFSI TSYFWNWIRQFPGNKLEWMGHI
Mim_F8-1   EVQLEESGPGLVKPSQSLSLTCSVTGFSI TSYFWNWIRQFPGNKLEWMGHI
Mim_F8-2   EVQLEESGPGLVKPSQSLSLTCSVTGFSI TSYFWNWIRQFPGNKLEWMGHI
3S         EVQLEESGPGLVKPSQSLSLTCSVTGFSI TSYFWNWIRQFPGNKLEWMGHI
IGHV3-6    D...Q.....................Y..TSG.Y.................Y.

W614A-3S   TYDGRKKYNPSLKNRLSITRDTSKNQFFLNLNSVTAEDTATYYCYGYGYWGQG
Mim_F8-1   TYDGRKKYNPSLKNRLSITRDTSKNQFFLNLNSVTAEDTATYYCYGYGYWGQG
Mim_F8-2   TYDGRKKYNPSLKNRLSITRDTSKNQFFLNLNSVTAEDTATYYCYGYGYWGQG
3S         TYDGRKKYNPSLKNRLSITRDTSKNQFFLNLNSVTAEDTATYYCYGYGYWGQG
IGHV3-6    S...SNN........I.............K.....T........AR
```

Figure 4: Molecular interaction between the F8 mAb and peptides. The target peptides are indicated in the first column. The amino acid sequences of both the VL and the VH domains are indicated in the second column. CDRs are underlined and indicated in bold letters while residues involved in the interaction with the peptide are indicated in red. The closest F8 germline-encoded V regions, identified in Supplemental Table I, are indicated in blue.

Finally, to investigate the impact of multivalent presentation of the mimotope for the binding to the F8 mAb, complexes between biotinylated Mim_F8-1 peptide and streptavidin beads were constructed. Monitoring of interactions by BLI using an anti-mouse IgG Fc capture biosensor to immobilize the F8 mAb did not allow detection of specific binding with those complexes of linear or cyclic Mim_F8-1 peptides (data not shown). These results suggest that only pIII-fused mimotopes will be able to bind the F8 mAb and to induce the cognate antibody *in vivo*.

3.3. Validation of the Neutralizing Epitope by Mice Immunization. Regarding the F8 mAb, 24 residues are mutated from the closest germline-encoded V regions, including 3 and 10 amino acids into the CDRs of the VL and VH domains, respectively (Figure 4). The molecular docking approach was used to compare the structural interactions of the different peptides with the F8 mAb. The data indicate that 13 and 8 residues from the VL and VH domains, respectively, interact with W614A-3S. The Mim_F8-1 mimotope, as well as the W614A-3S peptide, interacts with all CDRs of both the VH and VL domains (Figure 5). As shown in Figure 4, the predicted interactions of these peptides with the F8 mAb are very similar and involve six residues closely juxtaposed in the light chain CDR3 (CDR L3) and three and two residues of the CDR H3 for Mim_F8-1 and W614A-3S, respectively. From the opposite point of view, F8 CDR residues are predicted to interact mainly around the alanine residue, corresponding to the W614A mutation into the 3S derivative peptide and around the ECAGC motif of Mim_F8-1, as shown in Figure 5. The predicted interactions involved in antigen binding of Mim_F8-2 with F8 are slightly different, with a non-substantial reduced number of interactions (Figures 4 and 5). In conclusion, the three peptides are predicted to be anchored in the binding site of the F8 mAb as illustrated by the 3D model shown in Figure 5(b).

It is of note that the docking prediction of the 3S peptide, based on the BG505 SOSIP structure, is very different from that of the W614A-3S peptide, with the engagement of only few residues of four CDRs of the F8 mAb (Figures 4 and 5). Overall, *in silico* analysis suggests that the W614A mutation in the 3S motif generates a conformational change, giving its shape to the epitope and allowing a better interaction with F8 mAb.

Finally, to obtain proof of concept of its immunogenic potential, four mice were immunized with Mim_F8-1 phagotope (Supplemental Figure 1). As expected, all showed robust amounts of anti-phage Abs at day 53, with end-point titers reaching a 10^5 dilution factor (Figure 6(a)). Interestingly, anti-W614A-3S IgG were also detected by ELISA at days 39

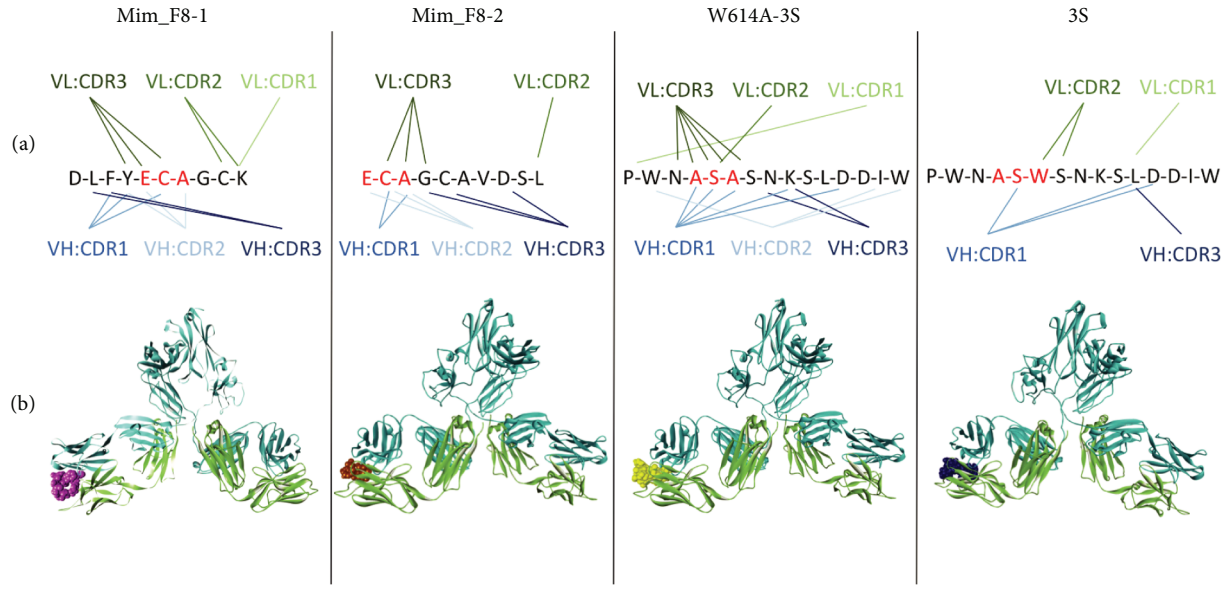

FIGURE 5: *In silico* docking studies of the 3S derivatives with F8 mAb. Predominant molecular interactions between peptide residues and F8 CDRs are indicated in (a) for each antigen, and the binding interactions of the peptides (hard spheres) with the F8 mAb (cartoon representation) are illustrated in a 3D model (b).

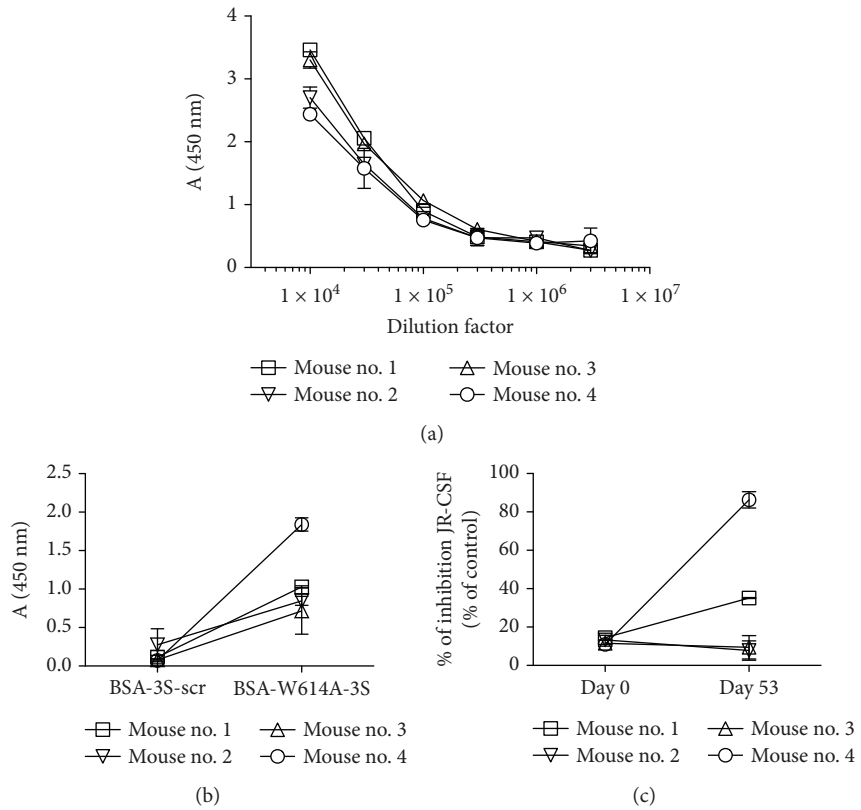

FIGURE 6: Serum reactivity of mice immunized with the Mim_F8-1 phagotope. (a) Titers of serum IgG directed at phage proteins were determined by ELISA against immobilized Mim-F8 phagotope. (b) IgG binding reactivity of the sera (1 : 50 dilution) against immobilized BSA-W614A-3S was assayed by ELISA at day 53. BSA-3S-scr functioned as negative control. Binding activity is expressed as mean OD at 450 nm of duplicate wells and bars indicate SD. (c) Neutralizing activity of the sera (1 : 2 dilution) at day 53 was performed as mentioned in Figure 1 using the JR-CSF strain. Sera at day 0 were used as negative control. Experiments were run in duplicate and bars indicate SD.

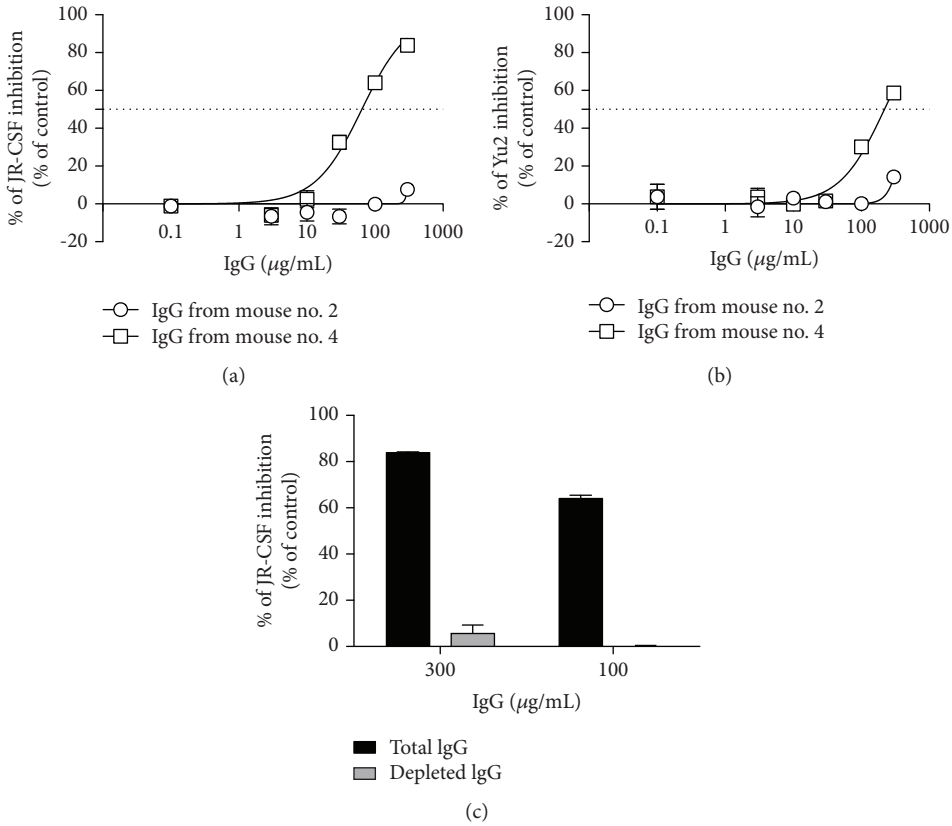

Figure 7: Neutralizing properties of purified IgG from mice immunized with the Mim_F8-1 phagotope. Dose-response curves of total purified IgG from poor (Mouse no. 2) and good (Mouse no. 4) responder mice tested to neutralize JRCSF (a) and YU-2 (b) HIV-1 strains. Neutralizing activity was performed as in Figure 1. Experiments were run in triplicate and bars indicate SD. (c) Reactivity of the purified IgG at 100 and 300 μg/mL from the good responder mouse, before (black bar) and after depletion of the W614A-3S Abs (grey bar). Neutralizing activity was performed as above using the JR-CSF strain. Experiments were run in duplicate and bars indicate SD.

and 53, at titers that varied among the immunized mice (Figure 6(b)). More importantly, among the four immunized mice, the one with the most anti-W614A-3S Abs displayed neutralizing activity against the tier 2 JR-CSF HIV-1 strain with up to 80% of inhibition (Figure 6(c)). Purified IgG from a poor responder mouse did not neutralize the virus ($IC_{50} > 300\,\mu$g/mL for JRCSF and YU-2), while purified IgG from a good responder mouse had IC_{50} values of 49 and 218 μg/mL for JRCSF and YU-2, respectively (Figures 7(a) and 7(b)). To confirm the involvement of the anti-W614A-3S Abs in the neutralization process, purified IgG were adsorbed on CRM-W614A-3S. Anti-W614A-3S depleted IgG from the good responder mouse failed to neutralize the JRCSF strain ($IC_{50} > 300\,\mu$g/mL), as shown in Figure 7(c).

4. Discussion

The identification of the molecular specificities of Abs that mediate neutralizing breadth and potency is key in the design and development of suitable Env-based immunogens for vaccination. The epitope-based vaccine design consists in grafting an epitope of interest onto a heterologous protein scaffold. Numerous epitope-scaffold designs, focusing MPER, CD4 binding, or glycan V3 sites of vulnerability, have been tested without eliciting cross-reactive serum neutralization of most primary strains of HIV-1 [45–47]. Recently, structure-based optimization of an epitope-based vaccine design provided fusion peptide-directed antibodies that neutralize diverse strains of HIV-1 [24]. In the present study, we sought to determine the molecular specificity of mAbs generated by immunization with the W614A-3S-modified peptide derived from gp41. Among the three mAbs tested for their neutralizing activity, two were non-neutralizing, as previously reported with the wild-type 3S peptide [30, 31], whereas the F8 mAb showed moderate neutralizing activity against tier 1 and tier 2 HIV-1 clade B and clade C strains with values of IC_{50} that are similar to those described for the human anti-gp41 MPER 2F5 and 4E10 mAbs [48, 49]. In SPR experiments, the F8 mAb exhibited similar association rates (kon) with BSA-coupled W614A-3S and wild-type 3S peptides but the dissociation rate (koff) of BSA-W614A-3S is significantly slower. Thus, apparent constant affinity (KD) of the F8 mAb is very low, reflecting its high affinity for this epitope. Similar observations have been described previously with various human and mouse mAbs, where koff values are highly predictive of anti-HIV-neutralizing activity [50]. This suggests that the F8 mAb recognizes different binding sites on wild-type 3S and W614A-3S peptides. This is highlighted in *in silico* molecular

modeling studies of the F8 mAb that show different docking interactions with both peptides, illustrating the dramatic impact of the W614A mutation on the epitope conformation.

In the structure of the HIV-1 envelope trimer [35, 36], the 3S motif appears to be exposed at the surface in the trimeric prefusion structure of the HIV-1 envelope [34] and possibly adopts different conformations during the viral entry steps. This suggests that the neutralizing F8 mAb could recognize a conformational intermediate epitope [2, 51, 52] mimicked by the W614A-3S peptide. It has been reported that few neutralizing Abs targeting gp41 bind transient epitopes exposed during the conformational changes of the Env protein in the course of the viral entry process [24, 53, 54]. The W614 residue is highly conserved into the 3S motif of gp41 in all HIV-1 strains. Thus, the generation of W614A-3S Abs is very unlikely to result from the occurrence of dominant W614A-3S mutant viral strains in HIV-infected individuals, since they are non-infectious [32]. Anti-W614A-3S cross-reactive Abs would rather have been generated in the process of somatic hypermutation generated by non-W614A-3S-bearing strains.

To gain insight into the characterization of the W614A-3S nAbs, a phage peptide library [37] was screened with the neutralizing F8 mAb to select specific mimotopes. The preferentially selected mimotope (Mim_F8-1) interacts with F8, but not with the non-neutralizing mAbs, and competes with the W614A-3S peptide for the binding to the F8 mAb. These data suggest that W614A-3S and Mim_F8-1 share a similar conformation, even if there is no sequence homology which is consistent with the notion that most neutralizing Abs have conformational epitopes [55, 56]. Molecular docking indicated that the W614A-3S peptide and the selected mimotopes adopt the same conformation: they are anchored in the binding site of the F8 mAb, interacting with residues of all the CDRs of both the VH and the Vk domains. Notably, the CDR L3 of the F8 mAb is predicted to interact mainly with the mutated residue W614A into the 3S peptide and with the ECAGC motif of the mimotopes. It is now evident that the exposure of epitopes on HIV-1 and Env features increases nAb emergence; conversely, lack of neutralization is due to an inability of an antibody to access its epitope in the context of Env on the virus [57]. Consequently, structures capable of mimicking neutralizing transient epitopes, such as Mim_F8-1, might be useful in the molecular design of new immunogens. It is likely that interactions with the phage pIII protein constrain the peptide mimotope into a specific conformation, essential for binding to the F8 mAb [38, 58]. Therefore, the phage particle, or at least the pIII protein, should be considered an important element in vaccine formulation [59, 60]. Immunization of mice with the phage bearing the Mim_F8-1 mimotope led to the induction of anti-HIV-neutralizing Abs in the serum, demonstrating that structural mimicry of the Mim_F8-1 allows functional activity. It is of note that all immunized mice developed low titers of neutralizing Ab, which is certainly due to the strong response against the phage proteins. To increase the immunogenicity while retaining the constrained conformation imposed by the phage protein, the mimotope could be fused to soluble recombinant pIII and used as vaccine instead of a phagotope [61]. Finally, additional animal studies should be conducted, using rabbit and non-human primate models, to determine if immunization with Mim_F8-1 is superior to immunization with KLH-W614A-3S peptide in its capacity to elicit serum neutralization. At this point, our work is suggesting that it is indeed possible to preferably orientate an immune response towards the recognition of "F8-like" specificities, at the expense of "B8-like" or "G6-like" non-neutralizing responses.

Thus, in addition to revealing features of the W614A-3S motif that allows for neutralizing activity, the molecular survey of the F8 mAb provides new insight into molecular conformations of a highly conserved motif of gp41. Future structural studies will allow better understanding of the W614A-3S motif as a promising HIV-1 vaccine.

Data Availability

Sequences of F8 mAb reported in this paper have been deposited in the GenBank Database under accession numbers MK110657 and MK110658. All other data used to support the findings of this study are included within the supplementary information files or available from the corresponding author upon request.

Disclosure

Affoune Amel's present address is the Assistance Publique-Hôpitaux de Paris (AP-HP), Hôpital Bichat, FAVA-Multi, F-75018 Paris, France. Lucar Olivier's present address is the Harvard Medical School, Center for Virology and Vaccine Research, Beth Israel Deaconess Medical Center, Boston, MA, USA.

Conflicts of Interest

The authors declare that there is no conflict of interest regarding the publication of this paper.

Authors' Contributions

KD, NP, AA, OL, TB, SC, CeP, ChP, and VV performed experiments and interpreted and analyzed the data. KD and VV designed the assays and wrote the manuscript. All authors edited the manuscript.

Acknowledgments

This work was supported by Sorbonne Université and the Institut National de la Santé et de la Recherche Médicale (INSERM). The authors acknowledge Delphine Lucas from Minka Therapeutics and Julien Puech and Noemi Asfogo, both students of the CIMI-Paris, for their technical assistance.

Supplementary Materials

Supplemental Figure 1: mice immunization protocol with the Mim_F8-1 phagotope. Supplemental Figure 2: sequence analysis of the F8 mAb by mass spectrometry. Supplemental

Figure 3: construction and characterization of the chimeric F8 mAb. Supplemental Figure 4: SPR sensorgrams of F8 mAb binding to BSA-W614S-3S and BSA-3S. Supplemental Table I: molecular characterization of the anti-W614A-3S mAbs. Supplemental Table II: sequence of the peptides used in this study. *(Supplementary Materials)*

References

[1] D. Corti and A. Lanzavecchia, "Broadly neutralizing antiviral antibodies," *Annual Review of Immunology*, vol. 31, no. 1, pp. 705–742, 2013.

[2] D. R. Burton and L. Hangartner, "Broadly neutralizing antibodies to HIV and their role in vaccine design," *Annual Review of Immunology*, vol. 34, no. 1, pp. 635–659, 2016.

[3] C. Moog, H. J. A. Fleury, I. Pellegrin, A. Kirn, and A. M. Aubertin, "Autologous and heterologous neutralizing antibody responses following initial seroconversion in human immunodeficiency virus type 1-infected individuals," *Journal of Virology*, vol. 71, no. 5, pp. 3734–3741, 1997.

[4] X. L. Wu, Z. Y. Yang, Y. X. Li et al., "Rational design of envelope identifies broadly neutralizing human monoclonal antibodies to HIV-1," *Science*, vol. 329, no. 5993, pp. 856–861, 2010.

[5] T. Zhou, I. Georgiev, X. Wu et al., "Structural basis for broad and potent neutralization of HIV-1 by antibody VRC01," *Science*, vol. 329, no. 5993, pp. 811–817, 2010.

[6] I. Mikell, D. N. Sather, S. A. Kalams, M. Altfeld, G. Alter, and L. Stamatatos, "Characteristics of the earliest cross-neutralizing antibody response to HIV-1," *PLoS Pathogens*, vol. 7, no. 1, article e1001251, 2011.

[7] L. E. Mccoy and R. A. Weiss, "Neutralizing antibodies to HIV-1 induced by immunization," *Journal of Experimental Medicine*, vol. 210, no. 2, pp. 209–223, 2013.

[8] D. Peterhoff and R. Wagner, "Guiding the long way to broad HIV neutralization," *Current Opinion in HIV and AIDS*, vol. 12, no. 3, pp. 257–264, 2017.

[9] M. S. Cohen and L. Corey, "Broadly neutralizing antibodies to prevent HIV-1," *Science*, vol. 358, no. 6359, pp. 46-47, 2017.

[10] J. R. Mascola, M. G. Lewis, G. Stiegler et al., "Protection of macaques against pathogenic simian/human immunodeficiency virus 89.6PD by passive transfer of neutralizing antibodies," *Journal of Virology*, vol. 73, no. 5, pp. 4009–4018, 1999.

[11] R. Shibata, T. Igarashi, N. Haigwood et al., "Neutralizing antibody directed against the HIV–1 envelope glycoprotein can completely block HIV–1/SIV chimeric virus infections of macaque monkeys," *Nature Medicine*, vol. 5, no. 2, pp. 204–210, 1999.

[12] T. W. Baba, V. Liska, R. Hofmann-Lehmann et al., "Human neutralizing monoclonal antibodies of the IgG1 subtype protect against mucosal simian–human immunodeficiency virus infection," *Nature Medicine*, vol. 6, no. 2, pp. 200–206, 2000.

[13] P. W. H. I. Parren, P. A. Marx, A. J. Hessell et al., "Antibody protects macaques against vaginal challenge with a pathogenic R5 simian/human immunodeficiency virus at serum levels giving complete neutralization in vitro," *Journal of Virology*, vol. 75, no. 17, pp. 8340–8347, 2001.

[14] F. Ferrantelli, R. Hofmann-Lehmann, R. A. Rasmussen et al., "Post-exposure prophylaxis with human monoclonal antibodies prevented SHIV89.6P infection or disease in neonatal macaques," *AIDS*, vol. 17, no. 3, pp. 301–309, 2003.

[15] S. Nakowitsch, H. Quendler, H. Fekete, R. Kunert, H. Katinger, and G. Stiegler, "HIV-1 mutants escaping neutralization by the human antibodies 2F5, 2G12, and 4E10: in vitro experiments versus clinical studies," *AIDS*, vol. 19, no. 17, pp. 1957–1966, 2005.

[16] A. Trkola, H. Kuster, P. Rusert et al., "Delay of HIV-1 rebound after cessation of antiretroviral therapy through passive transfer of human neutralizing antibodies," *Nature Medicine*, vol. 11, no. 6, pp. 615–622, 2005.

[17] R. M. Ruprecht, "Passive immunization with human neutralizing monoclonal antibodies against HIV-1 in macaque models: experimental approaches," *Methods in Molecular Biology*, vol. 525, pp. 559–566, 2009.

[18] A. J. Hessell, P. Poignard, M. Hunter et al., "Effective, low-titer antibody protection against low-dose repeated mucosal SHIV challenge in macaques," *Nature Medicine*, vol. 15, no. 8, pp. 951–954, 2009.

[19] J. F. Scheid, H. Mouquet, N. Feldhahn et al., "Broad diversity of neutralizing antibodies isolated from memory B cells in HIV-infected individuals," *Nature*, vol. 458, no. 7238, pp. 636–640, 2009.

[20] G. Frey, J. Chen, S. Rits-Volloch, M. M. Freeman, S. Zolla-Pazner, and B. Chen, "Distinct conformational states of HIV-1 gp41 are recognized by neutralizing and non-neutralizing antibodies," *Nature Structural & Molecular Biology*, vol. 17, no. 12, pp. 1486–1491, 2010.

[21] R. Kong, K. Xu, T. Zhou et al., "Fusion peptide of HIV-1 as a site of vulnerability to neutralizing antibody," *Science*, vol. 352, no. 6287, pp. 828–833, 2016.

[22] G. Stiegler, R. Kunert, M. Purtscher et al., "A potent cross-clade neutralizing human monoclonal antibody against a novel epitope on gp41 of human immunodeficiency virus type 1," *AIDS Research and Human Retroviruses*, vol. 17, no. 18, pp. 1757–1765, 2001.

[23] A. Manrique, P. Rusert, B. Joos et al., "In vivo and in vitro escape from neutralizing antibodies 2G12, 2F5, and 4E10," *Journal of Virology*, vol. 81, no. 16, pp. 8793–8808, 2007.

[24] K. Xu, P. Acharya, R. Kong et al., "Epitope-based vaccine design yields fusion peptide-directed antibodies that neutralize diverse strains of HIV-1," *Nature Medicine*, vol. 24, no. 6, pp. 857–867, 2018.

[25] O. Ringel, V. Vieillard, P. Debré, J. Eichler, H. Büning, and U. Dietrich, "The hard way towards an antibody-based HIV-1 Env vaccine: lessons from other viruses," *Viruses*, vol. 10, no. 4, 2018.

[26] M. Montero, N. E. van Houten, X. Wang, and J. K. Scott, "The membrane-proximal external region of the human immunodeficiency virus type 1 envelope: dominant site of antibody neutralization and target for vaccine design," *Microbiology and Molecular Biology Reviews*, vol. 72, no. 1, pp. 54–84, 2008.

[27] L. Scharf, J. F. Scheid, J. H. Lee et al., "Antibody 8ANC195 reveals a site of broad vulnerability on the HIV-1 envelope spike," *Cell Reports*, vol. 7, no. 3, pp. 785–795, 2014.

[28] V. Vieillard, J. L. Strominger, and P. Debré, "NK cytotoxicity against $CD4^+$ T cells during HIV-1 infection: a gp41 peptide induces the expression of an NKp44 ligand," *Proceedings of the National Academy of Sciences of the United States of America*, vol. 102, no. 31, pp. 10981–10986, 2005.

[29] V. Vieillard, S. Gharakhanian, O. Lucar et al., "Perspectives for immunotherapy: which applications might achieve an HIV functional cure?," *Oncotarget*, vol. 7, no. 25, pp. 38946–38958, 2016.

[30] V. Vieillard, R. E. Habib, P. Brochard et al., "CCR5 or CXCR4 use influences the relationship between CD4 cell depletion, NKp44L expression and NK cytotoxicity in SHIV-infected macaques," *AIDS*, vol. 22, no. 2, pp. 185–192, 2008.

[31] V. Vieillard, N. Dereuddre-Bosquet, I. Mangeot-Méderlé, R. Le Grand, and P. Debré, "An HIVgp41 vaccine protects CD4 central memory T cells in SHIV-infected macaques," *Vaccine*, vol. 30, no. 48, pp. 6883–6891, 2012.

[32] C. Petitdemange, A. Achour, S. Dispinseri et al., "A single amino-acid change in a highly conserved motif of gp41 elicits HIV-1 neutralization and protects against CD4 depletion," *Clinical Infectious Diseases*, vol. 57, no. 5, pp. 745–755, 2013.

[33] T. Bradley, A. Trama, N. Tumba et al., "Amino acid changes in the HIV-1 gp41 membrane proximal region control virus neutralization sensitivity," *eBioMedicine*, vol. 12, pp. 196–207, 2016.

[34] O. Lucar, B. Su, V. Potard et al., "Neutralizing antibodies against a specific human immunodeficiency virus gp41 epitope are associated with long-term non-progressor status," *eBioMedicine*, vol. 22, pp. 122–132, 2017.

[35] M. Pancera, T. Zhou, A. Druz et al., "Structure and immune recognition of trimeric pre-fusion HIV-1 Env," *Nature*, vol. 514, no. 7523, pp. 455–461, 2014.

[36] J. H. Lee, G. Ozorowski, and A. B. Ward, "Cryo-EM structure of a native, fully glycosylated, cleaved HIV-1 envelope trimer," *Science*, vol. 351, no. 6277, pp. 1043–1048, 2016.

[37] I. Fisch, R. E. Kontermann, R. Finnern et al., "A strategy of exon shuffling for making large peptide repertoires displayed on filamentous bacteriophage," *Proceedings of the National Academy of Sciences of the United States of America*, vol. 93, no. 15, pp. 7761–7766, 1996.

[38] K. Dorgham, I. Dogan, N. Bitton et al., "Immunogenicity of HIV type 1 gp120 CD4 binding site phage mimotopes," *AIDS Research and Human Retroviruses*, vol. 21, no. 1, pp. 82–92, 2005.

[39] L. J. Harris, E. Skaletsky, and A. McPherson, "Crystallographic structure of an intact IgG1 monoclonal antibody," *Journal of Molecular Biology*, vol. 275, no. 5, pp. 861–872, 1998.

[40] J. Maupetit, P. Derreumaux, and P. Tuffery, "PEP-FOLD: an online resource for de novo peptide structure prediction," *Nucleic Acids Research*, vol. 37, Supplement 2, pp. W498–W503, 2009.

[41] R. Chen and Z. Weng, "A novel shape complementarity scoring function for protein-protein docking," *Proteins: Structure, Function, and Genetics*, vol. 51, no. 3, pp. 397–408, 2003.

[42] O. Elemento and M. P. Lefranc, "IMGT/PhyloGene: an on-line tool for comparative analysis of immunoglobulin and T cell receptor genes," *Developmental & Comparative Immunology*, vol. 27, no. 9, pp. 763–779, 2003.

[43] G. Pialoux, J. L. Excler, Y. Rivière et al., "A prime-boost approach to HIV preventive vaccine using a recombinant canarypox virus expressing glycoprotein 160 (MN) followed by a recombinant glycoprotein 160 (MN/LAI)," *AIDS Research and Human Retroviruses*, vol. 11, no. 3, pp. 373–381, 1995.

[44] S. Delhalle, J. C. Schmit, and A. Chevigne, "Phages and HIV-1: from display to interplay," *International Journal of Molecular Sciences*, vol. 13, no. 4, pp. 4727–4794, 2012.

[45] D. R. Burton and J. R. Mascola, "Antibody responses to envelope glycoproteins in HIV-1 infection," *Nature Immunology*, vol. 16, no. 6, pp. 571–576, 2015.

[46] A. Escolano, J. M. Steichen, P. Dosenovic et al., "Sequential immunization elicits broadly neutralizing anti-HIV-1 antibodies in Ig knockin mice," *Cell*, vol. 166, no. 6, pp. 1445–1458.e12, 2016.

[47] P. D. Kwong and J. R. Mascola, "HIV-1 vaccines based on antibody identification, B cell ontogeny, and epitope structure," *Immunity*, vol. 48, no. 5, pp. 855–871, 2018.

[48] A. Trkola, A. B. Pomales, H. Yuan et al., "Cross-clade neutralization of primary isolates of human immunodeficiency virus type 1 by human monoclonal antibodies and tetrameric CD4-IgG," *Journal of Virology*, vol. 69, no. 11, pp. 6609–6617, 1995.

[49] M. B. Zwick, R. Jensen, S. Church et al., "Anti-human immunodeficiency virus type 1 (HIV-1) antibodies 2F5 and 4E10 require surprisingly few crucial residues in the membrane-proximal external region of glycoprotein gp41 to neutralize HIV-1," *Journal of Virology*, vol. 79, no. 2, pp. 1252–1261, 2004.

[50] T. C. Vancott, F. R. Bethke, V. R. Polonis et al., "Dissociation rate of antibody-gp120 binding interactions is predictive of V3-mediated neutralization of HIV-1," *Journal of Immunology*, vol. 153, no. 1, pp. 449–459, 1994.

[51] R. Wyatt and J. Sodroski, "The HIV-1 envelope glycoproteins: fusogens, antigens, and immunogens," *Science*, vol. 280, no. 5371, pp. 1884–1888, 1998.

[52] A. F. Labrijn, P. Poignard, A. Raja et al., "Access of antibody molecules to the conserved coreceptor binding site on glycoprotein gp120 is sterically restricted on primary human immunodeficiency virus type 1," *Journal of Virology*, vol. 77, no. 19, pp. 10557–10565, 2003.

[53] M. Kim, Z. Y. J. Sun, K. D. Rand et al., "Antibody mechanics on a membrane-bound HIV segment essential for GP41-targeted viral neutralization," *Nature Structural & Molecular Biology*, vol. 18, no. 11, pp. 1235–1243, 2011.

[54] J. M. Kovacs, E. Noeldeke, H. J. Ha et al., "Stable, uncleaved HIV-1 envelope glycoprotein gp140 forms a tightly folded trimer with a native-like structure," *Proceedings of the National Academy of Sciences of the United States of America*, vol. 111, no. 52, pp. 18542–18547, 2014.

[55] P. D. Kwong and J. R. Mascola, "Human antibodies that neutralize HIV-1: identification, structures, and B cell ontogenies," *Immunity*, vol. 37, no. 3, pp. 412–425, 2012.

[56] J. R. Mascola and B. F. Haynes, "HIV-1 neutralizing antibodies: understanding nature's pathways," *Immunological Reviews*, vol. 254, no. 1, pp. 225–244, 2013.

[57] R. A. Pantophlet, "Antibody epitope exposure and neutralization of HIV-1," *Current Pharmaceutical Design*, vol. 16, no. 33, pp. 3729–3743, 2010.

[58] K. B. Jensen, M. Larsen, J. S. Pedersen et al., "Functional improvement of antibody fragments using a novel phage coat protein III fusion system," *Biochemical and Biophysical Research Communications*, vol. 298, no. 4, pp. 566–573, 2002.

[59] L. Aghebati-Maleki, B. Bakhshinejad, B. Baradaran et al., "Phage display as a promising approach for vaccine development," *Journal of Biomedical Science*, vol. 23, no. 1, p. 66, 2016.

[60] A. Prisco and P. De Berardinis, "Filamentous bacteriophage Fd as an antigen delivery system in vaccination," *International Journal of Molecular Sciences*, vol. 13, no. 4, pp. 5179–5194, 2012.

[61] R. Krishnan, H. Tsubery, M. Y. Proschitsky et al., "A bacteriophage capsid protein provides a general amyloid interaction motif (GAIM) that binds and remodels misfolded protein assemblies," *Journal of Molecular Biology*, vol. 426, no. 13, pp. 2500–2519, 2014.

Hindawi
Journal of Immunology Research
Volume 2019, Article ID 8303648, 13 pages
https://doi.org/10.1155/2019/8303648

Review Article

Alternative Methods of Vaccine Delivery: An Overview of Edible and Intradermal Vaccines

E. Criscuolo,[1] **V. Caputo**,[1,2] **R. A. Diotti**,[1,2] **G. A. Sautto**,[3] **G. A. Kirchenbaum**,[4] **and N. Clementi**[1]

[1]*Microbiology and Virology Unit, "Vita-Salute San Raffaele" University, Milan, Italy*
[2]*Pomona Ricerca S.r.l., Turin, Italy*
[3]*Center for Vaccines and Immunology, University of Georgia, Athens, GA, USA*
[4]*Cellular Technology Ltd., Shaker Heights, OH, USA*

Correspondence should be addressed to R. A. Diotti; diotti.robertaantonia@hsr.it

Received 26 November 2018; Revised 8 February 2019; Accepted 14 February 2019; Published 4 March 2019

Academic Editor: Isabella Quinti

Vaccines are recognized worldwide as one of the most important tools for combating infectious diseases. Despite the tremendous value conferred by currently available vaccines toward public health, the implementation of additional vaccine platforms is also of key importance. In fact, currently available vaccines possess shortcomings, such as inefficient triggering of a cell-mediated immune response and the lack of protective mucosal immunity. In this regard, recent work has been focused on vaccine delivery systems, as an alternative to injectable vaccines, to increase antigen stability and improve overall immunogenicity. In particular, novel strategies based on edible or intradermal vaccine formulations have been demonstrated to trigger both a systemic and mucosal immune response. These novel vaccination delivery systems offer several advantages over the injectable preparations including self-administration, reduced cost, stability, and elimination of a cold chain. In this review, the latest findings and accomplishments regarding edible and intradermal vaccines are described in the context of the system used for immunogen expression, their molecular features and capacity to induce a protective systemic and mucosal response.

1. Introduction

One of the ten greatest public health achievements of the last century was preventative vaccination [1]. Vaccines have successfully reduced the spread of diseases and mitigated mortality associated with infectious agents such as diphtheria, tetanus, polio, measles, mumps, rubella, and hepatitis B [2]. In spite of the many successes achieved by vaccines, novel technologies and administration routes remain one of the main focuses in the vaccinology field. Although many licensed vaccines are administered by injection, in certain cases, this administration route suffers from limitations. In particular, injectable vaccines require trained personnel for the administration of the vaccine and may require multiple doses or inclusion of an adjuvant. Moreover, injectable vaccines may require specialized storage and transport conditions. From an immunological point of view, injectable vaccines are capable of eliciting robust systemic humoral responses while conferring weaker T cell-mediated immunity and mucosal protection [3, 4]. Importantly, T cell effector activity and mucosal immunity both contribute to prevention and control of infection from pathogens targeting the mucosa [5].

To improve on this limitation, alternative vaccine delivery methods coupled with novel formulations and production systems have recently been proposed. Numerous studies have focused on vaccines delivered to the mucosal interface or intradermally, demonstrating rapid and wide biodistribution of the antigen and the capacity to induce both protective mucosal (mainly mediated by secretory IgA [SIgA]) and systemic cellular and humoral responses [6–8].

In this review, we discuss current advances and advantages of edible systems based on plants, algae, yeast,

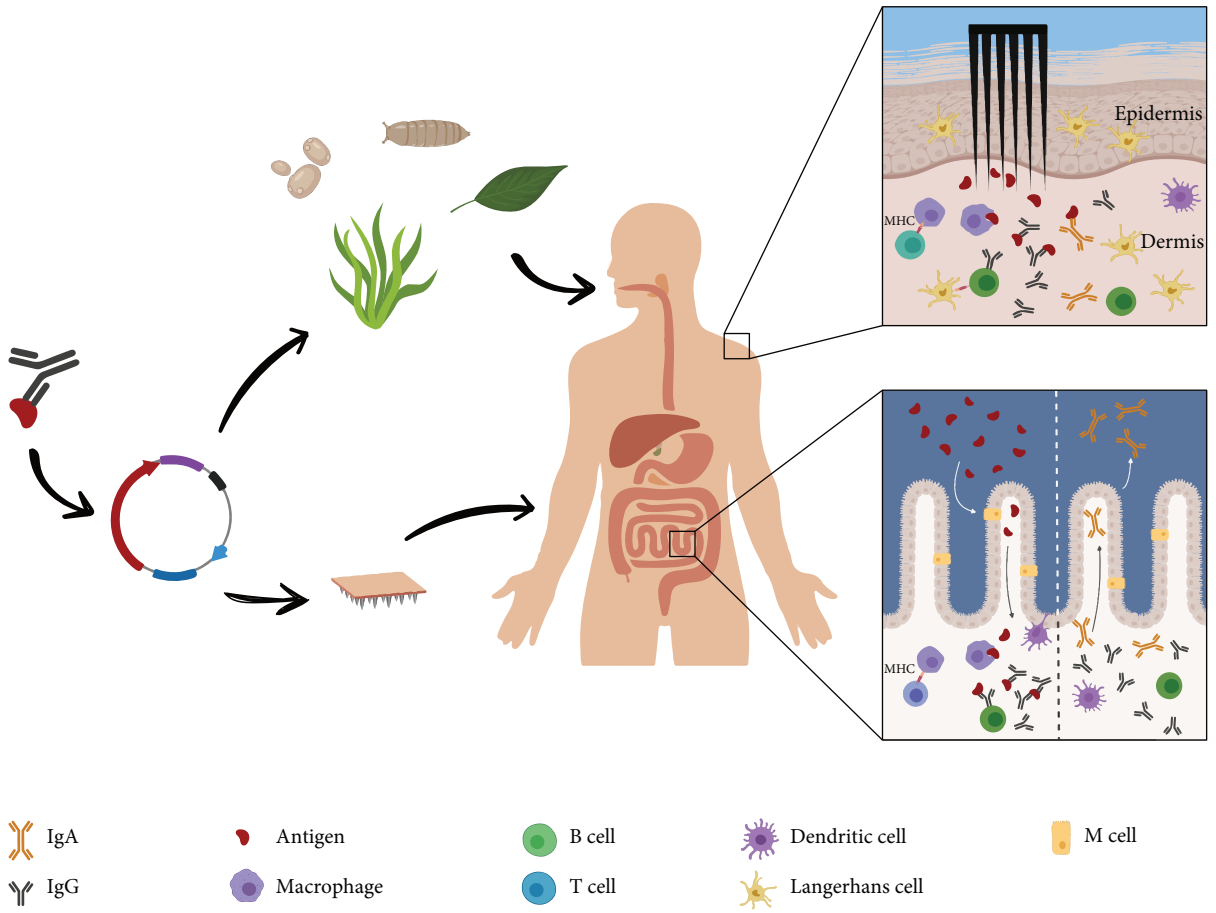

Figure 1: Alternative methods of vaccine delivery. Development of rationally designed vaccines starts with the identification of the gene encoding for the protective antigenic protein(s). Subsequently, the antigen(s) can be incorporated into different edible systems, as plants, algae, insects, or yeasts, or used for intradermal formulations to induce a mucosal protective response. Following the administration of the edible vaccine and the subsequent passage of the antigen(s) through the M cell compartment delivering it to dendritic cells, the individual's immune system triggers a response leading also to specific IgA production and secretion. Similarly, patches with coated microprojections or biodegradable needles activate Langerhans cells and dermal dendritic cells in the skin dermis. These cells capture and present the antigen(s) to T and B lymphocytes, triggering both a mucosal and a systemic immunity.

insect cells, and lactic acid bacteria and of the intradermal immunization route.

1.1. The Mucosal Delivery and the Immune Response. The efficacy of the mucosal administration route is largely based on the fact that mucous membranes constitute the largest immunologic organ in the body. Moreover, this interface is endowed with well-organized lymphatic structures, termed mucosa-associated lymphoid tissue (MALT), containing both the innate and adaptive (T and B cells) arms of the immune system [9]. Furthermore, antigen-specific SIgA plays a pivotal role in protecting mucosal surfaces from both microbe adhesion and toxin activities [8]. Thus, the development of novel vaccine delivery platforms implementing the elicitation of pathogen- or toxin-specific SIgA, as well as systemic IgG, is pivotal to improve vaccine effectiveness [10].

To date, the most well-studied vaccine delivery platforms capable of eliciting both mucosal and systemic immunities are edible or intradermal vaccine formulations (Figure 1). Oral vaccines stimulate the generation of immunity in gut-associated lymphoid tissue (GALT), which includes lymph nodes, Peyer's patches (in which lymphocytes are the major component: ~75% are B cells, while ~20% are T cells), and isolated lymphoid follicles in the gastrointestinal tract (GIT). An effective immunization using oral vaccines is achieved when sufficient quantities of antigen are transported across the mucosal barrier by M cells into Peyer's patches and subsequently presented to T cells by antigen-presenting cells (APCs) [11]. Briefly, professional APCs display peptide fragments of the antigen in the context of the major histocompatibility complex (MHC) on their surface, which leads to activation of $CD4^+$ T cells [12]. Subsequently, activated $CD4^+$ T cells support germinal center development, including B cell affinity maturation and class switching to IgA, through providing CD40/CD40 ligand interactions and cytokine secretion [13–15]. Moreover, through the expression of specific chemokine homing receptors (e.g., CXCR5 or CCR10), antigen-experienced B cells migrate to distant effector regions where they differentiate into plasma cells capable of secreting dimeric or polymeric

IgA molecules that are transported into the intestinal lumen as SIgA [10, 16].

In the context of edible vaccines aimed at eliciting pathogen-specific responses, it will be necessary to overcome mucosal tolerance. Briefly, mucosal tolerance is achieved against certain foreign antigens, such as those contained in our food, and serves to prevent unnecessary and potentially detrimental immune responses in the gut mucosa. Due to this phenomenon, an erroneous mucosal vaccine formulation could induce a T_{reg}-based tolerogenic response instead of Th17-mediated protective immunity [17]. This potential shortcoming can be circumvented using several strategies, including incorporation of an appropriate adjuvant in the vaccine formulation or using sufficiently high doses of antigen to promote induction of effector rather than regulatory cells [5, 11]. Moreover, in the context of edible-based vaccine immunizations, it will also be important to consider the characteristics of the GIT, in which several factors, including proteolytic enzymes, acidic pH, bile salts, and limited permeability, may hinder the induction of a protective immune response [10]. To this end, conjugation of the vaccine antigen with specific ligands that enhance their uptake by M cells represents a focus of ongoing studies aimed at improving immunogenicity [18]. Moreover, antigen bioencapsulation avoids degradation and conformational alterations [19].

1.2. Overview of Edible Vaccines. In the following sections, we review the various strategies underlying the development of edible vaccines. In particular, we focused on plant, algae, insect cells, whole yeast, and lactic acid bacteria-based vaccines and describe the advantages and limitations of individual systems.

1.3. Plant-Based Vaccines. Plants have been extensively used for developing novel biopharmaceutical-producing platforms in recent years, as they promote proper folding of exogenous proteins and are economically sustainable [20, 21]. This is also known in the context of "molecular farming," in which biomolecules of commercial value are produced in genetically engineered plants. There are several ongoing clinical trials using purified antigens transiently produced in tobacco plants (*Nicotiana benthamiana*) for injectable vaccine formulations. For example, Medicago recently completed a phase II clinical trial using a plant-derived, virus-like particle (VLP) quadrivalent influenza vaccine and announced a phase III clinical study in the last year (ClinicalTrials.gov identifier: NCT03301051) [22].

Owing to the fact that plants are edible, the notion that they could serve as a delivery vehicle, as well as biofactories, led to their use for oral vaccination in the early 1990s [23]. In recent years, additional studies have sought to overcome the limitations of conventional vaccines through development of edible formulations [24, 25]. Since the inception of the idea, it has been evident that using plants to produce vaccines would have several advantages. First, plant vaccines would likely have a low production cost and could be easily scaled-up, as has been demonstrated by the biopharmaceutical industry. Molecular farming gained visibility thanks to the success of ZMapp, the experimental drug against the Ebola virus that was produced in *Nicotiana* plants [26]. However, unlike biomolecule production, edible vaccine formulations do not need processing or purification steps before administration, which serves to further lower production-associated costs. Indeed, another advantage of this strategy is that plant cells would provide antigen protection due to their rigid cell wall. This is also known as the bioencapsulation effect and could increase bioavailability of antigenic molecules to the GALTs through preserving structural integrity of vaccine components through the stomach to elicit both a mucosal and a systemic immune response. Additional strategies for antigen protection can be achieved through targeting biomolecule expression inside chloroplasts or other storage organelles [27] or in the protein bodies of seeds [28, 29]. This technology also offers advantages in terms of storage and cold chain-free delivery due to the high stability of the expressed antigens bioencapsulated within the plant and seed tissues. Moreover, plant materials can be stored at elevated temperatures for longer periods and grown where needed, making this strategy even more attractive for developing countries [30]. Finally, plant-based oral vaccines are characterized by improved safety relative to traditional recombinant vaccine platforms, especially since contamination from mammalian-specific pathogens can be eliminated [30]. Indeed, some studies using lyophilized leaves have shown their advantages over fresh materials such as long-term stability, higher antigen content, and lower microbial contamination. As an example, freeze-dried CTB-EX4-expressing (CTB: cholera toxin B subunit; EX4: exendin-4) leaves were shown to be stable for up to 10 months at room temperature, and lettuces expressing soluble antigen (PA; protective antigen from *Bacillus anthracis*) were successfully stored for up to 15 months at room temperature without showing antigen degradation [31]. The antigen content in lyophilized leaf materials was also 24-fold higher than fresh leaves. An additional benefit of lyophilization was its ability to remove microbial contamination. While lyophilized lettuce had no detectable microbes, fresh leaves contained up to approximately 6000 cfu/g microbes when plated on various growing media [31].

To date, vaccine antigens have been transformed into many edible species including lettuce, tomato, potato, papaya, carrot, quinoa, and tobacco [32]. Their proper folding and enhanced expression have also been tested in animal models, proving the immunogenicity of antigens produced in these systems [24, 33].

To obtain high quantities of the protein of interest, both nuclear and chloroplast genomes have been successfully engineered. However, the latter option is preferred owing to some advantages including high levels of transgene expression (up to 70% of total soluble proteins (TSP)) [34, 35], bioencapsulation effect, and regulatory concerns since transgene containment is assured by the fact that plastids are not spread via pollen in most plants. Moreover, incorporation of vaccine antigens into the chloroplast genome would also enable the expression of multiple genes in a single operon, which would be very attractive for multivalent vaccine development. Likewise, this approach may enable the production of vaccines conferring protection against multiple infectious

Table 1: Status of development of plant-based vaccines.

Pathogen	Antigen	Plant host	Expression system	Indication	Route of administration	Clinical trial status	Clinical trial ID	Refs
Enterotoxigenic *E. coli*	LT-B	Potato	Transgenic	Diarrhea	Edible	Early phase 1	►	[42]
Enterotoxigenic *E. coli*	LT-B	Maize	Transgenic	Diarrhea	Edible	Early phase 1	►	[43]
Norwalk virus	CP	Potato	Transgenic	Diarrhea	Edible	Early phase 1	►	[44]
Rabies virus	GP/NP (fusion)	Spinach	Viral vector (transient)	Rabies	Edible	Early phase 1	►	[45]
HBV	HBsAg	Lettuce	Transgenic	Hepatitis B	Edible	Early phase 1	►	[46]
HBV	HBsAg	Potato	Transgenic	Hepatitis B	Edible	Phase 1	NCT01292421	[47]
Vibrio cholerae	CTB	Rice	Transgenic	Cholera	Edible	Phase 1	UMIN000009688	[48–51]

HBsAg: hepatitis B surface antigen; CP: capsid protein; GP: glycoprotein; NP: nucleoprotein; CTB: cholera toxin subunit B. ►: restricted cohort study design.

agents and would serve to further reduce costs associated with vaccine production and administration [36].

Unfortunately, there are some disadvantages undermining their applications. First, plastids are not suitable for production of antigens that require glycosylation for proper folding or those antigens in which a protective immune response requires glycan recognition. However, nuclear transformation represents a valid option. Secondly, antigen expression can be either transient or stable in plants, but the second is preferred in order to obtain a stable genetic resource. In fact, transgenic seeds represent a constant resource to grow the transgenic plants and to extract proteins. However, stable transformation is time-consuming [25]. Moreover, expression in stable transformed crop plants suffers from low yields, typically less than 1% of TSP [36]. On the other hand, transient expression technology using either *Agrobacterium* or viral vectors is robust, quick, and easy to manipulate [37]. However, this expression is typically unstable [30]. Another important challenge of plant-based oral vaccines is the lack of a proper dosing strategy because low doses may not be able to induce a sufficient immune response and high doses, as previously described, may lead to immune tolerance. To this end, freeze-drying methods were implemented to stabilize plant biomass, concentrate the antigen, and achieve an accurate dosage by quantifying the antigen in terms of dry biomass weight, as mentioned above [31, 38].

To date, there are some plant-based vaccines for the hepatitis B virus (HBV), rabies virus, Norwalk virus, enterotoxigenic *E. coli*, and *Vibrio cholerae* in phase 1 clinical trials (Table 1). Many others are still in preclinical development, including vaccines targeting a variety of pathogens such as avian influenza viruses (HPAI H5N1) [39], *Helicobacter pylori* [40], and coronaviruses [41].

1.4. Algae-Based Vaccines. Green microalgae, such as *Chlamydomonas reinhardtii*, represent another viable option for vaccine production. However, some disadvantages of plant-derived vaccines, such as low expression levels and improper glycosylation of antigen proteins, have been described [52]. Thus far, only chloroplast transformation is possible [52], and only a single organelle is present, even if it occupies half of the cell volume [53].

Stable transformed lines of green algae are easy to obtain and can lead to increased yield of expressed antigens. In fact, unicellular green algae have all the positive characteristics of plant systems, plus unique advantages over terrestrial plants. Biomass accumulation is extremely fast and can be used in its entirety. Their growth neither has seasonal constraints nor relies on soil fertility. Cross-contamination of nearby crops cannot occur, as algae can be cultured with enclosed bioreactors [54]. Furthermore, in regard to regulatory aspects, green algae, such as *C. reinhardtii*, are generally recognized as safe (GRAS) by the FDA. Finally, algae can be easily lyophilized and, when dried, can be stored at room temperature for up to 20 months without losing antigenic efficacy [55]. In fact, the algae cell wall assures the bioencapsulation effect, as it was proven to prevent antigen degradation by enzymes of the GIT [55].

Collectively, these characteristics indicate that algae would be an ideal host for vaccine transport without a cold chain supply. Thus, as already described for plant-derived edible vaccines, the low cost and simpler logistic in terms of manufacturing, storage, delivery, and administration of the algae-based technology make it an ideal system in the context of resource-limited settings compared to conventional vaccine formulations.

There are no algae-based vaccines currently in clinical trials; however, preclinical formulations against human papillomavirus (HPV), HBV, and foot-and-mouth disease virus (FMDV) are under development [32, 52, 56] to overcome some technical problems, such as a low expression level from the nuclear genome and lack of glycosylation following chloroplast expression [52].

1.5. Insect Cell-Based Vaccines. Insect cell systems have been widely adopted because of their capacity to produce high levels of proteins and to perform cotranslational and posttranslational modifications, including glycosylation, phosphorylation, and protein processing. This expression platform allows for generation of stable transformed cell lines or transient expression driven by recombinant baculovirus

Table 2: Status of development of whole yeast-based vaccines.

Pathogen	Antigen	Yeast host	Expression system	Indication	Clinical trial status	Clinical trial ID	Refs
HBV	HBV (X/S/core)	*Saccharomyces cerevisiae*	Stable	Chronic HBV	Phase 2	NCT01943799 NCT02174276	[73]
HCV	HCV (NS3/core)	*Saccharomyces cerevisiae*	Stable	Chronic HCV	Phase 2	NCT00606086	[74]

X: hepatitis B regulatory protein; S: hepatitis B surface antigen; NS3: hepatitis C nonstructural protein.

infection. The baculovirus-insect cell expression system, referred to as BEVS, is one of the most well-known and used systems for large-scale production of complex proteins and, most recently, for the development of subunit vaccines [57]. To date, there are three commercially available vaccines produced in insect cells for different indications: Cervarix (GSK) for cervical cancer, Flublok (Protein Sciences, now owned by Sanofi Pasteur) for influenza, and PROVENGE (Dendreon) for prostate cancer [58].

Importantly, the baculovirus expression system is not limited only to cultured cells. Insect larvae or pupae can be used for protein production. In the context of edible vaccines using insect larvae or pupae, silkworm *Bombyx mori* larvae or pupae have been commercially used for the production of recombinant proteins and also as a feasible delivery system for the vaccine [59, 60]. As mentioned above, the baculovirus-silkworm expression system is able to perform cotranslational and posttranslational modifications and also able to produce large amount and multiple proteins. Moreover, since baculovirus is unable to replicate in vertebral animals, it can be considered a GRAS. Furthermore, the presence of protease inhibitors and biocapsule-like fat in the silkworms may protect recombinant proteins from enzymatic digestion in the GIT [23, 61].

Several vaccine prototypes are currently under evaluation, and strong systemic immune protective responses support the use of silkworm as a mucosal vaccine vector, as shown, for example, by high immunogenicity in mice of the urease B subunit of *Helicobacter pylori* produced in silkworm [60, 62]. While the data collected so far support the possible use of baculovirus-silkworm vaccines as a promising edible vaccine platform, it is only approved for food ingestion in a few Asian countries.

1.6. Whole-Cell Yeast-Based Vaccines. The industrial usage of yeasts cells for production of heterologous proteins has been well described [63, 64]. Additionally, the capability of this system to perform posttranslational modifications, the GRAS status, and the cellular wall that could protect the antigen across the GIT make engineered yeasts an attractive vaccine delivery system [23, 65]. In addition, the major drawback of this system is hyperglycosylation of recombinant proteins, but it has been already addressed by generating defective N-glycosylation strains of yeasts [66, 67].

Whole-cell yeast-based vaccines have been studied for their ability to elicit an immune response. Remarkably, some preclinical studies based on orally administrated *Saccharomyces cerevisiae* and developed for different infectious agents, such as HPV and *Actinobacillus pleuropneumoniae*, showed that this delivery system is able to induce a protective mucosal and a systemic immune response [68–70].

Moreover, the increased immunogenicity of this delivery system could be explained by the adjuvant activity of β-glucans on the yeast cell wall, which demonstrates immunomodulatory and adjuvant effects through binding of innate pathogen receptors on macrophages, DC, and neutrophils [71]. Currently, two clinical trials have been developed: GS-4774 for HBV treatment and GI-5005 for hepatitis C virus (HCV) treatment (Table 2). Regarding the clinical trial for GS-4774, despite the positive results obtained from phase 1 [72], the second phase, conducted in virally suppressed, noncirrhotic patients with chronic HBV infection did not show a clinical benefit. However, other safety and efficacy studies have been conducted on another group of patients (in particular, in treatment-naïve patients with chronic HBV) [73]. Regarding the clinical trial for GI-5005, phases I and II reported promising results [74]. In particular, in this trial, GI-5005 was used also in combination with Peg-IFN/ribavirin. However, data on efficacy have not been published yet.

1.7. Lactic Acid Bacteria-Based Vaccines. Lactic acid bacteria (LAB) are Gram-positive, nonsporulating, and nonpathogenic bacteria that have been used for decades for the production and preservation of food as well as for therapeutic heterologous gene expression, like the production of different anti-human immunodeficiency virus (anti-HIV) antibodies (scFV-m9, dAb-m36, and dAb-m36.4) by *Lactobacillus jensenii* and the production and functional expression of the antilisterial bacteriocin EntA in *L. casei* [75–77]. Given these and the ability of LAB to elicit a specific immune response against recombinant foreign antigens, these bacteria have been considered potential candidates as mucosal vaccine vectors. This delivery system can confer protection against antigen degradation and, thanks to its uptake at the GIT level, can activate both innate and adaptive immune responses [78, 79].

Many LAB, in particular, *Lactobacillus spp* and *Bacillus subtilis*, were used in preclinical studies against different infectious diseases. Different results have been obtained from these studies, but an elicited immune response was observed in all of them. As an example, the production of high levels of specific IgA and systemic IgG after immunization with *bacillus* spores expressing toxin A peptide repeat was reported [80], while in another paper, *L. lactis* expressing HEV antigen ORF2 vaccine was tested and a specific Th2-based cell-mediated immune response was revealed as well as the production of specific mucosal IgA and serum IgG [81].

Another study reported a Th1/Th2 immune response elicited after the immunization with Csenolase-expressing *Bacillus subtilis* [82]. Another example is the oral administration of *B. subtilis* spores expressing urease B of *Helicobacter pylori* that provide protection against *Helicobacter* infection [83].

An important feature of LAB is their natural adjuvanticity and their immunomodulatory effects, although the molecular mechanism of these capabilities is not completely understood [84]. Moreover, other studies reported an effect on dendritic cell maturation and an induction of cytokine secretion [85, 86]. Despite the promising characteristics of recombinant LAB as mucosal vaccine vectors and given the encouraging results from murine studies, some aspects need to be taken into consideration, namely, the fact that vaccine strains cannot be considered avirulent, even if it could be listed as GRAS, due to potential transfer of antibiotic selection markers among microbes [78, 87]. Furthermore, other factors are important for the development of LAB-based vaccines. As an example, the necessity of a suitable delivery system since different administration routes produce different immune effects. Additionally, the role of specific adjuvants and the correct localization (intracellularly or on the bacterial surface) of each expressed antigen need consideration [88]. Overall, additional studies and clinical trials are needed for the development of efficient vaccines based on LAB.

A different carrier system based on nonrecombinant *Lactococcus lactis* bacteria was recently developed. This system, called Gram-positive enhancer matrix (GEM), is composed of the rigid peptidoglycan (PGN) cell wall of the bacterium resulting in a nonliving particle that preserves the shape and the size as the original bacterium [89]. GEMs are used in two different ways: mixed with vaccine antigens as adjuvants or as antigen protein carriers, with the antigens bound to the surface of GEMs.

Regarding the use of GEMs as adjuvants, because of their nature, GEMs are safer adjuvants compared to others. Moreover, they retain the inflammatory properties of live bacteria and enhanced specific mucosal and systemic immune responses of the influenza subunit vaccine [90–92]. Therefore, the use of GEMs was further examined in a study investigating the immune response elicited by intranasal delivery of the influenza subunit vaccine coadministrated with GEM (FluGEM). In detail, an influenza-specific memory B cell response and the presence of long-lived antibody-secreting plasma cells were reported. Additionally, this immune response was able to confer protection from influenza infections [91]. These important results obtained in murine studies have led to a phase I clinical trial which confirmed the positive preclinical data. Systemic hemagglutination inhibition (HAI) titers and local SIgA responses were reported. Further studies will assess if this immune response confers protection against the influenza virus [93].

GEMs have also been used as antigen protein carriers. In particular, antigens are bound to GEM through the presence of a PGN-binding tag (Protan) in the antigen. Several works used this vaccination strategy, and the data support the potential of GEMs as safe vaccine delivery vehicles and their ability to elicit systemic antibodies [94–97]. Moreover, GEMs are also able to present several antigens at the same time which could be helpful for the preparation of multivalent vaccines [98]. Furthermore, the delivery of an adjuvant (GEMs) and an antigen together has been correlated with enhanced vaccine immunogenicity [97]. Lastly, as opposed to a vaccine based on LAB, the absence of recombinant DNA avoids its dissemination into the environment. However, the inability of GEMs to colonize any compartment does not allow the reduction of the number of vaccine doses.

These promising premises allowed the development of a vaccine against respiratory syncytial virus (RSV). In particular, an intranasal formulation based on the trimeric RSV fusion protein coupled with GEMs and named SynGEM was developed. Also, in this case, positive results from studies in mice and rats have been obtained, and as for FluGEM, vaccination with SynGEM resulted in the induction of a robust systemic and mucosal immune response as well as a balanced cytokine profile. These data supported further study of this vaccine in phase I clinical trial, which is currently ongoing [97]. In conclusion, GEMs represent an interesting vaccination strategy either as adjuvant or as antigen protein carriers, but as in the case of vaccine based on LAB, further studies are needed.

1.8. The Intradermal Vaccine Delivery and Its Associated Immune Response. Another vaccine delivery route capable of triggering both systemic and mucosal immunities is the intradermal route, in which the antigen is delivered through the skin using recently developed self-administrable devices. In particular, the application of microneedle technology overcomes the skin permeation barrier imposed by the stratum corneum and facilitates antigen delivery. The efficacy of this new microneedle-based immunization approach is due to the presence of several types of immune cells (such as DCs, T lymphocytes, NK cells, macrophages, and mast cells) in the epithelium [99, 100]. In fact, the cells that are responsible for triggering the inflammation cascade in the skin are the Langerhans cells (comprising 2-4% of epithelial cells). Langerhans cells are a specific DC subset that migrates into the lymph node following antigen capture and aids in the initiation of an adaptive immune response [101]. These cells are also efficiently stimulated by pathogen-associated molecular patterns (PAMPs) using an array of germline-encoded pattern recognition receptors (PRR), including toll-like receptors (TLR) and langerin (CD207) [100]. Importantly, skin resident mast cells are also key drivers of the innate immune response in the skin through the release of granules containing inflammatory mediators [102].

1.9. Intradermal Vaccination. Using conventional syringes for intramuscular or subcutaneous vaccinations, large volumes of vaccine solution can be injected ($\geq$1 mL). Thus, the choice of the muscle or hypodermis as vaccination targets is mainly based on convenience [99]. Intradermal immunization for vaccine delivery is an upcoming strategy showing significant advantages over conventional vaccination routes. In particular, in the last few years, intradermal vaccination has gained momentum as an alternative and more effective

Table 3: Status of development of some intradermal vaccines.

Pathogen	Formulation/antigen	Indication	Clinical trial status	Clinical trial ID	Refs
Influenza virus	Split virus	Influenzas A and B	Approved	NCT01712984, NCT02563093, NCT02258334, NCT01946438	[118]
Enterotoxigenic *E. coli*	dmLT*	Gastroenteritis	Phase 1	NCT02531685	[119]
HBV	HBsAg	Hepatitis B	Phase 1	NCT02186977	[120]
Dengue virus	Attenuated virus	Dengue fever	Phase 1	NCT01765426	[121]
Poliovirus	Inactivated virus	Poliomyelitis	Phase 3	NCT03239496	[122]
HIV-1	HIV-1 DNA	AIDS	Phase 2a	PACTR2010050002122368	[123]

*dmLT: double mutant heat-labile enterotoxin.

vaccine delivery route, both from a scientific and a commercial point of view (Table 3).

Intradermal vaccination designates the delivery of an antigen directly into the dermis with a syringe, a needle, a microneedle, or a pressure injector. The standard intradermal immunization technique was invented by the French physician Charles Mantoux in 1910, while he was developing the tuberculin test. This technique allows the injection of 100-200 μL of vaccine solution. However, Mantoux's technique requires skilled medical personnel to be performed [103]. Recent advancements have led to the development of techniques and instruments that can overcome the difficulties associated with intradermal administration [104]. In fact, different devices have been developed over the years for intradermal vaccination. Among them, solid microneedles, particle injectors, and self-administrable patches with coated microprojections or biodegradable needles have been described [105]. As previously mentioned, intradermal vaccination can induce mucosal and systemic immunities. These immunological capabilities, coupled with its ease of access, make the intradermal route an attractive vaccination delivery target [106].

Intradermal vaccination has been demonstrated to be very safe. In fact, novel devices involve the use of needles with a smaller size than the usual (25 μm and 1 mm) and make it possible to bypass the corneous layer of epidermis by creating transient micropores in the cutaneous tissues. Even if some studies have shown that intradermal vaccination can be associated with a higher incidence of local reactogenicity, including primarily mild pain, swelling, and redness, systemic side effects have not been reported. In fact, the intradermal route limits the transfer of vaccine components to the blood circulation (and the risk of septic shock) and the possible toxicity due to hepatic first-pass effect [107]. Typically, when present, local effects resolve quickly, as reported in a study comparing the safety and immunogenicity of a large number of intradermal versus intramuscular influenza vaccines [108].

Another important aspect is the possibility of improving the immunogenicity of various vaccines in immunocompromised hosts as well as during pregnancy via the intradermal route [109, 110]. As an example, it has been reported that the HBV vaccine fails to yield seroconversion in 3-5% of recipients. However, a significant improvement was observed following intradermal vaccination [111]. Additionally, it has been demonstrated that in patients on dialysis or in HIV-positive subjects, the intradermal route was more immunogenic than the standard intramuscular route [112].

From a commercial point of view, intradermal vaccination has been primarily explored for its ability to elicit equivalent antibody responses at lower doses, a phenomenon typically described as "dose sparing" [113]. In this regard, the advantage of a low dose is most evident in high-surge situations, such as during pandemic and seasonal influenza waves, in which large populations are at an increased risk and large amounts of new antigen preparations are quickly required each year [114–116]. Above all, dose sparing is also important in a large-scale setting and in reducing the production-associated costs, especially in developing countries, where the price of the vaccine limits its use and coverage. In this regard, the U.S. Food and Drug Administration (FDA) approved the trivalent inactivated intradermal influenza vaccine for use in adults 18-64 years of age for use during the 2012-2013 season, and a quadrivalent formulation was subsequently approved in 2014. However, similar to intramuscular vaccines, the formulation of these approved intradermal vaccines is liquid and thus still dependent on the cold chain and administered through a syringe. For these reasons, novel dried solid microneedle devices, while eliciting comparable immunogenicity to intramuscular-administered vaccines, represent an innovative approach to facilitate self-administration and allow vaccine storage at room temperature [117].

2. Conclusions

Infectious diseases represent a global concern, and the most effective strategy to reduce them is vaccination. Unfortunately, not every disease can currently be prevented through vaccines. However, many strategies have been developed against infectious agents, such as the generation of neutralizing antibodies, antibiotics, and antiviral drugs [124–130], and innovative approaches are currently under development [131–133].

Many vaccines have been developed and approved against various pathogens, and countless studies have been conducted to improve their efficacy by testing new adjuvants and performing the rational identification of the antigen formulations and pathogen contaminations [134–136]. Promising results have been also achieved by changing the delivery strategy. In fact, most of the approved vaccines are administrated by injection with intrinsic limitations like

Table 4: Edible and intradermal vaccines: pros and cons.

Route of administration	Host	Pros	Cons
Edible	Plant	Mucosal and systemic immunities, scale-up production, stable transformation, transient transformation, no antigen purification, long-term storage at RT, antigen bioencapsulation, no microbial contaminations	Lack of a proper dosing strategy, improper glycosylation, low antigen expression yields, unstable antigen expression
	Algae	Mucosal and systemic immunities, scale-up production (bioreactors), fast biomass accumulation, easy stable transformation, antigen bioencapsulation, long-term storage at RT	Improper glycosylation, low antigen expression yields
	Insect	Mucosal and systemic immunities, cotranslational modifications, posttranslational modifications, high antigen expression yields, antigen bioencapsulation, stable transformation, transient transformation, high immunogenicity	Improper glycosylation; further studies are needed; cultural barrier
	Yeast	Mucosal and systemic immunities, posttranslational modifications, antigen bioencapsulation, high immunogenicity	Inaccurate glycosylation; further studies are needed
	LAB	Mucosal and systemic immunities, antigen bioencapsulation, high immunogenicity	Possible transfer of antibiotic selection markers
Intradermal		Mucosal and systemic immunities, no systemic side effects, dose sparing, storage at room temperature	Trained personnel for administration, local reactogenicity

LAB: lactic acid bacteria; RT: room temperature.

those concerning the immunological aspect. Injected vaccines are able to elicit a strong humoral immunity but a weak cellular response. In addition, this type of administration is strongly associated with a systemic immunity but with a lack of mucosal response, which is helpful to block the early stages of infection since most pathogens infect through the mucosal membranes.

For these reasons, new vaccination strategies have been proposed. In particular, edible vaccines, triggering the GALT, and intradermal approaches, involving Langerhans cells, are able to elicit both a mucosal and a systemic immune response. The increased knowledge of these approaches has led to the progression of many preclinical studies and several promising clinical trials (Tables 1, 2, and 3). Moreover, these vaccine strategies are considered safe and cost-effective as no extensive antigen processing is needed [137, 138] and they are easy to administrate (Table 4). In fact, due to the opportunity of self-administration and ease of distribution compared to an injection-based approach, these two vaccination systems could improve the overall coverage.

There remain a number of obstacles and drawbacks associated with each antigen delivery platform that still need to be addressed (Table 4). Presently there are no FDA-approved compounds for edible vaccination, but new emerging technologies like nanoparticles (NPs) could help to control antigen bioavailability to avoid mucosal tolerance. NPs are particles with a mean size of 10-100 nm (up to 2000 nm), which can be used as carriers and/or adjuvants in vaccine preparation [139–141]. Moreover, NPs can be targeted to specific cell populations. As an example, NPs can be coated with antibodies recognizing a surface protein on dendritic cells [142, 143]. This approach enabled a more accurate measurement of the quantity of antigen required to elicit an immune response [144]. Finally, a more efficient immunization was demonstrated using NP-based approaches combined with an intradermal vaccine delivery [145], while oral delivery needed further investigations as they have been tested only *in vitro* [146, 147].

In conclusion, novel approaches eliciting a stronger mucosal response are showing promising results both in preclinical and clinical studies. Further studies are needed to implement and improve these delivery systems; however, mucosal delivery is becoming the most preferred mode of vaccination.

Conflicts of Interest

The authors declare that they have no conflicts of interest.

Authors' Contributions

E.C. and V.C. contributed equally to this work.

References

[1] Centers for Disease Control and Prevention (CDC), "Ten great public health achievements—United States, 1900-1999," *Morbidity and Mortality Weekly Report*, vol. 281, no. 16, pp. 1481–1483, 1999.

[2] R. Rappuoli, H. I. Miller, and S. Falkow, "The intangible value of vaccination," *Science*, vol. 297, no. 5583, pp. 937–939, 2002.

[3] J. Wang, L. Thorson, R. W. Stokes et al., "Single mucosal, but not parenteral, immunization with recombinant adenoviral-based vaccine provides potent protection from pulmonary tuberculosis," *Journal of Immunology*, vol. 173, no. 10, pp. 6357–6365, 2004.

[4] N. Lycke and M. Bemark, "Mucosal adjuvants and long-term memory development with special focus on CTA1-DD and other ADP-ribosylating toxins," *Mucosal Immunology*, vol. 3, no. 6, pp. 556–566, 2010.

[5] N. Lycke, "Recent progress in mucosal vaccine development: potential and limitations," *Nature Reviews Immunology*, vol. 12, no. 8, pp. 592–605, 2012.

[6] Y.-H. Fu, J.-S. He, X.-B. Wang et al., "A prime–boost vaccination strategy using attenuated *Salmonella typhimurium* and a replication-deficient recombinant adenovirus vector elicits protective immunity against human respiratory syncytial virus," *Biochemical and Biophysical Research Communications*, vol. 395, no. 1, pp. 87–92, 2010.

[7] J. Holmgren and C. Czerkinsky, "Mucosal immunity and vaccines," *Nature Medicine*, vol. 11, pp. S45–S53, 2005.

[8] P. Brandtzaeg, "Function of mucosa-associated lymphoid tissue in antibody formation," *Immunological Investigations*, vol. 39, no. 4-5, pp. 303–355, 2010.

[9] G. Dietrich, M. Griot-Wenk, I. C. Metcalfe, A. B. Lang, and J. F. Viret, "Experience with registered mucosal vaccines," *Vaccine*, vol. 21, no. 7-8, pp. 678–683, 2003.

[10] J. Kunisawa, Y. Kurashima, and H. Kiyono, "Gut-associated lymphoid tissues for the development of oral vaccines," *Advanced Drug Delivery Reviews*, vol. 64, no. 6, pp. 523–530, 2012.

[11] J. E. Vela Ramirez, L. A. Sharpe, and N. A. Peppas, "Current state and challenges in developing oral vaccines," *Advanced Drug Delivery Reviews*, vol. 114, pp. 116–131, 2017.

[12] D. J. Brayden, M. A. Jepson, and A. W. Baird, "Keynote review: intestinal Peyer's patch M cells and oral vaccine targeting," *Drug Discovery Today*, vol. 10, no. 17, pp. 1145–1157, 2005.

[13] S. Fagarasan, S. Kawamoto, O. Kanagawa, and K. Suzuki, "Adaptive immune regulation in the gut: T cell-dependent and T cell-independent IgA synthesis," *Annual Review of Immunology*, vol. 28, no. 1, pp. 243–273, 2010.

[14] M. Fischer and R. Küppers, "Human IgA- and IgM-secreting intestinal plasma cells carry heavily mutated VH region genes," *European Journal of Immunology*, vol. 28, no. 9, pp. 2971–2977, 1998.

[15] C. Lindner, I. Thomsen, B. Wahl et al., "Diversification of memory B cells drives the continuous adaptation of secretory antibodies to gut microbiota," *Nature Immunology*, vol. 16, no. 8, pp. 880–888, 2015.

[16] R. Burioni, F. Canducci, D. Saita et al., "Antigen-driven evolution of B lymphocytes in coronary atherosclerotic plaques," *Journal of Immunology*, vol. 183, no. 4, pp. 2537–2544, 2009.

[17] A. M. Mowat, O. R. Millington, and F. G. Chirdo, "Anatomical and cellular basis of immunity and tolerance in the intestine," *Journal of Pediatric Gastroenterology and Nutrition*, vol. 39, Supplement 3, pp. S723–S724, 2004.

[18] K. Hase, K. Kawano, T. Nochi et al., "Uptake through glycoprotein 2 of $FimH^+$ bacteria by M cells initiates mucosal immune response," *Nature*, vol. 462, no. 7270, pp. 226–230, 2009.

[19] S. Rosales-Mendoza and R. Nieto-Gómez, "Green therapeutic biocapsules: using plant cells to orally deliver biopharmaceuticals," *Trends in Biotechnology*, vol. 36, no. 10, pp. 1054–1067, 2018.

[20] M. Hernández, G. Rosas, J. Cervantes, G. Fragoso, S. Rosales-Mendoza, and E. Sciutto, "Transgenic plants: a 5-year update on oral antipathogen vaccine development," *Expert Review of Vaccines*, vol. 13, no. 12, pp. 1523–1536, 2014.

[21] E. P. Rybicki, "Plant-based vaccines against viruses," *Virology Journal*, vol. 11, no. 1, pp. 205–220, 2014.

[22] N. Landry, B. J. Ward, S. Trépanier et al., "Preclinical and clinical development of plant-made virus-like particle vaccine against avian H5N1 influenza," *PLoS One*, vol. 5, no. 12, article e15559, 2010.

[23] S. Rosales-Mendoza, C. Angulo, and B. Meza, "Food-grade organisms as vaccine biofactories and oral delivery vehicles," *Trends in Biotechnology*, vol. 34, no. 2, pp. 124–136, 2016.

[24] H.-T. Chan and H. Daniell, "Plant-made oral vaccines against human infectious diseases-are we there yet?," *Plant Biotechnology Journal*, vol. 13, no. 8, pp. 1056–1070, 2015.

[25] M. T. Waheed, M. Sameeullah, F. A. Khan et al., "Need of cost-effective vaccines in developing countries: what plant biotechnology can offer?," *SpringerPlus*, vol. 5, no. 1, p. 65, 2016.

[26] Q. Chen and K. R. Davis, "The potential of plants as a system for the development and production of human biologics," *F1000Res*, vol. 5, p. 912, 2016.

[27] I. Khan, R. M. Twyman, E. Arcalis, and E. Stoger, "Using storage organelles for the accumulation and encapsulation of recombinant proteins," *Biotechnology Journal*, vol. 7, no. 9, pp. 1099–1108, 2012.

[28] F. Takaiwa, "Seed-based oral vaccines as allergen-specific immunotherapies," *Human Vaccines*, vol. 7, no. 3, pp. 357–366, 2011.

[29] M. Sack, A. Hofbauer, R. Fischer, and E. Stoger, "The increasing value of plant-made proteins," *Current Opinion in Biotechnology*, vol. 32, pp. 163–170, 2015.

[30] E. P. Rybicki, "Plant-produced vaccines: promise and reality," *Drug Discovery Today*, vol. 14, no. 1-2, pp. 16–24, 2009.

[31] K.-C. Kwon, R. Nityanandam, J. S. New, and H. Daniell, "Oral delivery of bioencapsulated exendin-4 expressed in chloroplasts lowers blood glucose level in mice and stimulates insulin secretion in beta-TC6 cells," *Plant Biotechnology Journal*, vol. 11, no. 1, pp. 77–86, 2013.

[32] C. Concha, R. Cañas, J. Macuer et al., "Disease prevention: an opportunity to expand edible plant-based vaccines?," *Vaccine*, vol. 5, no. 2, pp. 14–23, 2017.

[33] M. T. Waheed, H. Ismail, J. Gottschamel, B. Mirza, and A. G. Lössl, "Plastids: the green frontiers for vaccine production," *Frontiers in Plant Science*, vol. 6, article 1005, 2015.

[34] M. Oey, M. Lohse, B. Kreikemeyer, and R. Bock, "Exhaustion of the chloroplast protein synthesis capacity by massive expression of a highly stable protein antibiotic," *The Plant Journal*, vol. 57, no. 3, pp. 436–445, 2009.

[35] T. Ruhlman, D. Verma, N. Samson, and H. Daniell, "The role of heterologous chloroplast sequence elements in transgene integration and expression," *Plant Physiology*, vol. 152, no. 4, pp. 2088–2104, 2010.

[36] A. G. Lössl and M. T. Waheed, "Chloroplast-derived vaccines against human diseases: achievements, challenges and scopes," *Plant Biotechnology Journal*, vol. 9, no. 5, pp. 527–539, 2011.

[37] T. V. Komarova, S. Baschieri, M. Donini, C. Marusic, E. Benvenuto, and Y. L. Dorokhov, "Transient expression systems for plant-derived biopharmaceuticals," *Expert Review of Vaccines*, vol. 9, no. 8, pp. 859–876, 2010.

[38] A. M. Walmsley, M. L. Alvarez, Y. Jin et al., "Expression of the B subunit of *Escherichia coli* heat-labile enterotoxin as a fusion protein in transgenic tomato," *Plant Cell Reports*, vol. 21, no. 10, pp. 1020–1026, 2003.

[39] Y. Shoji, C. E. Farrance, J. Bautista et al., "A plant-based system for rapid production of influenza vaccine antigens," *Influenza and Other Respiratory Viruses*, vol. 6, no. 3, pp. 204–210, 2012.

[40] H. Zhang, M. Liu, Y. Li et al., "Oral immunogenicity and protective efficacy in mice of a carrot-derived vaccine candidate expressing UreB subunit against *Helicobacter pylori*," *Protein Expression and Purification*, vol. 69, no. 2, pp. 127–131, 2010.

[41] N. Pogrebnyak, M. Golovkin, V. Andrianov et al., "Severe acute respiratory syndrome (SARS) S protein production in plants: development of recombinant vaccine," *Proceedings of the National Academy of Sciences of the United States of America*, vol. 102, no. 25, pp. 9062–9067, 2005.

[42] C. O. Tacket, H. S. Mason, G. Losonsky, J. D. Clements, M. M. Levine, and C. J. Arntzen, "Immunogenicity in humans of a recombinant bacterial antigen delivered in a transgenic potato," *Nature Medicine*, vol. 4, no. 5, pp. 607–609, 1998.

[43] C. O. Tacket, M. F. Pasetti, R. Edelman, J. A. Howard, and S. Streatfield, "Immunogenicity of recombinant LT-B delivered orally to humans in transgenic corn," *Vaccine*, vol. 22, no. 31-32, pp. 4385–4389, 2004.

[44] C. O. Tacket, H. S. Mason, G. Losonsky, M. K. Estes, M. M. Levine, and C. J. Arntzen, "Human immune responses to a novel Norwalk virus vaccine delivered in transgenic potatoes," *The Journal of Infectious Diseases*, vol. 182, no. 1, pp. 302–305, 2000.

[45] V. Yusibov, D. C. Hooper, S. V. Spitsin et al., "Expression in plants and immunogenicity of plant virus-based experimental rabies vaccine," *Vaccine*, vol. 20, no. 25-26, pp. 3155–3164, 2002.

[46] J. Kapusta, A. Modelska, M. Figlerowicz et al., "A plant-derived edible vaccine against hepatitis B virus," *The FASEB Journal*, vol. 13, no. 13, pp. 1796–1799, 1999.

[47] Y. Thanavala, M. Mahoney, S. Pal et al., "Immunogenicity in humans of an edible vaccine for hepatitis B," *Proceedings of the National Academy of Sciences of the United States of America*, vol. 102, no. 9, pp. 3378–3382, 2005.

[48] T. Nochi, Y. Yuki, Y. Katakai et al., "A rice-based oral cholera vaccine induces macaque-specific systemic neutralizing antibodies but does not influence pre-existing intestinal immunity," *Journal of Immunology*, vol. 183, no. 10, pp. 6538–6544, 2009.

[49] Y. Yuki, M. Mejima, S. Kurokawa et al., "Induction of toxin-specific neutralizing immunity by molecularly uniform rice-based oral cholera toxin B subunit vaccine without plant-associated sugar modification," *Plant Biotechnology Journal*, vol. 11, no. 7, pp. 799–808, 2013.

[50] K. Kashima, Y. Yuki, M. Mejima et al., "Good manufacturing practices production of a purification-free oral cholera vaccine expressed in transgenic rice plants," *Plant Cell Reports*, vol. 35, no. 3, pp. 667–679, 2016.

[51] S. Kurokawa, R. Nakamura, M. Mejima et al., "MucoRice-cholera toxin B-subunit, a rice-based oral cholera vaccine, down-regulates the expression of α-amylase/trypsin inhibitor-likeprotein family as major rice allergens," *Journal of Proteome Research*, vol. 12, no. 7, pp. 3372–3382, 2013.

[52] E. A. Specht and S. P. Mayfield, "Algae-based oral recombinant vaccines," *Frontiers in Microbiology*, vol. 5, p. 60, 2014.

[53] S. E. Franklin and S. P. Mayfield, "Recent developments in the production of human therapeutic proteins in eukaryotic algae," *Expert Opinion on Biological Therapy*, vol. 5, no. 2, pp. 225–235, 2005.

[54] R. Franconi, O. C. Demurtas, and S. Massa, "Plant-derived vaccines and other therapeutics produced in contained systems," *Expert Review of Vaccines*, vol. 9, no. 8, pp. 877–892, 2010.

[55] I. A. J. Dreesen, G. C. E. Hamri, and M. Fussenegger, "Heat-stable oral alga-based vaccine protects mice from *Staphylococcus aureus* infection," *Journal of Biotechnology*, vol. 145, no. 3, pp. 273–280, 2010.

[56] D.-M. He, K.-X. Qian, G.-F. Shen et al., "Recombination and expression of classical swine fever virus (CSFV) structural protein E2 gene in *Chlamydomonas reinhardtii* chroloplasts," *Colloids and Surfaces B: Biointerfaces*, vol. 55, no. 1, pp. 26–30, 2007.

[57] J. A. Mena and A. A. Kamen, "Insect cell technology is a versatile and robust vaccine manufacturing platform," *Expert Review of Vaccines*, vol. 10, no. 7, pp. 1063–1081, 2011.

[58] I. Legastelois, S. Buffin, I. Peubez, C. Mignon, R. Sodoyer, and B. Werle, "Non-conventional expression systems for the production of vaccine proteins and immunotherapeutic molecules," *Human Vaccines & Immunotherapeutics*, vol. 13, no. 4, pp. 947–961, 2017.

[59] Z. Gong, Y. Jin, and Y. Zhang, "Oral administration of a cholera toxin B subunit-insulin fusion protein produced in silkworm protects against autoimmune diabetes," *Journal of Biotechnology*, vol. 119, no. 1, pp. 93–105, 2005.

[60] X. Zhang, W. Shen, Y. Lu et al., "Expression of UreB and HspA of *Helicobacter pylori* in silkworm pupae and identification of its immunogenicity," *Molecular Biology Reports*, vol. 38, no. 5, pp. 3173–3180, 2011.

[61] T. Kato, M. Kajikawa, K. Maenaka, and E. Y. Park, "Silkworm expression system as a platform technology in life science," *Applied Microbiology and Biotechnology*, vol. 85, no. 3, pp. 459–470, 2010.

[62] H. Feng, G.-Q. Hu, H.-L. Wang et al., "Canine parvovirus VP2 protein expressed in silkworm pupae self-assembles into virus-like particles with high immunogenicity," *PLoS One*, vol. 9, no. 1, article e79575, 2014.

[63] D. Mattanovich, P. Branduardi, L. Dato, B. Gasser, M. Sauer, and D. Porro, "Recombinant protein production in yeasts," *Methods in Molecular Biology*, vol. 824, pp. 329–358, 2012.

[64] T. Treebupachatsakul, H. Nakazawa, H. Shinbo et al., "Heterologously expressed *Aspergillus aculeatus* β-glucosidase in *Saccharomyces cerevisiae* is a cost-effective alternative to commercial supplementation of β-glucosidase in industrial ethanol production using *Trichoderma reesei* cellulases," *Journal of Bioscience and Bioengineering*, vol. 121, no. 1, pp. 27–35, 2016.

[65] D. Jacob, C. Ruffie, M. Dubois et al., "Whole *Pichia pastoris* yeast expressing measles virus nucleoprotein as a production and delivery system to multimerize *Plasmodium* antigens," *PLoS One*, vol. 9, no. 1, article e86658, 2014.

[66] K. Tomimoto, Y. Fujita, T. Iwaki et al., "Protease-deficient *Saccharomyces cerevisiae* strains for the synthesis of human-compatible glycoproteins," *Bioscience, Biotechnology, and Biochemistry*, vol. 77, no. 12, pp. 2461–2466, 2013.

[67] M. Han and X. Yu, "Enhanced expression of heterologous proteins in yeast cells via the modification of *N*-glycosylation sites," *Bioengineered*, vol. 6, no. 2, pp. 115–118, 2015.

[68] S. J. Shin, J. L. Bae, Y.-W. Cho et al., "Induction of antigen-specific immune responses by oral vaccination with *Saccharomyces cerevisiae* expressing *Actinobacillus pleuropneumoniae* ApxIIA," *FEMS Immunology and Medical Microbiology*, vol. 43, no. 2, pp. 155–164, 2005.

[69] A. Bolhassani, M. Muller, F. Roohvand et al., "Whole recombinant *Pichia pastoris* expressing HPV16 L1 antigen is superior in inducing protection against tumor growth as compared to killed transgenic *Leishmania*," *Human Vaccines & Immunotherapeutics*, vol. 10, no. 12, pp. 3499–3508, 2014.

[70] H. J. Kim, J. Y. Lee, H. A. Kang, Y. Lee, E. J. Park, and H. J. Kim, "Oral immunization with whole yeast producing viral capsid antigen provokes a stronger humoral immune response than purified viral capsid antigen," *Letters in Applied Microbiology*, vol. 58, no. 3, pp. 285–291, 2014.

[71] H. Huang, G. R. Ostroff, C. K. Lee, C. A. Specht, and S. M. Levitz, "Characterization and optimization of the glucan particle-based vaccine platform," *Clinical and Vaccine Immunology*, vol. 20, no. 10, pp. 1585–1591, 2013.

[72] A. Gaggar, C. Coeshott, D. Apelian et al., "Safety, tolerability and immunogenicity of GS-4774, a hepatitis B virus-specific therapeutic vaccine, in healthy subjects: a randomized study," *Vaccine*, vol. 32, no. 39, pp. 4925–4931, 2014.

[73] A. S. Lok, C. Q. Pan, S.-H. B. Han et al., "Randomized phase II study of GS-4774 as a therapeutic vaccine in virally suppressed patients with chronic hepatitis B," *Journal of Hepatology*, vol. 65, no. 3, pp. 509–516, 2016.

[74] A. A. Haller, G. M. Lauer, T. H. King et al., "Whole recombinant yeast-based immunotherapy induces potent T cell responses targeting HCV NS3 and core proteins," *Vaccine*, vol. 25, no. 8, pp. 1452–1463, 2007.

[75] A. Marcobal, X. Liu, W. Zhang et al., "Expression of human immunodeficiency virus type 1 neutralizing antibody fragments using human vaginal lactobacillus," *AIDS Research and Human Retroviruses*, vol. 32, no. 10-11, pp. 964–971, 2016.

[76] J. J. Jiménez, D. B. Diep, J. Borrero et al., "Cloning strategies for heterologous expression of the bacteriocin enterocin A by *Lactobacillus sakei* Lb790, *Lb. plantarum* NC8 and *Lb. casei* CECT475," *Microbial Cell Factories*, vol. 14, no. 1, p. 166, 2015.

[77] T. W. Overton, "Recombinant protein production in bacterial hosts," *Drug Discovery Today*, vol. 19, no. 5, pp. 590–601, 2014.

[78] K. L. Roland, S. A. Tinge, K. P. Killeen, and S. K. Kochi, "Recent advances in the development of live, attenuated bacterial vectors," *Current Opinion in Molecular Therapeutics*, vol. 7, no. 1, pp. 62–72, 2005.

[79] X. Wang, X. Zhang, D. Zhou, and R. Yang, "Live-attenuated *Yersinia pestis* vaccines," *Expert Review of Vaccines*, vol. 12, no. 6, pp. 677–686, 2013.

[80] P. Permpoonpattana, H. A. Hong, J. Phetcharaburanin et al., "Immunization with *Bacillus* spores expressing toxin A peptide repeats protects against infection with *Clostridium difficile* strains producing toxins A and B," *Infection and Immunity*, vol. 79, no. 6, pp. 2295–2302, 2011.

[81] S. Gao, D. Li, Y. Liu, E. Zha, T. Zhou, and X. Yue, "Oral immunization with recombinant hepatitis E virus antigen displayed on the *Lactococcus lactis* surface enhances ORF2-specific mucosal and systemic immune responses in mice," *International Immunopharmacology*, vol. 24, no. 1, pp. 140–145, 2015.

[82] X. Wang, W. Chen, Y. Tian et al., "Surface display of *Clonorchis sinensis* enolase on Bacillus subtilis spores potentializes an oral vaccine candidate," *Vaccine*, vol. 32, no. 12, pp. 1338–1345, 2014.

[83] Z. Zhou, S. Gong, X.-M. Li et al., "Expression of *Helicobacter pylori* urease B on the surface of *Bacillus subtilis* spores," *Journal of Medical Microbiology*, vol. 64, Part_1, pp. 104–110, 2015.

[84] K. Szatraj, A. K. Szczepankowska, and M. Chmielewska-Jeznach, "Lactic acid bacteria - promising vaccine vectors: possibilities, limitations, doubts," *Journal of Applied Microbiology*, vol. 123, no. 2, pp. 325–339, 2017.

[85] J. You, H. Dong, E. R. Mann, S. C. Knight, and P. Yaqoob, "Probiotic modulation of dendritic cell function is influenced by ageing," *Immunobiology*, vol. 219, no. 2, pp. 138–148, 2014.

[86] P. Rigaux, C. Daniel, M. Hisbergues et al., "Immunomodulatory properties of Lactobacillus plantarum and its use as a recombinant vaccine against mite allergy," *Allergy*, vol. 64, no. 3, pp. 406–414, 2009.

[87] N. Toomey, D. Bolton, and S. Fanning, "Characterisation and transferability of antibiotic resistance genes from lactic acid bacteria isolated from Irish pork and beef abattoirs," *Research in Microbiology*, vol. 161, no. 2, pp. 127–135, 2010.

[88] M. Wang, Z. Gao, Y. Zhang, and L. Pan, "Lactic acid bacteria as mucosal delivery vehicles: a realistic therapeutic option," *Applied Microbiology and Biotechnology*, vol. 100, no. 13, pp. 5691–5701, 2016.

[89] T. Bosma, R. Kanninga, J. Neef et al., "Novel surface display system for proteins on non-genetically modified Gram-positive bacteria," *Applied and Environmental Microbiology*, vol. 72, no. 1, pp. 880–889, 2006.

[90] V. Saluja, M. R. Visser, W. ter Veer et al., "Influenza antigen-sparing by immune stimulation with Gram-positive enhancer matrix (GEM) particles," *Vaccine*, vol. 28, no. 50, pp. 7963–7969, 2010.

[91] V. Saluja, J. P. Amorij, M. L. van Roosmalen et al., "Intranasal delivery of influenza subunit vaccine formulated with GEM particles as an adjuvant," *The AAPS Journal*, vol. 12, no. 2, pp. 109–116, 2010.

[92] Y. Zhang, X. Yu, L. Hou et al., "CTA1: purified and display onto gram-positive enhancer matrix (GEM) particles as mucosal adjuvant," *Protein Expression and Purification*, vol. 141, pp. 19–24, 2018.

[93] A. Wyszyńska, P. Kobierecka, J. Bardowski, and E. K. Jagusztyn-Krynicka, "Lactic acid bacteria—20 years exploring their potential as live vectors for mucosal vaccination," *Applied Microbiology and Biotechnology*, vol. 99, no. 7, pp. 2967–2977, 2015.

[94] S. A. L. Audouy, M. L. van Roosmalen, J. Neef et al., "*Lactococcus lactis* GEM particles displaying pneumococcal antigens induce local and systemic immune responses following intranasal immunization," *Vaccine*, vol. 24, no. 26, pp. 5434–5441, 2006.

[95] S. A. L. Audouy, S. van Selm, M. L. van Roosmalen et al., "Development of lactococcal GEM-based pneumococcal vaccines," *Vaccine*, vol. 25, no. 13, pp. 2497–2506, 2007.

[96] R. Ramasamy, S. Yasawardena, A. Zomer, G. Venema, J. Kok, and K. Leenhouts, "Immunogenicity of a malaria parasite

antigen displayed by *Lactococcus lactis* in oral immunisations," *Vaccine*, vol. 24, no. 18, pp. 3900–3908, 2006.

[97] N. Van Braeckel-Budimir, B. J. Haijema, and K. Leenhouts, "Bacterium-like particles for efficient immune stimulation of existing vaccines and new subunit vaccines in mucosal applications," *Frontiers in Immunology*, vol. 4, p. 282, 2013.

[98] P. Kobierecka, A. Wyszyńska, M. Maruszewska et al., "Lactic acid bacteria as a surface display platform for *Campylobacter jejuni* antigens," *Journal of Molecular Microbiology and Biotechnology*, vol. 25, no. 1, pp. 1–10, 2015.

[99] J.-F. Nicolas and B. Guy, "Intradermal, epidermal and transcutaneous vaccination: from immunology to clinical practice," *Expert Review of Vaccines*, vol. 7, no. 8, pp. 1201–1214, 2008.

[100] S. Henri, M. Guilliams, L. F. Poulin et al., "Disentangling the complexity of the skin dendritic cell network," *Immunology and Cell Biology*, vol. 88, no. 4, pp. 366–375, 2010.

[101] H. K. Lee and A. Iwasaki, "Innate control of adaptive immunity: dendritic cells and beyond," *Seminars in Immunology*, vol. 19, no. 1, pp. 48–55, 2007.

[102] J. M. Schröder, K. Reich, K. Kabashima et al., "Controversies in experimental dermatology: who is really in control of skin immunity under physiological circumstances - lymphocytes, dendritic cells or keratinocytes?," *Experimental Dermatology*, vol. 15, no. 11, pp. 913–916, 2006.

[103] P. H. Lambert and P. E. Laurent, "Intradermal vaccine delivery: will new delivery systems transform vaccine administration?," *Vaccine*, vol. 26, no. 26, pp. 3197–3208, 2008.

[104] J. A. Mikszta and P. E. Laurent, "Cutaneous delivery of prophylactic and therapeutic vaccines: historical perspective and future outlook," *Expert Review of Vaccines*, vol. 7, no. 9, pp. 1329–1339, 2008.

[105] S. Marshall, L. J. Sahm, and A. C. Moore, "The success of microneedle-mediated vaccine delivery into skin," *Human Vaccines & Immunotherapeutics*, vol. 12, no. 11, pp. 2975–2983, 2016.

[106] Z. Zheng, D. Diaz-Arévalo, H. Guan, and M. Zeng, "Noninvasive vaccination against infectious diseases," *Human Vaccines & Immunotherapeutics*, vol. 14, no. 7, pp. 1717–1733, 2018.

[107] C. Ponvert and P. Scheinmann, "Vaccine allergy and pseudo-allergy," *European Journal of Dermatology*, vol. 13, no. 1, pp. 10–15, 2003.

[108] F. Marra, F. Young, K. Richardson, and C. A. Marra, "A meta-analysis of intradermal versus intramuscular influenza vaccines: immunogenicity and adverse events," *Influenza and Other Respiratory Viruses*, vol. 7, no. 4, pp. 584–603, 2013.

[109] N. G. Rouphael and M. J. Mulligan, "Microneedle patch for immunization of immunocompromised hosts," *Oncotarget*, vol. 8, pp. 93311-93312, 2017.

[110] E. S. Esser, J. A. Pulit-Penaloza, H. Kalluri et al., "Microneedle patch delivery of influenza vaccine during pregnancy enhances maternal immune responses promoting survival and long-lasting passive immunity to offspring," *Scientific Reports*, vol. 7, no. 1, p. 5705, 2017.

[111] M. Filippelli, E. Lionetti, A. Gennaro et al., "Hepatitis B vaccine by intradermal route in non responder patients: an update," *World Journal of Gastroenterology*, vol. 20, no. 30, pp. 10383–10394, 2014.

[112] T. Chanchairujira, N. Chantaphakul, T. Thanwandee, and L. Ong-Ajyooth, "Efficacy of intradermal hepatitis B vaccination compared to intramuscular vaccination in hemodialysis patients," *Journal of the Medical Association of Thailand*, vol. 89, Supplement 2, pp. S33–S40, 2006.

[113] R. T. Kenney, S. A. Frech, L. R. Muenz, C. P. Villar, and G. M. Glenn, "Dose sparing with intradermal injection of influenza vaccine," *The New England Journal of Medicine*, vol. 351, no. 22, pp. 2295–2301, 2004.

[114] L. E. Brown, "The role of adjuvants in vaccines for seasonal and pandemic influenza," *Vaccine*, vol. 28, no. 50, pp. 8043–8045, 2010.

[115] J. Nordin, J. Mullooly, S. Poblete et al., "Influenza vaccine effectiveness in preventing hospitalizations and deaths in persons 65 years or older in Minnesota, New York, and Oregon: data from 3 health plans," *The Journal of Infectious Diseases*, vol. 184, no. 6, pp. 665–670, 2001.

[116] G. A. Sautto, G. A. Kirchenbaum, and T. M. Ross, "Towards a universal influenza vaccine: different approaches for one goal," *Virology Journal*, vol. 15, no. 1, p. 17, 2018.

[117] G. J. P. Fernando, J. Hickling, C. M. Jayashi Flores et al., "Safety, tolerability, acceptability and immunogenicity of an influenza vaccine delivered to human skin by a novel high-density microprojection array patch (Nanopatch™)," *Vaccine*, vol. 36, no. 26, pp. 3779–3788, 2018.

[118] G. J. Gorse, A. R. Falsey, A. Ozol-Godfrey, V. Landolfi, and P. H. Tsang, "Safety and immunogenicity of a quadrivalent intradermal influenza vaccine in adults," *Vaccine*, vol. 33, no. 9, pp. 1151–1159, 2015.

[119] S. S. El-Kamary, M. B. Cohen, A. L. Bourgeois et al., "Safety and immunogenicity of a single oral dose of recombinant double mutant heat-labile toxin derived from enterotoxigenic *Escherichia coli*," *Clinical and Vaccine Immunology*, vol. 20, no. 11, pp. 1764–1770, 2013.

[120] T. J. S. Van Mulder, S. Verwulgen, K. C. L. Beyers et al., "Assessment of acceptability and usability of new delivery prototype device for intradermal vaccination in healthy subjects," *Human Vaccines & Immunotherapeutics*, vol. 10, no. 12, pp. 3746–3753, 2014.

[121] L. A. Jackson, R. Rupp, A. Papadimitriou, D. Wallace, M. Raanan, and K. J. Moss, "A phase 1 study of safety and immunogenicity following intradermal administration of a tetravalent dengue vaccine candidate," *Vaccine*, vol. 36, no. 27, pp. 3976–3983, 2018.

[122] S. Resik, A. Tejeda, P. M. Lago et al., "Randomized controlled clinical trial of fractional doses of inactivated poliovirus vaccine administered intradermally by needle-free device in Cuba," *Journal of Infectious Diseases*, vol. 201, no. 9, pp. 1344–1352, 2010.

[123] P. J. Munseri, A. Kroidl, C. Nilsson et al., "Priming with a simplified intradermal HIV-1 DNA vaccine regimen followed by boosting with recombinant HIV-1 MVA vaccine is safe and immunogenic: a phase IIa randomized clinical trial," *PLoS One*, vol. 10, no. 4, article e0119629, 2015.

[124] R. A. Diotti, N. Mancini, N. Clementi et al., "Cloning of the first human anti-JCPyV/VP1 neutralizing monoclonal antibody: epitope definition and implications in risk stratification of patients under natalizumab therapy," *Antiviral Research*, vol. 108, pp. 94–103, 2014.

[125] N. Clementi, E. Criscuolo, F. Cappelletti et al., "Entry inhibition of HSV-1 and -2 protects mice from viral lethal challenge," *Antiviral Research*, vol. 143, pp. 48–61, 2017.

[126] R. A. Diotti, G. A. Sautto, L. Solforosi, N. Mancini, M. Clementi, and R. Burioni, "Neutralization activity and kinetics of two broad-range human monoclonal IgG1 derived from recombinant Fab fragments and directed against hepatitis C virus E2 glycoprotein," *The New Microbiologica*, vol. 35, no. 4, pp. 475–479, 2012.

[127] R. Burioni, F. Canducci, N. Mancini et al., "Monoclonal antibodies isolated from human B cells neutralize a broad range of H1 subtype influenza A viruses including swine-origin influenza virus (S-OIV)," *Virology*, vol. 399, no. 1, pp. 144–152, 2010.

[128] G. Sautto, N. Mancini, R. A. Diotti, L. Solforosi, M. Clementi, and R. Burioni, "Anti-hepatitis C virus E2 (HCV/E2) glycoprotein monoclonal antibodies and neutralization interference," *Antiviral Research*, vol. 96, no. 1, pp. 82–89, 2012.

[129] R. Burioni, Y. Matsuura, N. Mancini et al., "Diverging effects of human recombinant anti-hepatitis C virus (HCV) antibody fragments derived from a single patient on the infectivity of a vesicular stomatitis virus/HCV pseudotype," *Journal of Virology*, vol. 76, no. 22, pp. 11775–11779, 2002.

[130] L. Solforosi, N. Mancini, F. Canducci et al., "A phage display vector optimized for the generation of human antibody combinatorial libraries and the molecular cloning of monoclonal antibody fragments," *The New Microbiologica*, vol. 35, no. 3, pp. 289–294, 2012.

[131] N. Mancini, G. A. Sautto, N. Clementi, R. Burioni, and M. Clementi, "Chimeric antigen receptor (CAR)-redirected T cells: is there a place for them in infectious diseases?," *Clinical Microbiology and Infection*, vol. 21, no. 8, pp. 715-716, 2015.

[132] G. A. Sautto, K. Wisskirchen, N. Clementi et al., "Chimeric antigen receptor (CAR)-engineered T cells redirected against hepatitis C virus (HCV) E2 glycoprotein," *Gut*, vol. 65, no. 3, pp. 512–523, 2016.

[133] N. Mancini, L. Marrone, N. Clementi, G. A. Sautto, M. Clementi, and R. Burioni, "Adoptive T-cell therapy in the treatment of viral and opportunistic fungal infections," *Future Microbiology*, vol. 10, no. 4, pp. 665–682, 2015.

[134] M. Castelli, F. Cappelletti, R. A. Diotti et al., "Peptide-based vaccinology: experimental and computational approaches to target hypervariable viruses through the fine characterization of protective epitopes recognized by monoclonal antibodies and the identification of T-cell-activating peptides," *Clinical & Developmental Immunology*, vol. 2013, Article ID 521231, 12 pages, 2013.

[135] N. Clementi, N. Mancini, E. Criscuolo, F. Cappelletti, M. Clementi, and R. Burioni, "Epitope mapping by epitope excision, hydrogen/deuterium exchange, and peptide-panning techniques combined with in silico analysis," in *Monoclonal Antibodies: Methods and Protocols*, pp. 427–446, Humana Press, Totowa, NJ, USA, 2014.

[136] G. A. Sautto, G. A. Kirchenbaum, J. W. Ecker, A. G. Bebin-Blackwell, S. R. Pierce, and T. M. Ross, "Elicitation of broadly protective antibodies following infection with influenza viruses expressing H1N1 computationally optimized broadly reactive hemagglutinin antigens," *ImmunoHorizons*, vol. 2, no. 7, pp. 226–237, 2018.

[137] J. Li, M. Zeng, H. Shan, and C. Tong, "Microneedle patches as drug and vaccine delivery platform," *Current Medicinal Chemistry*, vol. 24, no. 22, pp. 2413–2422, 2017.

[138] Y. Hao, W. Li, X. Zhou, F. Yang, and Z. Y. Qian, "Microneedles-based transdermal drug delivery systems: a review," *Journal of Biomedical Nanotechnology*, vol. 13, no. 12, pp. 1581–1597, 2017.

[139] A. Seth, F. K. Ritchie, N. Wibowo, L. H. L. Lua, and A. P. J. Middelberg, "Non-carrier nanoparticles adjuvant modular protein vaccine in a particle-dependent manner," *PLoS One*, vol. 10, no. 3, article e0117203, 2015.

[140] A. E. Gregory, R. Titball, and D. Williamson, "Vaccine delivery using nanoparticles," *Frontiers in Cellular and Infection Microbiology*, vol. 3, p. 13, 2013.

[141] R. Rietscher, M. Schröder, J. Janke et al., "Antigen delivery via hydrophilic PEG-*b*-PAGE-*b*-PLGA nanoparticles boosts vaccination induced T cell immunity," *European Journal of Pharmaceutics and Biopharmaceutics*, vol. 102, pp. 20–31, 2016.

[142] L. Shen, S. Tenzer, W. Storck et al., "Protein corona-mediated targeting of nanocarriers to B cells allows redirection of allergic immune responses," *The Journal of Allergy and Clinical Immunology*, vol. 142, no. 5, pp. 1558–1570, 2018.

[143] O. Gamucci, A. Bertero, M. Gagliardi, and G. Bardi, "Biomedical nanoparticles: overview of their surface immune-compatibility," *Coatings*, vol. 4, no. 1, pp. 139–159, 2014.

[144] S. M. Gheibi Hayat and M. Darroudi, "Nanovaccine: a novel approach in immunization," *Journal of Cellular Physiology*, vol. 58, article 1491, 2019.

[145] L. Niu, L. Y. Chu, S. A. Burton, K. J. Hansen, and J. Panyam, "Intradermal delivery of vaccine nanoparticles using hollow microneedle array generates enhanced and balanced immune response," *Journal of Controlled Release*, vol. 294, pp. 268–278, 2019.

[146] A. Akbari, A. Lavasanifar, and J. Wu, "Interaction of cruciferin-based nanoparticles with Caco-2 cells and Caco-2/HT29-MTX co-cultures," *Acta Biomaterialia*, vol. 64, pp. 249–258, 2017.

[147] M. Nuzzaci, A. Vitti, V. Condelli et al., "In vitro stability of cucumber mosaic virus nanoparticles carrying a hepatitis C virus-derived epitope under simulated gastrointestinal conditions and in vivo efficacy of an edible vaccine," *Journal of Virological Methods*, vol. 165, no. 2, pp. 211–215, 2010.

Hindawi
Journal of Immunology Research
Volume 2019, Article ID 2463731, 10 pages
https://doi.org/10.1155/2019/2463731

Research Article

High-Titre Neutralizing Antibodies to H1N1 Influenza Virus after Mouse Immunization with Yeast Expressed H1 Antigen: A Promising Influenza Vaccine Candidate

Edyta Kopera,[1] **Konrad Zdanowski**,[1,2] **Karolina Uranowska**,[3] **Piotr Kosson**,[4] **Violetta Sączyńska**,[5] **Katarzyna Florys**,[5] **and Bogusław Szewczyk**[3]

[1]*Institute of Biochemistry and Biophysics, Polish Academy of Sciences, Pawinskiego 5A, 02-106 Warsaw, Poland*
[2]*Institute of Chemistry, University of Natural Sciences and Humanities, 3 Maja 54, 08-110 Siedlce, Poland*
[3]*Department of Recombinant Vaccines, Intercollegiate Faculty of Biotechnology, University of Gdansk and Medical University of Gdansk, Abrahama 58, 80-307 Gdansk, Poland*
[4]*Mossakowski Medical Research Centre Polish Academy of Sciences, Pawinskiego 5, 02-106 Warsaw, Poland*
[5]*Institute of Biotechnology and Antibiotics, Staroscinska 5, 02-516 Warsaw, Poland*

Correspondence should be addressed to Edyta Kopera; ekopera@ibb.waw.pl

Received 28 June 2018; Revised 26 September 2018; Accepted 9 October 2018; Published 8 January 2019

Guest Editor: Elena Criscuolo

H1N1 influenza virus is still regarded as a serious pandemic threat. The most effective method of protection against influenza virus and the way to reduce the risk of epidemic or pandemic spread is vaccination. Influenza vaccine manufactured in a traditional way, though well developed, has some drawbacks and limitations which have stimulated interest in developing alternative approaches. In this study, we demonstrate that the recombinant H1 vaccine based on the hydrophilic haemagglutinin (HA) domain and produced in the yeast system elicited high titres of serum haemagglutination-inhibiting antibodies in mice. Transmission electron microscopy showed that H1 antigen oligomerizes into functional higher molecular forms similar to rosette-like structures. Analysis of the N-linked glycans using mass spectrometry revealed that the H1 protein is glycosylated at the same sites as the native HA. The recombinant antigen was secreted into a culture medium reaching approximately 10 mg/l. These results suggest that H1 produced in *Pichia pastoris* can be considered as the vaccine candidate against H1N1 virus.

1. Introduction

Influenza is an infectious disease occurring around the world both in humans and animals. Influenza epidemics occur every year, causing high morbidity and mortality. Since 1918, two subtypes of haemagglutinin (HA) (H1 and H3) and two subtypes of neuraminidase (NA) (N1 and N2) have always been found in the human population [1, 2]. Vaccination is still the most effective way of protecting against the influenza infection and a way to reduce the risk of an epidemic or pandemic. Classical influenza vaccines are produced by culturing the virus in embryonated eggs and subsequently inactivating the virus after purification. However, the time required to produce the vaccine is 7-8 months, and this has always been the Achilles' heel of the traditional approach. Mutations during virus growth in the eggs have been reported to reduce the effectiveness of the influenza vaccine [3]. To overcome the egg-dependent production of influenza vaccines, several novel strategies have been provided. As the influenza virus neutralizing antibodies currently are directed primarily against the haemagglutinin, recombinant HA-based vaccines provide a promising alternative for influenza vaccine manufacture. Such a vaccine comprises a recombinant haemagglutinin obtained by genetic engineering using various expression systems [4–10].

Haemagglutinin is a homotrimeric glycoprotein, most prolifically found on the surface of the virus. It occurs in homotrimeric form. Each monomer consists of two subunits—HA1 and HA2—linked by a disulphide bond. A monomer molecule is synthesized as an inactive precursor (HA0).

The protein undergoes N-linked glycosylation, and this post-translational modification has been shown to play an important role in the proper folding, trimer stabilization, and elicitation of neutralizing antibodies [11–14].

A challenging task for the production of subunit vaccine is the development of a simple and efficient purification process for the desired antigen. The final vaccine product should contain only highly purified compound. In our study, we utilized *Pichia pastoris* cells. This expression system enables efficient secretion of the overexpressed polypeptide facilitating purification of the protein product. *Pichia pastoris* offers the possibility to produce a high level of the desired protein and is suitable for large-scale production since *Pichia* cells can easily grow in a fermenter [15–17]. Several attempts have been made to utilize the *P. pastoris* system for HA polypeptide production. The full-length HA protein of H1N1 [18, 19] and H5N2 virus [20] was expressed in *P. pastoris* as partially secreted proteins. However, the levels of expression appeared to be very low. Expression of the H5 antigen was also reported by Subathra and colleagues [21], but the protein was not exported out of the cells, which hindered its purification process.

The aim of this study was to test an H1N1pdm09 influenza virus HA produced in a yeast expression system as a potential vaccine antigen. Our previous study showed that the H5 antigen produced in the *P. pastoris* cells is capable of inducing a specific immune response in mice [8, 10] and providing full protection in chicken [9]. Ease of preparation, low cost of production, and high immunogenicity of the yeast-derived antigen prompted us to test an H1N1pdm09 influenza virus antigen.

2. Results

2.1. Purification of Yeast-Derived H1 Antigen. Our previous results showed that the recombinant H5 protein encompassing residues from the extracellular domain adopted the correct three-dimensional structure required for oligomerization. Moreover, the H5 vaccine produced in *Pichia* cells proved to be protective for chickens challenged with a lethal dose of the highly pathogenic H5N1 virus [9]. Therefore, in this study, the transmembrane region and cytoplasmic tail of the H1 protein were also excluded. *In silico* analysis of the amino acid sequence of H1N1 haemagglutinin (A/H1N1/Gdansk/036/2009) revealed that the extracellular domain of H1 haemagglutinin comprises amino acids from 18 to 540. A DNA fragment encoding this amino acid sequence of HA (with His_6-tag at the N-terminus) was cloned as *EcoR*I and *Sac*II insert in the pPICZαA expression vector. As expected, the majority of expressed H1 represented an uncleaved HA polypeptide. No significant proteolytic processing into the HA1 and HA2 domains was detected. Coomassie blue staining after the SDS-PAGE separation of the purified H1 protein showed a high level of purity after one-step purification (Figure 1(a)). Furthermore, the purified H1 antigen typically migrates as a mixture of monomers and disulphide-linked dimers under nonreducing conditions (Figure 1(b)).

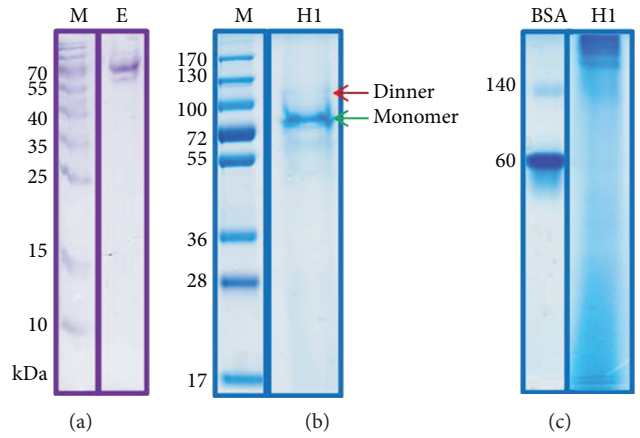

Figure 1: SDS-PAGE analysis of H1 antigen after IMAC purification. Protein was eluted with 250 mM imidazole. Collected fractions were analysed on 4-12% SDS-PAGE following Coomassie staining in reducing (a) and nonreducing (b) conditions. M: molecular weight marker; E: H1 protein eluted from Ni-NTA column by 250 mM imidazole. Fractions with H1 protein were pooled and lyophilized after being run on 4-7% Native PAGE (c).

Table 1: N-glycosylated peptides from the H1 protein confirmed by LC/MS/MS analysis. *N*-linked glycosylation sites are underlined.

Residue	Region	Amino acid sequence
N39	HA1	NVTVTHSVNILEDK
N292	HA1	NAGSGIIISDTPVHDCNTTCQTPK
N303	HA1	GAINTSLPFQNIHPITIGK
N497	HA2	NGTYDYPK

2.2. Characterization of H1 Antigen. The theoretical molecular weight of His-tagged HA lacking a C-terminal transmembrane anchor and cytoplasmic domain is 59.5 kDa. SDS-PAGE analysis showed that the H1 protein displayed a band of 70 kDa. The difference between the calculated molecular weight of H1 and the apparent molecular weight of the SDS-PAGE band indicates protein modification. Haemagglutinin is a glycosylated protein. In silico analysis of the H1 sequence using the NetNGlyc tool revealed 7 potential N-glycosylation sites (six in the HA1 domain and one in the HA2 domain). Using LC/MS-MS analysis, we examined the carbohydrate profile of the H1 antigen. Four of the seven potential N-glycosylation sites of yeast-produced recombinant H1 antigen (N39, N292, N303, and N497) were glycosylated (Table 1 and Figure 2).

Electrophoresis under native conditions allowed visualization of the high molecular weight molecules in the sample eluted from the affinity column (Figure 1(c)). The recombinant antigen appeared to be a mixture of various oligomeric forms. The same elution fractions of the recombinant antigen were further analysed by size exclusion chromatography (SEC), revealing two major peaks of the H1 antigen (Figure 3). The first peak, eluted prior to a thyroglobulin molecular weight standard (~670 kDa), demonstrates that the recombinant antigen forms high molecular weight

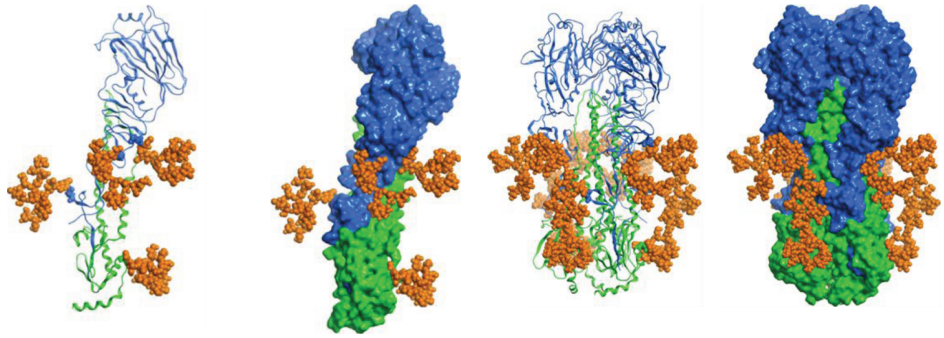

(a) (b)

Figure 2: Structural representation of the molecular model of the N-glycosylated H1 monomer (a) and trimer (b). The HA1 domain is depicted with the blue ribbon, the HA2 domain is depicted with the green, and the oligosaccharides are represented by orange atomistic balls. The sugar-bonded asparagines are depicted in atomistic representations, according to their respective domain colours. The models were constructed based on the crystallographic structure of the H1 haemagglutinin (PDB ID code 3LZG, [27]).

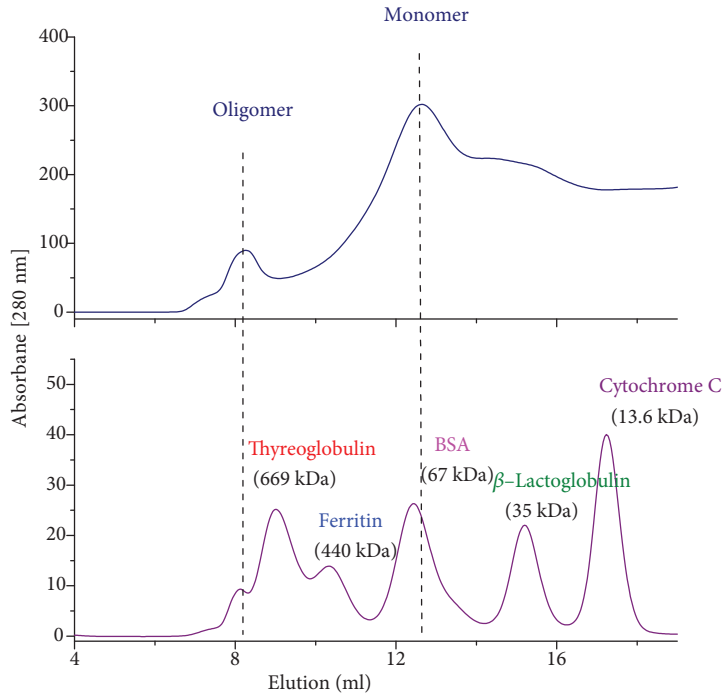

Figure 3: Size exclusion chromatography of the H1 antigen on Superdex 200 10/300 GL column. Chromatogram of the IMAC: elution fractions (upper plot) and molecular weight standards (lower plot). Fractions of the H1 protein were liophilised and dissolved in water, followed by injection into a Superdex 200 10/300 GL column preequilibrated with 10 mM Tris pH 7.6 with 200 mM NaCl. Absorbance at 280 nm is shown.

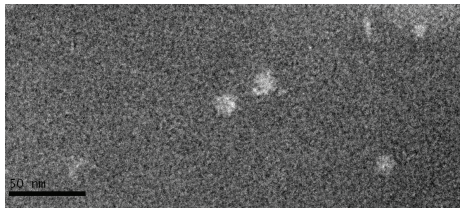

Figure 4: Transmission electron microscopy of the purified H1 antigen. Image was obtained at nominal 30000 magnification. The black scale bar represents 50 nm. Rosette-like structures were visualized.

complexes. The second peak, eluted between γ-globulin (158 kDa) and ovalbumin (44 kDa) molecular weight standards, indicates the presence of monomers.

Transmission electron microscopy (TEM) showed that oligomers eluted from the SEC column formed rosette-like structures (Figure 4).

In a modified ELISA, we examined whether H1N1pdm09 recombinant protein reacts with FI6 human neutralizing antibody. We performed a binding analysis of the glycosylated and deglycosylated H1 antigen with neutralizing antibody. The reactivity of the FI6 antibody with the

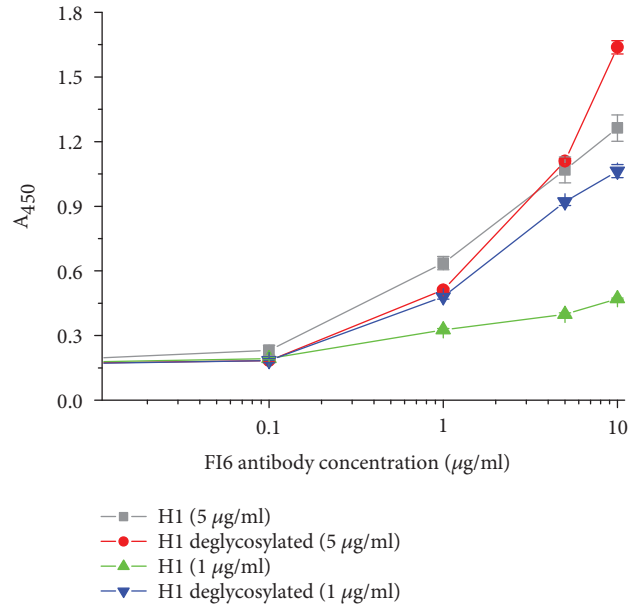

Figure 5: ELISA of the glycosylated and deglycosylated H1N1pdm09 recombinant protein using FI6 antibody. The H1 protein was deglycosylated with Endo H in native condition (pH 7.0). Two concentrations of the H1 protein were tested. Efficient HA-mediated haemagglutination was observed at high H1 concentration (data not shown). This is consistent with previous data, which suggested that only high HA oligomers are able to bind to multiple red blood cells to create the latticed structures that are measured in the haemagglutination assay [10].

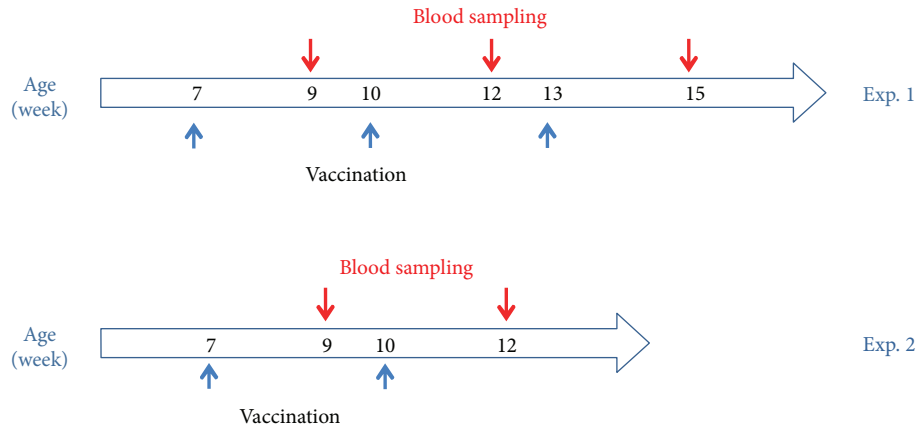

Figure 6: Scheme of mouse vaccination with H1 antigen. Exp. 1: mice were vaccinated subcutaneously (blue arrows) three times at three-week intervals. Blood samples were taken two weeks after each injection (red arrows). Exp. 2: mice were vaccinated intradermally twice at three-week intervals. Blood samples were taken two weeks after each injection (red arrows).

glycosylated H1 antigen was observed only at a high protein concentration. Much better results were seen for the deglycosylated H1N1pdm09 recombinant protein (Figure 5).

2.3. Immunization of Mice with H1 Vaccine Generated High Titres of Anty-H1N1pdm09 Antibodies. Immunogenicity studies in mice were conducted to evaluate the immunogenic potential of the H1 antigen and to determine the minimal effective dose that generates protective correlates of immunity. Two sets of immunization experiment were performed using prime/boost strategy. In the first immunization, experiment groups of mice were vaccinated subcutaneously with different doses of the H1 antigen (ranging from 1 μg to 25 μg) and boosted twice at three-week intervals (Figure 6, Exp. 1).

The control group received only saline plus Alhydrogel. Following immunization, the mice showed no adverse effects suggesting that the H1 vaccine was well tolerated. The results of the ELISA test demonstrated that the H1 antigen is strongly immunogenic. A single administration of the H1 vaccine at a dose as low as 1 μg in a presence of aluminium hydroxide elicited specific anti-HA antibodies with an end-point titre of 2×10^3. A second antigen injection significantly boosted the antibody response in all groups, and strong dose dependence was observed. Interestingly, after the third injection, the highest HA-specific IgG titre of 6×10^5 was

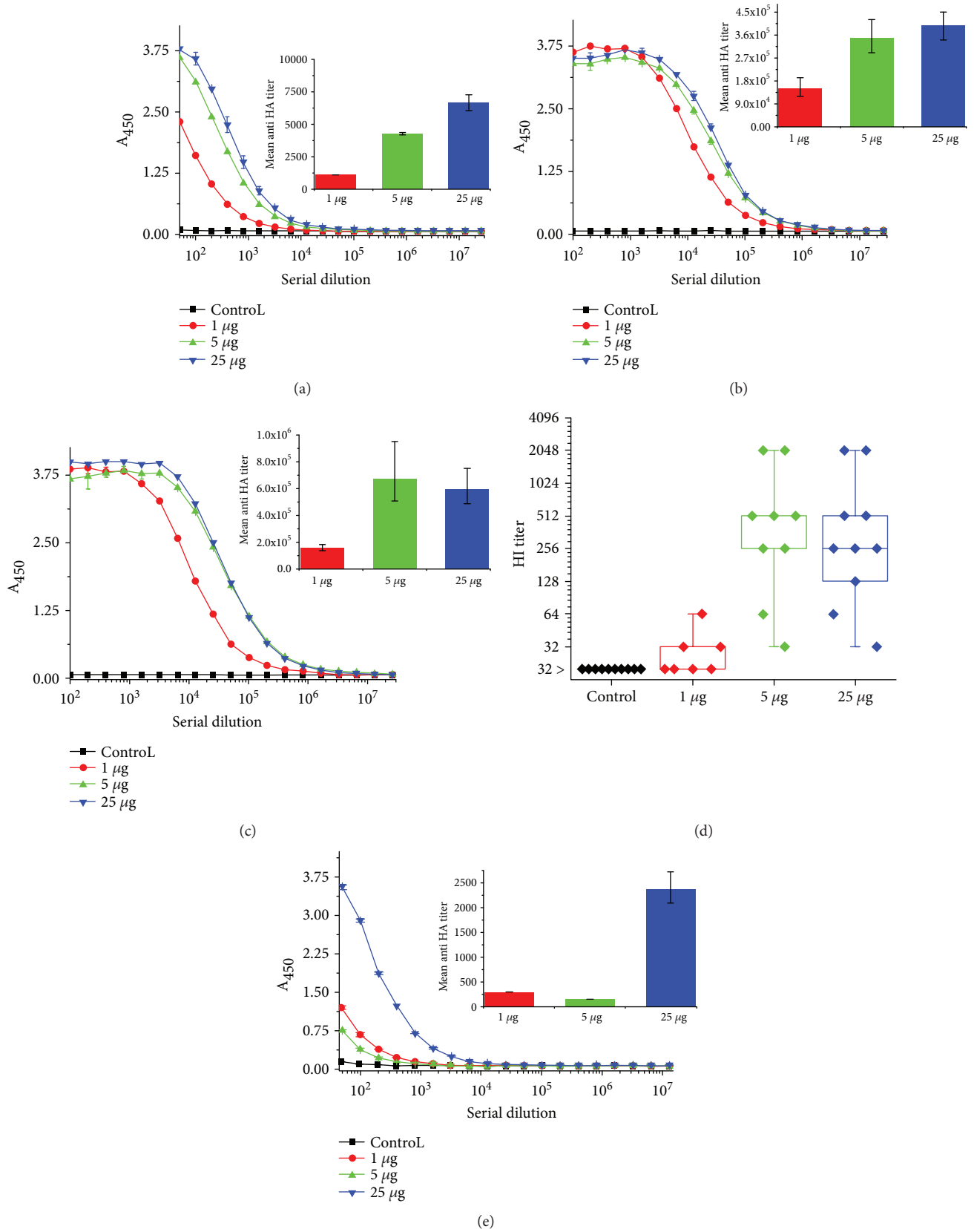

Figure 7: Continued.

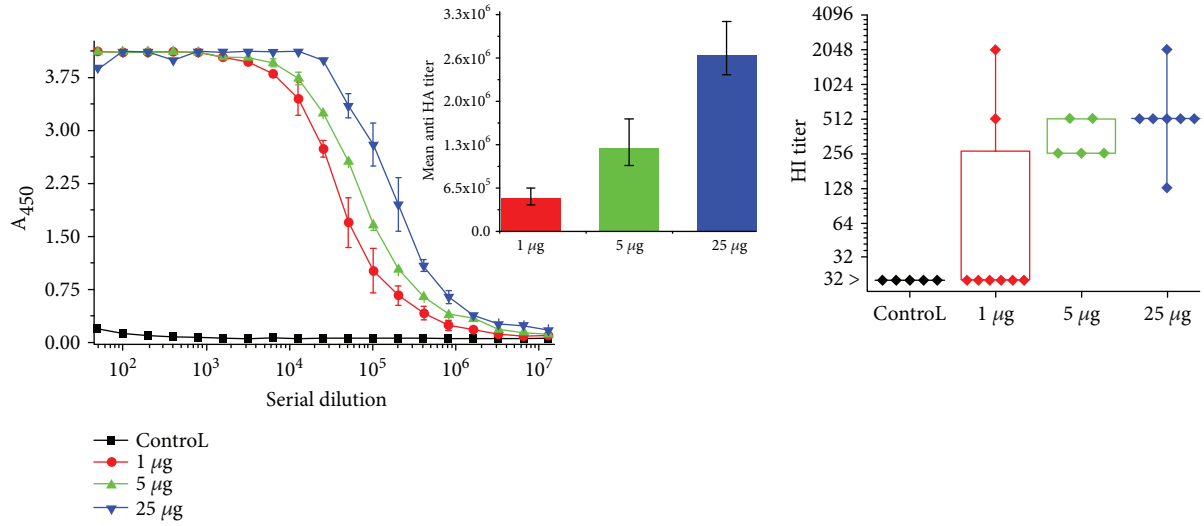

(f)

FIGURE 7: Humoural response in mice after immunization with the H1 antigen. Sera samples of mice immunized with 1, 5, and 25 μg of H1 adjuvanted with Alhydrogel were pooled and the immune responses were measured two weeks after immunization (a), booster (b), and second booster (c) by indirect ELISA (nonlinear fitting plots: bars represent standard deviation; column plots: bars represent 95% confidence level) and two weeks after second booster by HI test (d). Data for individuals (raw data, ✦), mean (○), and the medians (□) are shown for each group. During the second immunization experiment, two doses of 1, 5, and 25 μg of H1 adjuvanted with Sigma Adjuvant System were tested. Sera samples of mice immunized twice were measured two weeks after the first antigen injection (e) and booster (f) by indirect ELISA (bars represent 95% confidence level). Two weeks after booster, the HI test was performed with homologous H1N1pdm09 virus (f). Data for individuals (raw data, ✦), mean (○), and the medians (□) are shown for each group.

detected in mice immunized with 5 μg of the H1 vaccine (Figures 7(a)–7(c)). No increase was observed in the serum IgG response in the control mice on any of the days tested. The sera from the individual groups were pooled for testing using ELISA. For the HI assay, the sera of individual mice were tested to pinpoint the differences in protective efficacy of each of the H1 vaccine doses. The level of HI antibodies was tested after the final vaccine doses. HI antibody titres were not very high in the group immunized with 1 μg, and only 40% of this group was positive. Groups of mice immunized with 5 μg and 25 μg of H1 vaccine were 100% positive, with HI titres as high as 1 : 2048, and no significant differences among these two groups were detected (Figure 7(d)). These results prompted us to study the protective efficacy of only one booster of the H1 vaccine. The second immunization experiment was similar to the previous one; however, a different adjuvant was used. Based on our results obtained from the immunization experiment with H5 antigen [8], the H1 vaccine formulation contained the Sigma Adjuvant System. The same doses of the H1 antigen were tested. The mice were immunized intradermally twice, at three-week intervals (Figure 6, Exp. 2). A single immunization with the H1 vaccine in the presence of the Sigma Adjuvant System elicited a rather low level of specific anti-HA antibodies, and titre $< 2 \times 10^3$ was detected only for the 25 μg dose of the H1 antigen (Figure 7(e)). A massive increase in the immune response was detected after the booster in all three groups of immunized mice (Figure 7(f)). The HA-specific IgG titre, which was as high as 2.6×10^6, was detected in mice immunized with 25 μg of the H1 vaccine. No immune response to the HA antigen was detected in the control group. HI titres (determined for individual animals) were also very high. As in the first immunization experiment, most of the mice immunized with 1 μg of H1 vaccine were HI negative. One hundred percent of the animals in groups immunized with 5 μg or 25 μg of H1 vaccine were HI positive, and no significant difference was observed in the HI titres between these two doses (Figure 7(f)). These results suggest that two doses of 5 μg of the H1 vaccine might be protective against H1N1pdm09 virus infection.

3. Discussion

Influenza haemagglutinin is the primary target of almost all neutralizing antibodies, and it is regarded as a crucial component of current influenza vaccines. Previously, we showed that immunization with the subunit vaccine based on the extracellular region of the H5 haemagglutinin with deletion of the multibasic cleavage site elicited serum haemagglutination-inhibiting antibodies and fully protected chickens from lethal infections by the highly pathogenic H5N1 virus [9]. We also demonstrated the feasibility of producing H5N1 HA antigen in yeast [9, 10]. Therefore, testing this expression system for production of other influenza antigens, especially those HAs which are components of strains typical for humans, was successful. The biochemical and immunological characterization of purified *Pichia*-produced H1 antigen was achieved in this study.

The level of H1 protein oligomerization has been evaluated using various techniques: electrophoresis under native conditions, size exclusion chromatography, and transmission electron microscopy. Based on these results, one can

conclude that most H1 antigen exists in a monomeric form; however, the higher molecular weight species are also present. Transmission electron microscopy visualized rosette-like structures of the H1 protein. We also examined whether the extracellular region of H1 protein preserves the conformational epitope. For this analysis, we used the FI6 antibody. This antibody was originally isolated from plasma cells from blood samples of donors exposed to pH1N1 [22]. FI6 targeted a distinct site on the stem region of HA and may be able to neutralize the majority of influenza A virus subtypes [23, 24]. According to reports, FI6 may be used to test the correct immunogenic conformation of HA [25]. Therefore, we used this antibody to study FI6 reactivity with recombinant H1 antigen. A relatively good reactivity of FI6 antibody with the deglycosylated H1 protein was observed suggesting that the binding site for the conformational antibody was preserved. The reactivity of the FI6 antibody with the glycosylated H1 antigen was rather poor, especially at low protein concentration. This result was consistent with the structural model of the N-glycosylated H1 protein, since all the glycosylated sites are located in its stem region. However, for both H1 protein states, low signals from FI6 might be explained by the oligomeric forms of the recombinant antigen.

Our immunization experiments showed that the H1 antigen induced a strong HI-immune response in mice. The mean anti-HA antibody titre as high as 8×10^5 after the third dose of the H1 vaccine adjuvanted with Alhydrogel was detected. An even higher mean anti-HA antibody titre (6×10^6) was detected after the second dose of the H1 vaccine adjuvanted with the Sigma Adjuvant System. Most anti-HA neutralizing antibodies are conformation dependent. Antibodies that are generated against haemagglutinin, especially against the receptor-binding region, have a high neutralizing potential and are able to prevent viral infection. These antibodies can be easily quantified using the HI test. A strong correlation of protection exists for serum HI titres, and this assay is commonly used for evaluation of effectivity of influenza vaccines [FDA, https://www.fda.gov/downloads/BiologicsBloodVaccines/guidanceComplianceRegulatoryInformation/Guidances/Vaccines/ucm091990.pdf]. HI tests performed by us showed that the H1 antigen induced high neutralizing antibodies titre.

The crucial issue for a vaccine to be licensed for medical use is to develop an effective process for the purification of the protein product [10]. Our work addresses both vaccine production steps: the expression and the purification. In this study, we investigated the use of the *Pichia* cells to produce a soluble H1N1 HA antigen. The *P. pastoris* expression system has been commonly utilized as a platform to produce various proteins significant to the medical industry, including vaccine antigens (Shanvac™, Elovac™, and Gavac™) [10]. We proved that the *Pichia*-based production process is also effective for the H1 antigen. The manufacturing method is simple and inexpensive compared to the existing solutions. A good efficiency of up to 10 mg of highly purified protein from 1 litre of culture medium (400 doses) for the H1 antigen was obtained. The efficiency of the H1 vaccine antigen production presumably could be easily scaled up in a bioreactor.

4. Materials and Methods

4.1. Production and Purification of H1 Antigen. Plasmid pPICZαA (Invitrogen) and plasmid pJET/H1 carrying H1N1 virus haemagglutinin gene (A/H1N1/Gdansk/036/2009) have been used for the construction of the expression vector pPICZαA/H1. The plasmid contains an α factor sequence, which ensures the secretion of recombinant protein to the medium. cDNA of 1569 bp, which codes the hydrophilic domain (18-540 aa) of the H1N1 virus haemagglutinin (A/H1N1/Gdansk/036/2009), was amplified in a PCR reaction. The sequence encoding the His-Tag was added to the cDNA sequence by forward primer. The PCR product was cloned into the pPICZαA expression vector under the control of the AOX promoter. *Pichia pastoris* cells (KM 71 strain, his4, aox1::ARG4, arg4) (Invitrogen) were transformed with recombinant plasmids by electroporation. Integration of the haemagglutinin gene into the *P. pastoris* genome was confirmed by PCR. KM 71 transformant selection was performed using a medium containing Zeocin (multiple passaging). The presence of recombinant protein, in the medium and in the cells (control), was detected by SDS-PAGE and Western blotting. Recombinant haemagglutinin was purified from culture medium by affinity chromatography, using Ni-NTA Agarose resin. Protein binding to the Ni-NTA Agarose was carried out in phosphate buffer solution (PBS) with 450 mM NaCl. The HA protein was eluted from the column with 250 mM imidazole in PBS pH 7.4. The protein was then dialyzed against PBS pH 7.4. After dialysis, the protein was lyophilized and stored at a temperature of −20°C.

4.2. Enzymatic and MS/MS Analysis of Recombinant HA Glycosylation. 5 μg of H1 protein was incubated with 750 U of endoglycosidase H (New England BioLabs) at 37°C for 18 h. The reaction samples were analysed by Western blotting and SDS-PAGE after. A band corresponding to the deglycosylated HA protein was cut from the gel for MS/MS analysis. The protein was digested by trypsin. The mixture of peptides (without reduction or alkylation) was applied in an RP-18 precolumn (Waters nanoAcquity 20 mm × 180 μm) with water and 0.1% trifluoroacetic acid and then into an HPLC RP-18 column (Waters nanoAcquity UPLC column 250 mm × 75 μm), using a line gradient of acetonitrile (0-50% in 30 minutes) with 0.1% formic acid. The elution fraction from the HPLC column was directed to the MS ionization chamber (LTQ-FTICR, Thermo Electron). The Protein Bank Data PDB (National Center of Biotechnology Information NCBI no. Version 20080624) and Mascot software (http://www.matrixscience.com) were used for the analysis of the resulting mass spectra.

4.3. Size Exclusion Chromatography. The H1 antigen was analysed according to a procedure previously published [9]. Shortly, a Superdex 200 10/300 GL column (GE Healthcare, UK) was preequilibrated with 10 mM Tris pH 7.6 with 200 mM NaCl, and the protein was injected with the equilibration buffer. Elution of the H1 antigen was monitored at 280 nm. Molecular weight standards (Bio-Rad, USA) were

used to calibrate the column and to identify the molecular weights of the proteins present in the samples.

4.4. Transmission Electron Microscopy. TEM analysis was performed in collaboration with Electron Microscopy platform of the Integrated Structural Biology of Grenoble. A procedure previously published was applied [9]. Shortly, 100 μg of the H1 protein sample was applied to the clean side of the carbon on mica and negatively stained with 2% (w/v) sodium silico tungstate. A grid was then placed on top of the carbon film which was subsequently air-dried. Images were taken under low-dose conditions (less than 20 e−/A2) with a T12 FEI electron microscope at 120 kV using an ORIUS SC1000 camera (Gatan, Inc., Pleasanton, CA).

4.5. Immunization. Seven-week-old, pathogen-free, female BALB/c mice were used for vaccination. The animals were housed in a temperature-controlled environment at 24°C with 12 h day-night cycles and received food and water *ad libitum*. Immunization experiments were conducted in the animal house of the Institute of Experimental Medicine PAS (Warsaw) under control of the Bioethics Committee (Permission no. 11/2012). The experimental groups in the first trial consisted of 10 mice. The control group of 10 mice was administered adjuvant only. The recombinant antigen suspended in saline solution supplemented with Alhydrogel (aluminium hydroxide) was administered subcutaneously (sc) into the neck skin-fold. The antigen was administered at three doses: 1, 5, and 25 μg. Sera samples were taken from all groups one week before the application of the first dose. There were three injections (first application of antigen and/or adjuvant + two booster shots) at an interval of three weeks between each dose in order to monitor immunological response. Blood samples were taken two weeks after each injection to determine the level of antibodies. Sera were stored at −20°C. The experimental groups in the second immunization experiment consisted of 8 7-week-old BALB/c mice. Five mice were in the control group. The antigen was administered at three doses, the same ones as described above. For immunization, 25 μg of the Sigma Adjuvant System containing 0.5 mg monophosphoryl Lipid A (detoxified endotoxin) from *Salmonella minnesota* and 0.5 mg synthetic Trehalose Dicorynomycolate in 2% oil (squalene)-Tween® 80-water was used. The booster injection was adjuvanted with 25 μg monophosphoryl lipid A and 25 μg muramyl dipeptide (Sigma-Aldrich). The control group was administered with only the specific adjuvant. Administration of 100 μl of vaccine was by intradermal injection (i.d.) in the walking pad of the hind paw. As in the first experiment, blood samples were taken two weeks after each injection in order to determine the level of antibodies. Sera were stored at −20°C.

4.6. ELISA. Collected sera were assayed for antibodies against H1 HA by an ELISA method, using MaxiSorp plates (Nunc, Denmark) coated with purified HA (coating concentration 1.6 μg/ml). Sera samples from mice immunized with the H1 protein were tested in parallel with sera from sham-immunized mice (negative controls). A procedure previously published was applied [10]. Sera samples, taken from individual mice at each time point of the experiment, were pooled in groups, serially diluted in 2% BSA/PBS and applied onto the plates (overnight, 2-8°C) and blocked with 2% BSA/PBS (1.5 h, 37°C). The tested samples were then incubated overnight at 2–8°C together with blanks (sample diluent). Bound antibodies were subsequently detected with goat-generated and horseradish peroxidase- (HRP-) labelled antibodies against mouse IgG (γ-chain specific) at 1 : 1000 dilution in 2% BSA/PBS (1 h, 37°C). TMB was used as a HRP substrate. After incubation for 30 min at room temperature, the reaction was stopped by the addition of 0.5 M sulfuric acid. The absorbance was measured at 450 nm with a microplate reader (Synergy 2; BioTek Instruments, USA). The endpoint titre was defined as the highest dilution producing an A_{450} value 4-fold higher than the mean A_{450} value of the control group.

In an enzyme-linked immunosorbent assay (ELISA), 50 μl of FI6 antibody at the concentrations of 10 μg/ml-0.01 μg/ml was coated on 96-well ELISA MediSorp plates (Nunc, Denmark) and allowed to bind overnight at 4°C. Plates were then washed four times with washing buffer (PBS, 0.1% Tween, pH 7.6) and blocked with 2% BSA/PBS (blocking buffer) at 37°C for 1.5 h. After the plates had been washed two times with washing buffer, 50 μl of glycosylated or deglycosylated H1 antigen (5 μg/ml or 1 μg/ml) in PBS was then added to the plates and incubated at room temperature for 1.5 h. Plates were again washed four times with washing buffer. Bound antigens were detected with horseradish peroxidase- (HRP-) labelled antibodies against His-Tag at 1 : 5000 dilution in 2% BSA/PBS (37°C, 1 h). After incubation for 30 min at room temperature with the TMB, 0.5 M sulfuric acid was added to stop the reaction. The absorbance was measured at 450 nm with a microplate reader (Synergy 2; BioTek Instruments, USA).

4.7. Haemagglutination Inhibition Test. Sera samples were heat inactivated at 56°C for 30 min and then were pretreated with kaolin to avoid a false-positive reaction in the HI test [26]. The pretreated sera samples (25 μl of sera in serial two-fold dilutions) were incubated for 25 min in a titration plate with 4 HA units of the inactivated antigen [10]. Next, the suspension of 1% hen erythrocytes was added and incubated for 30 min. The HI titre was determined as the reciprocal of the highest dilution in which haemagglutination is inhibited. Samples were assigned as positive when their titre was ≥16. Sera samples from the immunization experiments (trials 1 and 2) were tested using the homologous strain H1N1.

Abbreviations

HA: Haemagglutinin
AOX: Alcohol oxidase
Endo H: Endoglycosidase H
IV: Influenza virus
PAGE: Polyacrylamide gel electrophoresis
SEC: Size exclusion chromatography
TEM: Transmission electron microscopy
HI: Haemagglutination inhibition
IMAC: Immobilized metal ion affinity chromatography.

Data Availability

The models were constructed based on the crystallographic data deposited in PDB (ID code 3LZG).

Conflicts of Interest

The authors declare that the research was conducted in the absence of any commercial or financial relationships that could be construed as a potential conflict of interest.

Authors' Contributions

EK, KZ, and KU performed the experiments; PK conducted the mice experiment. EK, KF, and VS performed the ELISA analysis. EK, KZ, KU, and BSz participated in the study design and data analysis. All authors participated in the manuscript and figure preparation; all authors have read and approved the final manuscript.

Acknowledgments

This work was supported by the Ministry of Science and Higher Education, Grant No. IP2011/025571, and in part by Grant No. PBS2/A7/14/2014 from the National Centre for Research and Development. We thank Dr. Marcin Mielecki for constructing the molecular models of the glycosylated monomeric and trimeric haemagglutinin H1. We thank Dr. Krzysztof Lacek and Alfredo Nicosia for the FI6 antibody. This work used the platforms of the Grenoble Instruct Centre (ISBG; UMS 3518 CNRS-CEA-UJF-EMBL) with support from FRISBI (ANR-10-INSB-05-02) and GRAL (ANR-10-LABX-49-01) within the Grenoble Partnership for Structural Biology (PSB). We thank Dr. Christine Moriscot and Dr. Guy Schoehn from the Electron Microscopy platform of the Integrated Structural Biology of Grenoble. The equipment used was sponsored in part by the Centre for Preclinical Research and Technology (CePT), a project cosponsored by European Regional Development Fund and Innovative Economy, The National Cohesion Strategy of Poland [Innovative economy 2007–13, Agreement POIG.02.02.00-14-024/08-00].

References

[1] C. R. Parrish and Y. Kawaoka, "The origins of new pandemic viruses: the acquisition of new host ranges by canine parvovirus and influenza A viruses," *Annual Review of Microbiology*, vol. 59, no. 1, pp. 553–586, 2005.

[2] J. K. Taubenberger and J. C. Kash, "Influenza virus evolution, host adaptation, and pandemic formation," *Cell Host & Microbe*, vol. 7, no. 6, pp. 440–451, 2010.

[3] D. M. Skowronski, N. Z. Janjua, G. de Serres et al., "Low 2012–13 influenza vaccine effectiveness associated with mutation in the egg-adapted H3N2 vaccine strain not antigenic drift in circulating viruses," *PLoS One*, vol. 9, no. 3, article e92153, 2014.

[4] J. J. Treanor, H. E. Sahly, J. King et al., "Protective efficacy of a trivalent recombinant hemagglutinin protein vaccine (FluBlok®) against influenza in healthy adults: a randomized, placebo-controlled trial," *Vaccine*, vol. 29, no. 44, pp. 7733–7739, 2011.

[5] M. M. J. Cox and Y. Hashimoto, "A fast track influenza virus vaccine produced in insect cells," *Journal of Invertebrate Pathology*, vol. 107, pp. S31–S41, 2011.

[6] Y. Shoji, A. Prokhnevsky, B. Leffet et al., "Immunogenicity of H1N1 influenza virus-like particles produced in *Nicotiana benthamiana*," *Human Vaccines & Immunotherapeutics*, vol. 11, no. 1, pp. 118–123, 2015.

[7] F. Krammer, S. Nakowitsch, P. Messner, D. Palmberger, B. Ferko, and R. Grabherr, "Swine-origin pandemic H1N1 influenza virus-like particles produced in insect cells induce hemagglutination inhibiting antibodies in BALB/c mice," *Biotechnology Journal*, vol. 5, no. 1, pp. 17–23, 2010.

[8] E. Kopera, A. Dvornyk, P. Kosson et al., "Expression, purification and characterization of glycosylated influenza H5N1 hemagglutinin produced in Pichia pastoris," *Acta Biochimica Polonica*, vol. 61, no. 3, pp. 597–602, 2014.

[9] M. Pietrzak, A. Macioła, K. Zdanowski et al., "An avian influenza H5N1 virus vaccine candidate based on the extracellular domain produced in yeast system as subviral particles protects chickens from lethal challenge," *Antiviral Research*, vol. 133, pp. 242–249, 2016.

[10] A. K. Macioła, M. A. Pietrzak, P. Kosson et al., "The length of *N*-glycans of recombinant H5N1 hemagglutinin influences the oligomerization and immunogenicity of vaccine antigen," *Frontiers in Immunology*, vol. 8, p. 444, 2017.

[11] C. S. Copeland, R. W. Doms, E. M. Bolzau, R. G. Webster, and A. Helenius, "Assembly of influenza hemagglutinin trimers and its role in intracellular transport," *Journal of Cell Biology*, vol. 103, no. 4, pp. 1179–1191, 1986.

[12] P. C. Roberts, W. Garden, and H. D. Klenk, "Role of conserved glycosylation sites in maturation and transport of influenza A virus hemagglutinin," *Journal of Virology*, vol. 67, no. 6, pp. 3048–3060, 1993.

[13] X. Sun, A. Jayaraman, P. Maniprasad et al., "N-linked glycosylation of the hemagglutinin protein influences virulence and antigenicity of the 1918 pandemic and seasonal H1N1 influenza A viruses," *Journal of Virology*, vol. 87, no. 15, pp. 8756–8766, 2013.

[14] R. A. Medina, S. Stertz, B. Manicassamy et al., "Glycosylations in the globular head of the hemagglutinin protein modulate the virulence and antigenic properties of the H1N1 influenza viruses," *Science Translational Medicine*, vol. 5, no. 187, article 187ra70, 2013.

[15] M. Romanos, "Advances in the use of *Pichia pastoris* for high-level gene expression," *Current Opinion in Biotechnology*, vol. 6, no. 5, pp. 527–533, 1995.

[16] M. Rodríguez, V. Martínez, K. Alazo et al., "The bovine IFN-ω1 is biologically active and secreted at high levels in the yeast *Pichia pastoris*," *Journal of Biotechnology*, vol. 60, no. 1-2, pp. 3–14, 1998.

[17] C. E. White, N. M. Kempi, and E. A. Komives, "Expression of highly disulfide–bonded proteins in *Pichia pastoris*," *Structure*, vol. 2, no. 11, pp. 1003–1005, 1994.

[18] T. N. Athmaram, S. Saraswat, S. R. Santhosh et al., "Yeast expressed recombinant hemagglutinin protein of novel H1N1 elicits neutralising antibodies in rabbits and mice," *Virology Journal*, vol. 8, no. 1, p. 524, 2011.

[19] T. N. Athmaram, S. Saraswat, A. K. Singh et al., "Influence of copy number on the expression levels of pandemic influenza

hemagglutinin recombinant protein in methylotrophic yeast *Pichia pastoris*," *Virus Genes*, vol. 45, no. 3, pp. 440–451, 2012.

[20] C. Y. Wang, Y. L. Luo, Y. T. Chen et al., "The cleavage of the hemagglutinin protein of H5N2 avian influenza virus in yeast," *Journal of Virological Methods*, vol. 146, no. 1-2, pp. 293–297, 2007.

[21] M. Subathra, P. Santhakumar, M. L. Narasu, S. S. Beevi, and S. K. Lal, "Evaluation of antibody response in mice against avian influenza A (H5N1) strain neuraminidase expressed in yeast *Pichia pastoris*," *Journal of Biosciences*, vol. 39, no. 3, pp. 443–451, 2014.

[22] D. Corti, J. Voss, S. J. Gamblin et al., "A neutralizing antibody selected from plasma cells that binds to group 1 and group 2 influenza A hemagglutinins," *Science*, vol. 333, no. 6044, pp. 850–856, 2011.

[23] D. C. Ekiert and I. A. Wilson, "Broadly neutralizing antibodies against influenza virus and prospects for universal therapies," *Current Opinion in Virology*, vol. 2, no. 2, pp. 134–141, 2012.

[24] C. Dreyfus, D. C. Ekiert, and I. A. Wilson, "Structure of a classical broadly neutralizing stem antibody in complex with a pandemic H2 influenza virus hemagglutinin," *Journal of Virology*, vol. 87, no. 12, pp. 7149–7154, 2013.

[25] Y. Lu, J. P. Welsh, and J. R. Swartz, "Production and stabilization of the trimeric influenza hemagglutinin stem domain for potentially broadly protective influenza vaccines," *Proceedings of the National Academy of Sciences of the United States of America*, vol. 111, no. 1, pp. 125–130, 2014.

[26] G. Bizanov and V. Tamosiunas, "Immune response induced in mice after intragastral administration with Sendai virus in combination with extract of Uncaria tomentosa," *Scandinavian Journal of Laboratory Animal Science*, vol. 32, pp. 201–207, 2005.

[27] R. Xu, D. C. Ekiert, J. C. Krause, R. Hai, J. E. Crowe, and I. A. Wilson, "Structural basis of preexisting immunity to the 2009 H1N1 pandemic influenza virus," *Science*, vol. 328, no. 5976, pp. 357–360, 2010.

Hindawi
Journal of Immunology Research
Volume 2018, Article ID 3734207, 14 pages
https://doi.org/10.1155/2018/3734207

Review Article

Defensive Driving: Directing HIV-1 Vaccine-Induced Humoral Immunity to the Mucosa with Chemokine Adjuvants

Ebony N. Gary[1] **and Michele A. Kutzler**[1,2]

[1]*The Department of Microbiology and Immunology, Drexel University College of Medicine, Philadelphia, PA, USA*
[2]*The Division of Infectious Diseases and HIV Medicine, The Department of Medicine, Drexel University College of Medicine, Philadelphia, PA, USA*

Correspondence should be addressed to Michele A. Kutzler; mkutzler@drexelmed.edu

Received 30 June 2018; Revised 17 September 2018; Accepted 3 October 2018; Published 13 December 2018

Guest Editor: Roberta A. Diotti

A myriad of pathogens gain access to the host via the mucosal route; thus, vaccinations that protect against mucosal pathogens are critical. Pathogens such as HIV, HSV, and influenza enter the host at mucosal sites such as the intestinal, urogenital, and respiratory tracts. All currently licensed vaccines mediate protection by inducing the production of antibodies which can limit pathogen replication at the site of infection. Unfortunately, parenteral vaccination rarely induces the production of an antigen-specific antibody at mucosal surfaces and thus relies on transudation of systemically generated antibody to mucosal surfaces to mediate protection. Mucosa-associated lymphoid tissues (MALTs) consist of a complex network of immune organs and tissues that orchestrate the interaction between the host, commensal microbes, and pathogens at these surfaces. This complexity necessitates strict control of the entry and exit of lymphocytes in the MALT. This control is mediated by chemoattractant chemokines or cytokines which recruit immune cells expressing the cognate receptors and adhesion molecules. Exploiting mucosal chemokine trafficking pathways to mobilize specific subsets of lymphocytes to mucosal tissues in the context of vaccination has improved immunogenicity and efficacy in preclinical models. This review describes the novel use of MALT chemokines as vaccine adjuvants. Specific attention will be placed upon the use of such adjuvants to enhance HIV-specific mucosal humoral immunity in the context of prophylactic vaccination.

1. Introduction

Many pathogens access the host via mucosal barrier surfaces. Thus, developing vaccines that elicit robust effector and memory responses at mucosal sites is a crucial public health goal. The mucosa-associated lymphoid tissues (MALTs) are an interactive network of organs and tissues that are responsible for the education of mucosal lymphocytes and the orchestration of responses against commensal microbes and pathogens. As the mucosal immune system must balance the ability to respond to pathogens with tolerance of commensal microbes, effector cell access to the MALT is tightly regulated. Peripherally activated lymphocytes are rarely able to traffic to mucosal sites due to low, or lack of expression, specific adhesion and chemokine receptors required for entry into these sites. Due to the exclusion of these peripheral lymphocytes, generating mucosal immunity with parenteral vaccination is rarely successful. While it has been demonstrated that peripheral vaccination can generate mucosal humoral responses, it does so by relying on the magnitude of the response. Vaccinating with adjuvants in the periphery induces large quantities of antigen-specific antibodies. This increased concentration of the antigen-specific antibody can then transudate to mucosal surfaces. Thus, even in the context of peripheral vaccination, successful mucosal targeting of responses has the potential to have dose-sparing a effects on vaccine development.

Before the discovery of mucosa-specific chemokines, it was known that a common mucosal immune system existed. Czerkinsky et al. and Bienenstock et al. reported that following adoptive transfer, labeled antibody-secreting cells (ASCs) from mesenteric lymph nodes (MLNs) of donor mice were

more likely to be recovered from the intestines, mammary glands, cervix, vagina, and MLN of recipient mice [1–3]. These data supported the idea that mucosal immunity is a coordinated phenomenon, namely, that there are cell-intrinsic differences in the ability of lymphocytes to access the MALT. Subsequent studies in mice and other animal models confirmed the existence of the common mucosal immune system [4]. We now know that access to the MALT is dependent upon the expression of specific chemokine receptors. Chemokines are small 8–14 kD secretory proteins classified by the arrangement of four canonical cysteines into four classes—the CXC or alpha chemokines, the CC or beta chemokines, the C or gamma, and the CX3C or delta chemokines. The cell-expressed G-protein chemokine receptors that bind them are similarly classified [5]. Directing immune responses to the mucosa remains a challenge for HIV vaccine design. As human immunodeficiency virus-1 (HIV-1) is primarily transmitted sexually, with infection occurring in the gastrointestinal and genital mucosae, the induction of robust humoral responses in the mucosa is critical to the development of an efficacious prophylactic vaccine. Harnessing the extant chemokine/receptor system responsible for trafficking antibody-secreting cells to mucosal surfaces during and after immunization is a viable strategy for enhancing antigen-specific immunity in the mucosa. Here, we discuss HIV-1 infection in the mucosa, and the necessity and challenges of designing an HIV-1 vaccine. We will also discuss the chemokines and receptors responsible for mucosal trafficking of lymphocytes and review recent studies using chemokines to augment mucosal responses to viral vaccine antigens including HIV, HSV, and influenza.

1.1. Mucosal Pathogenesis of HIV. Human immunodeficiency virus-1 (HIV-1) currently infects more than thirty-five million people, and the WHO estimates that 0.8% of all adults between ages 15 and 50 are HIV infected. More than 2.5 million new infections occur each year, highlighting the need for an effective prophylactic vaccine. Unfortunately, the nature of the virus lifecycle and the lack of definitive correlates of protection make vaccine design challenging [6–8]. HIV-1 transmission occurs primarily through sexual contact, at mucosal surfaces. Once the virus accesses tissue resident $CD4^+$T cells, its primary targets, integration of the viral genome into the host genome establishes lifelong infection. An effective prophylactic vaccine must therefore engender a robust, neutralizing antibody response directed specifically to the mucosal compartment. Directing vaccine-induced responses to mucosal sites remains remarkably challenging. The concentration of antigen-specific antibody in the mucosal compartment following immunization depends on several factors, namely, the dose of antigen and the route of delivery. It is generally known that oral vaccination is the best delivery route for generation of mucosal antibody responses; unfortunately, oral antigen delivery requires large doses to overcome the tolerogenic environment of the gastrointestinal tract. Similarly, direct delivery of the antigen to mucosal sites, such as intranasal administration, while effective, requires large amounts of the antigen to mediate immunity. Conversely, relatively small doses of the protein antigen delivered parenterally induce robust IgG responses, including neutralizing antibody production, but little to no mucosal antibody of either IgG or IgA isotypes. Increasing dosages of the protein antigen and the addition of adjuvants can promote high titers of the antibody that can passively diffuse into the mucosa, leading to protection against infection.

Despite the substantial number of HIV-1 vaccine clinical trials completed and underway, almost no successes have been recorded. The only trial to ever demonstrate efficacy was the RV144 or Thai trial, which began in 2003 [9]. The vaccine regimen consisted of a modified canarypox vector expressing HIV-1 *gag*, *pol*, and *env* proteins, followed by a recombinant HIV gp120 (envelope, *env*) boost. The trial demonstrated efficacy ranging from 26.4%–31%. It was determined after analysis of patient samples that protection correlated with HIV-specific serum IgG which mediated antibody-dependent cellular cytotoxicity (ADCC). This indicated that nonneutralizing antibodies (nNAbs) may play an important role in preventing HIV infection (for a review of nNAbs in HIV, see Excler et al. [10]). Interestingly, subsequent analysis of serum from RV144 vaccinees determined that while env-binding IgG inversely correlated with risk of infection, env-binding IgA in serum positively correlated with infection risk [9]. For in-depth review of the analysis of correlates of protection in this trial, see Kim et al. [8]. It should be noted that mucosal IgA is mostly found in dimeric form (dIgA) and serum IgA is mostly found as monomeric IgA [11]. Unfortunately, no mucosal samples were taken from RV144 vaccinees; thus, the effect of mucosal dIgA on transmission could not be determined in subsequent analyses [12].

Very few studies have evaluated the ability of neutralizing antibodies of the IgA isotype to prevent infection. In one such study, Watkins and colleagues found that intrarectal application of dimeric IgA1 (dIgA1) to rhesus macaques prior to intrarectal challenge with simian-human immunodeficiency virus (SHIV) led to 83% protection from challenge [13]. While analysis from RV144 trial vaccinees indicated that serum IgA positively correlated with infection risk, Sholukh and colleagues found that the combination of dIgA and IgG (targeting the same HGN194 (a neutralizing epitope in env)), applied intrarectally, led to 100% protection from intrarectal challenge [14]. These results suggest different roles for serum IgA and mucosal dIgA. Recently, to understand the role of vaccine-induced IgA, HIV-specific IgA monoclonal antibodies (MAbs) were cloned from memory B cells present in the blood of RV144 vaccinees. These HIV-specific IgA MAbs were capable of mediating antibody-dependent cellular phagocytosis (ADCP) by monocytes and blocked env-binding to the alternative HIV receptor galactosylceramide [15]. In support of this, several studies have determined that there is an association of HIV-specific mucosal IgA with reduction of infection. Decreased risk of mother to child transmission was associated with anti-env IgA in breast milk [16]. Similarly, decreased infection rates in exposed seronegative women were associated with HIV-1 neutralizing IgA in genital secretions [17]. Finally,

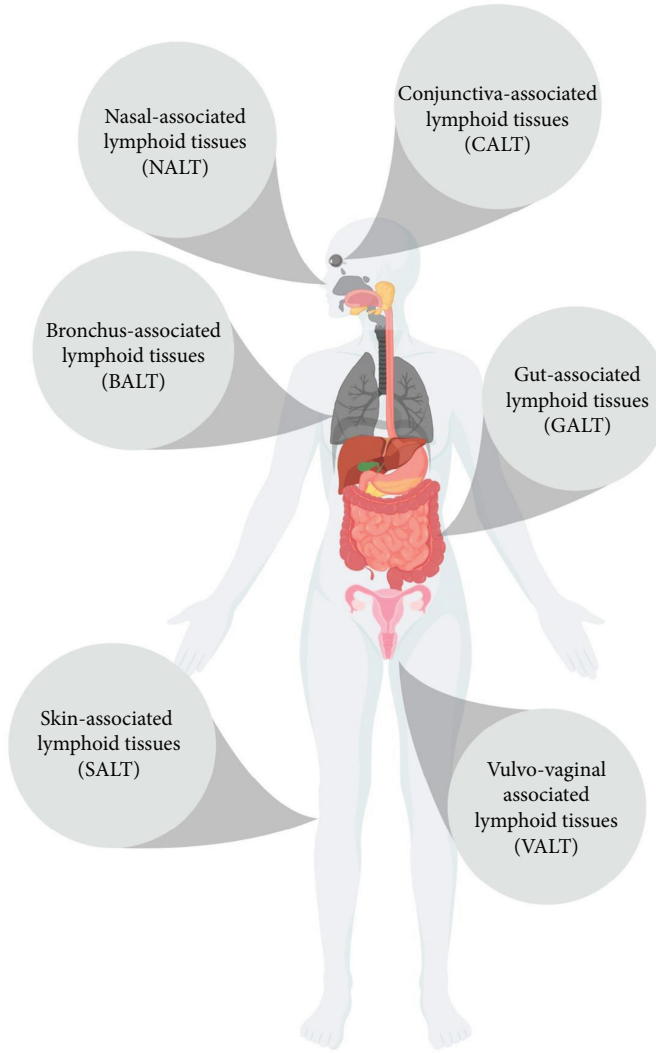

Figure 1: Mucosa-associated lymphoid tissues. MALT provides protection from pathogenic incursion and promotes the development of tolerance to commensal microbes. The lymphoid tissues in these sites sample the antigen directly from the environment to initiate immune exclusion or immune tolerance, and these responses are propagated in associated draining lymph nodes.

neutralizing mucosal IgA was detected in a cohort of exposed, seronegative Kenyan sex workers [18]. These data indicate that both neutralizing and nonneutralizing IgA antibodies at mucosal surfaces may be an important correlate of HIV-1 protection. The potential role of mucosal IgA in mediating protection from HIV infection necessitates a clear understanding of the function of inductive and effector mucosal immune organs, as IgA-secreting B cells are induced and educated at these sites.

2. The Mucosal Immune System

Mucosal surfaces present a barrier between the host and the environment and must balance tolerogenic responses to commensal microbes while maintaining the ability to respond to pathogens. The mucosal immune system consists of lymph nodes and nonorganized lymphoid tissues present in the respiratory, digestive, ocular, mammary, and urogenital tracts. There is also evidence of a connection between the skin immune system and the classical mucosal immune system [19, 20] (Figure 1—MALTs). IgA is found at high concentration in mucosal sites (where IgG is also present in substantial quantities) and at low concentration in the serum. In humans, two isotypes of IgA exist, IgA1 and IgA2 [21]. Interestingly, in the female genitourinary tract, antibodies of the IgG isotype are found in greater quantities than IgA [22]. The regulation of production and secretion of IgA is a key component of the mucosal barrier system. Differences in affinity of secretory IgA (sIgA) can determine if an antigen is subject to immune protection or tolerance [23–26]. Low-affinity binding to commensals is proposed to induce immune exclusion or tolerance to these bacteria, and this is required for the development and homeostasis of the mucosal immune system. Conversely, high-affinity IgA is proposed to bind pathogens and subject them to immune control.

The gut-associated lymphoid tissues (GALTs) are the largest lymphoid tissue organization in mammals. It consists of discrete organs: Peyer's patches (PPs), appendix, and isolated lymphoid follicles (ILFs). The GALT also contains diffuse lymphoid tissues including intraepithelial lymphocytes (IELs) and lamina propria (LP) lymphocytes. The appendix, ILFs, and PPs are considered inductive sites of mucosal immunity, while the MLNs and LP are considered effector sites. The GALT is part of the MALT (which encompasses all mucosa-associated lymphoid tissues) but distinct from the nasopharynx-associated lymphoid tissues (NALTs) which begin in the upper palate and include the nasal and upper respiratory tract mucosa. As IgA^+ B cells leave inductive sites in the MALT, they terminally differentiate to plasma cells, resulting in a greater number of IgA-secreting B cells in mucosal effector sites (MLNs and LP) than in inductive sites (PPs and appendix) [27]. This phenomenon is termed the "IgA cycle" [28] and is supported by genomics studies linking the immunoglobulin variable heavy (Ig_vH) chains of PP B cells to those of LP B cells [29–31]. Mesenteric lymph nodes are considered a part of the MALT, as activated mucosal lymphocytes can drain here and undergo expansion, but some researchers have suggested that they cannot be included in the MALT as the MALT proper samples antigen directly from intestinal lumen [32]. It is important to note that like the PPs, all MALT organs/organelles are similar in structure to peripheral lymph nodes, with discreet B cell zones separated by T cell areas, and contain dendritic cells and other antigen-presenting cells. Importantly, MALT organs and organelles lack afferent lymphatics. This lack of afferent lymphatics is possible as the characteristic follicle-associated epithelium (FAE) of the MALT contains microfold or M cells, which directly sample luminal antigens [33], and only efferent lymphatics are required for activated cells to exit and access other sites.

Peyer's patches are the primary inductive sites of IgA responses in the intestine [34, 35]. These patches are small, domed structures, visible to the naked eye, containing lymphocytes including B cells, T cells, and dendritic cells. In mice, the small intestines contain 7–12 PPs along its length. In humans, the number ranges from 30 to more than 200 [36]. Peyer's patches have distinct anatomical regions. B cell zones or follicles are surrounded by a FAE. The subepithelial dome (SED) lies between the FAE and the B cell follicles. Small T cell zones are also present in the PP [37] (see ref. [29] for a complete review of PP biology). The FAE microfold cells (M cells) sample luminal antigens and present them in Peyer's patches [38]. Germinal centers (GCs) are formed in the SED where follicular helper T cells (T_{FH}) induce T-dependent IgA class switching in B cells [37, 39] (Figure 2—Peyer's patch). The size and complexity of the mucosal immune system and the crosstalk between individual units of the MALT present challenges for vaccine design. However, the concept of a "unified" mucosal immune system implies that vaccine modalities that enhance mucosal responses will produce effects in multiple mucosal sites. This is especially helpful in the context of HIV vaccines as HIV transmission occurs primarily at gastrointestinal and urogenital mucosal sites.

3. Mucosal Chemokines and Their Receptors

The intestinal epithelial lining is dynamic and mediates interactions between the environment and the host. Intestinal epithelial cells (IECs) and the immune cells which reside in the tissue beneath the epithelial layer are responsible for maintaining the balance between responding to pathogens and tolerance of commensals. IECs express more than twenty unique chemokines, which bind ten distinct receptors (see Kulkarni et al. for a review of chemokines expressed by IECs [40]) (Figure 3—chemokine trafficking in the mucosa). The CXC chemokines CXCL8, 9, 10, 11, 12, and CXCL13 are expressed in the MALT. CXCL8 binds the receptors CXCR1 and CXCR2 expressed on eosinophils [41], mast cells [42], neutrophils [43], and some macrophages [44]. CXCL9, 10, and 11 all bind the receptor CXCR3 expressed on T_H1 cells [45]. CXCL12 binds the receptor CXCR4 which is expressed on IgA^+ and IgG^+ plasma cells [46, 47], and T cells (and is also a coreceptor for HIV infection). CXCL13 is expressed in peripheral and mucosal secondary lymphoid organs and grants B cells, T cells, and dendritic cells access to GCs via expression of the receptor CXCR5 [48]. The GC is the primary site of T-dependent class switch and affinity maturation [49, 50]. PP T_{FH} are most likely to induce IgA class switching. Importantly, in the context of HIV-1 infection, T_{FH} cells residing within lymphoid tissue GCs are a reservoir of infection-competent virus [51–54]. The CX3C chemokine CX3CL1 (fractalkine) binds the receptor CX3CR1, which is expressed on macrophages and dendritic cells [55, 56].

A variety of CC chemokines are also expressed by MALT IECs. The CC chemokine receptor CCR3 is expressed on eosinophils [57], macrophages [58], and T cells [59] and binds the chemokines CCL5, CCL7, CCL11, CCL13, CCL24, and CCL24, all of which are expressed by IECs. CCR5 is expressed on monocytes, macrophages [60], and T cells [61] and binds the ligands CCL3, CCL4, and CCL5. Importantly, CCR5 and CCR3 [62–64] to a lesser extent, along with the chemokine receptor CXCR4, are known coreceptors for HIV-1 infection. CCR6, an important mucosal homing receptor is expressed on dendritic cells, mature B cells, and T cells including T_H17 cells. CCR6 has only one known ligand, CCL20 [65]. CCR7 which is expressed by activated T cells [66] as well as innate lymphoid type 3 cells (ILC3) [66, 67] binds both CCL19 and CCL21.

The three most well-studied mucosal chemokines are CCL25, CCL27, and CCL28. The chemokine CCL25 (also called thymus-expressed chemokine or TECK), a well-studied skin-homing chemokine, has only one receptor, CCR9, and attracts gamma-delta T cells ($\gamma\delta$T) [68], $CD8^+$ T cells [69], $CD4^+$ T cells [70], dendritic cells [71], and IgA^+ plasma cells [72] to the MALT [73]. The CCR9/CCL25 axis is associated with oral tolerance [74], and perturbations in this axis are associated with pathogenic inflammation [75, 76]. CCL28 or mucosa-associated epithelial chemokine (MEC) is secreted by epithelial cells at many mucosal surfaces including the colon, salivary glands, mammary glands, and respiratory and urogenital tracts [77, 78]. CCL28 binds the receptor CCR10 and was first described by Mora et al. and Wang and colleagues [20, 79]. CCL28

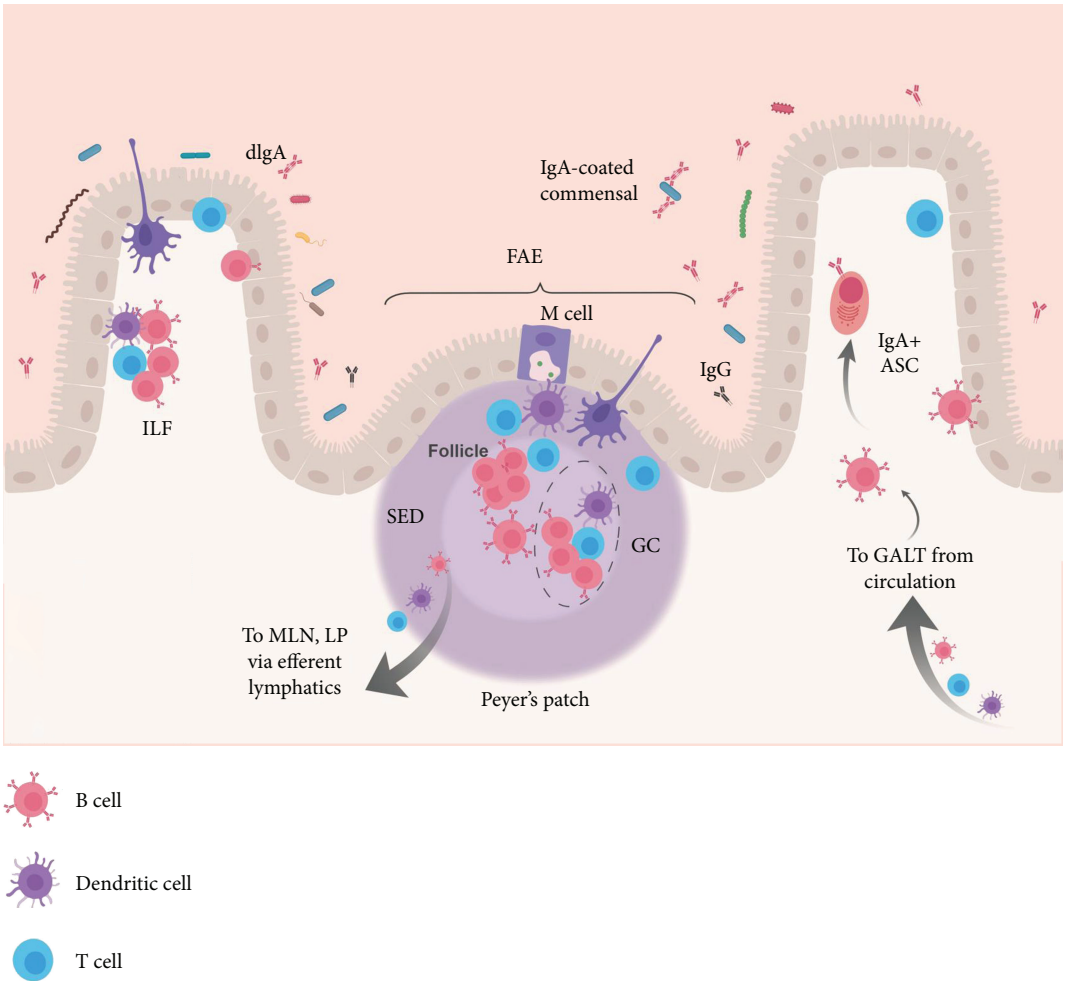

Figure 2: The Peyer's patch (PP) is the inductive site of GALT responses. M cells in the follicle-associated epithelium (FAE) of the PP directly sample luminal antigens and deliver them to antigen-presenting cells in the basolateral tissue. Dendritic cells (purple) may also stretch across the FAE and sample antigen directly. Antigen is presented to T cells (blue) within the PP. $CD4^+$ T cells (blue) provide help to PP B cells (red). Within the subepithelial zone (SED), PP germinal centers (GC), T_{FH} induce T-dependent IgA class switching of BCRs. Similarly, isolated lymphoid follicles (ILFs) are also inductive sites of MALT responses. Activated lymphocytes can exit the PP via efferent lymphatics and traffic to the mesenteric lymph node (MLN) or lamina proria (LP), and return to the GALT from circulation. In the GALT, antibody-secreting cells (ASCs) secrete antibodies including dimeric IgA (dIgA) which are translocated into the lumen.

is the most well-studied mucosal chemokine and is associated almost exclusively with the homing of IgA^+ antibody-secreting cells [73, 80–84]. Both CCL25, CCL28, and their receptors are expressed early in gestation in the thymus and mucosal tissues, suggesting involvement in the ontogeny of the common mucosal immune system [85]. The second ligand of CCR10 is CCL27 (also called cutaneous T cell-attracting chemokine or CTACK) [86] which is associated most commonly with the homing of T lymphocytes to the skin [87], but is indeed expressed by IECs.

The expression of the various receptors is "imprinted" on naïve lymphocytes following antigen stimulation. In the case of T cells, the antigen presented by mucosal dendritic ($CD103^+$) cells leads to the upregulation of CCR9 and the adhesion molecule $\alpha 4\beta 7$ which binds MALT-expressed mucosal vascular addressin cell adhesion molecule 1 (MADCAM1). For B cells, the expression of CCR9, CCR10, and $\alpha 4\beta 7$ provides access to the MALT. The end results of these complex interactions and receptor profiles are the attachment and extravasation of all the major types of lymphocytes into the MALT.

HIV transmission occurs primarily in the mucosa, and these surfaces are the sites of initial virus replication before dissemination and latency. Much research has therefore been focused on the role of chemokines and inflammatory cytokines at mucosal surfaces and HIV susceptibility or resistance. Recently, Arnold et al. demonstrated a striking correlation between inflammatory chemokines, decreased mucosal barrier integrity, and susceptibility to HIV infection [88]. The recruitment of $CD4^+$ T cells and other infection-permissive cells increases the number of target cells and can enhance HIV infection at the mucosa. Interestingly, increased levels of HIV coreceptor-binding mucosal chemokines CCL3 [89] and CCL5 [90] have been associated with decreased susceptibility to HIV infection. This is thought to be due to competition for coreceptor binding. Elevated levels

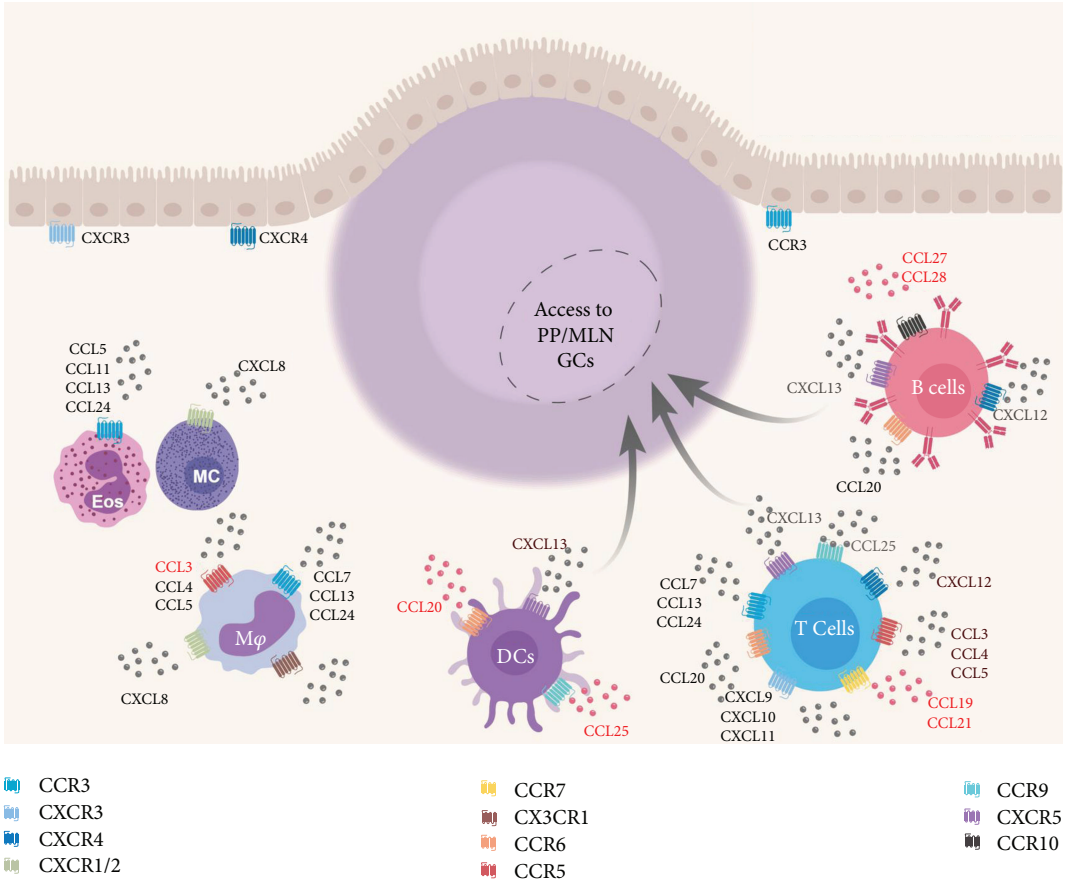

Figure 3: GALT chemokines and their receptors. All currently known GALT chemokines and their associated receptors are depicted. Chemokines and receptors are separated by the cell type. Chemokine adjuvants that have been used in the context of vaccination are depicted in red.

of the mucosal chemokine CCL20 in cervicovaginal wash from HIV-infected and uninfected women correlated with inhibition of HIV infection *in vitro* [91]. As the receptor for CCL20, CCR6, is not a known HIV coreceptor, it has been suggested that CCL20 might have anti-HIV antimicrobial activity. It was subsequently reported that the CCR6/CCL20 interaction stimulates cell-intrinsic immunity via cellular restriction factors [92]. For a complete review of barrier chemokines and their role in HIV pathogenesis, see Rancez et al. [93]. These studies strongly indicate a role for chemokine/receptor signaling in HIV infection, pathogenesis, and resistance. This supports the hypothesis that the chemokine trafficking system of the MALT could be strategically employed to prevent HIV infection.

4. Chemokine Adjuvants for Antiviral Mucosal Vaccines

The recruitment of activated lymphocytes to mucosal surfaces is strictly controlled, requiring the expression of specific chemokine receptors and adhesion molecules. This selection helps prevent pathogenic mucosal inflammation but presents a challenge for parenteral vaccination. Herpes virus infections are typically transmitted at mucosal surfaces. In the context of herpes infection, $CD8^+$ T cell responses are critical to protection; however, neutralizing antibodies can also prevent transmission. In a landmark publication, Shin and Iwasaki proposed the topical application of chemokines to "pull" antigen-experienced T lymphocytes that had been primed by peripheral vaccination, to the vaginal tract [94]. They called this approach "prime and pull," and it was remarkably effective. Following subcutaneous immunization with an attenuated herpes virus type-2 (HSV-2) and a topical application of the T cell chemokines CXCL9 and CXCL10 (CXCR3 ligands—CXCR3L) in the vaginal tract, HSV-2 glycoprotein B (gB)-specific $CD8^+$ T cells were detected in the vaginal mucosa. Specifically, the detected cells were CXCR3-expressing and had an activated phenotype. Importantly, these cells remained in the vaginal mucosa for up to twelve weeks post-"pull," and this led to 100% protection from lethal vaginal challenge [94]. The prime and pull approach definitively proved that the mucosal chemokine system could be used to direct antigen-specific responses to mucosal surfaces.

There are technical and logistical challenges associated with producing recombinant chemokines and delivering them to the genital mucosa in human patients. The DNA vaccine platform solves many of these technical issues.

Delivering DNA-encoded chemokines peripherally would enhance MALT receptor expression on antigen-specific cells, enabling them to traffic to the mucosa more effectively, bypassing the need for direct delivery of the chemokine to the genital mucosa. DNA vaccines typically consist of naked plasmids encoding the DNA sequence of the protein of interest. Upon delivery, this DNA is taken up by cells, transcribed and translated within the cell, processed and presented on MHC molecules, and secreted as a soluble antigen from transformed cells [95]. DNA is incredibly stable, can be synthesized in the lab, and requires no cold chain transport. Finally, the advent of electroporation for delivery and the optimization of plasmid generation has enhanced the immunogenicity of DNA vaccines [96, 97]. The DNA platform also allows for the inclusion of plasmid-encoded adjuvants, termed "molecular adjuvants," such as chemokines, to be codelivered with antigens in a single formulation. Importantly, DNA vaccines have been used in humans for over two decades and have an excellent safety profile [98].

Herpes DNA vaccines have capitalized on the flexibility of the DNA platform to deliver HSV antigens and mucosa-directing chemokines to target vaccine responses to the genital tract. In 2001, when comparing intramuscular versus intranasal vaccine delivery, Eo and colleagues reported that intranasal codelivery of plasmids encoding Herpes gB and murine CCL19 and CCL21 leads to a transient increase in HSV-specific IgA in vaginal wash, while intramuscular immunization did not enhance mucosal antibody [99]. Similarly, the Rouse lab demonstrated an increase in vaginal IgA in response to a viral vector prime, the DNA boost vaccine regimen. The formulation included plasmid-expressed gB, CCL21 or CCL19, and recombinant vaccinia virus, encoding herpes gB. Unfortunately, these responses did not lead to the generation of long-lasting memory [100].

Using a slightly modified approach, Yan and colleagues created a fusion plasmid encoding both HSV-2 gB and CCL19 and injected 5 μg of this single plasmid into female mice twice, separated by two weeks. The animals were rested for seven weeks and then given a lethal intravaginal challenge with HSV-2. The fusion construct was superior to immunization with separate plasmids encoding gB and CCL19. However, immunization with either the fusion construct or two individual plasmids leads to statistically significant increases in serum and vaginal HSV-specific IgA and serum IgG. The group also observed increases in IgA-secreting cells in the colorectal mucosa and enhancement of spleen and MLN lymphocyte migrations toward CCL19, indicating increased expression of the receptor CCR7 and explaining the increased mucosal antibody responses. These enhanced antibody responses lead to protection from challenge. Animals immunized with either the two plasmids or the single fusion plasmid had decreased mortality; however, animals receiving the individual plasmids lost weight and had mild, clinical disease, while those immunized with the fusion construct lost no weight and exhibited no clinical disease [101]. This indicates a benefit of having the chemokine adjuvant and antigen expressed in the same transformed cell.

Influenza vaccines face similar challenges in that flu-specific immunity needs to be present in the upper respiratory mucosa to protect against viral infection. In the context of influenza, neutralizing antibodies at the site of transmission are critical to preventing infection. $CD8^+$ T cell responses are equally critical in that the recognition and killing of influenza-infected cells will limit replication and protect against disease. Traditional intramuscular influenza vaccines with protein antigens and chemical adjuvants induce robust peripheral responses, generating high titers of neutralizing IgG which can diffuse form circulation into the BALT and NALT. Our laboratory evaluated the use of CCL27 and CCL28 to augment responses to an influenza hemagglutinin- (HA-) encoding DNA vaccine [102]. This was the first use of these chemokines as molecular (plasmid-encoded) adjuvants in the context of a DNA vaccine. We observed 2–3-fold increases in HA-specific IgA in the fecal extract of vaccinated animals, which remained detectable at 8 weeks after a second intramuscular immunization. The presence of antigen-specific antibodies at distal mucosal sites is indicative of coordinated mucosal homing. That peripherally activated lymphocytes can traffic to the mucosa following chemokine-adjuvanted vaccination suggests that these chemokine molecules imprint such cells with the receptors necessary for mucosal trafficking. We also detected increased IgG in the serum of chemokine coimmunized animals. This neutralizing IgG led to 100% protection from lethal influenza infection in these animals [102]. The Kutzler laboratory has also used CCL25 (TECK) to enhance influenza-specific T cell responses at mucosal surfaces. Again, we detected increased HA-specific IgA in the fecal extracts and vaginal wash from CCL25 coimmunized animals as well as increased IgA ASCs in the lungs of these animals. Importantly, increased IFNγ-secreting T cells in the spleens and MLNs of these animals were also evident. Upon challenge, pCCL25 and pHA coimmunized animals lost less weight and were 100% protected from mortality [103].

Creating an effective anti-HIV vaccine requires the generation of effective humoral and cell-mediated responses. Binding, neutralizing, and ADCC/ADCP-mediating antibody responses are as critical as the generation of effector $CD8^+$ T cells. Importantly, the vast majority of these responses need to be directed to mucosal surfaces to prevent transmission of the virus. In keeping with this, HIV vaccine researchers have used mucosal chemokines to enhance B and T cell responses to HIV-1 immunogens. Song and colleagues reported that immunization with 50 μg of HIV gag (capsid proteins) plasmid in the presence of CCL3, CCL19, and CCL20 leads to enhanced recruitment of macrophages and $CD8^+$ T cells. Unfortunately, B cell activation was lacking, and only a modest enhancement in HIV-specific IgG was reported in animals receiving pgag and pCCL19 [104].

CCL25, CCL27, and CCL28 are some of the most well-studied mucosal chemokines and are used to promote the generation of antigen-specific mucosal immunity following immunization. We reported on the use of CCL25 to drive T cell responses to the mucosa following HIV DNA immunization, finding that after immunization via electroporation, increased IFNγ-secreting cells were detected in the spleen

and MLN of coimmunized animals, and increased HIV-specific IgA in the serum and fecal extracts was also detected in these mice [103]. Our laboratory was the first to report the use of CCL27 and CCL28 as molecular adjuvants in the context of a DNA vaccine [102]. Other groups have confirmed our findings and used these chemokines in the context of HIV-1 vaccines. Hu et al. completed a comparative study of the ability of chemokine and cytokine adjuvants to augment an HIV-1 env gp140 DNA vaccine when delivered either intramuscularly with electroporation or intranasally as naked DNA. The group vaccinated mice with either pgp140 alone, plasmid-encoded CCL19 and CCL28, or a proliferation-inducing ligand (APRIL, a known B cell-stimulating cytokine). The results demonstrated that coimmunization with pCCL19 or pCCL28 enhanced mucosal and systemic anti-HIV IgA responses. Importantly, neutralizing IgA from vaginal secretions was reported in this study. Finally, Hu and colleagues reported detecting increased $CCR10^+$ B cells in the MLNs of CCL28 coimmunized animals when the vaccine was delivered intramuscularly with electroporation but not when delivered intranasally [105]. These results also demonstrated that expression of the associated chemokine receptor is required for chemokine adjuvanticity. In this study, 15 μg of chemokine adjuvant was delivered with 4 μg of the env antigen in PEI (transfection reagent) intranasally, while 30 μg of the antigen and 100 μg of adjuvant were used for intramuscular delivery via electroporation. Intranasal delivery may have been less successful in these studies due to the decreased concentration of the antigen and adjuvant used. These results however, indicate that CCR10 expression mediated CCL28-induced responses.

In an attempt to replicate the Iwaski "prime and pull" method of classical protein immunization and topical application of chemokine in the context of an HIV-1 vaccine, Tregoning and colleagues vaccinated animals with trimeric HIV-1 gp140 and applied CCL28 to the vaginal surface six days after each immunization. They detected an increase in total, but not HIV-specific IgA in the vaginal wash of immunized animals [106]. The group did not examine CCR10 expression on the surface of IgA-secreting cells in this study. These results further support the need for expression of chemokine and antigen together during priming as being critical for enhancing mucosal homing of antigen-specific cells.

Following the encouraging results reported by our laboratory and others using CCL28 to enhance HIV-specific IgA responses in the mucosal tract, we performed similar experiments in nonhuman primates. Female macaques were vaccinated five times, separated by 6 weeks, with plasmids encoding consensus simian immunodeficiency virus (SIV—the NHP analogue of HIV) gag, pol, and env, followed by a boost with SIV nef-rev plasmids. HIV antigens were administered either alone or with plasmids encoding rhesus CCL25 (CCR9L) or CCL27 and CCL28 (CCR10L). All immunizations were given by intramuscular injection followed by electroporation. In these studies, we detected increased mucosal and systemic IgG and IgA in coimmunized animals. The primates which received CCR10L-encoding plasmids had an 89% protection rate from SIV challenge compared to only 68% protection in the other vaccine groups and 14% in naïve primates [107]. These increased antibody responses were correlated with a decrease risk of infection during challenge. Our studies and those performed in other laboratories have demonstrated the ability of CCL27 and CCL28 to enhance mucosal IgA responses to HIV vaccines, promoting increased antigen-specific IgA in the mucosal secretions of animals, which can mediate transmission prevention (Table 1—chemokine vaccine studies targeting HIV). Importantly, all the studies described above demonstrate that peripheral immunization, using molecules that target antigen-specific cells to the mucosa, can induce mucosal immunity.

5. Discussion

The characterization of the chemokines and receptors involved in the tissue-specific migration of immune cells has yielded a greater understanding of how vaccine adjuvants can be used to target antigen-specific immunity to the mucosa. This understanding will be crucial to the development of vaccines against mucosal pathogens. Poor mucosal responsiveness to parenterally delivered vaccine antigens highlights the need to develop vaccine modalities that direct antigen-specific cells to barrier surfaces. There is an urgent need to develop a safe, immunogenic HIV-1 vaccine that generates binding and neutralizing antibodies, effector T cells, and promotes the formation of long-lasting memory at mucosal surfaces. The challenges associated with HIV vaccine development, namely, the lack of clear correlates of protection, make this difficult. However, immunity at the genital mucosa will obviously play a role in preventing transmission.

The prime and pull method effectively pulls antigen-primed cells to mucosal surfaces; however, the longevity of these responses needs to be explored. DNA vaccines are an established platform for the codelivery of molecular chemokine adjuvants. Interestingly, even though DNA vaccines are almost exclusively delivered parenterally, the inclusion of plasmid-encoded chemokines as molecular adjuvants enhances responses in the distal mucosa. We propose that ligation of chemokine with its cognate receptor creates an autocrine amplification loop that increases expression of the cognate receptor on the cell surface. This phenomenon polarizes the cell such that it is more responsive to the chemokine gradient. This suggests that transformed cells secreting the chemokine adjuvant create an artificial, temporary gradient which recruits receptor-bearing immunocytes and leads to upregulation of the chemokine receptor in question. If any of these immunocytes can respond to the antigen being secreted and presented by the transformed cell, they will become activated, traffic to draining lymph nodes, expand in population, and eventually home back to mucosal sites by virtue of enhanced mucosal chemokine receptor expression and the homeostatic gradient created by IECs (Figure 4—MALT molecular chemokine adjuvants in DNA vaccines). Very little is known about the regulation of chemokine receptor expression. It will be important to characterize cognate chemokine receptor expression on mucosal effector cells following vaccination with mucosal chemokine

Table 1: HIV-1 vaccine studies using chemokine adjuvants. Italicized adjuvants are not discussed in this review.

Study (ref)	Antigen	Platform	Chemokine adjuvants	Target cells	Results
Kathuria et al. [103]	HIV gag and also influenza HA	DNA vaccine	CCL25	CTLs and $CD4^+$ T cells	Increased $IFN\gamma^+$ T cells in the spleen and MLN. Increased IgA^+ ASCs in PPs and increased HIV-specific IgA in serum.
Hu et al. [105]	HIV gp140 (env)	DNA vaccine	CCL19, CCL28, and *also APRIL*		Enhanced HIV-specific serum and vaginal IgA. Neutralizing IgA in vaginal wash and increased $CCR10^+$ B cells in MLNs.
Tregoning et al. [106]	HIV gp140 (env and trimeric)	Protein	CCL28 and *also TLR4L*		No increase in HIV-specific IgA in vaginal wash.
Kutzler et al. [107]	SIV gag, pol, env, and nef-rev	DNA vaccine	CCL25, CCL27, and CCL28		Increased HIV-specific IgG and IgA in serum and vaginal wash. Highest protection from SIV challenge (CCR10L group).
Song et al. [104]	HIV gag	DNA vaccine	CCL3, CCL19, and CCL20	CTLs and macrophages	Increased Mφ recruitment and CTL activity.

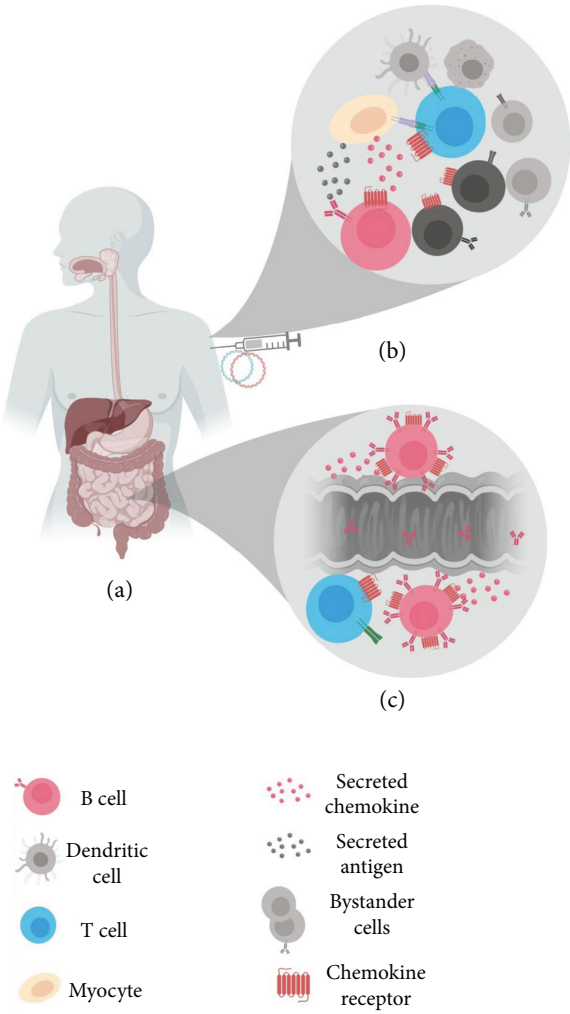

Figure 4: MALT molecular chemokine adjuvants in DNA vaccines. (a) Following parenteral delivery of antigen and chemokine plasmid DNA, transformed cells (tan) will transcribe, translate, process, and present the antigen. (b) Antigen (black circles) is also secreted from transformed cells, as is the chemokine adjuvant (red circles), creating a local chemokine gradient which will recruit chemokine receptor-bearing cells (red chemokine receptors). Some recruited cells will be unable to respond to antigen (dark gray); others will be recruited as a result of vaccination-induced inflammation (light gray). Recruited cells bearing the appropriate receptors and capable of responding to antigen (red B cell and blue T cell), will upregulate the chemokine receptor and proliferate. (c) Receptor upregulation following chemokine ligation and antigen-experience imprints these antigen-experienced cells with the ability to traffic to the MALT effector site, resulting in antigen-specific mucosal responses.

adjuvants; this knowledge will be critical to further development of chemokine adjuvants. Similarly, vaccination studies where chemokines are used as adjuvants should evaluate the effect of chemokine adjuvantation on receptor expression on antigen-specific and bystander cells.

Having determined that chemokines can be used effectively to enhance vaccine-mediated mucosal immunity, it will be important to study whether vaccination with these adjuvants induces the establishment of immune memory at mucosal sites. Furthermore, it is important to continue to study the basic mechanisms by which expression and kinetics of tissue-specific homing receptors are regulated. This knowledge will inform the development of other methods to promote receptor-ligand-mediated homing. For example, it is known that colonization of the intestines by commensal microbes promotes increased CCL28 secretion by intestinal epithelial cells [108].

In conclusion, an increased understanding of chemokine-mediated trafficking in the mucosa has prompted the use of these molecules as adjuvants to direct activated, antigen-experienced effector cells to mucosal surfaces. Chemokine molecular adjuvants, particularly CCL28, have proven especially useful for generating humoral anti-HIV immunity at mucosal sites, leading to protection from challenge in SIV models. DNA vaccines are well-suited for the delivery of chemokine adjuvants and represent a parenteral delivery method that can promote mucosal immunity. Thus, the combined use of the DNA platform and mucosal chemokine adjuvants has potential to induce robust anti-HIV responses in the mucosa and represents a new modality for generating antigen-specific mucosal immunity. The final challenge for successful delivery of chemokines as vaccine adjuvants is the generation of long-lived immunity at mucosal surfaces. Thus, future studies should address the ability of chemokines to promote mucosal memory in the context of vaccination.

Disclosure

M. Kutzler receives grant funding, participates in industry collaborations, has received speaking honoraria, and honoraria for her service in reviewing federal research grants at the National Institute of Health and Department of Defense. M. Kutzler has received funding through a sponsored research agreement with Pfizer Inc. and has received royalties from a patent licensure through Inovio Pharmaceuticals. These financial relationships do not relate to the content of this review article and in no way pose a potential conflict of interest.

Conflicts of Interest

The authors declare that they have no conflicts of interest.

Acknowledgments

Writing of this review article is supported by the following grants to M. Kutzler: W. W. Smith Charitable Trust Foundation, the Pennsylvania Department of Health CURE program, and the Philadelphia Health and Education Corporation funds. E. Gary is partially funded by Drexel University's Interdisciplinary and Translational Research Training Grant in NeuroAIDS, funded by the National Institutes of Health (National Institute of Mental Health) grant T32-MH079785.

References

[1] M. McDermott and J. Bienenstock, "Evidence for a common mucosal immunologic system. I. Migration of B immunoblasts into intestinal, respiratory, and genital tissues," *The Journal of Immunology*, vol. 122, no. 5, pp. 1892–1898, 1979.

[2] C. Czerkinsky, S. J. Prince, S. M. Michalek et al., "IgA antibody-producing cells in peripheral blood after antigen ingestion: evidence for a common mucosal immune system in humans," *Proceedings of the National Academy of Sciences of the United States of America*, vol. 84, no. 8, pp. 2449–2453, 1987.

[3] J. Bienenstock, M. McDermott, D. Befus, and M. O'Neill, "A common mucosal immunologic system involving the bronchus, breast and bowel," in *Secretory Immunity and Infection. Advances in Experimental Medicine and Biology, vol 107*, J. R. McGhee, J. Mestecky, and J. L. Babb, Eds., pp. 53–59, Springer, Boston, MA, USA, 1978.

[4] H. L. Wilson and M. R. Obradovic, "Evidence for a common mucosal immune system in the pig," *Molecular Immunology*, vol. 66, no. 1, pp. 22–34, 2015.

[5] A. Zlotnik and O. Yoshie, "The chemokine superfamily revisited," *Immunity*, vol. 36, no. 5, pp. 705–716, 2012.

[6] G. D. Tomaras and S. A. Plotkin, "Complex immune correlates of protection in HIV-1 vaccine efficacy trials," *Immunological Reviews*, vol. 275, no. 1, pp. 245–261, 2017.

[7] L. Corey, P. B. Gilbert, G. D. Tomaras, B. F. Haynes, G. Pantaleo, and A. S. Fauci, "Immune correlates of vaccine protection against HIV-1 acquisition," *Science Translational Medicine*, vol. 7, no. 310, article 310rv317, 2015.

[8] J. H. Kim, J.-L. Excler, and N. L. Michael, "Lessons from the RV144 Thai phase III HIV-1 vaccine trial and the search for correlates of protection," *Annual Review of Medicine*, vol. 66, no. 1, pp. 423–437, 2015.

[9] S. Rerks-Ngarm, P. Pitisuttithum, S. Nitayaphan et al., "Vaccination with ALVAC and AIDSVAX to prevent HIV-1 infection in Thailand," *The New England Journal of Medicine*, vol. 361, no. 23, pp. 2209–2220, 2009.

[10] J.-L. Excler, J. Ake, M. L. Robb, J. H. Kim, and S. A. Plotkin, "Nonneutralizing functional antibodies: a new "old" paradigm for HIV vaccines," *Clinical and Vaccine Immunology*, vol. 21, no. 8, pp. 1023–1036, 2014.

[11] J. M. Woof and J. Mestecky, "Mucosal immunoglobulins," *Immunological Reviews*, vol. 206, no. 1, pp. 64–82, 2005.

[12] B. F. Haynes, P. B. Gilbert, M. J. McElrath et al., "Immune-correlates analysis of an HIV-1 vaccine efficacy trial," *The New England Journal of Medicine*, vol. 366, no. 14, pp. 1275–1286, 2012.

[13] J. A. Watkins, A. M. Sholukh, M. M. Mukhtar et al., "Anti-HIV IgA isotypes: differential virion capture and inhibition of transcytosis are linked to prevention of mucosal R5 SHIV transmission," *AIDS*, vol. 27, no. 9, pp. F13–F20, 2013.

[14] A. M. Sholukh, J. D. Watkins, H. K. Vyas et al., "Defense-in-depth by mucosally administered anti-HIV dimeric IgA2 and systemic IgG1 mAbs: complete protection of rhesus monkeys from mucosal SHIV challenge," *Vaccine*, vol. 33, no. 17, pp. 2086–2095, 2015.

[15] S. Wills, K. K. Hwang, P. Liu et al., "HIV-1-specific IgA monoclonal antibodies from an HIV-1 vaccinee mediate galactosylceramide blocking and phagocytosis," *Journal of Virology*, vol. 92, no. 7, 2018.

[16] J. Pollara, E. McGuire, G. G. Fouda et al., "Association of HIV-1 envelope-specific breast milk IgA responses with reduced risk of postnatal mother-to-child transmission of HIV-1," *Journal of Virology*, vol. 89, no. 19, pp. 9952–9961, 2015.

[17] J. M. Lund, K. Broliden, M. N. Pyra et al., "HIV-1-neutralizing IgA detected in genital secretions of highly HIV-1-exposed seronegative women on oral preexposure prophylaxis," *Journal of Virology*, vol. 90, no. 21, pp. 9855–9861, 2016.

[18] R. Kaul, F. Plummer, M. Clerici, M. Bomsel, L. Lopalco, and K. Broliden, "Mucosal IgA in exposed, uninfected subjects: evidence for a role in protection against HIV infection," *AIDS*, vol. 15, no. 3, pp. 431-432, 2001.

[19] Z. Xu, D. Parra, D. Gómez et al., "Teleost skin, an ancient mucosal surface that elicits gut-like immune responses," *Proceedings of the National Academy of Sciences of the United States of America*, vol. 110, no. 32, pp. 13097–13102, 2013.

[20] J. R. Mora, G. Cheng, D. Picarella, M. Briskin, N. Buchanan, and U. H. von Andrian, "Reciprocal and dynamic control of CD8 T cell homing by dendritic cells from skin- and gut-associated lymphoid tissues," *Journal of Experimental Medicine*, vol. 201, no. 2, pp. 303–316, 2005.

[21] S. Crago, W. Kutteh, I. Moro et al., "Distribution of IgA1-, IgA2-, and J chain-containing cells in human tissues," *The Journal of Immunology*, vol. 132, no. 1, pp. 16–18, 1984.

[22] R. K. Naz, "Female genital tract immunity: distinct immunological challenges for vaccine development," *Journal of Reproductive Immunology*, vol. 93, no. 1, pp. 1–8, 2012.

[23] S. Fagarasan and T. Honjo, "Intestinal IgA synthesis: regulation of front-line body defences," *Nature Reviews Immunology*, vol. 3, no. 1, pp. 63–72, 2003.

[24] A. J. Macpherson, K. D. McCoy, F. E. Johansen, and P. Brandtzaeg, "The immune geography of IgA induction and function," *Mucosal Immunology*, vol. 1, no. 1, pp. 11–22, 2008.

[25] A. Cerutti, "The regulation of IgA class switching," *Nature Reviews Immunology*, vol. 8, no. 6, pp. 421–434, 2008.

[26] E. Slack, M. L. Balmer, J. H. Fritz, and S. Hapfelmeier, "Functional flexibility of intestinal IgA–broadening the fine line," *Frontiers in Immunology*, vol. 3, p. 100, 2012.

[27] D. Parrott, "The gut as a lymphoid organ," *Clinics in Gastroenterology*, vol. 5, no. 2, pp. 211–228, 1976.

[28] M. E. Lamm, "Cellular aspects of immunoglobulin A," *Advances in Immunology*, vol. 22, pp. 223–290, 1976.

[29] D. K. Dunn-Walters, P. G. Isaacson, and J. Spencer, "Sequence analysis of human IgVH genes indicates that ileal lamina propria plasma cells are derived from Peyer's patches," *European Journal of Immunology*, vol. 27, no. 2, pp. 463–467, 1997.

[30] J. Tseng, "Transfer of lymphocytes of Peyer's patches between immunoglobulin allotype congenic mice: repopulation of the IgA plasma cells in the gut lamina propria," *The Journal of Immunology*, vol. 127, no. 5, pp. 2039–2043, 1981.

[31] J. Tseng, "A population of resting IgM-IgD double-bearing lymphocytes in Peyer's patches: the major precursor cells for IgA plasma cells in the gut lamina propria," *The Journal of Immunology*, vol. 132, no. 6, pp. 2730–2735, 1984.

[32] P. Brandtzaeg, H. Kiyono, R. Pabst, and M. W. Russell, "Terminology: nomenclature of mucosa-associated lymphoid tissue," *Mucosal Immunology*, vol. 1, no. 1, pp. 31–37, 2008.

[33] M. R. Neutra, N. J. Mantis, and J.-P. Kraehenbuhl, "Collaboration of epithelial cells with organized mucosal lymphoid tissues," *Nature Immunology*, vol. 2, no. 11, pp. 1004–1009, 2001.

[34] J. R. Mora, M. Iwata, B. Eksteen et al., "Generation of gut-homing IgA-secreting B cells by intestinal dendritic cells," *Science*, vol. 314, no. 5802, pp. 1157–1160, 2006.

[35] J. R. Mora and U. H. Von Andrian, "Differentiation and homing of IgA-secreting cells," *Mucosal Immunology*, vol. 1, no. 2, pp. 96–109, 2008.

[36] J. S. Cornes, "Number, size, and distribution of Peyer's patches in the human small intestine: part I the development of Peyer's patches," *Gut*, vol. 6, no. 3, pp. 225–229, 1965.

[37] A. Reboldi and J. G. Cyster, "Peyer's patches: organizing B-cell responses at the intestinal frontier," *Immunological Reviews*, vol. 271, no. 1, pp. 230–245, 2016.

[38] W. Bye, C. Allan, and J. Trier, "Structure, distribution, and origin of M cells in Peyer's patches of mouse ileum," *Gastroenterology*, vol. 86, 5, Part 1, pp. 789–801, 1984.

[39] A. T. Cao, S. Yao, B. Gong, R. I. Nurieva, C. O. Elson, and Y. Cong, "Interleukin (IL)-21 promotes intestinal IgA response to microbiota," *Mucosal Immunology*, vol. 8, no. 5, pp. 1072–1082, 2015.

[40] N. Kulkarni, M. Pathak, and G. Lal, "Role of chemokine receptors and intestinal epithelial cells in the mucosal inflammation and tolerance," *Journal of Leukocyte Biology*, vol. 101, no. 2, pp. 377–394, 2017.

[41] H. Petering, O. Götze, D. Kimmig, R. Smolarski, A. Kapp, and J. Elsner, "The biologic role of interleukin-8: functional analysis and expression of CXCR1 and CXCR2 on human eosinophils," *Blood*, vol. 93, no. 2, pp. 694–702, 1999.

[42] U. Lippert, M. Artuc, A. Grützkau et al., "Expression and functional activity of the IL-8 receptor type CXCR1 and CXCR2 on human mast cells," *The Journal of Immunology*, vol. 161, no. 5, pp. 2600–2608, 1998.

[43] G. Godaly, G. Bergsten, L. Hang et al., "Neutrophil recruitment, chemokine receptors, and resistance to mucosal infection," *Journal of Leukocyte Biology*, vol. 69, no. 6, pp. 899–906, 2001.

[44] E. J. Williams, S. Haque, C. Banks, P. Johnson, P. Sarsfield, and N. Sheron, "Distribution of the interleukin-8 receptors, CXCR1 and CXCR2, in inflamed gut tissue," *The Journal of Pathology*, vol. 192, no. 4, pp. 533–539, 2000.

[45] J. R. Groom and A. D. Luster, "CXCR3 in T cell function," *Experimental Cell Research*, vol. 317, no. 5, pp. 620–631, 2011.

[46] G. Muehlinghaus, L. Cigliano, S. Huehn et al., "Regulation of CXCR3 and CXCR4 expression during terminal differentiation of memory B cells into plasma cells," *Blood*, vol. 105, no. 10, pp. 3965–3971, 2005.

[47] A. E. Hauser, G. F. Debes, S. Arce et al., "Chemotactic responsiveness toward ligands for CXCR3 and CXCR4 is regulated on plasma blasts during the time course of a memory immune response," *The Journal of Immunology*, vol. 169, no. 3, pp. 1277–1282, 2002.

[48] D. F. Legler, M. Loetscher, R. S. Roos, I. Clark-Lewis, M. Baggiolini, and B. Moser, "B cell–attracting chemokine 1, a human CXC chemokine expressed in lymphoid tissues, selectively attracts B lymphocytes via BLR1/CXCR5," *Journal of Experimental Medicine*, vol. 187, no. 4, pp. 655–660, 1998.

[49] C.-H. Jenh, M. A. Cox, W. Hipkin et al., "Human B cell-attracting chemokine 1 (BCA-1; CXCL13) is an agonist for the human CXCR3 receptor," *Cytokine*, vol. 15, no. 3, pp. 113–121, 2001.

[50] P. Schaerli, K. Willimann, A. B. Lang, M. Lipp, P. Loetscher, and B. Moser, "CXC chemokine receptor 5 expression defines follicular homing T cells with B cell helper function," *Journal of Experimental Medicine*, vol. 192, no. 11, pp. 1553–1562, 2000.

[51] C. H. Fox, K. Tenner-Rácz, P. Rácz, A. Firpo, P. A. Pizzo, and A. S. Fauci, "Lymphoid germinal centers are reservoirs of human immunodeficiency virus type 1 RNA," *Journal of Infectious Diseases*, vol. 164, no. 6, pp. 1051–1057, 1991.

[52] E. N. Gary and M. A. Kutzler, "A little help from the follicles: understanding the germinal center response to human immunodeficiency virus 1 infection and prophylactic vaccines," *Clinical Medicine Insights: Pathology*, vol. 10, article 117955571769554, 2017.

[53] S. Gratton, R. Cheynier, M.-J. Dumaurier, E. Oksenhendler, and S. Wain-Hobson, "Highly restricted spread of HIV-1 and multiply infected cells within splenic germinal centers," *Proceedings of the National Academy of Sciences of the United States of America*, vol. 97, no. 26, pp. 14566–14571, 2000.

[54] M. Perreau, A.-L. Savoye, E. De Crignis et al., "Follicular helper T cells serve as the major CD4 T cell compartment for HIV-1 infection, replication, and production," *Journal of Experimental Medicine*, vol. 210, no. 1, pp. 143–156, 2013.

[55] J. H. Niess, S. Brand, X. Gu et al., "CX3CR1-mediated dendritic cell access to the intestinal lumen and bacterial clearance," *Science*, vol. 307, no. 5707, pp. 254–258, 2005.

[56] O. Pabst and G. Bernhardt, "The puzzle of intestinal lamina propria dendritic cells and macrophages," *European Journal of Immunology*, vol. 40, no. 8, pp. 2107–2111, 2010.

[57] A. A. Humbles, B. Lu, D. S. Friend et al., "The murine CCR3 receptor regulates both the role of eosinophils and mast cells in allergen-induced airway inflammation and hyperresponsiveness," *Proceedings of the National Academy of Sciences of the United States of America*, vol. 99, no. 3, pp. 1479–1484, 2002.

[58] A. Mantovani, A. Sica, S. Sozzani, P. Allavena, A. Vecchi, and M. Locati, "The chemokine system in diverse forms of macrophage activation and polarization," *Trends in Immunology*, vol. 25, no. 12, pp. 677–686, 2004.

[59] E. Danilova, I. Skrindo, E. Gran et al., "A role for CCL28–CCR3 in T-cell homing to the human upper airway mucosa," *Mucosal Immunology*, vol. 8, no. 1, pp. 107–114, 2015.

[60] A. Kaufmann, R. Salentin, D. Gemsa, and H. Sprenger, "Increase of CCR1 and CCR5 expression and enhanced functional response to MIP-1α during differentiation of human monocytes to macrophages," *Journal of Leukocyte Biology*, vol. 69, no. 2, pp. 248–252, 2001.

[61] C. C. Bleul, L. Wu, J. A. Hoxie, T. A. Springer, and C. R. Mackay, "The HIV coreceptors CXCR4 and CCR5 are differentially expressed and regulated on human T lymphocytes," *Proceedings of the National Academy of Sciences of the United States of America*, vol. 94, no. 5, pp. 1925–1930, 1997.

[62] H. Choe, M. Farzan, Y. Sun et al., "The β-chemokine receptors CCR3 and CCR5 facilitate infection by primary HIV-1 isolates," *Cell*, vol. 85, no. 7, pp. 1135–1148, 1996.

[63] J. He, Y. Chen, M. Farzan et al., "CCR3 and CCR5 are co-receptors for HIV-1 infection of microglia," *Nature*, vol. 385, no. 6617, pp. 645–649, 1997.

[64] A. Ghorpade, M. Q. Xia, B. T. Hyman et al., "Role of the β-chemokine receptors CCR3 and CCR5 in human immunodeficiency virus type 1 infection of monocytes and microglia," *Journal of Virology*, vol. 72, no. 4, pp. 3351–3361, 1998.

[65] E. Schutyser, S. Struyf, and J. Van Damme, "The CC chemokine CCL20 and its receptor CCR6," *Cytokine & Growth Factor Reviews*, vol. 14, no. 5, pp. 409–426, 2003.

[66] A. Habtezion, L. P. Nguyen, H. Hadeiba, and E. C. Butcher, "Leukocyte trafficking to the small intestine and colon," *Gastroenterology*, vol. 150, no. 2, pp. 340–354, 2016.

[67] E. C. Mackley, S. Houston, C. L. Marriott et al., "CCR7-dependent trafficking of RORγ^+ ILCs creates a unique microenvironment within mucosal draining lymph nodes," *Nature Communications*, vol. 6, no. 1, p. 5862, 2015.

[68] E. R. Mann, N. E. McCarthy, S. T. C. Peake et al., "Skin- and gut-homing molecules on human circulating $\gamma\delta$ T cells and their dysregulation in inflammatory bowel disease," *Clinical & Experimental Immunology*, vol. 170, no. 2, pp. 122–130, 2012.

[69] M. Svensson, J. Marsal, A. Ericsson et al., "CCL25 mediates the localization of recently activated CD8$\alpha\beta^+$ lymphocytes to the small-intestinal mucosa," *The Journal of Clinical Investigation*, vol. 110, no. 8, pp. 1113–1121, 2002.

[70] H. Stenstad, A. Ericsson, B. Johansson-Lindbom et al., "Gut-associated lymphoid tissue–primed CD4$^+$ T cells display CCR9-dependent and -independent homing to the small intestine," *Blood*, vol. 107, no. 9, pp. 3447–3454, 2006.

[71] M. Wendland, N. Czeloth, N. Mach et al., "CCR9 is a homing receptor for plasmacytoid dendritic cells to the small intestine," *Proceedings of the National Academy of Sciences of the United States of America*, vol. 104, no. 15, pp. 6347–6352, 2007.

[72] E. P. Bowman, N. A. Kuklin, K. R. Youngman et al., "The intestinal chemokine thymus-expressed chemokine (CCL25) attracts IgA antibody-secreting cells," *Journal of Experimental Medicine*, vol. 195, no. 2, pp. 269–275, 2002.

[73] N. Feng, M. C. Jaimes, N. H. Lazarus et al., "Redundant role of chemokines CCL25/TECK and CCL28/MEC in IgA$^+$ plasmablast recruitment to the intestinal lamina propria after rotavirus infection," *The Journal of Immunology*, vol. 176, no. 10, pp. 5749–5759, 2006.

[74] B. Cassani, E. J. Villablanca, F. J. Quintana et al., "Gut-tropic T cells that express integrin $\alpha4\beta7$ and CCR9 are required for induction of oral immune tolerance in mice," *Gastroenterology*, vol. 141, no. 6, pp. 2109–2118, 2011.

[75] M.-A. Wurbel, M. G. McIntire, P. Dwyer, and E. Fiebiger, "CCL25/CCR9 interactions regulate large intestinal inflammation in a murine model of acute colitis," *PLoS One*, vol. 6, no. 1, article e16442, 2011.

[76] J. D. Wermers, E. N. McNamee, M.–. A. Wurbel, P. Jedlicka, and J. Rivera–Nieves, "The chemokine receptor CCR9 is required for the T-cell–mediated regulation of chronic ileitis in mice," *Gastroenterology*, vol. 140, no. 5, pp. 1526–1535.e3, 2011.

[77] E. J. Kunkel and E. C. Butcher, "Plasma-cell homing," *Nature Reviews Immunology*, vol. 3, no. 10, pp. 822–829, 2003.

[78] H. Ogawa, M. Iimura, L. Eckmann, and M. F. Kagnoff, "Regulated production of the chemokine CCL28 in human colon epithelium," *American Journal of Physiology-Gastrointestinal and Liver Physiology*, vol. 287, no. 5, pp. G1062–G1069, 2004.

[79] W. Wang, H. Soto, E. R. Oldham et al., "Identification of a novel chemokine (CCL28), which binds CCR10 (GPR2)," *Journal of Biological Chemistry*, vol. 275, no. 29, pp. 22313–22323, 2000.

[80] N. H. Lazarus, E. J. Kunkel, B. Johnston, E. Wilson, K. R. Youngman, and E. C. Butcher, "A common mucosal chemokine (mucosae-associated epithelial chemokine/CCL28) selectively attracts IgA plasmablasts," *The Journal of Immunology*, vol. 170, no. 7, pp. 3799–3805, 2003.

[81] E. Wilson and E. C. Butcher, "CCL28 controls immunoglobulin (Ig) A plasma cell accumulation in the lactating mammary gland and IgA antibody transfer to the neonate," *Journal of Experimental Medicine*, vol. 200, no. 6, pp. 805–809, 2004.

[82] M. Berri, F. Meurens, F. Lefevre et al., "Molecular cloning and functional characterization of porcine CCL28: possible involvement in homing of IgA antibody secreting cells into the mammary gland," *Molecular Immunology*, vol. 45, no. 1, pp. 271–277, 2008.

[83] P. Sundström, S. B. Lundin, L. Å. Nilsson, and M. Quiding-Järbrink, "Human IgA-secreting cells induced by intestinal, but not systemic, immunization respond to CCL25 (TECK) and CCL28 (MEC)," *European Journal of Immunology*, vol. 38, no. 12, pp. 3327–3338, 2008.

[84] K. Hieshima, Y. Kawasaki, H. Hanamoto et al., "CC chemokine ligands 25 and 28 play essential roles in intestinal extravasation of IgA antibody-secreting cells," *The Journal of Immunology*, vol. 173, no. 6, pp. 3668–3675, 2004.

[85] F. Meurens, J. Whale, R. Brownlie, T. Dybvig, D. R. Thompson, and V. Gerdts, "Expression of mucosal chemokines TECK/CCL25 and MEC/CCL28 during fetal development of the ovine mucosal immune system," *Immunology*, vol. 120, no. 4, pp. 544–555, 2007.

[86] B. Homey, W. Wang, H. Soto et al., "Cutting edge: the orphan chemokine receptor G protein-coupled receptor-2 (GPR-2, CCR10) binds the skin-associated chemokine CCL27 (CTACK/ALP/ILC)," *The Journal of Immunology*, vol. 164, no. 7, pp. 3465–3470, 2000.

[87] J. Morales, B. Homey, A. P. Vicari et al., "CTACK, a skin-associated chemokine that preferentially attracts skin-homing memory T cells," *Proceedings of the National Academy of Sciences of the United States of America*, vol. 96, no. 25, pp. 14470–14475, 1999.

[88] K. B. Arnold, A. Burgener, K. Birse et al., "Increased levels of inflammatory cytokines in the female reproductive tract are associated with altered expression of proteases, mucosal barrier proteins, and an influx of HIV-susceptible target cells," *Mucosal Immunology*, vol. 9, no. 1, pp. 194–205, 2016.

[89] J. Lajoie, J. Poudrier, M. Massinga Loembe et al., "Chemokine expression patterns in the systemic and genital tract compartments are associated with HIV-1 infection in women from Benin," *Journal of Clinical Immunology*, vol. 30, no. 1, pp. 90–98, 2010.

[90] S. M. Iqbal, T. B. Ball, J. Kimani et al., "Elevated T cell counts and RANTES expression in the genital mucosa of HIV-1–resistant Kenyan commercial sex workers," *The Journal of Infectious Diseases*, vol. 192, no. 5, pp. 728–738, 2005.

[91] M. Ghosh, J. V. Fahey, Z. Shen et al., "Anti-HIV activity in cervical-vaginal secretions from HIV-positive and -negative

women correlate with innate antimicrobial levels and IgG antibodies," *PLoS One*, vol. 5, no. 6, article e11366, 2010.

[92] M. K. Lafferty, L. Sun, L. DeMasi, W. Lu, and A. Garzino-Demo, "CCR6 ligands inhibit HIV by inducing APOBEC3G," *Blood*, vol. 115, no. 8, pp. 1564–1571, 2010.

[93] M. Rancez, A. Couëdel-Courteille, and R. Cheynier, "Chemokines at mucosal barriers and their impact on HIV infection," *Cytokine & Growth Factor Reviews*, vol. 23, no. 4-5, pp. 233–243, 2012.

[94] H. Shin and A. Iwasaki, "A vaccine strategy that protects against genital herpes by establishing local memory T cells," *Nature*, vol. 491, no. 7424, pp. 463–467, 2012.

[95] M. A. Kutzler and D. B. Weiner, "DNA vaccines: ready for prime time?," *Nature Reviews Genetics*, vol. 9, no. 10, pp. 776–788, 2008.

[96] N. Y. Sardesai and D. B. Weiner, "Electroporation delivery of DNA vaccines: prospects for success," *Current Opinion in Immunology*, vol. 23, no. 3, pp. 421–429, 2011.

[97] S. A. Abdulhaqq and D. B. Weiner, "DNA vaccines: developing new strategies to enhance immune responses," *Immunologic Research*, vol. 42, no. 1–3, pp. 219–232, 2008.

[98] R. R. MacGregor, J. D. Boyer, K. E. Ugen et al., "First human trial of a DNA-based vaccine for treatment of human immunodeficiency virus type 1 infection: safety and host response," *Journal of Infectious Diseases*, vol. 178, no. 1, pp. 92–100, 1998.

[99] S. K. Eo, S. Lee, U. Kumaraguru, and B. T. Rouse, "Immunopotentiation of DNA vaccine against herpes simplex virus via co-delivery of plasmid DNA expressing CCR7 ligands," *Vaccine*, vol. 19, no. 32, pp. 4685–4693, 2001.

[100] F. N. Toka, M. Gierynska, and B. T. Rouse, "Codelivery of CCR7 ligands as molecular adjuvants enhances the protective immune response against herpes simplex virus type 1," *Journal of Virology*, vol. 77, no. 23, pp. 12742–12752, 2003.

[101] Y. Yan, K. Hu, X. Deng et al., "Immunization with HSV-2 gB-CCL19 fusion constructs protects mice against lethal vaginal challenge," *The Journal of Immunology*, vol. 195, no. 1, pp. 329–338, 2015.

[102] M. A. Kutzler, K. A. Kraynyak, S. J. Nagle et al., "Plasmids encoding the mucosal chemokines CCL27 and CCL28 are effective adjuvants in eliciting antigen-specific immunity *in vivo*," *Gene Therapy*, vol. 17, no. 1, pp. 72–82, 2010.

[103] N. Kathuria, K. A. Kraynyak, D. Carnathan, M. Betts, D. B. Weiner, and M. A. Kutzler, "Generation of antigen-specific immunity following systemic immunization with DNA vaccine encoding CCL25 chemokine immunoadjuvant," *Human Vaccines & Immunotherapeutics*, vol. 8, no. 11, pp. 1607–1619, 2012.

[104] R. Song, S. Liu, and K. W. Leong, "Effects of MIP-1α, MIP-3α, and MIP-3β on the induction of HIV gag-specific immune response with DNA vaccines," *Molecular Therapy*, vol. 15, no. 5, pp. 1007–1015, 2007.

[105] K. Hu, S. Luo, L. Tong et al., "CCL19 and CCL28 augment mucosal and systemic immune responses to HIV-1 gp140 by mobilizing responsive immunocytes into secondary lymph nodes and mucosal tissue," *The Journal of Immunology*, vol. 191, no. 4, pp. 1935–1947, 2013.

[106] J. S. Tregoning, V. Buffa, A. Oszmiana, K. Klein, A. A. Walters, and R. J. Shattock, "A "prime-pull" vaccine strategy has a modest effect on local and systemic antibody responses to HIV gp140 in mice," *PLoS One*, vol. 8, no. 11, article e80559, 2013.

[107] M. A. Kutzler, M. C. Wise, N. A. Hutnick et al., "Chemokine-adjuvanted electroporated DNA vaccine induces substantial protection from simian immunodeficiency virus vaginal challenge," *Mucosal Immunology*, vol. 9, no. 1, pp. 13–23, 2016.

[108] F. Meurens, M. Berri, R. H. Siggers et al., "Commensal bacteria and expression of two major intestinal chemokines, TECK/CCL25 and MEC/CCL28, and their receptors," *PLoS One*, vol. 2, no. 7, article e677, 2007.

Hindawi
Journal of Immunology Research
Volume 2018, Article ID 8087916, 12 pages
https://doi.org/10.1155/2018/8087916

Research Article

An O-Antigen Glycoconjugate Vaccine Produced Using Protein Glycan Coupling Technology Is Protective in an Inhalational Rat Model of Tularemia

Laura E. Marshall,[1] Michelle Nelson,[1] Carwyn H. Davies,[1] Adam O. Whelan,[1] Dominic C. Jenner,[1] Madeleine G. Moule,[2] Carmen Denman,[2] Jon Cuccui,[2] Timothy P. Atkins,[1,3] Brendan W. Wren,[2] and Joann L. Prior[1,2,3]

[1]*Defence Science and Technology Laboratory, Porton Down, Salisbury, Wiltshire SP4 0JQ, UK*
[2]*Department of Pathogen Molecular Biology, London School of Hygiene and Tropical Medicine, Keppel Street, London WC1E 7HT, UK*
[3]*School of Biosciences, University of Exeter, Devon, UK*

Correspondence should be addressed to Adam O. Whelan; aowhelan@dstl.gov.uk and Joann L. Prior; jlprior@dstl.gov.uk

Received 19 June 2018; Revised 22 August 2018; Accepted 10 September 2018; Published 29 November 2018

Guest Editor: Roberta A. Diotti

There is a requirement for an efficacious vaccine to protect people against infection from *Francisella tularensis*, the etiological agent of tularemia. The lipopolysaccharide (LPS) of *F. tularensis* is suboptimally protective against a parenteral lethal challenge in mice. To develop a more efficacious subunit vaccine, we have used a novel biosynthetic technique of protein glycan coupling technology (PGCT) that exploits bacterial N-linked glycosylation to recombinantly conjugate *F. tularensis* O-antigen glycans to the immunogenic carrier protein *Pseudomonas aeruginosa* exoprotein A (ExoA). Previously, we demonstrated that an ExoA glycoconjugate with two glycosylation sequons was capable of providing significant protection to mice against a challenge with a low-virulence strain of *F. tularensis*. Here, we have generated a more heavily glycosylated conjugate vaccine and evaluated its efficacy in a Fischer 344 rat model of tularemia. We demonstrate that this glycoconjugate vaccine protected rats against disease and the lethality of an inhalational challenge with *F. tularensis* Schu S4. Our data highlights the potential of this biosynthetic approach for the creation of next-generation tularemia subunit vaccines.

1. Introduction

Tularemia is caused by the intracellular bacterium *Francisella tularensis*. This bacterium can cause a range of presentations of disease in humans. In the most severe cases where infection is acquired by the pulmonary route, the mortality rate was found to be between 30 and 60% prior to the introduction of antibiotics [1]. The more virulent *F. tularensis* subsp. *tularensis* strains are endemic across North America. Lower virulence strains, including *F. tularensis* subsp. *holarctica* are endemic more widely in the Northern Hemisphere across Europe, America, and Asia. These high- and low-virulence strains are commonly designated as type A and type B strains, respectively [2]. Extrapolation of data from human aerosol infection studies has estimated that lung deposition of a single colony forming unit (CFU) may be sufficient to establish infection [3]. The bacterium is categorised by the US Centers for Disease Control and Prevention as a Tier 1 biological select agent due to its low infectious dose via the aerosol route and disease severity. Development of a safe and effective vaccine to protect against aerosol challenge with this bacterium remains a priority.

F. tularensis subsp. *holarctica* live vaccine strain (LVS) has been previously used in humans to protect against tularemia in at-risk populations such as laboratory workers. This vaccine was tested in humans experimentally and shown to

protect against disease resulting from aerosol challenges of up to 20,000 CFU [4, 5]. Whilst demonstrating good efficacy, the mechanisms of its attenuation remain poorly defined. Phase II clinical trials to determine the safety and immunogenicity of LVS remain ongoing [6]. To provide a more defined alternative to LVS, several engineered live attenuated vaccines have been constructed which have demonstrated efficacy in animal models of disease [7–12]. In comparison with live attenuated candidates, safety compliance requirements for potential licensure are expected to be easier to achieve with subunit vaccines. However, overcoming efficacy limitations of subunit candidates has been the challenge to date. The only protein subunit candidate that has provided partial protection against type A strains of *F. tularensis* is IglC, but that was when delivery was through the use of a live attenuated *Listeria monocytogenes* vector [13]. Currently, lipopolysaccharide (LPS) is the only defined subunit *F. tularensis* vaccine antigen that has been reported to provide protection to immunised animals, although principally only against the lower virulence strains [14–17]. Therefore, whilst LPS remains a promising subunit candidate, strategies to improve its efficacy are warranted.

As LPS is a T cell-independent antigen, a strategy employed to enhance protective immunity for vaccines developed and licensed for other human pathogens is the incorporation of an antigenic carrier protein to the polysaccharide subunit. This approach has been successfully employed for several licensed public health vaccines including against *Neisseria meningitidis*, *Haemophilus influenzae* type B, and *Streptococcus pneumoniae* [18]. As proof of concept for the benefits of this approach in the field of tularemia, conjugation of *F. tularensis* LPS to bovine serum albumin induced protective immunity against type B, but not type A, strains of *F. tularensis* in mice [17].

These traditional conjugation approaches require the purification of the glycan from the native bacteria and then chemical conjugation of the glycans to a suitable carrier protein. This multistep approach can be time consuming, costly, and susceptible to variations between bioconjugation preparation batches. An alternative protein conjugation strategy adopted by our laboratory is the use of protein glycan coupling technology (PGCT) which facilitates the *in vitro* transfer of glycans to a recombinant acceptor protein using the glycosylating enzyme PglB from *Campylobacter jejuni* [19–22]. The presence of the PglB gene locus allows coupling of glucans to recombinantly expressed proteins containing the acceptor sequon D/E-X-N-Y-S/T, where X and Y are any amino acid except proline. We previously utilised PGCT to transfer recombinantly synthesized *F. tularensis* subsp. *tularensis* O-antigen to the carrier protein *Pseudomonas aeruginosa* exoprotein A (ExoA). This glycoconjugate was engineered to contain two glycosylation sequons and was produced using an *Escherichia coli* expression system [23]. We demonstrated that this glycoconjugate significantly improved the protection from disease in mice infected with *F. tularensis* subsp. *holarctica* compared to immunisation with LPS alone [23].

In the current study, we have introduced a further eight sequons into the sequence of ExoA resulting in a protein conjugate more highly glycosylated with *F. tularensis* O-antigen sugars. To allow stringent efficacy evaluation of this next-generation vaccine, we have developed a Fischer 344 (F344) rat inhalational challenge model and demonstrated that this subunit glycoconjugate vaccine can protect rats against an aerosol challenge of the high-virulence strain of *F. tularensis* Schu S4.

2. Materials and Methods

2.1. Francisella Bacterial Strains and Culture. For vaccination of rats with LVS, a lyophilised vial of LVS (National Drug Biologic Research Company, USA, lot number 4) was reconstituted in phosphate-buffered saline (PBS, Life Technologies, UK), inoculated onto blood cysteine glucose agar (BCGA), and incubated at 37°C for 48 h. Bacterial growth was recovered from the agar and resuspended in PBS, and the optical density at 600 nm (OD_{600}) was adjusted to 0.14. The suspension was serially diluted ten-fold to the desired concentration for immunisation.

For challenge studies, *F. tularensis* Schu S4 was inoculated onto BCGA and incubated at 37°C for 24 h. Growth was recovered from agar, resuspended in PBS, and the OD_{600} adjusted to 0.1. One mL of this suspension was inoculated into 100 mL of modified cysteine partial hydrolysate (MCPH) broth with 4% glucose and incubated with shaking at 180 rpm, at 37°C for 48 h. OD_{600} of the culture was adjusted to 0.1 in PBS and serially diluted to the desired concentration for aerosol challenge. Challenge inoculum quantification was determined by plating serially diluted cultures onto BCGA and incubating at 37°C for 48–72 h.

To determine bacterial load in organs, organs were weighed, homogenised through a 40 μm cell sieve, serially diluted in PBS, plated onto BCGA, and incubated at 37°C for 48–72 h.

2.2. Production of the Glycoconjugate Vaccine (GtExoA)

2.2.1. Bacterial Strains and Plasmid Construction. Escherichia coli CLM24 [24] was used as the host strain for protein expression and glycoconjugate production. CLM24 (a ligase negative strain) was stably transformed with the plasmid pGab2 [23], a construct created from the insertion of the *F. tularensis* subspecies *tularensis* strain Schu S4 O-antigen coding region into the low copy number expression plasmid pLAFR [25]. pGab2 is tetracycline selectable and constitutively expressed. Following confirmation of the expression of the *F. tularensis* O-antigen, the resulting strain was then transformed with the plasmid CLM24 containing a plasmid-encoded *C. jejuni* pglB, pGVXN114, which expresses the *C. jejuni* oligosaccharyltransferase PglB. Finally, the resulting strain was transformed with the plasmid pGVXN150: GtExoA, creating a three plasmid system for the production of the glycoconjugate. The GtExoA construct was engineered to express a modified version of *P. aeruginosa* exotoxin A that was synthesized by Celtek Bioscience LLC, USA in the vector pGH and closed into a vector derived from pEC415 using the restriction enzymes NheI and

EcoRI (NEB, UK). The synthesized protein contains two internal modifications that allow glycosylation of the protein by PglB [23], as well as containing four *N*-glycosylation sequons at the N terminus and an additional 4 at the C terminus. In addition, a hexahistidine tag was added to the C terminus of the protein to facilitate purification and an *E. coli* DsbA signal peptide was added to the N-terminal sequences enabling Sec-dependent secretion to the periplasm. pGVXN150: GtExoA is ampicillin resistant and L-(+)-arabinose inducible. The construct sequence was then confirmed using Sanger sequencing with the primers GtExoA NF (GCGCTGGCTGGTTTAGTTT), GtExoA NR (CGCA TTCGTTCCAGAGGT), GtExoA CF (GACAAGGAACA GGCGATCAG), and GtExoA CR (TGGTGATGATGGTG ATGGTC).

2.2.2. Culture and GtExoA Glycoprotein Expression Conditions. For all experiments, *E. coli* CLM24 was cultured in Luria-Bertani (LB) broth (Fisher Scientific, UK) supplemented with appropriate antibiotics in the following concentrations: ampicillin 100 μg/mL, tetracycline 20 μg/mL, and spectinomycin 80 μg/mL. The addition of manganese chloride at the time of protein and PglB induction was at a final concentration of 4 mM, and made up as a 1 M stock fresh prior to each experiment. Cultures were incubated at 37°C shaking at 110 rpm for 16–20 hrs for large-scale preparation. For three-plasmid system glycoconjugate production, an overnight LB culture of *E. coli* CLM24 harbouring pGVXN114, pGVXN150: GtExoA, and pGab2 were subcultured in a 1 : 10 dilution of LB broth (Fisher Scientific) with antibiotics, and grown to mid log phase. pGVXN150: GtExoA was induced by the addition of 0.2% L-(+)-arabinose (Sigma-Aldrich, UK), and *C. jejuni* PglB was induced with 1 mM IPTG, followed by incubation for an initial 4 hours. Another addition of 0.4% L-(+)-arabinose was then added and cultures were incubated overnight.

2.2.3. Production and Purification of Glycoconjugate Vaccine. 1.8 L of LB was inoculated with a 200 mL starter culture and grown to an OD_{590} of 0.60–0.80, then induced as described above. The next day, induced glycoconjugate pellets were harvested via centrifugation at 5300 ×g at 4°C for 30 minutes and were resuspended in ice-cold lysis buffer (50 mM NaH_2PO_4, 300 mM NaCl, and 10 mM imidazole) containing 1 mg/mL lysozyme (Sigma-Aldrich) and 0.15 μL Benzonase® Nuclease (Novagen®, UK). Lysis, wash, and elution buffer were all adjusted to pH 8 with 5 M NaOH. Resuspended cells were subjected to five rounds of lysis using a prechilled Stansted High Pressure Cell Disruptor (Stansted Fluid Power Ltd., UK) under 60,000 psi (410 MPa) in continuous mode. Cell debris was subsequently pelleted by spinning at 7840 ×g at 4°C for 60 minutes. The resulting supernatant was kept on ice whilst being loaded onto a GE Healthcare, UK, HIS-trap HP 1 mL column. Then, the column was washed in buffer containing 50.0 mM NaH_2PO_4, 300 mM NaCl, and 20 mM imidazole whilst attached to an AKTA purifier. Material was eluted and collected in 1 mL fractions with an imidazole gradient of 30–500 mM elution buffer that also contained 20% v/v glycerol and 5% w/v glucose. The collected fractions were visualised by Western blot, and the glycosylated GtExoA fractions were pooled and concentrated using buffer exchange columns (Vivaspin 2 (Vivaproducts, UK)) into PBS 20% v/v glycerol, prior to quantification with a BCA Protein Assay Kit (Pierce Biotechnology, USA).

2.2.4. Western Blot Analysis. To assess protein expression and glycosylation levels, a two-channel simultaneous Western blot (Odyssey LI-COR, LI-COR Biosciences, Hamburg Germany) was used to analyse AKTA purified elution fractions. Freshly eluted samples were resuspended in 2x Laemmli buffer and boiled at 95°C for 6 minutes. Boilates, and a PageRuler Plus Prestained Protein Ladder (Life Technologies) were separated on a NuPAGE 10% Bis-Tris Gel Novex®, then transferred to a Hybond™-C Extra nitrocellulose membrane (Amersham Biosciences, UK). The membrane was then blocked in 2% w/v skim milk and PBS 0.2% v/v Tween 20 (Sigma-Aldrich) overnight at 4°C. The next day, membranes were probed simultaneously with two primary antibodies: O-antigen presence was detected using the mouse monoclonal antibody FB-11 (1 : 10,000) (Abcam, UK) and GtExoA was detected with rabbit anti-HIS polyclonal antibodies (1 : 5000) (Abcam). Secondary antibodies were Goat anti-Rabbit IRDye® 680RD and Goat anti-Mouse IRDye® 800CW (Odyssey® LI-COR Biosciences, UK) both diluted 1 : 10,000.

2.3. Animal Procedures

2.3.1. Ethics Statement. Animals were kept in accordance with the UK Animals (Scientific Procedures) Act 1986 and Codes of Practice for the Housing and Care of Animals used in Scientific Procedures 1989. The license application underwent approval by the local ethical review process with the Defence Science and Technology Laboratory (Dstl) Animal Welfare and Ethical Review Body (AWERB) before submission and approval with the UK Home Office and Animal Procedures Committee (an independent committee that offers advice to The Secretary of State of the ethics of the proposed work). The project license that covered this work was 30/3166. No prespecified effect size was predicted for the glycoconjugate, and therefore no sample size estimate was made. No randomisation of animals or blinding of investigators was used in this study. No animals were excluded from the study.

2.3.2. Animals. Female F344 rats were obtained from Envigo, UK. Rats were implanted with BioThermo microchips (Identipet, SA) by subcutaneous (s.c.) injection to allow individual rats to be tracked and have their temperature measured through the study. Rats used in vaccine studies were 12–16 weeks of age and weighed 190 ±20 g at the start of the procedures. On arrival in the conventional animal unit and on transfer of rats into containment level 3 animal facilities, rats were acclimatised to their new surroundings for 10 days before any procedures were performed. Rats were housed in cages of five, in polypropylene cages with a stainless steel mesh cover with an integral water bottle holder and diet hopper which conformed to the Code of Practice for the housing of animals bred, supplied, or used for scientific purposes

(December 2014). Rats were kept under a 12 hour light/dark cycle (350 to 400 Lux during the day, 10 Lux during the night, with a ramp up and ramp down period at "dawn" and "dusk") at 19 to 23°C and 45 to 65% relative humidity. Cages contained 8/10 and 10/14 grade corn cob (International Product Supplies, UK) as a nesting material with a range of environmental enrichment added throughout the studies (e.g., irradiated aspen wood, Des.Res. rat houses (LBS, UK)), and there was free access to food (Labdiet certified rodent diet 5002 and Labdiet EU rodent 22% diet 5LF5; International Product Supplies) and water throughout the study. During immunisation and the subsequent rest period, rats were housed in a conventional animal unit, in rooms supplied with rough filtered air giving 20 to 25 air changes per hour. For challenge with *F. tularensis* Schu S4, all animals were handled under UK Advisory Committee on Dangerous Pathogens animal containment level 3 conditions within a half-suit isolator compliant with British Standard BS5726, supplied with an inward flow of HEPA-filtered air giving 35 to 45 air changes per hour. The room was supplied with double HEPA-filtered air giving 20 to 25 air changes per hour.

2.3.3. Experimental Animal Procedures. Rats were vaccinated with LVS in PBS via the s.c. route. Rats were vaccinated with 10 μg GtExoA coadministered with the MF59 adjuvant (Novartis, UK) in a 100 μL volume via the s.c. or intraperitoneal (i.p.) route 3 times, 2 weeks apart. Control groups of rats ($n = 5$) were also immunised by the i.p. and s.c. routes with the MF59 adjuvant alone or with PBS by the s.c. route. Aerosol challenge with *F. tularensis* Schu S4 occurred five weeks following final vaccination. Following challenge, animals were observed twice daily and signs of disease and subcutaneous temperature were recorded. Disease signs were assigned a score. The presence of piloerection and eye problems were scored given a clinical score of 1 or 2 depending on severity. Hunched posture, rapid breathing, and pinched posture were each given a clinical score of 1 if present. If any additional abnormal clinical signs were observed (e.g., pale tail), they were assigned a score of 1. A cumulative score for disease at each observed timepoint was calculated. Animals were weighed once daily. A humane endpoint was applied to rats in a moribund state or where their temperature was less than 33°C. Animals underwent euthanasia with intraperitoneally administered sodium pentobarbitone.

2.3.4. Aerosol Challenge. Rats were exposed to an aerosol of *F. tularensis* Schu S4 by the inhalational route in a nose-only exposure unit (EMMS, UK) utilising a 6-jet Collison atomiser (Dstl, in-house) attached to a contained Henderson Piccolo arrangement to condition the aerosol to 50% (±5%) relative humidity. The nose-only exposure unit was controlled by the Aerosol Management Platform (AeroMP) aerosol system (Biaera Technologies L.L.C., USA). The animals were exposed to the aerosolised bacteria for 10 minutes, with impingement of the aerosol cloud sampled at the midway point of challenge into PBS via an All-Glass Impinger (AGI-30; Ace Glass, Vineland, NJ, USA). Following the challenge, the impinged aerosol was enumerated by serial dilution, plated onto BCGA plates, and incubated at 37°C for 48 h. The challenge dose was calculated from the aerosol concentration (CFU/L of air) using Guyton's formula [26] for minute respiratory volume and assuming 40% retention of 1–3 μm droplets [27].

2.4. Immunological Assays

2.4.1. Cell Isolation and Culture. Rat spleens were homogenised through a 40 μm sieve using a sterile syringe plunger and collected into L15 medium (Life Technologies). The isolated splenocytes were diluted to 2×10^6 cells/mL in medium and cultured in the presence of either medium alone, sonicated LVS whole cells (10 μg/mL, Dstl), sonicated Schu S4 whole cells (10 μg/mL, Dstl), purified ExoA (5 μg/mL, London School of Hygiene and Tropical Medicine, UK), or Concanavalin-A (Con-A, 5 μg/mL, Sigma-Aldrich). For cultures of cells from LVS-infected or PBS control rats, splenocytes were diluted in L15 medium supplemented with 10% foetal bovine serum (Sigma-Aldrich), nonessential amino acids (Life Technologies), 2-mercaptoethanol (Life Technologies), 100 U/mL penicillin, and 100 mg/mL streptomycin sulphate (Life Technologies) and then cultured at 37°C in the absence of a controlled CO_2 environment. For cultures of cells from vaccinated rats, splenocytes were diluted in RPMI 1640 medium (Life Technologies), supplemented as described above, and then cultured at 37°C with 5% CO_2.

2.4.2. Measurement of IFNγ by Enzyme-Linked Immunosorbent Assay (ELISA). Splenocytes (2×10^5 per assay well) were cultured in duplicate in the presence of the antigen for 72 hours (see above), and supernatants were harvested and stored at −20°C prior to use. The expression of IFNγ was determined in plasma supernatants using a commercial rat IFNγ ELISA kit (Mabtech, Sweden) with responses determined by the measurement of optical density at 450 nm (OD_{450nm}).

2.4.3. ELISA for Anti-GtExoA Antibody Titre. Plates were coated with 5 μg/mL GtExoA in PBS, 100 μL per well, and incubated at 4°C overnight. After blocking with 1% skimmed milk powder in PBS for 2 hours at 37°C, plates were washed three times with 0.05% Tween 20 (Sigma-Aldrich) in PBS. Sera from individual rats were applied to plates at 1 : 50 and serially diluted 1 : 2 across the plate, in 1% skimmed milk powder. Bound IgG rat antibody was detected using anti-rat antibody conjugated to HRP at 1 : 2000 in PBS and developed using 10 mM 2,2′-azino-bis(3-ethylbenzothiazoline-6-sulphonic acid) in citrate buffer with 0.01% H_2O_2. OD was measured at 450 nm. Antibody titre was defined as the reciprocal of the highest dilution of serum that had a mean OD value at least 3 standard deviations higher than the mean OD of nonvaccinated serum.

2.5. Statistical Analysis. Analysis of rat weight data was performed using IBM SPSS version 21.0. All other statistical analyses were performed using GraphPad Prism version 6.02. The statistical tests applied to the different data sets are described in the corresponding figure legends.

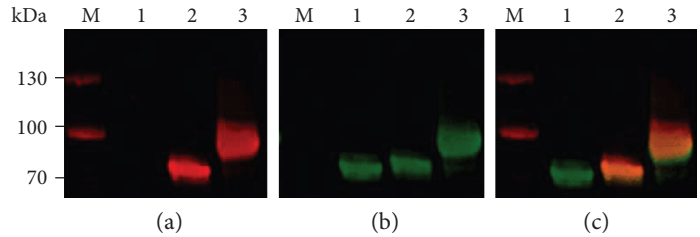

Figure 1: Recombinant ExoA modified to incorporate additional glycosylation sequons is heavily glycosylated by *F. tularensis* O-antigen by *C. jejuni* PglB in *E. coli* CLM24. Samples were separated by SDS-PAGE, and then two-colour Western blots were used to simultaneously detect the degree of glycosylation of ExoA using (a) a monoclonal mouse antibody (FB-11) with specificity to *F. tularensis* O-antigen (red) and (b) rabbit polyclonal antibodies with specificity to the 6x His sequence (green). The two IR secondary antibody channels when overlaid (IR 800/680) result in images with overall yellow colour indicating conjugation (c). M, protein ladder marker; lane 1, pGVXN150 only; lane 2, pGVXN150 ExoA glycosylated with the *F. tularensis* O-antigen (same construct from Cuccui et al. [23]); and lane 3, GtExoA heavily glycosylated with the *F. tularensis* O-antigen due to the presence of an additional eight glycosylation sequons.

3. Results

3.1. Production of the GtExoA Glycoconjugate Vaccine. The glycoconjugate vaccine previously evaluated by our group was glycosylated via two sequons incorporated into the ExoA carrier protein [23]. To improve the ratio of glycan to protein in the conjugate, a further 8 sequons were introduced into ExoA resulting in a more highly glycosylated conjugate, GtExoA. Recognition of GtExoA by a monoclonal antibody, FB-11, with specificity towards *F. tularensis* O-antigen demonstrated conservation of sugar moieties (Figure 1). No binding of FB-11 was observed in ExoA lacking the glycosylation sequons (Figure 1, lane 1). Western blot analysis of purified glycoconjugate vaccines demonstrated an increase in the molecular size of the decaglycosylated GtExoA compared with the biglycosylated first generation conjugate (Figure 1). This observation was commensurate with an expected increase in glycosylation resulting from the inclusion of the additional sequons. Due to the increased antigenic potential of this glycoconjugate vaccine, GtExoA was prioritised for efficacy evaluation.

3.2. Development of a F344 Rat Rodent Model of Inhalational Tularemia to Allow Efficacy Evaluation of Candidate Vaccines. F344 rats have recently gained popularity as a preferred rodent model for assessing tularemia vaccines. In comparison with mice, F344 rats are considered to provide a closer approximation of human disease [28, 29] and demonstrate a more comparable response to LVS vaccination [30]. We therefore first developed an in-house F344 model of inhalational tularemia to allow stringent evaluation of GtExoA. Groups of 5 rats were challenged with a range of doses of *F. tularensis* Schu S4 via the aerosol route to determine an appropriate infectious dose. The estimated inhaled dose ranged from approximately 10 CFU to 3.15×10^4 CFU. All rats challenged with 2.94×10^2 to 3.15×10^4 CFU succumbed to infection within 14 days of challenge (Figure 2(a)). Of rats challenged with approximately 10 CFU, only 1 animal out of 5 survived to the end of the experiment at 21 days postinfection. During the recovery of this animal, its disease signs resolved and some weight was recovered. The mean lethal dose (MLD) was therefore estimated to be less than 10 CFU via the aerosol route in our model.

Bacterial dissemination was determined at day 7 post-challenge in groups of up to five sacrificed rats. Animals sacrificed at this time had highly colonised lungs, liver, and spleens (Supplementary Figure S1). All infected rats showed severe signs of disease. Rats initially exhibited piloerection and developed eye problems, including secretion of porphyrin and ptosis of the eyelids until their eyes were completely closed, followed by a hunched posture alongside rapid breathing. Rats became more lethargic and less responsive to stimuli over the course of disease (Figure 2(b)). All infected rats lost weight in a dose-dependent manner (Figure 2(c)) and displayed a febrile stage, with subcutaneous temperatures which were raised at least 1.5°C above their baseline temperature (Figure 2(d)). Rats which received the highest challenge of 3.15×10^4 CFU rapidly lost between 7 and 10 percent of their body weight within 5 days of challenge. Those rats which received a lower challenge all lost at least 10 percent of their starting weight, and in some cases more than 25 percent of body weight, but over a greater length of time. These data were used to identify disease parameters useful for assessing candidate vaccine performance in the model.

3.3. GtExoA Glycoconjugate Vaccine Induces Memory Immunity in Vaccinated F344 Rats. To determine whether the GtExoA glycoconjugate vaccine could induce memory immunity in rats prior to proceeding to a biosafety level 3 efficacy challenge study, groups of 5 rats were vaccinated with GtExoA in combination with the MF59 adjuvant. Groups were vaccinated by i.p. or s.c. administration routes. We previously used the i.p. vaccination route to assess the first generation glycoconjugate vaccine in mice [13], whilst s.c. is the immunisation route routinely used for LVS, the tularemia gold-standard reference vaccine. Therefore, both immunisation routes were assessed to allow translation between mouse and rat models and to control for the s.c. immunisation route used for LVS administration. Rats were vaccinated on 3 occasions, 2 weeks apart. Control groups included PBS sham-vaccinated rats, MF59 adjuvant-only-immunised rats and a group vaccinated with LVS. Serum and splenocytes were recovered 28 days after the final vaccination to measure IgG- and cell-mediated responses, respectively. Sera from the MF59 adjuvant-only-vaccinated controls showed no

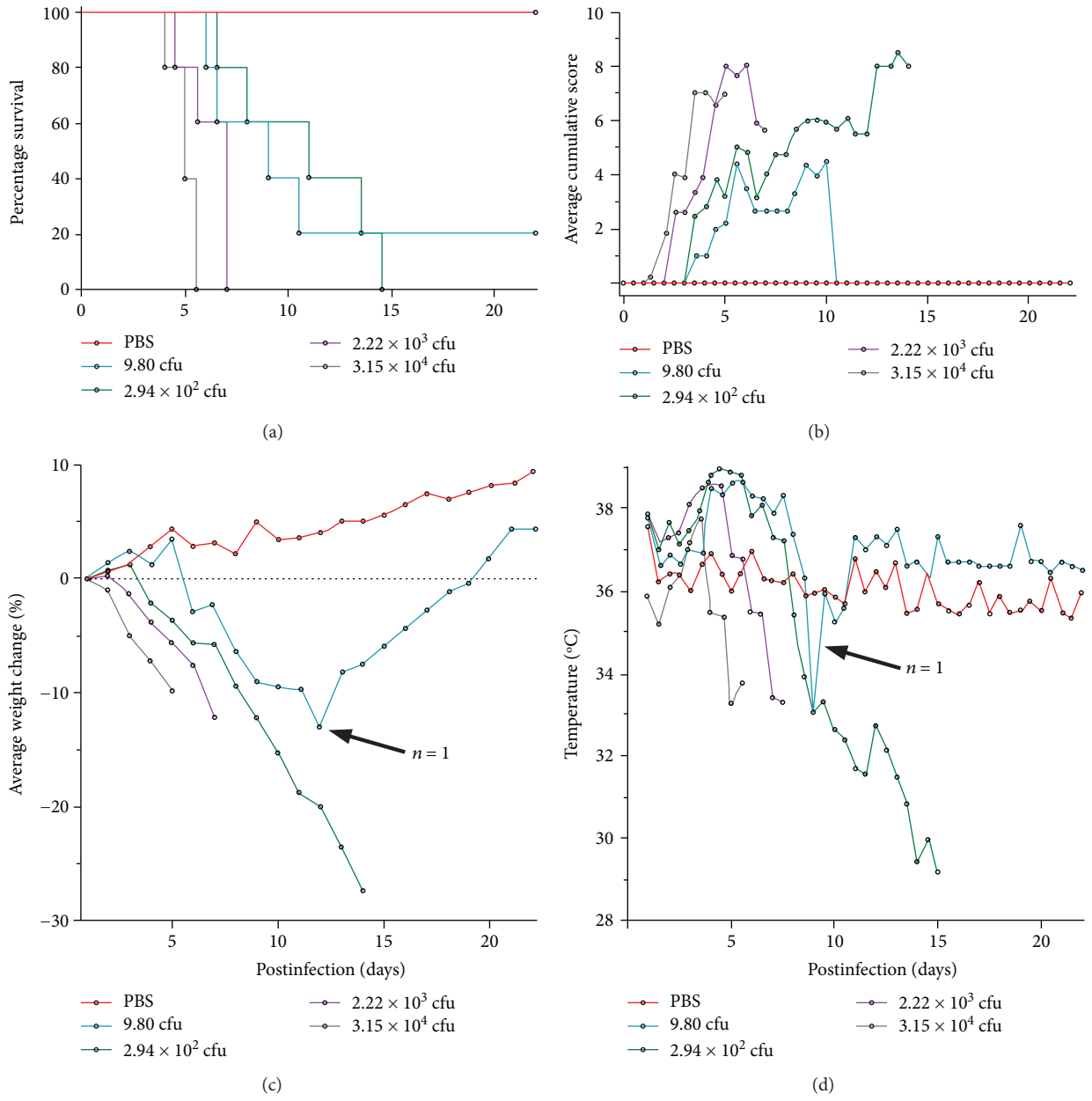

Figure 2: Survival and disease progression of rats following an aerosol challenge with a range of doses of *F. tularensis* Schu S4. (a) F344 rats ($n = 5$) were challenged via the aerosol route with a range of *F. tularensis* Schu S4 doses (see accompanying legend). Rats were monitored daily for mortality, and data were reported on the Kaplan-Meier survival curve. Calculated retained dose for each challenge group is shown on the Kaplan-Meier survival curve. (b) Clinical signs of disease were monitored twice daily. Average cumulative signs for each group are presented for animals which had not succumbed to disease. (c) Weight was monitored daily. Average weight change for each group is presented for animals which had not succumbed to disease. (d) Temperature was monitored twice daily. Average animal temperature for each group is presented for animals which had not succumbed to disease.

appreciable binding to the GtExoA antigen, whilst endpoint IgG titres from rats vaccinated with GtExoA by the i.p. or s.c. routes were 1 : 204800 and 1 : 102400, respectively (Figure 3(a)). Antigen-stimulated expression of IFNγ was used as a measure of T cell-mediated memory. Significantly elevated ExoA-stimulated IFNγ responses were only observed in rats immunised with GtExoA (Figure 3(b)) confirming the recognition of the ExoA conjugate protein by the cell-mediated compartment of these rats. No increase in ExoA-stimulated IFNγ from splenocytes isolated from rats immunised with the MF59 adjuvant by i.p. or s.c. routes was observed (data not shown). Stimulation of splenocytes with the crude *F. tularensis* antigen preparations only resulted in significantly elevated IFNγ expression in the group of rats vaccinated with LVS (Figure 3(b)). Elevated IFNγ responses stimulated by *F. tularensis* Schu S4 sonicate in the GtExoA-vaccinated groups of rats, potentially as a consequence of nonspecific stimulation by components in

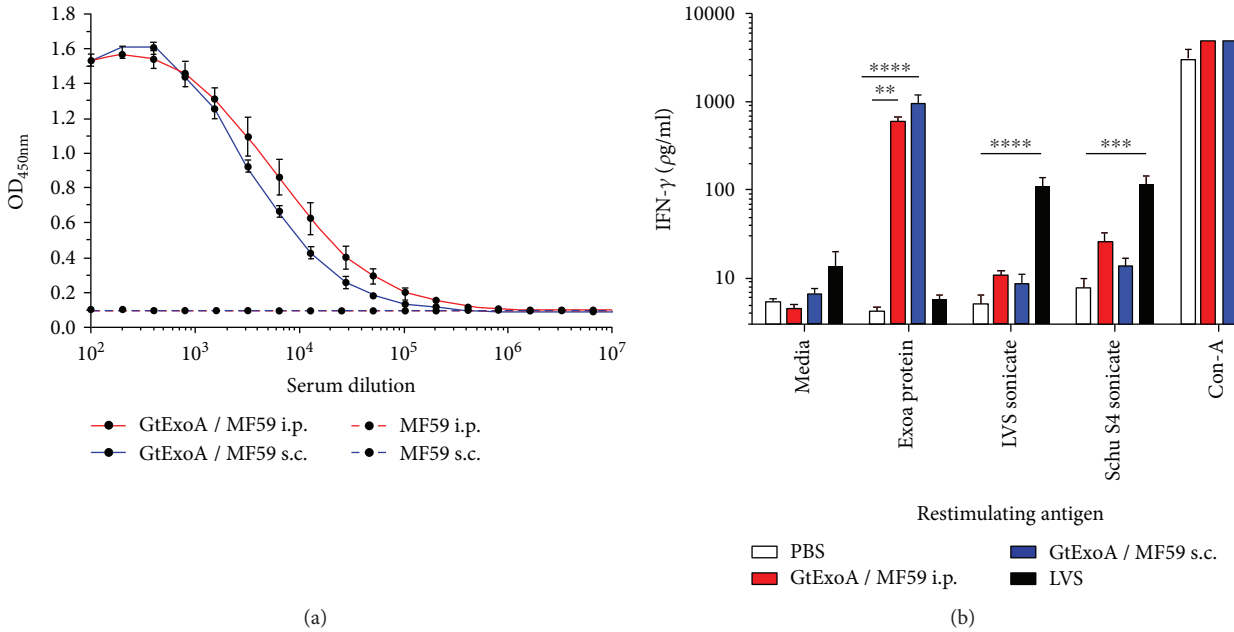

(a) (b)

Figure 3: GtExoA glycoconjugate stimulates memory immunity in vaccinated rats. Groups of F344 rats ($n = 5$) were vaccinated three times, two weeks apart with 10 μg of GtExoA coadministered with MF59, or immunised with MF59 alone, and immune responses were measured 28 days after the third immunisation. (a) Quantitation of rat IgG recognising the GtExoA glycoconjugate antigen was determined by ELISA for a serial dilution of sera from GtExoA and respective MF59 adjuvant control rats. The mean OD_{450nm} (±SEM) response is presented for each dilution for each vaccine group. The use of solid or dotted datapoint connecting lines identifies responses in sera from rats immunised with GtExoA + MF59 or with the MF59 adjuvant only, respectively. Responses in respective groups immunised via the i.p. or s.c. routes are identified using red or blue connecting lines, respectively (see legend). (b) Splenocytes were isolated from rats immunised with either GtExoA administered by i.p. (light blue bars) or s.c. (dark blue bars) routes and from rats immunised with LVS (black bars) or PBS. Splenocytes were cultured in the presence of purified ExoA protein, LVS sonicate, *F. tularensis* Schu S4 sonicate, Con-A, or medium. The expression of IFNγ in 72-hour culture supernatants was measured by ELISA. The OD_{450nm} results were normalised by transformation into units of ρg/mL by generating a standard curve using recombinant rat IFNγ. Statistical analysis of differences between groups was determined by one-way ANOVA with Holm-Sidak's posttests ($^{**}p < 0.01$, $^{***}p < 0.001$, or $^{****}p < 0.0001$). Data validity was tested using Bartlett's test for equal variance. IFNγ responses are presented as mean response for each group ($n = 5$) ±SEM.

this crude antigen extract, were not significantly stronger than responses observed in PBS-immunised rats (Figure 3(b)) or control rats immunised with MF59 alone (data not shown).

3.4. GtExoA Glycoconjugate Protects against Pulmonary Tularemia in F344 Rats. To evaluate the efficacy of our glycoconjugate vaccine, groups of 5 rats were vaccinated with the GtExoA by both the s.c. and i.p. routes along with appropriate MF59 adjuvant controls. A group of rats ($n = 5$) was also vaccinated with 5×10^7 CFU LVS via the s.c. route. The LVS group was included to validate the relevance of the model, whilst also providing a reference gold standard against which to assess the performance of our GtExoA vaccine candidate. Five weeks after the final vaccination, rats were challenged with an aerosol of 5.48×10^2 *F. tularensis* Schu S4 (the calculated retained dose). All LVS- and GtExoA bioconjugate-vaccinated rats survived 21 days postaerosol challenge (Figure 4(a)). One of the five rats vaccinated with the MF59 adjuvant alone via the s.c. route survived to 21 days postinfection but the group survival curve was still significantly different from rats vaccinated via the s.c. route with GtExoA ($p < 0.05$) (Figure 4(a)). Similarly, despite one of the five PBS-immunised rats surviving 21 days postinfection, survival was significantly different from rats vaccinated via the s.c. route with LVS (Figure 4(a), $p < 0.05$). However, as a consequence of three of the five rats vaccinated with MF59 alone via the i.p. route not succumbing to a lethal infection, the difference between their survival and that of the comparable i.p. GtExoA vaccine group did not reach significance ($p = 0.168$, log-rank test). The level of significance for the comparison of all survival curves is presented in Supplementary Table S1.

Rats vaccinated with GtExoA by either route, or with LVS, showed no clinical signs of disease (Figure 4(b)) and did not become febrile (Supplementary Figure S2). In contrast, rats vaccinated with PBS subcutaneously and MF59 only via i.p. and s.c. routes all became febrile with maximal febrile temperature being observed on day 5 postinfection. On day 5, the temperature of rats in the groups vaccinated with LVS or GtExoA (i.p. and s.c. routes) were all significantly lower than those in the PBS control group ($p < 0.001$, 0.001, and 0.01, respectively, ANOVA with Dunnett's postanalysis test), see Figure 4(c). There was no significant difference between the temperature of the PBS or MF59 (i.p. and s.c. routes) adjuvant control rats. Furthermore, all PBS- and MF59-only-immunised rats showed clinical signs of disease including those that did not ultimately succumb to a lethal infection (Figure 4(b)).

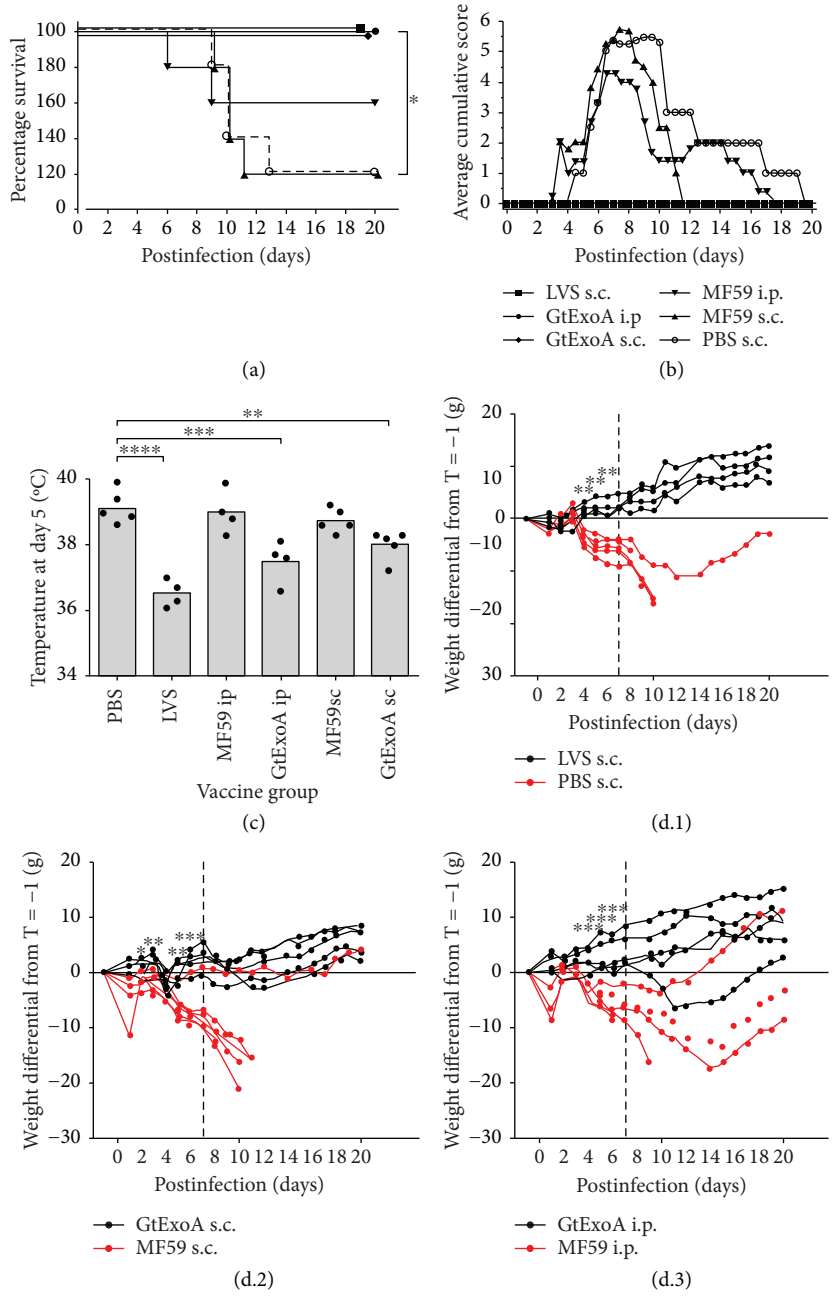

Figure 4: GtExoA protects F344 rats against aerosol infection with *F. tularensis* Schu S4. Groups of F344 rats ($n = 5$) were vaccinated three times, two weeks apart with 10 μg GtExoA coadministered with MF59, or immunised with MF59 alone, via the s.c. or i.p. route, or 5.38×10^7 LVS. 5 weeks after final vaccination, rats were challenged with a calculated retained dose of 5.48×10^2 *F. tularensis* Schu S4 via the aerosol route. (a) Rats were monitored twice daily and mortality and survival plotted on a Kaplan-Meier survival curve. For comparison of survival curves, a log-rank Mantel-Cox test was used ($^*p < 0.05$). (b) Signs of disease were recorded twice daily and average cumulative signs for surviving rats in each group of 5 presented. (c) The temperature for individual rats (black circles) in each treatment group is presented at day 5 postinfection, the day on which the maximal febrile temperature was detected. The grey bar is the average response for the group. Statistical analysis of differences between the temperatures of treatment and the PBS control group was determined by one-way ANOVA with Holm-Sidak's posttests ($^{**}p < 0.01$, $^{***}p < 0.001$, $^{****}p < 0001$). (d.1–d.3) Rats were weighed once daily and average weight change of surviving rats is presented. Each group is presented with its apposite control: LVS s.c. (black lines) and PBS s.c. (red lines) (d.1), GtExoA + MF59 s.c. (black lines) and MF59 s.c. (red lines) (d.2), and GtExoA + MF59 i.p. (black lines) and MF59 i.p. (red lines) (d.3). Significance in divergence of weight change between groups was found to fit the normal, Gaussian distribution using Q-Q plots (not shown). The data was analysed using a repeated measures general linear model. Validity of the data for this test was further established using Levene's tests for unequal variance (not shown). Individual comparisons, pairwise and dependent or independent of timepoints, were performed using Bonferroni's correction ($^*p < 0.05$, $^{**}p < 0.005$, and $^{***}p < 0.0005$). Due to culling of rats that reached their humane endpoint, the limit of analysis depicted by the dotted line is the timepoint up to which statistical comparisons could be performed across all groups with equivalent power.

Weight change in rats after challenge was shown to be significantly different over time between all groups of vaccinated rats and their relevant controls (Figure 4(d)). Weight change in rats vaccinated with LVS or with GtExoA via the i.p. route significantly diverged from their relevant controls on day 4 (Figures 4(d.1) and 4(d.3), $p < 0.005$, $p < 0.0005$, respectively). Weight change between rats vaccinated with GtExoA by the s.c. route and the relevant control rats significantly diverged on day 2 after challenge (Figure 4(d.2), $p < 0.05$). The control rats that did not reach a humane endpoint all resolved signs of disease and had recovered some weight by 21 days following infection. *F. tularensis* was not detected in the lungs, liver, or spleen of LVS- or GtExoA-vaccinated rats at 21 days postinfection whilst all surviving MF59- or PBS-only-vaccinated rats were colonised with *F. tularensis* in the lung, liver, and spleen at 21 days postinfection.

4. Discussion

The development of a subunit vaccine that can protect against inhalational infection with type A strains of *F. tularensis* remains an important goal for tularemia vaccine research. To this end, we have utilised PGCT to recombinantly express the immunogenic *P. aeruginosa* carrier protein ExoA glycosylated with O-antigen sugars of *F. tularensis* in a single-step process. We previously used this approach to engineer a glycoconjugate incorporating two sequons and demonstrated the protective potential of this biglycosylated vaccine in a murine model of tularemia [23]. Here, we have engineered a second generation vaccine by introducing a further 8 sequons into the conjugate protein ExoA to increase the antigen potential of the glycoconjugate. The glycans were recognised by a monoclonal antibody with specificity for the terminal moiety 4,6-dideoxy-4-formamido-D-glucose of the *F. tularensis* subsp. *tularensis* and subsp. *holarctica* O-antigen [31]. The recognition by this antibody confirmed the presence of structurally conserved sugars. Furthermore, increasing the number of sequons in the second generation conjugate successfully resulted in a more heavily glycosylated conjugate, as confirmed by its increased molecular size. Together, these data demonstrate the versatility of this technology for generating glycoconjugate vaccine candidates. It is currently unclear how many repeating units are transferred by *C. jejuni* PglB in this system. The native *F. tularensis* O-antigen consists of a repeating tetrasaccharide structure [14]. The absence of a ladder of multiple-sized products separated by SDS-PAGE suggests that GtExoA principally carries single repeat units at its sequon sites. Efforts to modulate the level of *C. jejuni* PglB to increase the chain length of repeat glycan units is ongoing in the Wren laboratory.

Recent development of a F344 rat model of respiratory tularemia for testing vaccine candidates has provided the opportunity for testing candidates in a closer approximation of human disease [28, 29]. Tularemia in rats is less acute than in mice, reflecting human disease progression more closely. In addition, F344 rats show similar sensitivity to *F. tularensis* strains as humans [32] and rats can be protected from disease by vaccination with LVS [30]. We consider that establishing an aerosol-initiated rat model of tularemia at our centre, commensurate with that developed by Hutt et al. [29], to be an important step in allowing efficacy evaluation of both GtExoA and future subunit tularemia vaccines. In our aerosol challenge model, lethal infection could be established with less than 10 CFU of *F. tularensis* Schu S4. This confirms the disease susceptibility of F344 rats to inhalation of type A strains of *F. tularensis* reported previously [28, 29, 33]. LVS has been shown to protect F344 rats against respiratory infection by *F. tularensis* Schu S4 delivered by the aerosol route [34] and more recently by the intratracheal route [28]. The inclusion of LVS as a comparative reference vaccine in our efficacy study confirms that this is also the case following infection by the aerosol delivery methodology employed in our study. These data mimic protection invoked by LVS against *F. tularensis* delivered by the aerosol route in humans reported during human experiments in the 1960s [5, 35], supporting the value of this model for efficacy evaluation of tularemia vaccine candidates.

Analysis of the GtExoA Kaplan-Meier survival curves indicated that a significant survival benefit was observed for the s.c. but not i.p. immunisation route when compared with the corresponding MF59 adjuvant control rats. This was due to survival of 3/5 rats that received the MF59 adjuvant by the i.p. route. Although we allowed a 5-week interval between the final vaccination and challenge with *F. tularensis*, we would hypothesise that i.p. immunisation with MFP59 results in a prolonged stimulation of innate immunity. However, it should be noted that none of the GtExoA-vaccinated rats, regardless of immunisation route, showed clinical signs of disease or demonstrated weight loss. In contrast, all of the control rats, including all those that did not succumb to the lethal infection, showed weight loss and adverse clinical signs. Therefore, even where significant protection against lethality was not observed, complete protection against clinical disease was. Given that pneumonic infections by high-virulence strains of *F. tularensis* exhibited <60% mortality in humans in the preantibiotic era [1], we would advocate the benefits of the rat model in being able to measure protection against lethal and nonlethal disease outcomes. The inclusion of the i.p. immunisation route in this study was primarily to provide consistency with the route used in our previous mouse efficacy study [19]. We would not envisage this as an appropriate immunisation route for future clinical extrapolation.

The protection provided by GtExoA delivered by the s.c. route was comparable to LVS in this study. This is a significant achievement for a tularemia subunit vaccine in view of the use of an aerosol challenge model using a type A strain of *F. tularensis*. Whilst undoubtedly promising, it would be premature to state the vaccine to be as protective as LVS. Since the data presented is derived from a single efficacy study, it provides proof of concept of efficacy in this preliminary study. The challenge dose employed in this study was approximately 500 CFU. LVS has demonstrated that it can protect F344 rats against lethal challenges approaching 10^5 CFU of *F. tularensis* Schu S4 delivered by the i.t. route [28]. Therefore, it will be important to test the efficacy of GtExoA in future dose escalation challenge studies to fully

establish its protective potential compared with the efficacy bench mark set by LVS.

Since the O-antigen of *F. tularensis* is a T cell-independent antigen, we would hypothesise that the protection observed was principally mediated by the generation of protective antibody responses. We detected strong titres of glycoconjugate-specific IgG in serum from GtExoA-vaccinated rats. Whilst O-antigen is widely acknowledged as a serodominant antigen, we did not formally quantitate the relative contribution of the O-antigen and ExoA protein-specific IgG. In mice, we previously demonstrated that the conjugation of the O-antigen glycans to the carrier protein ExoA resulted in enhanced antibody concentrations compared with using LPS alone [13]. This was believed to be due to ExoA providing T cell help to promote more efficient antibody generation. In the current study, we confirmed that vaccination of rats with GtExoA also resulted in the generation of ExoA-specific cell-mediated immunity supporting this hypothesis. Understanding the immunological basis and duration of the protective immunity generated by our glycoconjugate vaccine will be an important consideration for future studies.

The next step toward the development of glycoconjugate vaccines produced by this PGCT technology would be to incorporate *F. tularensis* peptide antigens as the O-antigen carrier protein, rather than *P. aeruginosa* ExoA. This approach has been successfully applied to a PGCT-produced *Staphylococcus aureus* glycoconjugate vaccine. Switching the carrier protein from ExoA to the *S. aureus*-specific protein Hla resulted in improved vaccine efficacy [36]. Whilst no single peptide antigen has been shown to be protective as a vaccine candidate for *F. tularensis* type A strains in mice, several recombinant *F. tularensis* proteins have been shown to invoke a cellular immune response [37–39]. Moreover, encapsulated recombinant peptide antigens [40], and recently a multiantigen Tobacco Mosaic virus-based vaccine [41], have been shown to protect against lethal LVS challenge to mice. An *F. tularensis* antigen expressed as part of a whole cell vaccine platform has also been shown to boost efficacy of a live attenuated vaccine [13]. It is therefore considered that incorporation of immunogenic *F. tularensis* antigens into a glycoconjugate vaccine is a desirable next step in the development of this candidate. A combination of the humoral response to the O-antigen, boosted by T cell help due to conjugation to protein, alongside the cellular response to *F. tularensis*-specific T cell epitopes has the potential to improve the protection demonstrated by the existing candidate. Future optimisation of dosing schedules and choice of adjuvant will also be important development considerations.

5. Conclusions

We have utilised PGCT technology to produce an *F. tularensis* O-antigen ExoA glycoconjugate vaccine. We have developed a F344 rat aerosol challenge model which has been used to generate proof of concept data demonstrating that this O-antigen glycoconjugate vaccine can protect against an aerosol challenge of *F. tularensis* Schu S4. Testing of the next generation of glycoconjugate vaccine candidates in this rat model of aerosol-delivered *F. tularensis* should allow delineation of the efficacies of this new source of candidates and would be the next strategic step towards development of a protective and licensable human vaccine to protect against tularemia.

Data Availability

The data used to support the findings of this study are available from the corresponding author upon request.

Conflicts of Interest

The authors declare no conflicts of interest.

Acknowledgments

The authors thank Dr. Thomas Laws (Dstl) for his assistance with statistical analysis. Additionally, we thank Novartis for supplying the MF59 vaccine adjuvant. We thank Dr. Michael Wacker and Dr. Michael Kowarik (GlycoVaxyn) for providing plasmids PGVXN114, pGVXN115, pGXVN150, and pLAFR1. This work was funded by the UK Ministry of Defence.

Supplementary Materials

Supplementary materials contain two data figures and a table supporting the analysis, interpretation, and discussion of associated study results. Figure S1: bacterial burden of *F. tularensis* Schu S4 in tissues of F344 rats 7 days after aerosol infection. Figure S2: temperature profile of vaccinated F344 rats following *F. tularensis* Schu S4 aerosol infection. Table S1: statistical comparison of Kaplan-Meier survival curves in groups of vaccinated F344 rats ($n = 5$) challenged with *F. tularensis* Schu S4 by the aerosol route. *(Supplementary Materials)*

References

[1] B. M. Stuart and R. L. Pullen, "Tularemic pneumonia—review of American literature and reports of 15 additional cases," *American Journal of the Medical Sciences*, vol. 210, no. 2, pp. 223–236, 1945.

[2] W. Jellison, *Tularemia in North America. 1930-1974*, University of Montana, Missoula, Montana, 1974.

[3] R. M. Jones, M. Nicas, A. Hubbard, M. D. Sylvester, and A. Reingold, "The infectious dose of *Francisella tularensis* (tularemia)," *Applied Biosafety*, vol. 10, no. 4, pp. 227–239, 2005.

[4] R. B. Hornick and H. T. Eigelsbach, "Aerogenic immunization of man with live tularemia vaccine," *Bacteriological Reviews*, vol. 30, no. 3, pp. 532–538, 1966.

[5] S. Saslaw, H. E. Wilson, J. A. Prior, and S. R. Carhart, "Studies on the evaluation of tularemia vaccines in man," *Journal of Laboratory and Clinical Medicine*, vol. 54, no. 6, pp. 941-942, 1959.

[6] A. Cardile, "Continued safety and immunogenicity study of a live *Francisella tularensis* vaccine," May 2016, https://clinicaltrials.gov2016.

[7] P. M. Ireland, H. LeButt, R. M. Thomas, and P. C. F. Oyston, "A *Francisella tularensis* SCHU S4 mutant deficient in (gamma)-glutamyltransferase activity induces protective immunity: characterization of an attenuated vaccine candidate," *Microbiology*, vol. 157, no. 11, pp. 3172–3179, 2011.

[8] I. Golovliov, S. M. Twine, H. Shen, A. Sjostedt, and W. Conlan, "A ΔclpB mutant of *Francisella tularensis* subspecies *holarctica* strain, FSC200, is a more effective live vaccine than *F. tularensis* LVS in a mouse respiratory challenge model of tularemia," *PLoS One*, vol. 8, no. 11, article e78671, 2013.

[9] S. Twine, H. Shen, G. Harris et al., "BALB/c mice, but not C57BL/6 mice immunized with a ΔclpB mutant of *Francisella tularensis* subspecies *tularensis* are protected against respiratory challenge with wild-type bacteria: association of protection with post-vaccination and post-challenge immune responses," *Vaccine*, vol. 30, no. 24, pp. 3634–3645, 2012.

[10] M. Mahawar, S. M. Rabadi, S. Banik et al., "Identification of a live attenuated vaccine candidate for tularemia prophylaxis," *PLoS One*, vol. 8, no. 4, p. e61539, 2013.

[11] A. L. Signarovitz, H. J. Ray, J. J. Yu et al., "Mucosal immunization with live attenuated *Francisella novicida* U112ΔiglB protects against pulmonary *F. tularensis* SCHU S4 in the Fischer 344 rat model," *PLoS One*, vol. 7, no. 10, p. e47639, 2012.

[12] P. Chu, A. L. Cunningham, J.-J. Yu et al., "Live attenuated *Francisella novicida* vaccine protects against *Francisella tularensis* pulmonary challenge in rats and non-human primates," *PLoS Pathogens*, vol. 10, no. 10, article e1004439, 2014.

[13] Q. Jia, B.-Y. Lee, D. L. Clemens, R. A. Bowen, and M. A. Horwitz, "Recombinant attenuated *Listeria monocytogenes* vaccine expressing *Francisella tularensis* IglC induces protection in mice against aerosolized type A *F. tularensis*," *Vaccine*, vol. 27, no. 8, pp. 1216–1229, 2009.

[14] J. L. Prior, R. G. Prior, P. G. Hitchen et al., "Characterization of the O antigen gene cluster and structural analysis of the O antigen of *Francisella tularensis* subsp. *tularensis*," *Journal of Medical Microbiology*, vol. 52, no. 10, pp. 845–851, 2003.

[15] M. Fulop, P. Mastroeni, M. Green, and R. W. Titball, "Role of antibody to lipopolysaccharide in protection against low- and high-virulence strains of *Francisella tularensis*," *Vaccine*, vol. 19, no. 31, pp. 4465–4472, 2001.

[16] M. Fulop, R. Manchee, and R. Titball, "Role of lipopolysaccharide and a major outer membrane protein from *Francisella tularensis* in the induction of immunity against tularemia," *Vaccine*, vol. 13, no. 13, pp. 1220–1225, 1995.

[17] J. W. Conlan, H. Shen, A. Webb, and M. B. Perry, "Mice vaccinated with the O-antigen of *Francisella tularensis* LVS lipopolysaccharide conjugated to bovine serum albumin develop varying degrees of protective immunity against systemic or aerosol challenge with virulent type A and type B strains of the pathogen," *Vaccine*, vol. 20, no. 29-30, pp. 3465–3471, 2002.

[18] F. Berti and R. Adamo, "Recent mechanistic insights on glycoconjugate vaccines and future perspectives," *ACS Chemical Biology*, vol. 8, no. 8, pp. 1653–1663, 2013.

[19] C. M. Szymanski, R. Yao, C. P. Ewing, T. J. Trust, and P. Guerry, "Evidence for a system of general protein glycosylation in *Campylobacter jejuni*," *Molecular Microbiology*, vol. 32, no. 5, pp. 1022–1030, 1999.

[20] V. S. Terra, D. C. Mills, L. E. Yates, S. Abouelhadid, J. Cuccui, and B. W. Wren, "Recent developments in bacterial protein glycan coupling technology and glycoconjugate vaccine design," *Journal of Medical Microbiology*, vol. 61, Part 7, pp. 919–926, 2012.

[21] M. Wacker, D. Linton, P. G. Hitchen et al., "N-linked glycosylation in *Campylobacter jejuni* and its functional transfer into *E. coli*," *Science*, vol. 298, no. 5599, pp. 1790–1793, 2002.

[22] M. Wacker, M. F. Feldman, N. Callewaert et al., "Substrate specificity of bacterial oligosaccharyltransferase suggests a common transfer mechanism for the bacterial and eukaryotic systems," *Proceedings of the National Academy of Sciences of the United States of America*, vol. 103, no. 18, pp. 7088–7093, 2006.

[23] J. Cuccui, R. M. Thomas, M. G. Moule et al., "Exploitation of bacterial N-linked glycosylation to develop a novel recombinant glycoconjugate vaccine against *Francisella tularensis*," *Open Biology*, vol. 3, no. 5, 2013.

[24] M. F. Feldman, M. Wacker, M. Hernandez et al., "Engineering N-linked protein glycosylation with diverse O antigen lipopolysaccharide structures in *Escherichia coli*," *Proceedings of the National Academy of Sciences of the United States of America*, vol. 102, no. 8, pp. 3016–3021, 2005.

[25] J. Karlsson, R. G. Prior, K. Williams et al., "Sequencing of the *Francisella tularensis* strain Schu 4 genome reveals the shikimate and purine metabolic pathways, targets for the construction of a rationally attenuated auxotrophic vaccine," *Microbial and Comparative Genomics*, vol. 5, no. 1, pp. 25–39, 2000.

[26] A. C. Guyton, "Measurement of the respiratory volumes of laboratory animals," *American Journal of Physiology-Legacy Content*, vol. 150, no. 1, pp. 70–77, 1947.

[27] G. J. Harper and J. D. Morton, "The respiratory retention of bacterial aerosols—experiments with radioactive spores," *Journal of Hygiene*, vol. 51, no. 3, pp. 372–385, 1953.

[28] T. H. Wu, J. L. Zsemlye, G. L. Statom et al., "Vaccination of Fischer 344 rats against pulmonary infections by *Francisella tularensis* type A strains," *Vaccine*, vol. 27, no. 34, pp. 4684–4693, 2009.

[29] J. A. Hutt, J. A. Lovchik, A. Dekonenko, A. C. Hahn, and T. H. Wu, "The natural history of pneumonic tularemia in female Fischer 344 rats after inhalational exposure to aerosolized *Francisella tularensis* subspecies *tularensis* strain SCHU S4," *American Journal of Pathology*, vol. 187, no. 2, pp. 252–267, 2017.

[30] G. Mara-Koosham, J. A. Hutt, C. R. Lyons, and T. H. Wu, "Antibodies contribute to effective vaccination against respiratory infection by type A *Francisella tularensis* strains," *Infection and Immunity*, vol. 79, no. 4, pp. 1770–1778, 2011.

[31] M. I. Roche, Z. Lu, J. H. Hui, and J. Sharon, "Characterization of monoclonal antibodies to terminal and internal O-antigen epitopes of *Francisella tularensis* lipopolysaccharide," *Hybridoma*, vol. 30, no. 1, pp. 19–28, 2011.

[32] H. J. Ray, P. Chu, T. H. Wu et al., "The Fischer 344 rat reflects human susceptibility to *Francisella* pulmonary challenge and provides a new platform for virulence and protection studies," *PLoS One*, vol. 5, no. 4, p. e9952, 2010.

[33] C. R. Raymond and J. W. Conlan, "Differential susceptibility of Sprague-Dawley and Fischer 344 rats to infection by *Francisella tularensis*," *Microbial Pathogenesis*, vol. 46, no. 4, pp. 231–234, 2009.

[34] J. V. Jemski, "Respiratory tularemia: comparison of selected routes of vaccination in Fischer 344 rats," *Infection and Immunity*, vol. 34, no. 3, pp. 766–772, 1981.

[35] S. Saslaw, H. E. Wilson, S. Carhart, E. HT, and J. A. Prior, "Tularemia vaccine studies. 2. Respiratory challenge," *Archives of Internal Medicine*, vol. 107, no. 5, p. 702, 1961.

[36] M. Wacker, L. Wang, M. Kowarik et al., "Prevention of *Staphylococcus aureus* infections by glycoprotein vaccines synthesized in *Escherichia coli*," *The Journal of Infectious Diseases*, vol. 209, no. 10, pp. 1551–1561, 2014.

[37] M. G. Hartley, M. Green, G. Choules et al., "Protection afforded by heat shock protein 60 from *Francisella tularensis* is due to copurified lipopolysaccharide," *Infection and Immunity*, vol. 72, no. 7, pp. 4109–4113, 2004.

[38] I. Golovliov, M. Ericsson, L. Akerblom, G. Sandstrom, A. Tarnvik, and A. Sjostedt, "Adjuvanticity of ISCOMs incorporating a T cell-reactive lipoprotein of the facultative intracellular pathogen *Francisella tularensis*," *Vaccine*, vol. 13, no. 3, pp. 261–267, 1995.

[39] A. Sjostedt, G. Sandstrom, and A. Tarnvik, "Humoral and cell mediated immunity in mice to a 17 kilodalton liprotein of *Francisella tularensis* expressed by *Salmonella typhimurium*," *Infection and Immunity*, vol. 60, no. 7, pp. 2855–2862, 1992.

[40] A. J. Hickey, K. R. O. Hazlett, G. S. Kirimanjeswara, and D. W. Metzger, "Identification of *Francisella tularensis* outer membrane protein A (FopA) as a protective antigen for tularemia," *Vaccine*, vol. 29, no. 40, pp. 6941–6947, 2011.

[41] A. A. McCormick, A. Shakeel, C. Yi, H. Kaur, A. M. Mansour, and C. S. Bakshi, "Intranasal administration of a two-dose adjuvanted multi-antigen TMV-subunit conjugate vaccine fully protects mice against *Francisella tularensis* LVS challenge," *PLoS One*, vol. 13, no. 4, article e0194614, 2018.

Hindawi
Journal of Immunology Research
Volume 2018, Article ID 8979838, 8 pages
https://doi.org/10.1155/2018/8979838

Research Article

Food-Grade Saponin Extract as an Emulsifier and Immunostimulant in Emulsion-Based Subunit Vaccine for Pigs

Yulia Burakova,[1,2] Rachel Madera,[1] Lihua Wang,[1] Sterling Buist,[1] Karen Lleellish,[1] John R. Schlup,[2] and Jishu Shi[1]

[1]*Department of Anatomy and Physiology, College of Veterinary Science, Kansas State University, 228 Coles Hall, 1620 Denison Ave, Manhattan, KS 66506, USA*
[2]*Department of Chemical Engineering, College of Engineering, Kansas State University, 1005 Durland Hall, 1701A Platt St, Manhattan, KS 66506, USA*

Correspondence should be addressed to Jishu Shi; jshi@ksu.edu

Received 13 June 2018; Revised 17 August 2018; Accepted 26 September 2018; Published 27 November 2018

Guest Editor: Francesca Ferrara

Subunit vaccines consisting of highly purified antigens require the presence of adjuvants to create effective and long-lasting protective immunity. Advances on adjuvant research include designing combination adjuvants which incorporate two or more adjuvants to enhance vaccine efficacy. Previously, an oil-in-water emulsion adjuvant (OW-14) composed of mineral oil and an inexpensive gum Arabic emulsifier has been reported demonstrating enhanced and robust immune responses when used as an adjuvant in swine subunit vaccines. This study presents a modified version of OW-14 prepared with food-grade *Quillaja* saponin extract (OWq). In new OWq emulsion, saponin extract served as an emulsifier for stabilization of emulsion droplets and as an immunoactive compound. The use of saponins allowed to reduce the required amount of emulsifier in the original OW-14. However, emulsion stabilized with saponins demonstrated extended physical stability even at elevated temperature (37°C). The two-dose vaccination with a classical swine fever virus (CSFV) glycoprotein E2-based vaccine formulated with OWq produced higher levels of E2-specific IgG and virus neutralizing antibodies in pigs in contrast with animals that received the vaccine adjuvanted with oil only. In addition, new OWq adjuvant was safe to use in the vaccination of pigs.

1. Introduction

The effectiveness of subunit vaccines relies on immunostimulatory adjuvants to induce potent and long-lasting antigen-specific immune responses. Early adjuvants, like aluminum salts and emulsions, are still the primary choice in vaccine formulations for livestock species because of their safety, simple formulation, and low cost [1, 2]. However, the efficacy of these conventional adjuvants in the induction of antibody responses warrants further improvements. Combination of aluminum salts or emulsions with immunostimulant substances is currently considered to be a promising approach in boosting of the vaccine performance [3, 4]. Combination of the adjuvants with different modes of action presents potential on both enhanced and tailored immune responses for long-lasting protection against the disease. Coadministration of two or more adjuvants in one vaccine has also been explored in veterinary medicine [2]. The combination of different immunostimulant substances, such as saponins, with emulsions and aluminum salts in vaccines for livestock has been actively studied by several research groups [5–7]. For instance, the addition of saponin extract Quil-A® to commercial emulsion-based vaccine was reported to improve humoral immune responses in pigs vaccinated for foot-and-mouth disease [7]. In this present study, we utilized saponin extract, not only as immunostimulatory compound but also as emulsifier to stabilize the emulsion adjuvant.

Saponins are naturally occurring triterpene glucoside compounds (Figure 1) that are commonly used in vaccine research studies against both animal and human pathogens [8]. *Quillaja saponaria* Molina tree is a main source of saponins for vaccine adjuvants, although there are reports of

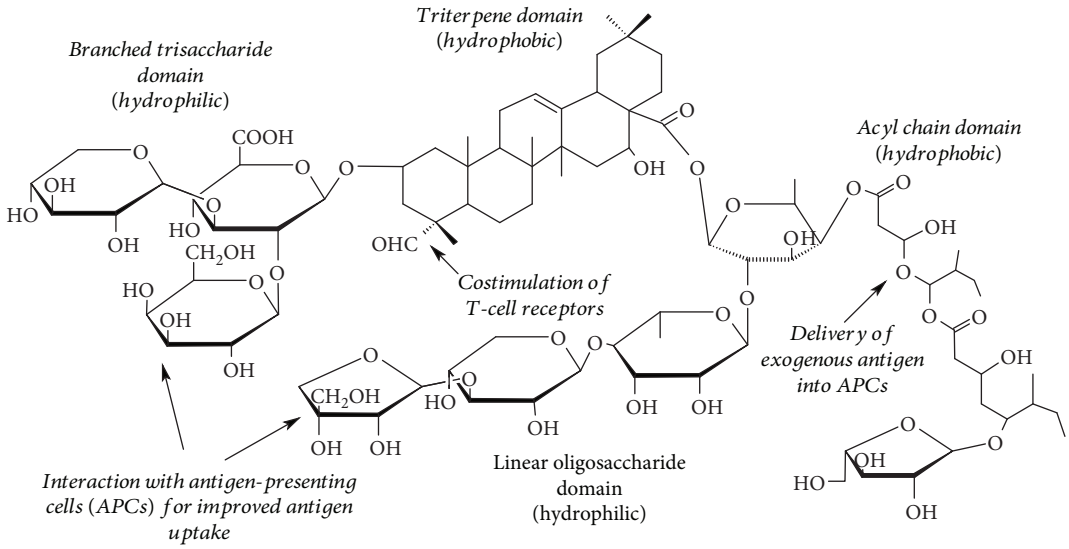

Figure 1: General structure of the saponin molecule reveals the presence of hydrophobic and hydrophilic regions responsible for surface activity of the molecule, while carbohydrate regions, acyl domain, and aldehyde group on triterpene domain demonstrate adjuvant properties. The structure representation is adapted from Yang et al. [14].

immunostimulant activity of saponins obtained from other plants [9] and semisynthetic saponins [10]. Commercial saponin adjuvants isolated from *Q. saponaria* tree such as Quil-A (Brenntag Biosector A/S, Denmark) and QS-21 (Desert King, USA) are very potent in inducing high antigen-specific immune responses of both T-helper 1 (Th1) and T-helper 2 (Th2) origins [11]. Studies show that the carbohydrate groups of the saponin molecule interact with receptors on antigen-presenting cells (APCs) and promote antigen phagocytosis and secretion of cytokines by APCs while acyl chain domain assists in the delivery of exogenous antigens into APCs and facilitates Th1 immunity [12]. Aldehyde group on the triterpene domain promotes costimulation of T cell surface receptors (Figure 1) [13]. However, the commercial application of these saponin extracts in animal vaccines is hindered by their high costs.

On the other hand, food-grade *Quillaja* saponin extracts are also used as emulsifiers to produce flavored and vitamin beverages. Saponin molecules contain both hydrophobic and hydrophilic domains making them good candidates for stabilization of oil-in-water food emulsions (Figure 1) [14, 15].

We have previously reported that OW-14, a low-cost emulsion adjuvant based on light mineral oil and food-grade gum Arabic emulsifier, can stimulate high-level antigen-specific antibody responses in vaccines for swine influenza (SI), *Mycoplasma hyopneumoniae*, and classical swine fever (CSF) [16, 17]. In the present study, a variation of the OW-14 emulsion adjuvant formulated with the food-grade saponin extract, Sapnov LS™ (Naturex, USA), in the subunit vaccine for CSF were tested.

CSF is caused by CSF virus, which is a small, enveloped RNA virus in the genus *Pestivirus* of the family *Flaviviridae* [18]. The disease is responsible for economic losses in the swine industry in many countries. Subunit vaccines based on envelope glycoprotein E2 of classical swine fever virus (CSFV) have been shown to induce high-level antigen-specific immune responses and clinical protection of pigs from CSFV challenge [17, 19].

The safety and efficacy of food-grade saponin extract as the emulsifier and immunostimulant in emulsion-based adjuvant coadministered with E2 antigen were investigated. Sapnov LS™ is a water extract of *Q. saponaria* with saponin content around 65% on the dry basis according to the manufacturer. This cost-effective nonionic surfactant is used for production of flavored and colored emulsions such as beverage concentrates and alcoholic drinks. To the best of our knowledge, this is the first report on application of food-grade saponin extract in emulsion-based vaccines for livestock. In addition, an experimental oil-based adjuvant (OBA) that produces an emulsion after low-energy mixing with aqueous solution of E2 antigen was tested in comparison with a saponin-based emulsion vaccine.

2. Materials and Methods

2.1. Materials. Light mineral oils, Drakeol 5 and Drakeol 6, were purchased from Calumet Panreco (Karns City, PA, USA). TICAmulsion A-2010 emulsifier (gum Arabic) was obtained from TIC Gums (White Marsh, MD, USA). *Quillaja* water extract Sapnov™ (65% saponin content) was provided by Naturex Inc. (Chicago, IL, USA). Polymeric surfactants Atlas G-5002L and Atlox 4916 were obtained from Croda Inc. (New Castle, DE, USA). Medium chain triglyceride oil (MCT oil) was purchased from Jedwards International Inc. (Braintree, MA, USA).

2.2. Formulation of Adjuvants and Vaccines. Emulsion adjuvant with saponin extract (OWq) was prepared by dissolving TICAmulsion A-2010 (5% *w*/*v*) in nanopure water and stirred overnight with a magnetic bar. *Quillaja* extract Sapnov emulsifier (0.5% *v*/*v*) was added to the TICAmulsion

solution and inverted several times to ensure complete mixing of both emulsifiers in water. Mineral oil Drakeol 5 (15% *v*/*v*) was added to the solution with emulsifiers. The coarse emulsion was mixed with high shear lab mixer (L5MA, Silverson Inc., East Longmeadow, MA, USA) at 10,000 rpm for 15 min and then passed through a microfluidizer M110P (Microfluidics, Westwood, MA, USA) for five times at 10,000 psi. OWq was stored at 4°C until use.

Insect cell-expressed CSFV E2 protein was prepared as described previously [17]. Subunit vaccine was formulated by mixing of 2 vol. of E2 protein solution dissolved in phosphate-buffered saline (PBS) and 1 vol. of OWq emulsion adjuvant using a vortex mixer for several seconds.

Oil-based adjuvant (OBA) was prepared by dissolving two nonionic block copolymer surfactants, Atlas G-5002L and Atlox 4916, in a 7 : 1 by weight ratio mixture of MCT oil and Drakeol 6 mineral oil, respectively. Oils and surfactants were mixed together in an 80 : 20 by weight ratio to produce a clear yellow mixture. To prepare emulsion-based subunit vaccine, OBA was slowly added to the solution of E2 protein in PBS in a 1 : 1 ratio of the adjuvant to aqueous phase and stirred using a magnetic stirrer for 30 min at room temperature.

The final concentration of the antigenic E2 protein in all vaccine formulations was 50 μg per dose.

2.3. Physical Characteristics and Stability Study of Adjuvants. Freshly prepared emulsions were analyzed using dynamic light scattering (DLS) with a Malvern Zetasizer Nano ZS 90 (Malvern Instruments, Westborough, MA, USA) to determine droplet size, polydispersity, and zeta potential. The OWq emulsion adjuvant was analyzed as prepared. OBA was mixed with PBS in a 1 : 1 weight ratio using a magnetic stirrer to obtain emulsion for DLS analysis and storage stability assessment.

Approximately 5 μl of each emulsion sample was diluted in 1 ml of deionized water to achieve a translucent solution and perform the measurements. All samples were measured 3 times at room temperature. Results are presented as a mean of 3 measurements ± the standard deviation (SD). The pH values of the emulsions were measured using a VWR SympHony digital pH meter SB21 (VWR International, Radnor, PA, USA), calibrated according to the manufacturer's manual. To assess the shelf stability, samples were stored at 4°C, room temperature (RT), and 37°C and then analyzed again for droplet size and pH after 6 months of storage. Emulsions were also observed visually for the presence of creaming, phase separation, and color change.

2.4. Pig Immunization. The animal study was conducted in accordance with Institutional Animal Care and Use Committee (IACUC). Animals were housed at the Large Animal Research Center (LARC) facility, Kansas State University. Conventional Large White-Duroc crossbreed weaned specific-pathogen free piglets (3 weeks of age) were randomly divided into two vaccine groups ($n = 6$ for each group) and 1 negative control group ($n = 2$). Pigs were immunized intramuscularly with 2 ml each of subunit vaccines. The first group received E2 protein co-administered with OWq (E2 + OWq). The second vaccine group was immunized with E2 and oil-based adjuvant (E2 + OBA). Three out of the 6 animals in each vaccine group received a second dose of the subunit vaccines 14 days after the first immunization (two-dose pigs). The negative control group received 2 ml intramuscularly of PBS. Blood samples were collected on days 0, 7, 14, 21, and 28 of the experiment. Sera was separated from the blood and stored at −20°C until further use in assays. Pig weights were measured weekly. Pig health was monitored daily including vaccine injection site reactions. Animals were humanely euthanized and disposed of at the end of the experiment (day 28).

2.5. Antibody Responses. E2-specific IgG, IgG1, and IgG2 antibody titers were determined in pig sera by enzyme-linked immunosorbent assay (ELISA) as described previously [17, 20]. Briefly, the 96-well flat-bottom microtiter plates (Corning®) were coated overnight with 62.5 ng/ml of purified E2 followed by washing with ELISA Wash Buffer (0.05% Tween 20 in PBS) and blocked with ELISA Blocking Buffer (2% fetal bovine serum in PBS) for 1 hour at 37°C. Diluted sera were added to plates and incubated for 1 hour at RT, followed by washing 3 times with ELISA Wash Buffer. Goat anti-swine IgG conjugated with horseradish peroxidase (HRP) (#sc-2914, Santa Cruz Biotechnology, USA, dilution 1/1,000), mouse anti-swine IgG1 (#MCA635GA, Bio-Rad Antibodies, USA, dilution 1/300), or mouse anti-swine IgG2 (#MCA636GA, Bio-Rad Antibodies, USA, dilution 1/300) in ELISA Blocking Buffer was added in wells at 100 μl/well as secondary antibodies and incubated 1 hour at RT followed by washing 3 times with ELISA Wash Buffer. HRP-conjugated goat anti-mouse IgG (H+L) (#115-035-003, Jackson ImmunoResearch, USA, dilution 1/1,000) was added to wells at 100 μl/well in case of IgG1 and IgG2 titer analysis and incubated 1 hour at RT followed by washing 3 times with washing buffer. 3,3,5,5-Tetramethylbenzidine- (TMB-) stabilized chromogen (Novex) was used to develop the ELISA plates following by 2N sulfuric acid to stop the reaction. Relative antibody concentration was determined with an optical spectrophotometer using a SpectraMAX microplate reader at 450 nm and was analyzed with Softmax® Pro 6.4 Software (Molecular Devices, USA).

2.6. Anti-CSFV Neutralization Assay of Pig Serum. The anti-CSFV neutralizing antibody levels were measured using indirect fluorescent antibody (IFA) assay in pig serum collected on day 21 after the first dose of subunit vaccines or PBS as described elsewhere [20]. Neutralizing titers in serum samples were calculated as the reciprocal of the highest dilution that caused neutralization of the virus in 50% of the wells.

2.7. Statistical Analysis. Data from pig experiments were reported as the mean values ± standard error of measurement (SEM). The differences between treatment groups were analyzed by one-way analysis of variance (ANOVA) using SigmaPlot 11.0 software (Systat Software Inc., USA). Differences were considered statistically significant when $p < 0.05$.

Table 1: Physical characteristics of fresh emulsion adjuvants and after 180-day storage at different temperatures.

Emulsion		Mean droplet size ± S.D., nm	Polydispersity ± S.D.	Zeta potential ± S.D., mV	pH
OWq	Fresh	203.40 ± 1.83	0.115 ± 0.008	−51.7 ± 0.2	7.1
	180 days at 4°C	272.50 ± 4.86	0.117 ± 0.025	−53.2 ± 0.7	6.2
	180 days at RT	266.57 ± 5.73	0.054 ± 0.035	−58.0 ± 3.1	7.1
	180 days at 37°C	277.80 ± 4.98	0.142 ± 0.022	−56.0 ± 3.9	6.3
OBA in PBS	Fresh	327.40 ± 4.59	0.270 ± 0.004	−25.0 ± 3.7	7.3
	180 days at 4°C	310.37 ± 2.29	0.193 ± 0.005	−12.4 ± 0.2	7.2
	180 days at RT	217.97 ± 1.85	0.147 ± 0.010	−6.8 ± 0.4	7.2
	180 days at 37°C	367.37 ± 0.51	0.242 ± 0.012	−11.5 ± 0.2	7.2

RT: room temperature; SD: standard deviation.

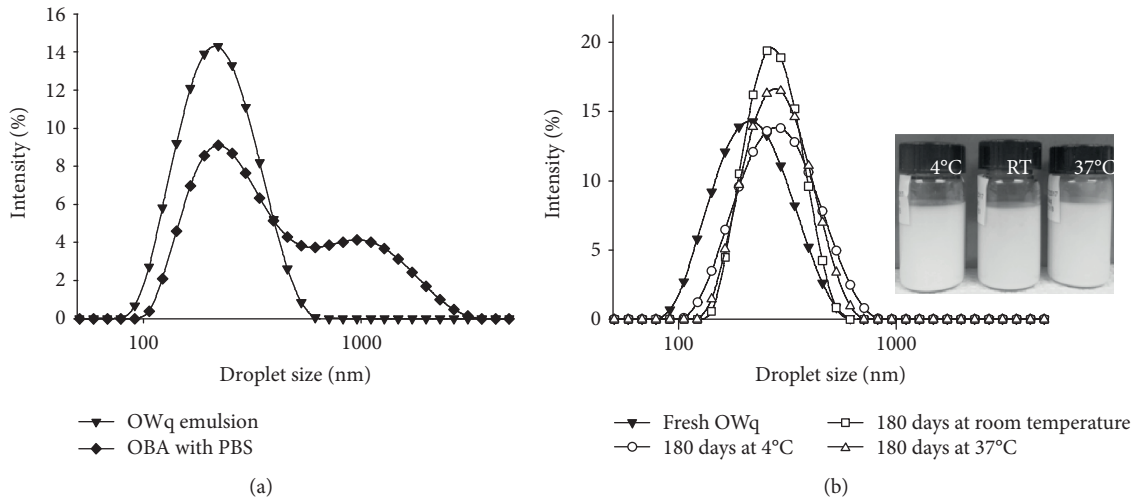

Figure 2: Size distribution of emulsion-based adjuvants obtained with dynamic light scattering (DLS). (a) Freshly prepared OWq emulsion had droplets within 90–600 nm size range, while oil-based adjuvant (OBA) mixed with PBS produced emulsion with droplets between 100 and 3000 nm. (b) After 180-day storage at different temperatures, the slight shift of size distributions towards bigger droplets was detected in OWq emulsion; however, no creaming or phase separation was observed in visual appearance of emulsion samples (photograph insertion).

3. Results

3.1. Designed Adjuvants Preserve Their Physical Characteristics after Prolonged Storage at Different Temperatures. According to DLS measurements, freshly prepared OWq emulsion adjuvant had nanoscale size of droplets with a mean value of approximately 200 nm and relatively low polydispersity, while emulsion prepared with OBA had droplets around 320 nm with higher difference in droplet sizes (Table 1). All formulations had pH values around 7 (Table 1). The OWq emulsion had a relatively narrow size distribution ranging from 91 to 531 nm, while an emulsion prepared from oil-based adjuvant had droplets with diameters from 106 nm up to 3090 nm (Figure 2(a)). In addition, a saponin-based emulsion had lower zeta potential value (−51.7 mV) than an emulsion prepared with OBA (−25.0 mV) (Table 1). After 6 months of storage at different temperatures, the OWq emulsion adjuvant did not undergo any significant changes in the mean size of emulsion droplets, polydispersity, zeta potential, and pH (Table 1). DLS analysis detected a small shift in the emulsion size distribution towards larger droplets for all OWq samples (4°C, RT, and 37°C) (Figure 2(b)). Thus, after 6-month storage at 37°C, the size of the OWq emulsion droplets ranged from 106 to 955 nm. However, no creaming, phase separation, and color changes were noticed in the appearance of the OWq emulsion after extended storage even at 37°C (Figure 2(b), photograph insertion). The mean droplet size of an emulsion prepared with OBA did not change after storage at 4°C and 37°C. However, a decrease from 320 nm to 217 nm was detected in samples stored at RT (Table 1). Visual observations did not detect any changes in appearance of all OBA emulsion samples (data not shown).

3.2. Subunit Vaccine with Saponin-Based Emulsion Did Not Produce Health Issues in Animals and Induced High Antibody Responses. After vaccination with E2 subunit vaccines, all pigs grew consistently, and no difference in weight gain was observed between the animals that received 1 dose and 2 doses of the subunit vaccines and negative control group injected with PBS (Figure 3(a)). The presence of small (1–2 cm) subcutaneous bumps was observed at the injection sites in the E2 + OWq-vaccinated pig groups. By day 28 of study, they decreased in size and mostly disappeared. The negative control group and the E2 + OBA-vaccinated pig

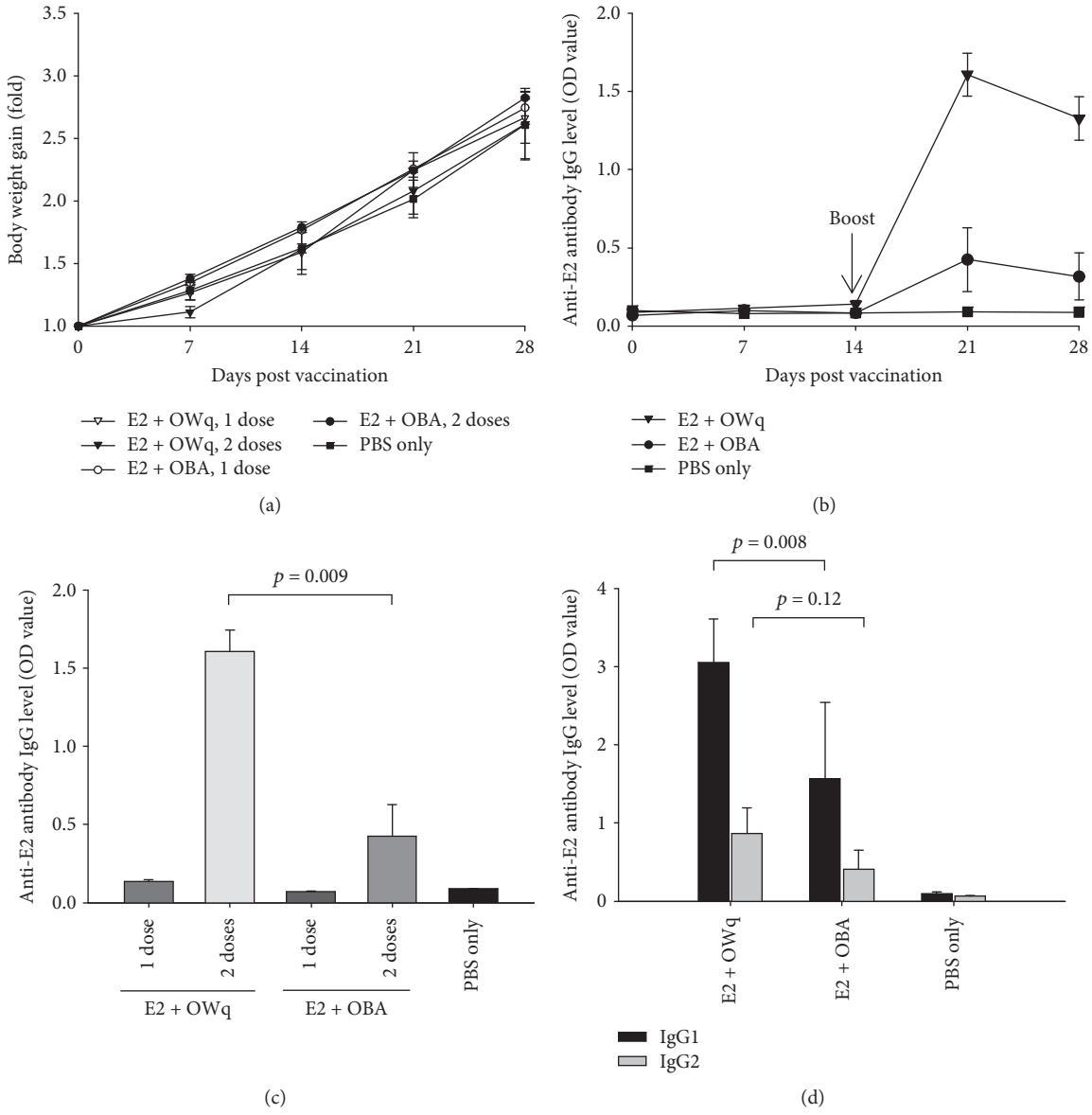

Figure 3: Safety and immunological effect of OWq and OBA injected with E2 antigenic protein. (a) E2 subunit vaccine administered with experimental adjuvants did not impact weight gain in pigs as both one-dose and two-dose animals had grown consistently and at the same level as negative control pigs (PBS only). (b) E2 protein coadministered with OWq adjuvant demonstrated higher E2-specific IgG antibody titer detected on days 21 and 28 in serum samples (dilution 1/5000) of two-dose pigs than subunit vaccine with OBA. (c) Two-dose pigs developed significantly higher IgG titer than animals receiving single vaccination on day 21 of the study (dilution 1/5000). (d) IgG1 and IgG2 titers in serum samples (dilution 1/1000) collected from two-dose pigs on day 21 of the study. Data are presented as a mean ± SEM.

group did not have any pathological changes at injection sites (data not shown). No issues were observed in pig health, and all animals survived by the end of the study.

Pigs that received the boost vaccine on day 14 of study had increased E2-specific IgG levels on days 21 and 28 of the experiment (Figure 3(b)). The animals immunized with E2 + OWq had statistically significant higher IgG titers in comparison with the vaccine group that received E2 with OBA ($p = 0.009$) and control group (Figure 3(c)). As expected, a two-dose immunization schedule provided significantly higher IgG titers than one dose in both vaccine groups on day 21 of the study (Figure 3(c)). The IgG1 and IgG2 antibody titers were also higher in E2 + OWq group in comparison with E2 + OBA vaccine group, although it should be noted that there was no statistically significant difference between the two groups ($p = 0.08$ and 0.12 for IgG1 and IgG2 titer analysis, respectively) (Figure 3(d)).

Table 2 represents the results of anti-CSFV neutralization assay performed with pig serum collected on day 21 of the study. The highest neutralizing antibody titers were detected in pigs immunized with two doses of E2 subunit vaccine adjuvanted with OWq emulsion. Very low or no detectable titers were detected in all other pigs including animals inoculated with PBS instead of the subunit vaccine (Table 2).

Table 2: Anti-CSFV neutralizing antibody titers (ND_{50}) in pigs on day 21 of the study.

Treatment group	Pig #	Day 21
E2 + OWq, 1 dose	178	<5
	181	5
	185	5
E2 + OWq, 2 doses	186	640
	188	960
	195	480
E2 + OBA, 1 dose	177	<5
	180	<5
	187	<5
E2 + OBA, 2 doses	189	480
	190	20
	193	40
PBS only	184	<5
	191	<5

4. Discussion

Emulsions are cost-effective vaccine adjuvants, and their combination with saponins is a promising way to increase the efficacy of veterinary vaccines. Saponins are very effective immunostimulants and have been studied in vaccine formulations for the past decades [2]. However, saponins' high toxicity due to their detergent properties presents a main drawback in their wide application in human and animal vaccines [11]. There are commercially available purified saponin extracts (Quil-A, QS-21); however, their high cost precludes their application as adjuvants in mass livestock immunization.

Safety, efficacy, and physical and chemical stability of the vaccine adjuvants are the key factors in designing novel vaccine formulations. In addition, the cost of materials and production are of paramount importance in the development of livestock vaccines [21]. In this study, a mineral oil-based emulsion with a food-grade inexpensive saponin extract (OWq) and oil-based adjuvant that produces an emulsion after gentle mixing with an aqueous phase were tested for safety and immunological activity in swine vaccination.

In OWq, the saponin extract served as an emulsifier for stabilization of emulsion droplets and as an immunostimulant in the subunit vaccine. Thus, the addition of saponin extract to original formulation (OW-14) [16] allowed reducing the amount of TICAmulsion A-2010 emulsifier from 7.5% w/v to 5% w/v without affecting the shelf stability of adjuvant. Moreover, OWq emulsion adjuvant demonstrated good physical stability after 180 days of storage at all tested temperatures. Mean droplet size remained less than 300 nm with low polydispersity among the droplets (Table 1, Figure 2(b)). The slight drop in pH values in samples stored at 4°C and 37°C was detected after 180 days. However, no physical changes in emulsion samples, such as creaming or phase separation, were observed. Physical stability is very important for livestock vaccines, especially in developing countries where refrigeration during transportation and storage of the vaccines is not always available or cost-effective.

The droplet diameters, polydispersity, and zeta potential of prepared emulsions are important factors in predicting the physical stability of the emulsions. Freshly prepared OWq emulsion had nanosize droplets in a range from 91 to 531 nm and low zeta potential (−51.7 mV), which provides electrostatic repulsion between the droplets and prevents their fast flocculation and coalescence. Vaccine can be easily prepared at the site by simple hand mixing or gentle agitation of OWq with antigenic solution. It can be readily administered through a standard syringe with 20-gauge needle.

OBA mixed with PBS by a low-energy mixing method produced an emulsion with high polydispersity, mean droplet size around 320 nm, and zeta potential around −25 mV. No significant changes in mean droplet size were detected after 180-day storage. However, a decrease in zeta potential value indicates lower colloidal stability over time in comparison with OWq emulsion.

The safety and immunological activity of designed adjuvants were tested in swine vaccination with E2 antigen. Pigs immunized with experimental adjuvants in subunit CSFV E2 vaccines did not experience any health issues and gained the weight on the same level as negative control pigs during the entire study (Figure 3(a)). Small subcutaneous bumps were observed at the injection sites of the OWq vaccine group, although they decreased in size significantly or disappeared towards the end of the experiment. These findings suggest that food-grade saponin extract can be safely utilized in veterinary vaccine formulations. Moreover, the group immunized with two doses of E2 subunit protein adjuvanted with OWq emulsion had higher E2-specific IgG levels (Figures 3(b)–3(d)) and anti-CSFV neutralizing antibody titers (Table 2) in comparison with vaccine group that received E2 formulated with emulsion and without saponins or other immunostimulant compounds.

The reason E2 + OBA vaccine did not induce strong IgG antibody responses and high anti-CSFV neutralizing titers can be attributed to the composition and physical characteristics of the adjuvant. OBA predominantly consisted of plant-derived MCT oil with small portion of mineral oil, while vaccines based on mineral oil generally produce more irritation at the injection sites and induce higher immune responses than vaccines with plant-derived oils [22]. In addition, the mean droplet size of emulsion fabricated from OBA was 327.40 nm. However, it has been demonstrated that particles less than 200 nm are processed more efficiently by the APCs [23]. Clearly, the changes in composition of the OBA should be done to reduce the size of emulsion droplets and improve the emulsion stability and efficacy as a vaccine adjuvant.

Animals that were immunized twice with subunit vaccines have developed significantly higher IgG titers (Figure 3(c)) and anti-CSFV neutralizing antibody titers (Table 2) in comparison with pigs receiving single vaccination. However, previous studies demonstrated that even one-dose vaccination with an emulsion-based subunit vaccine can protect the pigs from the challenge with CSF virus [17, 20].

Previous findings have shown that saponins promote the production of IgG2 over IgG1 antibody subclass and favor Th1 and cytotoxic T lymphocyte responses in contrast with conventional adjuvants such as aluminum salts and emulsions in murine models [9, 11]. These suggest that saponin adjuvants can be beneficial in vaccines against intracellular pathogens such as viruses. In the present study, IgG2 titer analysis of pig serum samples did not show statistically significant differences between saponin-based emulsion adjuvant and an emulsion without saponins ($p = 0.12$) (Figure 3(d)). This can be attributed to several factors such as the difference between mice and swine immune responses to the saponins, heterogeneous composition of food-grade saponin extract, or poor stability of the saponins resulting in stimulation of Th2 immunity rather than Th1. It has been demonstrated that various fractions of *Q. saponaria* extract have different immunological activity and can induce the production of different IgG antibody subclasses [11]. Another study showed that *Q. saponaria* extract are easily degraded during storage resulting in deacylation of the saponin molecules and the inability to promote a strong Th1 response and IgG2 production [24]. The exact fraction composition of the food-grade saponin extract used in this study is unknown and needed to be determined to verify these speculations. In addition, further investigation is required to confirm the level of protection of swine immunized with E2 protein and OWq saponin-based emulsion after the challenge with CSF virus.

5. Conclusion

Inexpensive food-grade saponin extract was employed to create emulsion-based adjuvant for swine subunit vaccine. Saponins served a dual purpose: stabilization of emulsion droplets and stimulation of immune responses. The addition of saponin extract helped to reduce the amount of emulsifier in the original OW-14 adjuvant. This change in composition did not impact droplet size stability of the emulsion adjuvant. Thus, OWq can be stored at least 180 days at different temperatures without dramatic changes in droplet size, creaming, or phase separation. A saponin-based emulsion adjuvant was safe to use in swine immunization as no significant inflammations at the injection sites and consistent weight gain in animals were observed after coadministration with E2 antigenic protein. Two doses of CSF E2 subunit vaccine with OWq adjuvant demonstrated high total IgG and anti-CSFV neutralizing antibody titers in pigs in comparison with the emulsion vaccine prepared with oil-based adjuvant without saponins. This is the first demonstration that a cost-effective food-grade saponin extract can be incorporated in an emulsion-based adjuvant and safely used in livestock immunization promoting strong antibody responses.

Data Availability

The datasets used to support the findings of this study are available from the corresponding author upon reasonable request.

Conflicts of Interest

The authors declare that they have no conflicts of interest.

Acknowledgments

We would like to thank the Comparative Medicine staff at Kansas State University for their help with the animal study. This research was supported by an award from the National Bio and Agro-Defense Facility Transition Fund and a USDA ARS Specific Cooperative Agreement (59-5430-001-23S, NP-103).

References

[1] T. L. Bowersock and S. Martin, "Vaccine delivery to animals," *Advanced Drug Delivery Reviews*, vol. 38, no. 2, pp. 167–194, 1999.

[2] Y. Burakova, R. Madera, S. McVey, J. R. Schlup, and J. Shi, "Adjuvants for animal vaccines," *Viral Immunology*, vol. 31, no. 1, pp. 11–22, 2018.

[3] G. Mutwiri, V. Gerdts, S. van Drunen Littel-van den Hurk et al., "Combination adjuvants: the next generation of adjuvants?," *Expert Review of Vaccines*, vol. 10, no. 1, pp. 95–107, 2011.

[4] B. Levast, S. Awate, L. Babiuk, G. Mutwiri, V. Gerdts, and S. van Drunen Littel-van den Hurk, "Vaccine potentiation by combination adjuvants," *Vaccines*, vol. 2, no. 2, pp. 297–322, 2014.

[5] J. Ren, H. Lu, S. Wen et al., "Enhanced immune responses in pigs by DNA vaccine coexpressing GP3 and GP5 of European type porcine reproductive and respiratory syndrome virus," *Journal of Virological Methods*, vol. 206, pp. 27–37, 2014.

[6] C. Çokçalışkan, T. Türkoğlu, B. Sareyyüpoğlu et al., "QS-21 enhances the early antibody response to oil adjuvant foot-and-mouth disease vaccine in cattle," *Clinical and Experimental Vaccine Research*, vol. 5, no. 2, pp. 138–147, 2016.

[7] C. Xiao, Z. I. Rajput, and S. Hu, "Improvement of a commercial foot-and-mouth disease vaccine by supplement of Quil A," *Vaccine*, vol. 25, no. 25, pp. 4795–4800, 2007.

[8] C. R. Kensil, "Saponins as vaccine adjuvants," *Critical reviews in therapeutic drug carrier systems*, vol. 13, no. 1-2, pp. 1–55, 1996.

[9] F. Silveira, S. P. Cibulski, A. P. Varela et al., "Quillaja brasiliensis saponins are less toxic than Quil A and have similar properties when used as an adjuvant for a viral antigen preparation," *Vaccine*, vol. 29, no. 49, pp. 9177–9182, 2011.

[10] A. Fernández-Tejada, D. S. Tan, and D. Y. Gin, "Development of improved vaccine adjuvants based on the saponin natural product QS-21 through chemical synthesis," *Accounts of Chemical Research*, vol. 49, no. 9, pp. 1741–1756, 2016.

[11] C. R. Kensil, U. Patel, M. Lennick, and D. Marciani, "Separation and characterization of saponins with adjuvant activity from Quillaja saponaria Molina cortex," *Journal of Immunology*, vol. 146, no. 2, pp. 431–437, 1991.

[12] D. J. Marciani, "Vaccine adjuvants: role and mechanisms of action in vaccine immunogenicity," *Drug Discovery Today*, vol. 8, no. 20, pp. 934–943, 2003.

[13] S. Soltysik, J. Y. Wu, J. Recchia et al., "Structure/function studies of QS-21 adjuvant: assessment of triterpene aldehyde

and glucuronic acid roles in adjuvant function," *Vaccine*, vol. 13, no. 15, pp. 1403–1410, 1995.

[14] Y. Yang, M. E. Leser, A. A. Sher, and D. J. McClements, "Formation and stability of emulsions using a natural small molecule surfactant: Quillaja saponin (Q-Naturale®)," *Food Hydrocolloids*, vol. 30, no. 2, pp. 589–596, 2013.

[15] J. Zhang, L. Bing, and G. A. Reineccius, "Formation, optical property and stability of orange oil nanoemulsions stabilized by Quallija saponins," *LWT - Food Science and Technology*, vol. 64, no. 2, pp. 1063–1070, 2015.

[16] A. Galliher-Beckley, L. K. Pappan, R. Madera et al., "Characterization of a novel oil-in-water emulsion adjuvant for swine influenza virus and mycoplasma hyopneumoniae vaccines," *Vaccine*, vol. 33, no. 25, pp. 2903–2908, 2015.

[17] R. Madera, W. Gong, L. Wang et al., "Pigs immunized with a novel E2 subunit vaccine are protected from subgenotype heterologous classical swine fever virus challenge," *BMC Veterinary Research*, vol. 12, no. 1, p. 197, 2016.

[18] V. Moennig, "Introduction to classical swine fever: virus, disease and control policy," *Veterinary Microbiology*, vol. 73, no. 2-3, pp. 93–102, 2000.

[19] G.-J. Lin, M. C. Deng, Z. W. Chen et al., "Yeast expressed classical swine fever E2 subunit vaccine candidate provides complete protection against lethal challenge infection and prevents horizontal virus transmission," *Vaccine*, vol. 30, no. 13, pp. 2336–2341, 2012.

[20] R. F. Madera, L. Wang, W. Gong et al., "Toward the development of a one-dose classical swine fever subunit vaccine: antigen titration, immunity onset, and duration of immunity," *Journal of Veterinary Science*, vol. 19, no. 3, pp. 393–405, 2018.

[21] T. J. D. Knight-Jones, K. Edmond, S. Gubbins, and D. J. Paton, "Veterinary and human vaccine evaluation methods," *Proceedings of the Royal Society B: Biological Sciences*, vol. 281, no. 1784, p. 20132839, 2014.

[22] T. Jansen, M. P. M. Hofmans, M. J. G. Theelen, F. Manders, and V. E. J. C. Schijns, "Structure- and oil type-based efficacy of emulsion adjuvants," *Vaccine*, vol. 24, no. 26, pp. 5400–5405, 2006.

[23] V. Kanchan and A. K. Panda, "Interactions of antigen-loaded polylactide particles with macrophages and their correlation with the immune response," *Biomaterials*, vol. 28, no. 35, pp. 5344–5357, 2007.

[24] D. J. Marciani, A. K. Pathak, R. C. Reynolds, L. Seitz, and R. D. May, "Altered immunomodulating and toxicological properties of degraded Quillaja saponaria Molina saponins," *International Immunopharmacology*, vol. 1, no. 4, pp. 813–818, 2001.

Hindawi
Journal of Immunology Research
Volume 2018, Article ID 3143189, 14 pages
https://doi.org/10.1155/2018/3143189

Research Article

Efficacy of a Recombinant Turkey Herpesvirus AI (H5) Vaccine in Preventing Transmission of Heterologous Highly Pathogenic H5N8 Clade 2.3.4.4b Challenge Virus in Commercial Broilers and Layer Pullets

Vilmos Palya,[1] **Tímea Tatár-Kis**,[1] **Edit Walkóné Kovács**,[1] **István Kiss**,[1] **Zalán Homonnay**,[1] **Yannick Gardin**,[2] **Krisztián Kertész**,[3] **and Ádám Dán**[4]

[1]*Scientific Support and Investigation Unit, Ceva-Phylaxia, Ceva Animal Health, Budapest 1107, Hungary*
[2]*Ceva Animal Health, Libourne 33500, France*
[3]*Ceva-Phylaxia, Ceva Animal Health, Budapest 1107, Hungary*
[4]*Veterinary Diagnostic Directorate, National Food Chain Safety Office (NEBIH), Budapest 1149, Hungary*

Correspondence should be addressed to Vilmos Palya; vilmos.palya@ceva.com

Received 15 June 2018; Revised 24 August 2018; Accepted 4 September 2018; Published 21 November 2018

Guest Editor: Giuseppe A. Sautto

Outbreaks caused by the highly pathogenic avian influenza virus (HPAIV) H5N8 subtype clade 2.3.4.4 were first reported in 2014 in South Korea then spread very rapidly in Asia, to Europe, and for the first time, to North America. Efficacy of a recombinant HVT-AI (H5) vaccine (rHVT-H5) to provide clinical protection as well as to significantly reduce the shedding of an H5N8 challenge virus has already been demonstrated in SPF chickens. The aim of our studies was to test the efficacy of the same rHVT-H5 vaccine in controlling the transmission of a recent Hungarian HPAIV H5N8 challenge virus in commercial chickens. Broilers and layers were vaccinated at day old according to the manufacturer's recommendation and then challenged with a 2017 Hungarian HPAIV H5N8 (2.3.4.4b) isolate at 5 or 7 weeks of age, respectively. Evaluation of clinical protection, reduction of challenge virus shedding, and transmission to vaccinated contact birds was done on the basis of clinical signs/mortality, detection, and quantitation of challenge virus in oronasal and cloacal swabs (regularly between 1 and 14 days postchallenge). Measurement of seroconversion to AIV nucleoprotein was used as an indicator of infection and replication of challenge virus. Our results demonstrated that rHVT-H5 vaccination could prevent the development of clinical disease and suppress shedding very efficiently, resulting in the lack of challenge virus transmission to vaccinated contact chickens, regardless the type of birds. Single immunization with the tested rHVT-H5 vaccine proved to be effective to stop HPAIV H5N8 (2.3.4.4b) transmission within vaccinated poultry population under experimental conditions.

1. Introduction

In recent years, several reassortant H5Nx subtype of highly pathogenic avian influenza (HPAI) viruses have emerged in East Asia. These new viruses, mostly of subtype H5N1, H5N2, H5N6, and H5N8, belonging to clade 2.3.4.4, have spread very rapidly in East Asia causing outbreaks in poultry in China, South Korea, and Vietnam. Virus strains related to the Eurasian H5N8 lineage of clade 2.3.4.4 have also spread over considerable distances reaching Europe (2014-2015 and 2016-2017) and for the first time, the North American continent (2014-2015). This lineage of clade 2.3.4.4 which is circulating in wild bird populations regularly infects backyard poultry as point source of introductions to industrial poultry and has caused repeated epidemics in several parts of the world [1, 2].

In several countries, the outbreaks of HPAI have been controlled by rapid depopulation of infected poultry premises, preemptive culling of neighbouring farms, movement restrictions, and sanitary measures [3]; however, the

application of this control method could have a devastating effect on the economy. The need for effective vaccines against HPAI has been arose by affected countries not only for the survival of the poultry industry but also because of the risk of future recurrence and persistence of the disease and its transmission potential to humans.

A number of H5 avian influenza vaccines, including the inactivated whole virus vaccines and live recombinant vaccines using fowlpox virus or turkey herpesvirus (HVT) or Newcastle disease virus (NDV) as vectors to express the HA antigen of a selected H5 subtype avian influenza virus (AIV) strain [4], are currently available for use in poultry. Traditional avian influenza (AI) vaccines are killed vaccines, produced either by conventional methods or by reverse genetics [5] which provide good protection against the clinical disease caused by HPAIVs and significant reduction in viral shedding, if the vaccine seed strain is antigenically matched to the challenge strain [6]. However, killed vaccines have several limitations including (i) the requirement for frequent update of vaccine seed strains to match with the circulating field strains, (ii) the interference of maternally derived antibodies (MDA) with vaccination, (iii) the lack of possibility to differentiate vaccinated birds from infected ones (DIVA) by serology unless the vaccine strain contains heterologous NA to all potentially circulating field viruses in the given geographical area/country, and (iv) the lack of stimulating strong cellular immunity (killed vaccines mostly stimulate a humoral immune response). Because of these shortcomings of killed vaccines, next generation technology has been used to develop a wide variety of AI vaccines to overcome some of these limitations [7].

HVT proved to be an excellent candidate for vector since it (i) confers long-term immunity due to its persistence in the host, (ii) has excellent safety characteristics, (iii) provides good protection when administered at hatch or in ovo, (iv) overcomes MDA, (v) can be used in validated combinations with certain other Marek's disease vaccines of other serotypes (e.g., [8, 9]), and (vi) may provide possibility to apply the DIVA strategy [10]. Attempts to use HVT as vector vaccine started in the early 1990s [11, 12]; however, it was not until more recently that HVT has been widely used as a vector for the development of recombinant vaccines against a number of poultry viral diseases, including the ones expressing AIV proteins for the protection against HPAI [13–16]. One of these candidate rHVT-AI vaccines has already reached marketing authorization in a number of countries and demonstrated promising results in poultry in several studies [17] including efficacy against H5Nx clade 2.3.4.4. isolates [18–20].

To asses the potential impact of control measures such as vaccination, it is crucial, however, to understand the transmission dynamics of AI virus both in susceptible and vaccinated populations. The potential of a vaccine to control the spread of infection at population level should be an important part of investigation when studying the effectiveness of a vaccine in the control of infectious diseases. Therefore, the goal of this study was not only to evaluate the efficacy of a commercial, live recombinant HVT-based AI vaccine against a recent H5N8 clade 2.3.4.4b virus in commercial broiler and layer chickens but to examine and quantify the effect of vaccination on virus transmission as well.

2. Materials and Methods

2.1. Vaccine. The commercial HVT vector-based live recombinant AI vaccine (Vectormune® AI, Ceva Biomune, Lenexa, KS) expressing the H5 gene (rHVT-H5) of a clade 2.2 H5N1 HPAIV was used in this study. Donor of the vaccine HA was the A/mute swan/Hungary/4999/2006 strain for which the cleavage site has been modified for a low pathogenic motif. The vaccine (lot number: 395-054) was diluted in the corresponding diluent (Ceva-Biomune, Lenexa, KS) to contain one dose in 200 μl.

2.2. Challenge Virus. The A/goose/Hungary/1030/2017 H5N8 HPAIV (HA clade 2.3.4.4b), isolated during the recent 2016-2017 epidemic of HPAI in Hungary, obtained from the virus repository of National Food Chain Safety Office Veterinary Diagnostic Directorate (NFCSO-VDD), Budapest, Hungary, was used in this study. The virus was propagated and titrated in specific-pathogen-free (SPF) embryonated chicken eggs according to standard procedures [21]. Titer was calculated using Spearman-Kärber method [22].

2.3. Antigenic Relatedness of Challenge Virus with the Vaccine

2.3.1. Comparison of Haemagglutinin Amino Acid Sequence of Vaccine Insert and Challenge Strain. The deduced amino acid sequences of challenge virus HA gene (accession number is EPI954663 in GISAID EpiFlu database) and the rHVT-H5 vaccine insert (accession number is KP969039 in GenBank) were aligned and pairwise comparison was prepared in CLC Main Workbench 7.9.1. Predicted H5 epitopes were annotated based on the identified epitopes by using polyclonal rabbit antisera for epitope scanning of baculovirus-expressed H5 HA protein [23]. Further antigenicity-associated sites [24, 25], predicted MHC antigenic sites [25, 26], and the previously identified MHCI/II peptide [27] were also compared between the vaccine and the challenge virus.

2.3.2. One-Way Cross-Haemagglutination Inhibition Test. The antigenic relatedness between the vaccine and challenge virus was determined by measuring the haemagglutination inhibition (HI) titer of antisera raised against the vaccine virus using HA antigens homologous with the vaccine or with the challenge virus (see in Serology paragraph). The antisera were collected six weeks after vaccination of day-old SPF chicks with the rHVT-H5 vaccine.

2.4. Experimental Design. The broiler (breed: Ross 308) and layer (breed: Tetra-SL) chicks used in the two transmission experiments which are described in this paper were obtained from commercial sources in Hungary (from hatcheries of Herbro Kft, Hernád and Tetra Kft, and Bábolna, respectively). Serum samples were collected at hatch from 10 individuals of each type of chicks to ascertain that the birds were serologically negative for antibodies to the nucleoprotein of influenza A viruses. During the postvaccination/

Table 1: Summary of the two transmission experiments set up.

Type of chickens	Group	Vaccination	Subgroup	Challenge	Abbreviation
Broiler chickens	Group 1	rHVT-H5 vaccine at hatch, s.c.	Vaccinated challenged	Direct challenge at 5 weeks of age	G1- VCh
			Vaccinated contact	Physical contact from 8 h postchallenge	G1- VC
	Group 2	No	Susceptible challenged	Direct challenge at 5 weeks of age	G2- SCh
			Susceptible contact	Physical contact from 8 h postchallenge	G2- SC
Layer chickens	Group 3	rHVT-H5 vaccine at hatch, s.c.	Vaccinated challenged	Direct challenge at 7 weeks of age	G3- VCh
			Vaccinated contact	Physical contact from 8 h postchallenge	G3-VC
	Group 4	No	Susceptible challenged	Direct challenge at 7 weeks of age	G4-SCh
			Susceptible contact	Physical contact from 8 h postchallenge	G4- SC

prechallenge period, chickens were housed in BSL-2 animal facilities and then transferred to BSL3 animal rooms for challenge (3 chickens/m^2). In both cases, chickens were kept on deep litter and water was provided through nipple drinkers or drinking towers which were controlled and changed daily. Appropriate food was provided *ad libitum*. All animals were housed separately according to group (i.e., one group in each room) in isolated animal rooms at Prophyl Kft. (Bar, Hungary).

The study has been conducted in compliance with the provisions of Directive 2010/63/EU, Hungarian Act No. XXVIII/1998, and the Hungarian Governmental Decree No. 40/2013 (II.14.) and with the permission of the Hungarian competent animal welfare and ethics authority (approval number: BAI/35/56-92/2017). No humane endpoint was used, since the study aimed at measuring the transmission rate of HPAIV and its outcome would be biased by the earlier removal of strong shedder diseased chickens. Generally, the birds died after short clinical phase (no clinical signs were observed on the day preceeding mortality in 22% of chickens; clinical signs were observed for less than 24 hours in 45%, for less than 48 hours in 26%, and for less than 72 hours in 7% of chickens). At the end of postchallenge observation period, all survived chickens were euthanized by injection of sodium pentobarbital (5 g/ml).

2.4.1. Transmission Experiment 1: Broilers. Two groups (groups 1 and 2) of broiler chicks were used (see Table 1). Each group consisted of 40, one-day-old chicks. 40 chicks of group 1 were vaccinated (designated G1-V for vaccinated) while the chicks of group 2 remained unvaccinated (designated G2-S for susceptible). All chicks of group 1 were vaccinated with a commercial dose of the rHVT-H5 vaccine subcutaneously (s.c.) on the nape of the neck, using a needle of $19G \times 1''$ at one day of age. The two groups were housed separately and were checked daily.

On day 31 postvaccination (p.v.), blood samples were taken from each animal for serology. Sera were separated from the blood clots by centrifugation, then inactivated at 56°C for 30 min, and stored at −20°C. On day 36 p.v., 20 animals from both the vaccinated (designated G1-VCh for vaccinated direct challenged) and from the nonvaccinated group (designated G2-SCh for susceptible direct challenged) were tranferred to separate BSL3 animal rooms and were challenged by inoculating them intranasally with 10^6 ELD_{50}/0.2 ml of the H5N8 virus. Eight hours postchallenge (pch.), the remaining 20 animals from each of the relevant groups were added as contact birds (designated G1-VC for vaccinated contact or G2-SC for susceptible contact).

The animals were observed for 14 days after challenge during which they were checked twice daily for clinical signs and mortality. Oronasal (ON) swabs taken from the choanal slit and cloacal (CL) swabs using Copan FLOQSwabs™ (ref 552C, Copan Diagnostics Inc., CA, USA) were collected daily between day 1 and 7 and then at day 10 pch. From the animals found dead, oronasal and cloacal swabs were also collected. In case the diagnosis of HPAI was not unambiguous based on the clinical signs and the gross lesions, organ samples (brain, heart, kidney, and spleen) were collected for qRRT-PCR. Those chickens, in which the cause of mortality was not attributable to challenge based on these laboratory tests, were omitted from the evaluation of clinical protection. At the end of the experiment (at 14 days pch., 50 days of age), oronasal and cloaca swabs as well as 5 ml of blood were collected from all surviving animals, and then the chickens were euthanized.

2.4.2. Transmission Experiment 2: Layers. In this experiment, two groups (groups 3 and 4), each consisting of 40, one-day-old layer chicks, were used (see Table 1). Chicks of group 3 were vaccinated (designated G3-V), while the chicks of group 4 remained unvaccinated (designated G4-S for susceptible). For vaccination, the same procedure as described for transmission experiment 1 was followed. The animals were housed in two rooms and were treated as described for transmission experiment 1. The chickens were blood sampled on day 21, 28, 35, and 45 p.v. On day 50 p.v., 20 animals from both the vaccinated (designated G3-VCh for vaccinated direct challenged) and from the nonvaccinated group (designated G4-SCh for susceptible direct challenged) were tranferred to separate BSL3 animal rooms and then challenged as described in transmission experiment 1. Sampling and

euthanasia protocols remained the same as described in transmission experiment 1. The experiment was terminated at 14 days pch. (i.e., 9 weeks of age).

2.5. Detection of rHVT-H5 Vaccine from Feather Pulp. To assess the take of rHVT-H5 vaccine (replication of vaccine virus in the bird), feather pulp samples were collected from five chickens of each vaccinated group at 3 weeks of age and from 5 vaccinated broilers and 10 vaccinated layers at 4 weeks of age. Five nonvaccinated animals were sampled the same way. Feather tips with substantial amount of pulp were homogenized in 1 ml phosphate-buffered saline by using Tissue Lyser II (Qiagen, Hilden, Germany). After centrifugation at 1500 × g at 4°C for 10 min, the supernatant of samples was processed as described previously [28].

2.6. Serology. Hemagglutination inhibition (HI) test performed according to standard procedure (OIE) was used to determine antibody responses elicited by vaccination and to check serological relatedness between the vaccine virus and the challenge virus. Two antigens have been used. One of them was closely related to the insert of the vaccine and considered as homologous antigen with the vaccine (reverse genetics antigen containing HA from clade 2.2.1 virus; Rg-A/duck/Egypt/M2583/10 (dH5N1)-A/PR/8/34/(R) (6 + 2), [29]) and the other one was prepared from the H5N8 challenge virus propagated in SPF hen eggs according to standard procedures [21] and then inactivated (Veterinary Diagnostic Directorate, National Food Chain Safety Office, Budapest, Hungary). Antiserum to the rHVT-H5 vaccine prepared in SPF chickens and serum samples collected in both transmission experiments before the challenge were checked against 4 HAU both of the antigen homologous to the vaccine and the antigen homologous to the challenge strain in order to evaluate cross-reactivity of vaccine-induced antibodies with the challenge virus. HI titers are reported as $\log_2$ values, with 3 $\log_2$ being the minimum titer considered as positive. Serum samples with HI titer below 1 : 2 were included with 0 $\log_2$ HI titer in the calculation of mean titer. Log_2 titers obtained with the two different antigens from the same serum samples were compared with paired *t*-test at 95% confidence level.

The ID Screen® Influenza A Nucleoprotein Indirect ELISA kit (for the specific detection of nucleoprotein antibodies; code: FLUNPS, IDVet, France) was used according to the manufacturer's instructions. Only the serum samples collected at day old to check the absence of MDA to AIV and serum samples collected at the termination of the experiments (14 days pch.) to check if the challenge caused infection and induction of antibodies to the nucleoprotein (NP) of AIV (DIVA) were tested by ELISA.

2.7. Challenge Virus RNA Quantification from Oronasal and Cloacal Swabs. To measure the number of challenge virus RNA copies present in the dry swabs collected during the transmission experiments, quantitative real-time reverse transcriptase PCR (qRRT-PCR) was used. After elution in 2 ml of PBS, 200 μl of swab supernatant was submitted to RNA extraction (MagNA Pure LC DNA and viral NA small volume nucleic acid isolation kit on the MagNA Pure LC robotic instrument (Roche Diagnostics, Indianapolis, IN)) according to the manufacturer's instructions. The extracted RNA was eluted in 100 μl elution buffer.

Real-time RT-PCR reactions were performed according to the EU diagnostic manual (2006) with protocol developed and validated at the European Reference Laboratory for AIV/NDV (Animal Health and Veterinary Laboratories Agency, Weybridge, UK) using the general influenza A primers and probe for matrix protein gene (M-gene) and one-step RT-PCR kit (Qiagen, Germany) as originally described by Spackman et al. [30].

All oronasal or cloaca swab samples which gave specific signal were considered positive regardless the Ct value. Standard curve was established with viral RNA extracted from serial dilution of the titrated challenge virus suspension, and AIV load in ELD_{50}/ml was calculated by extrapolation of Ct values of swab samples to this standard curve. The lowest limit of detection based on the swab samples from chickens was $10^{2.1}\text{ELD}_{50}$/ml. All negative samples were included in the calculation of mean with a value of $10^{1.5}\text{ELD}_{50}$/ml.

2.8. Statistical Analysis of Challenge Virus Transmission (Calculation of R). For the evaluation of challenge virus transmission, a bird was considered infectious at a certain sampling date if at least one of its swab samples (oronasal or cloaca) was positive. Virus transmission rate was estimated by the susceptible-infectious-recovered (SIR) stochastic model, using generalized linear models (GLM). The formulation of the transmission model is as follows. We accepted that the number of new cases (C (t)) is binomially distributed:

$$C(t) \sim \text{Binomial}[S(t), p(\Delta(\text{t}))], \tag{1}$$

where

$$p(\Delta(t)) = 1 - \exp\left(-\beta \frac{I(\text{t})}{N(\text{t})} \Delta(\text{t})\right). \tag{2}$$

$S(t)$ is the number of susceptible birds at beginning of day t, $I(t)$ is the number of infectious chickens at beginning of day t, $N(t)$ is the number of live chickens at the beginning of day t (animals that died were removed from the day of death), $\Delta(t)$ is the number of days elapsed between day t and day $t-1$, and β is the transmission rate parameter to be estimated.

The above model can be formulated as a GLM with a complementary log-log link, taking $\log((I(t)/N(t))\Delta(t))$ as offset variable. The intercept of GLM estimate is

$$\log(\beta). \tag{3}$$

The mean infectious period (T) was directly calculated from the data. For this, we used the data of the contact animals only as we tried to model the transmission in field conditions.

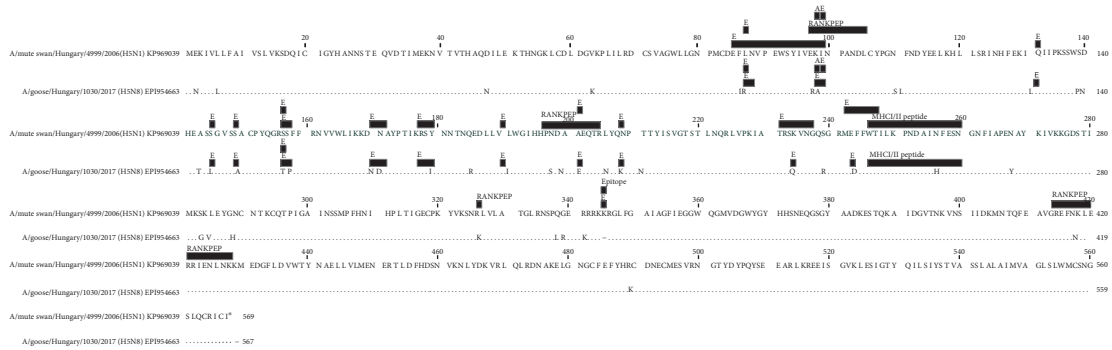

Figure 1: Alignment of A/mute swan/Hungary/4999/2006 (H5N1) and A/goose/Hungary/1030/2017 (H5N8) HA amino acid sequences. Identical residues are marked by dots. The sites of antigenic relevance (abbreviation: "A"), the predicted epitopes (abbreviation: "E"), the predicted MHC epitopes by RANKPEP, and the MHCI/II epitope identified for AIV H5 are marked by shaded boxes according to published reports [23–25, 27].

The reproduction ratio is given by the product of the transmission rate and the mean infectious period:

$$R = \beta T. \tag{4}$$

For the calculation of the confidence interval of R, we assumed independence between $\log(\beta)$ and $\log(T)$. Thus, by using the delta method to estimate $\mathrm{Var}(\log(T))$

$$\begin{aligned}\mathrm{Var}(\log(R)) &= \mathrm{Var}(\log(\beta)) + \mathrm{Var}(\log(T)) \\ &= \mathrm{Var}(\log(\beta)) + \frac{\mathrm{Var}(T)}{T^2}\end{aligned} \tag{5}$$

and the 95% confidence interval for R is

$$\exp\left[\log(\mathrm{R}) \pm 2 \cdot \sqrt{\mathrm{Var}(\log(\mathrm{R}))}\right]. \tag{6}$$

Statistical computations were performed using Stata software.

3. Results

3.1. Antigenic Relatedness between the Challenge Virus and the Vaccine

3.1.1. Sequence Comparison of rHVT-H5 Vaccine Insert and Challenge Virus HA Gene. Amino acid identity was 92%, which meant 45 amino acid differences between the sequences, including a single amino acid deletion from the sequence adjacent to the cleavage site, i.e., 337PQGERRRKKR/G347 and 337PLREKRRKR/G347 for the rHVT-H5 vaccine insert and for the challenge virus strain, respectively.

Several of the predicted epitopes or antigenic sites were affected by substitutions in the challenge virus compared to the rHVT-H5 vaccine insert sequence (see Figure 1). Haghighi et al. identified an MHCI/II peptide in the HA of A/turkey/Ireland/1378/83 (H5N8) which was able to stimulate both CD4+ and CD8+ lymphocytes [27]. This peptide motif ($H5_{246-260}$) can be found in the HA of both the vaccine and the challenge virus and shows a single amino acid difference between them at residue 256 being asparagine (N) in the vaccine and histidine (H) in the challenge virus.

3.1.2. Cross-Haemagglutination Inhibition Test. Testing of antisera prepared against the rHVT-H5 vaccine in SPF chickens resulted in 5.4 ± 0.6 $\log_2$ HI titer (mean and SD) with the antigen homologous to the vaccine, while only 0.3 ± 1.0 $\log_2$ HI titer (mean and SD) was measured with the challenge virus antigen indicating strong antigenic distance between the vaccine and the challenge virus.

3.2. Testing Day-Old Serum Samples from Commercial Broilers and Layers for MDA to AIV. ELISA detecting antibodies against nucleoprotein of influenza A virus was used to prove the negativity of the test chickens for AIV antibodies. Blood samples collected from both the broiler and layer chicks at one day of age were negative for AIV antibodies.

3.3. Vaccine Take and Antibody Response to Vaccination in Broilers and Layers without MDA to AIV. Vaccine virus was detected from the feather tips of all vaccinated chickens at 3 weeks of age, while 80% positivity was found at 4 weeks of age (4/5 positives in broilers and 8/10 positives in layers). Humoral immune response to rHVT-H5 vaccination was tested by HI test against HA antigens homologous either with the vaccine virus insert or with the challenge virus. All chickens, both in the broiler and layer experiments, were positive by HI test from four weeks of age onwards using the vaccine homologous HA antigen. On the contrary, the group mean HI titers measured against the challenge virus remained below the positivity threshold (see Figure 2) and were significantly lower compared to the titers measured with HA antigen homologous with the vaccine ($p \leq 0.001$). The nonvaccinated animals remained seronegative during the whole observation period before the challenge (all serum samples with HI titer below 1 : 2).

3.4. Transmission Experiment 1: Broilers

3.4.1. Clinical Signs and Mortality. The H5N8 challenge virus, consistent with the highly pathogenic nature of this virus strain, was lethal for the nonvaccinated broiler

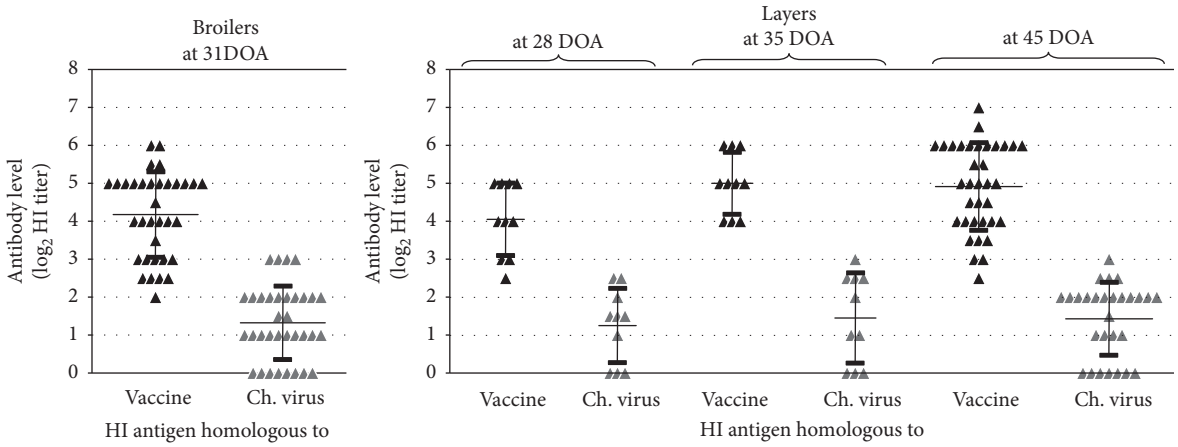

Figure 2: Humoral immune response to vaccination in commercial broilers and commercial layers without MDA to AIV H5N1. Hemagglutination inhibition test was performed parallel with the antigen homologous to the vaccine and with the antigen prepared from the challenge virus. Age of birds at sampling is shown above the graph (DOA = days of age). Mean titer and standard deviation is shown as a horizontal bar with whiskers. Positivity limit is at least 3 $\log_2$ HI titer.

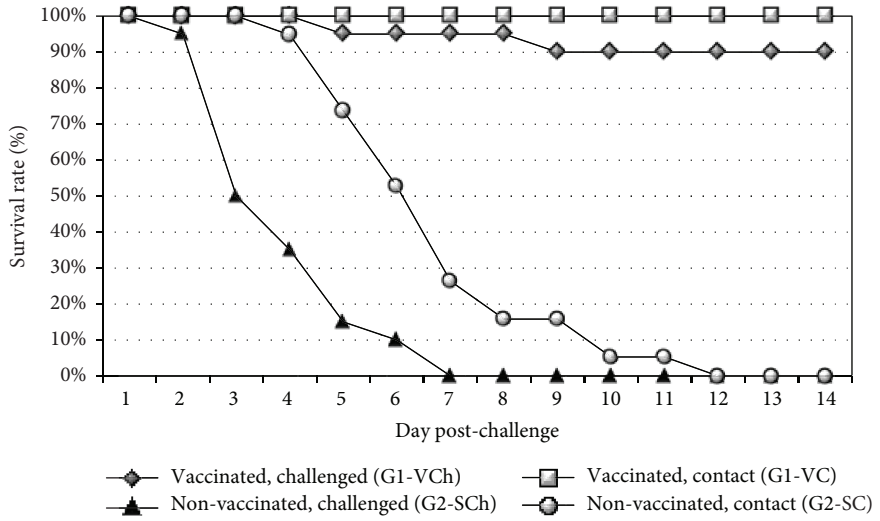

Figure 3: Time course of mortality in challenged broilers. Contact challenged groups were comingled with direct-challenged groups from 8 hours postchallenge. Recording date refers to the time after direct challenge.

chickens. After challenge infection, all animals both in the inoculated and contact groups (G2-SCh and G2-SC) developed clinical signs indicative of HPAI which was followed by 100% mortality in the direct challenged and in the contact group too (see Figure 3). The most prominent clinical signs in the nonvaccinated challenged broiler chickens were lethargy, anorexia, prostration, and neurologic signs.

By contrast, 90 percent of vaccinated chickens were protected against the HPAIV challenge and none of the vaccinated contact chickens died or showed clinical signs indicative of HPAIV infection during the postchallenge observation period (see Figure 3). Unfortunatelly, two vaccinated contacts died due to accidental physical injury (organ and swab samples collected from them proved to be negative with qRRT-PCR).

3.4.2. Virus Shedding and Transmission. In the nonvaccinated group, all of the direct challenged and contact animals shed high amount of challenge virus by the oronasal route (see Figure 4). After challenge, fast increasing virus load was measured in the direct inoculated birds, and similar, but slightly slower increase of virus shedding could be observed in the contact chickens 3-4 days later.

Fast increasing, high virus load was measured in the cloacal swabs of the nonvaccinated direct-challenge birds that was followed a few days later in the contact chickens reaching similar virus loads to the direct-challenged animals.

The majority of direct-challenged vaccinated chickens were negative by qRRT-PCR in ON swabs. Virus shedding could be detected at low level in ten percent of chickens mainly during the first 5 days pch. Only one inoculated

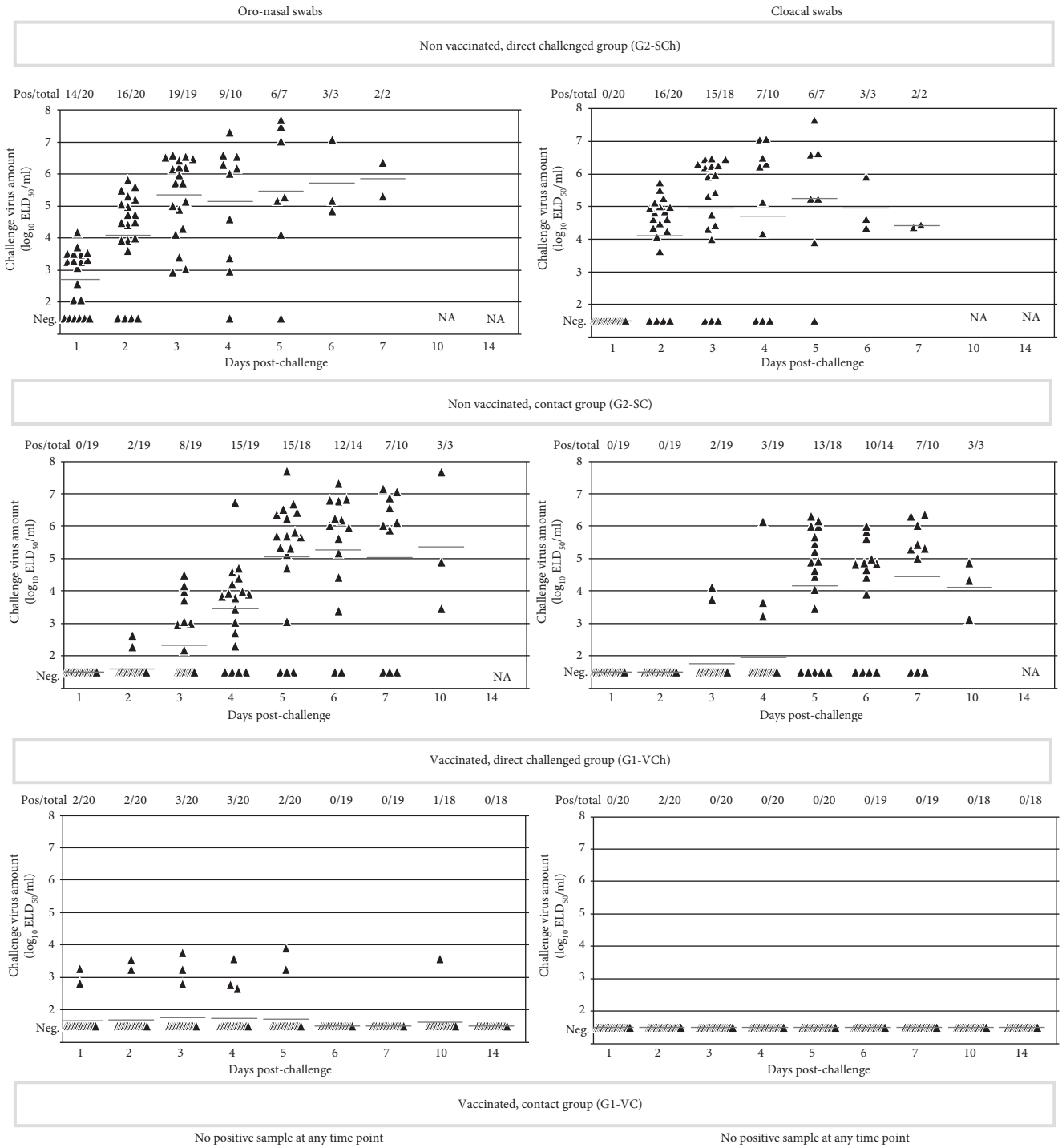

FIGURE 4: Oronasal and cloacal shedding by broilers. AIV load of swab samples measured by qRRT-PCR is presented as $\log_{10}ELD_{50}$/ml in the scatterplot; horizontal bars represent group mean value for each date. For calculation of mean, negative samples were given a value of 1.5 $\log_{10}$ ELD_{50}/ml. Contact challenged groups (G1-VC and G2-SC) were comingled with the direct-challenged control group (G1-VCh and G2-SCh) from 8 hours postchallenge. Sampling date refers to the time after direct challenge.

animal was found to be qRRT-PCR positive for the challenge virus in its ON swab with low virus load on day 10 pch. (see Figure 4). No virus shedding could be detected during the observation period in the vaccinated contact chickens (G1-VC).

A graphic representation of the progress of infection in the directly challenged and contact animals for the vaccinated groups for each day pch. is shown in Figure 4.

The challenge virus could not be detected in the cloacal swabs of vaccinated chickens, except one chicken with

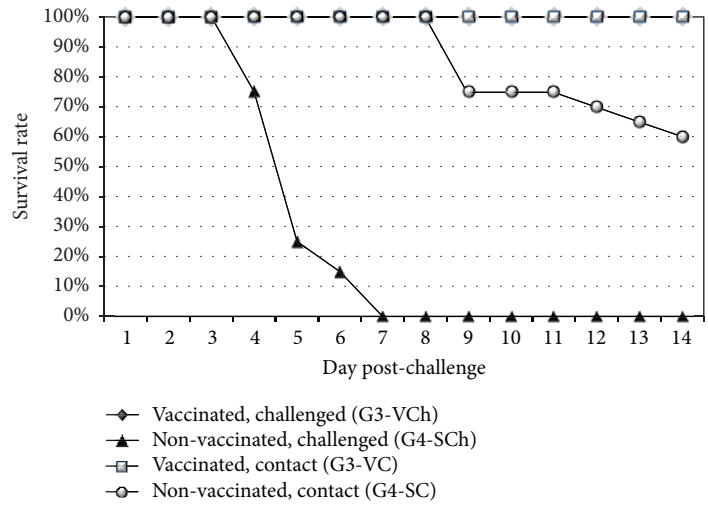

Figure 5: Time course of mortality in challenged layers. Contact challenged groups were comingled with direct-challenged groups from 8 hours postchallenge. Sampling date refers to the time after direct challenge.

moderate level of shedding at day 6 pch. All vaccinated contact chickens had negative cloaca swab samples during the observation period.

3.5. Transmission Experiment 2: Layers

3.5.1. Clinical Signs and Mortality. All of the unvaccinated direct-challenged birds (designated G4-SCh) died by 7 days pch. Spreading of challenge virus was slower in layer chickens than in broilers; morbidity of the nonvaccinated contacts (designated G4-SC) began five days later than in the direct-challenged chickens. Delayed infection of contact chickens resulted in lower morbidity and mortality (40%) compared to direct-challenged layers by the end of the postchallenge observation period (see Figure 5).

No mortality or clinical signs indicative of HPAIV infection occurred either in the vaccinated direct-challenged group (G3-VCh) or in the vaccinated contact chickens (G3-VC) during the postchallenge observation period (see Figure 5).

3.5.2. Virus Shedding and Transmission. Oronasal virus shedding by the unvaccinated direct-challenged birds was already high from the first day pch. and continued to be high until the day they died. Shedding of virus by the contact birds started on the 4th day pch. in 5% of the birds, which increased to 35% by the next day, but 60% of the birds survived till the end of the observation period without shedding virus in their oronasal swabs (see Figure 6). AIV load in the samples collected from affected contacts was similarly high as in the ones collected from the direct-challenged animals (see Figure 6).

Cloacal shedding by the nonvaccinated direct-challenged chickens started already on the 1st day pch. in 15% of the birds, increased rapidly, and continued until the day when the last bird died. Virus load in cloacal swabs was lower compared to oronasal swabs (see Figure 6). Delayed spreading of challenge virus to contact birds was observed, and the ratio of birds with detectable shedding at any date during the 14 days pch. observation period reached only 40% (see Figure 6).

Oronasal virus shedding by the vaccinated and direct-challenged chickens could be detected only in a small proportion (15%) of the birds and only at the first 5 days pch., while no virus could be detected in the ON swab samples of vaccinated contact chickens (see Figure 6).

Cloacal shedding of challenge virus by the direct-challenged vaccinated chickens was almost totally absent during the whole postchallenge observation period; only one chicken had moderate level of virus load in its cloacal swab at day 6 pch. Vaccinated contact chickens did not shed any detectable virus through the cloaca.

3.6. Reproduction Ratio (R). Length of infectious period, transmission rate, and reproduction ratio values in the unvaccinated groups are summarized in Table 2. The estimate of the reproduction ratio in the unvaccinated broiler chickens is 1.84 (95% confidence interval: 1.11, 3.06), which is significantly above 1. It means that the virus can spread easily in an unvaccinated population of broiler chickens. The estimate of R is 0.69 (0.33, 1.44) for the unvaccinated layers. As the confidence interval for the reproduction ratio covers 1, we cannot reject either that $R < 1$ or $R > 1$.

Vaccinated contact chickens showed lack of challenge virus spread; therefore, the R value for the vaccinated groups is 0.00 regardless the type of chicken (i.e., broiler or layer).

3.7. Humoral Immune Response to Challenge. Only a small proportion of the vaccinated direct-challenged birds developed antibody response to the NP of AIV in both the broiler and layer experiment (5 out of 18 in the broiler and 6 out of 20 in the layer experiment, see Figure 7), while the contact birds remained negative for NP antibodies. In the layer experiment, the survived unvaccinated contact chickens had no detectable antibody against the NP of AIV indicating the lack of virus transmission during the observed period.

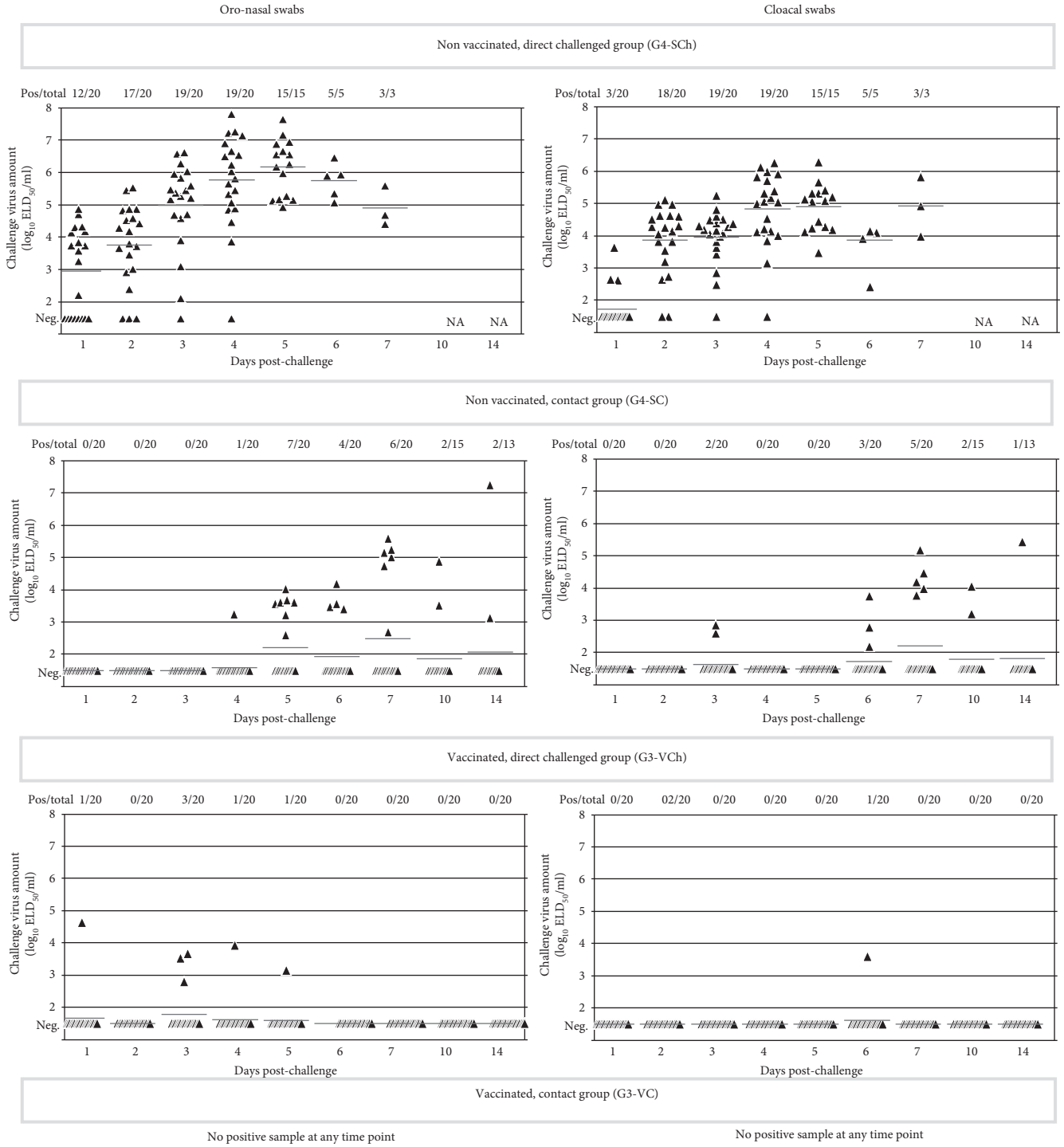

Figure 6: Oronasal and cloacal shedding by layers. AIV load of swab samples measured by qRRT-PCR is presented as $\log_{10}ELD_{50}$/ml in the scatterplot; horizontal bars represent group mean value for each date. For calculation of mean, negative samples were given a value of 1.5 $\log_{10}$ ELD_{50}/ml. Contact challenged groups (G3-VC and G4-SC) were comingled with the direct-challenged groups (G3-VCh and G4-SCh) from 8 hours postchallenge. Sampling date refers to the time after direct challenge.

4. Discussion

In poultry, vaccination against highly pathogenic avian influenza is not common; however, a number of countries (i.e., China, Hong Kong SAR, Vietnam, Indonesia, Bangladesh, South Korea, Pakistan, and Egypt) have used or continue to use vaccination in their fight against H5N1 avian influenza. The main objection against vaccination is that athough it provides clinical protection, it appears to be poorly effective in protecting against infection and controlling virus transmission; therefore, new infections can take place constantly without noticing [31].

Table 2: Overview of the statistical analyses (95% CI in brackets).

Group	Infectious period (day)		Transmission rate (β, 1/day)	Reproduction ratio (R)
	Challenged group	Contact group		
Unvaccinated broilers	3.55 (3.11–3.99)	3.42 (2.68–4.16)	0.54 (0.34–0.85)	1.84 (1.11–3.06)
Unvaccinated layers	4.55 (4.19–4.91)	4.70 (2.73–6.67)	0.15 (0.08–0.27)	0.69 (0.33–1.44)

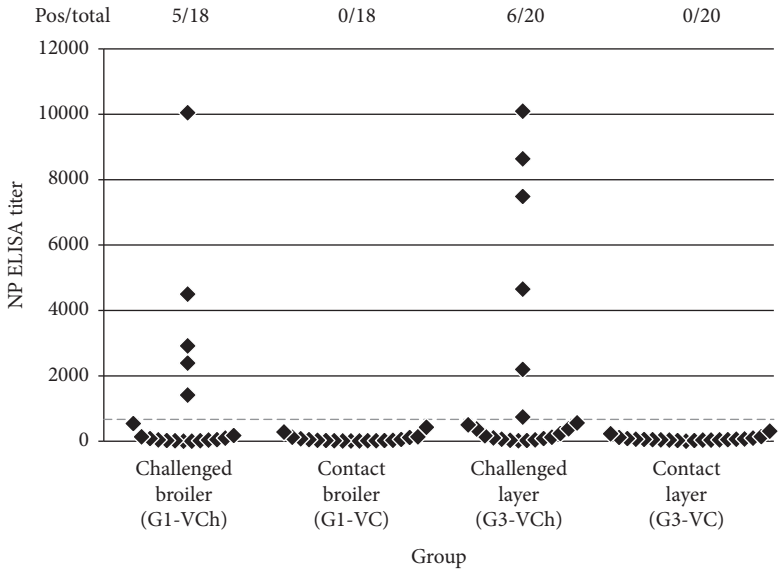

Figure 7: Presence of humoral immune response to challenge in vaccinated chickens was checked with commercial ELISA measuring antibodies against the NP protein. Positive results with ID Screen® Influenza A Nucleoprotein Indirect ELISA kit are above 668 titer (positivity limit is shown with dotted line).

We have used transmission experiments to study the efficacy of a rHVT-H5 vaccine-induced immunity on the transmission dynamics of HPAIV H5N8 strain both in commercial broilers and layers without MDA to AIV. In the unvaccinated groups, all direct-challenged birds became infected and died, which is in agreement with the highly pathogenic nature of the challenge virus. The mortality of the contact animals in the unvaccinated broiler group was also high (100%), indicating high transmission rate among unvaccinated individuals. Interestingly, only 40% of contacts in the unvaccinated layer group died and 45% got infected, indicating a less effective transmission of the virus to and among the contacts. More efficient spread of virus among broilers is reflected by the higher R value (1.84) compared to the one (0.69) in layers. High level of clinical protection (90% in broilers and 100% in layers) and very limited shedding followed by partial seroconversion to challenge was found in the direct-challenged vaccinated chickens, while the vaccinated contacts proved to be fully protected against infection (R value = 0.00). These results showed that information on morbidity and mortality, and quantification of virus shedding by the directly infected birds, as the regular method for the evaluation of vaccine efficacy, does not necessarily translate to transmission. Therefore, appropriate transmission experiments are needed that would allow to measure differences in infectivity of virus strains for different poultry species and breeds and to provide information on whether a vaccine is not only able to protect animals from morbidity and mortality but also to stop transmission with good effectiveness.

Other research groups that have tested the efficacy of this rHVT-H5 vaccine against clade 2.3.4.4 H5Nx viruses from Europe and the United States obtained also excellent cross protection (i.e., 90% or above [18, 20]) with the exception of a study performed with two US isolates from 2014, in which only 60% protection was found [19]. However, in that study [19], the prechallenge HI test of the vaccinated chickens (SPF) using an HA antigen homologous to the vaccine indicated only 70% seroconversion (7/10) with a range of HI titers from 5 to 7 $\log_2$, while the other 3 chickens were completely negative (1 $\log_2$ HI titer) at 4 weeks after vaccination. In the other published studies using the same rHVT-H5 vaccine in SPF chickens or broilers without MDA to AIV, more uniform seroconversion was reported at 4 weeks post-vaccination with no or rare negative HI titers [16, 18, 20]. This may indicate that the birds showing no seroconversion might have missed vaccination; therefore, it is very advisable to monitor vaccination efficiency in the field by checking "vaccine take" with the detection of vaccine virus by qPCR from the feather pulp of randomly selected birds between 2 and 5 weeks of age.

It is the general assumption that the closer the antigenic similarity between vaccine and field strain is, the better the vaccine efficacy is expected to be. Failure of vaccination to prevent infection and transmission of HPAIV strains in the field is usually attributed to the antigenic distances between

the inactivated vaccine and the circulating field strains and called for constant vaccine updating [32–34]. Our results reported here and the ones reviewed previously [17, 35], however, showed that rHVT-H5 vaccine could raise effective level of immunity against an antigenically distant virus.

Our results are in agreement with the findings, reported previously by others, that a sufficient level of host immunity induced by a vaccine can compensate for the antigenic difference between vaccine and field strain [36–40]. Immunity against avian influenza is largely based on the presence of antibodies against the surface proteins (NA and HA), from which the antibodies to HA are being far the most important [41]; therefore, this protein is expressed by most of the recombinant vaccines. Although the humoral immunity against HA protein is strong, its protective value is very strongly influenced by the difference between the inactivated vaccine strain and the challenge strain [6, 35]. In poultry, parenterally applied inactivated vaccines are widely used. In this case, humoral immune response to other cross-reactive proteins (e.g., transmembrane protein M2) is weak, which cannot compensate the effect of antigenic difference in HA [41].

Immunological background of cross protection against heterologous influenza infections has been investigated dominantly in mice and humans; only little information is available in chickens. Studies demonstrated that protection can occur in the absence or with very low level of serum HI antibodies against the challenge virus [18, 42], indicating that T cell-mediated immunity (CMI) plays a pivotal role in cross protection against drifted and heterologous strains [42–45]. Most of the studies on CMI focused on the conserved epitopes on internal proteins (e.g., NP and M), but it was revealed that HA specific T cell response can be detected after influenza vaccination or infection [46–48]. In chickens, a T cell epitope on AIV H5 HA molecule was identified by Haghighi et al. [27], which can be recognized by both CD4+ and CD8+ cells. This region showed only a single amino acid difference between the vaccine and the challenge virus used in our study, contrary to the presence of several amino acid differences in the other epitopes (see Figure 1). Clearance of influenza virus in the lungs of vaccinated mice was associated with significant CD4+ and CD8+ cell infiltration after heterologous challenge [42]. While CD8+ effector T cells kill the infected cells through their cytotoxic activity, CD4+ cells have a more diverse role mediating the maturing of CD8+ T cells, B cells, and the cytotoxic response [49]. Residence of memory CD4+ T cells in the lung afforded high level of protection in mice [50] and proved to be long lived with an enhanced capacity to protect against reinfection, due to their ability to respond rapidly and robustly [49]. On the contrary, Seo et al. found that the presence of memory CD8+ T cells expressing γIFN is the key for cross protection in chickens [51]. B cells and the B cell-derived soluble factors also contribute to the effector CD8+ T cell function [42]. Internal viral proteins contain B cell epitopes that are conserved among influenza viruses, and the mucosal IgA has broader specificity than serum IgM [52] which both may contribute to the control of heterologous influenza infection.

Efficacy studies conducted with the rHVT-H5 vaccine focused on humoral immune response to vaccination, clinical protection, and shedding reduction, but some of them addressed the presence of CMI. Rauw et al. [16] showed CMI by the ChIFNγ production after ex vivo antigenic recall activation of lymphocytes from the spleen in broilers at 3 and 4 weeks of age, while Kapczynski et al. [53] demonstrated the presence of cross-reactive cytotoxic lymphocytes in the spleen of 4-week-old SPF chickens which were vaccinated with the rHVT-H5 vaccine at day old. Based on the reports on the induction of both humoral and cell-mediated immune response against AIV after rHVT-H5 vaccination in chickens and the more extensive studies in mammals on the immunological background of cross-reactivity between antigenically distant influenza viruses, it is likely that CMI accounts for the good immunity even when antibody titers to the challenge virus strain are low.

Although a classical vaccination-challenge type of experiment can provide information on whether a vaccine is able to provide clinical protection and allow quantification of virus shedding, it does not bring the solid information on effectiveness of vaccine to control transmission. To the best of our knowledge, only few experimental studies exist where transmission was evaluated in birds vaccinated with a strain being antigenically distant from the challenge strain [35, 54–56]. Our results suggest that it is important to ascertain whether a vaccine selected to be used in a vaccination campaign is able to stop transmission by estimating the transmission magnitude of circulating field strains in vaccinated animals. Therefore, the results of our study further highlight the needs for carrying out appropriate transmission experiments that would allow the evaluation of any AI vaccine to be used in the control of HPAI for the effectiveness to stop transmission, which is one of the most important aims of vaccination, especially with regard to containing an epidemic.

Our study results offer evidence that rHVT- H5 vaccine could protect animals from infection and transmission, even if remarkable antigenic distance between vaccine and challenge strains exists. Using this type of vaccine in the prevention and control of HPAI could be attractive since the constant vaccine updating, required for inactivated whole virus antigen vaccines, could be reduced or eliminated. Apart from using a proper vaccine, it is equally important to make certain that the expected level of vaccination coverage is reached, and as a result, proper population immunity can be expected, which could be best accomplished when vaccination is done in the hatchery under controlled conditions, for which the use of HVT-based recombinant vaccine is well suited. If vaccination is not done properly, it will fail to elicit adequate level of herd immunity, which will in turn lead to insufficient protection against infection.

Data Availability

The data used to support the findings of this study are available from the corresponding author upon request.

Conflicts of Interest

The studies presented in this article were financed by the company that produces the vaccine tested, and the authors V. Palya, T. Tatár-Kis, E. Walkóné Kovács, I. Kiss, Z. Homonnay, K. Kertész, and Y. Gardin are employed by this company.

Acknowledgments

Authors would like to acknowledge A. Tábi, G. Somfai, M. Lénárd (at Ceva Phylaxia), K. Ursu, and Zs. Rónai (at Veterinary Diagnostic Directorate, National Food Chain Safety Office, Budapest, Hungary) for techincal assistance and E. Terzics (at Prophyl Ltd) for her help in animal work.

References

[1] D. H. Lee, K. Bertran, J. H. Kwon, and D. E. Swayne, "Evolution, global spread, and pathogenicity of highly pathogenic avian influenza H5Nx clade 2.3.4.4," *Journal of Veterinary Science*, vol. 18, no. S1, pp. 269–280, 2017.

[2] D. H. Lee, M. K. Torchetti, K. Winker, H. S. Ip, C. S. Song, and D. E. Swayne, "Intercontinental spread of Asian-origin H5N8 to North America through Beringia by migratory birds," *Journal of Virology*, vol. 89, no. 12, pp. 6521–6524, 2015.

[3] D. J. Alexander, "Summary of avian influenza activity in Europe, Asia, Africa, and Australasia, 2002–2006," *Avian Diseases*, vol. 51, no. s1, pp. 161–166, 2007.

[4] C. Li, Z. Bu, and H. Chen, "Avian influenza vaccines against H5N1 'bird flu'," *Trends in Biotechnology*, vol. 32, no. 3, pp. 147–156, 2014.

[5] D. E. Swayne, "Impact of vaccines and vaccination on global control of avian influenza," *Avian Diseases*, vol. 56, no. 4s1, pp. 818–828, 2012.

[6] D. E. Swayne, D. L. Suarez, E. Spackman et al., "Antibody titer has positive predictive value for vaccine protection against challenge with natural antigenic-drift variants of H5N1 high-pathogenicity avian influenza viruses from Indonesia," *Journal of Virology*, vol. 89, no. 7, pp. 3746–3762, 2015.

[7] J. Rahn, D. Hoffmann, T. C. Harder, and M. Beer, "Vaccines against influenza A viruses in poultry and swine: status and future developments," *Vaccine*, vol. 33, no. 21, pp. 2414–2424, 2015.

[8] S. Lemiere, S. Y. Wong, A. L. Saint-Gerand, S. Goutebroze, and F. X. Le Gros, "Compatibility of turkey herpesvirus–infectious bursal disease vector vaccine with Marek's disease rispens vaccine injected into day-old pullets," *Avian Diseases*, vol. 6, no. 1, pp. e28–e29, 2011.

[9] Y. Ishihara, M. Esaki, S. Saitoh, and A. Yasuda, "Combination of two Marek's disease virus vectors shows effective vaccination against Marek's disease, infectious bursal disease, and Newcastle disease," *Avian Diseases*, vol. 60, no. 2, pp. 473–479, 2016.

[10] V. Palya, T. Tatar-Kis, T. Mato, B. Felfoldi, E. Kovacs, and Y. Gardin, "Onset and long-term duration of immunity provided by a single vaccination with a turkey herpesvirus vector ND vaccine in commercial layers," *Veterinary Immunology and Immunopathology*, vol. 158, no. 1-2, pp. 105–115, 2014.

[11] R. W. Morgan, J. Gelb Jr., C. R. Pope, and P. J. Sondermeijer, "Efficacy in chickens of a herpesvirus of turkeys recombinant vaccine containing the fusion gene of Newcastle disease virus: onset of protection and effect of maternal antibodies," *Avian Diseases*, vol. 37, no. 4, pp. 1032–1040, 1993.

[12] P. J. A. Sondermeijer, J. A. J. Claessens, P. E. Jenniskens et al., "Avian herpesvirus as a live viral vector for the expression of heterologous antigens," *Vaccine*, vol. 11, no. 3, pp. 349–358, 1993.

[13] Y. Atsushi, M. Esaki, K. M. Dorsey et al., "Development of vaccines for poultry against H5 avian influenza based on turkey herpesvirus vector," in *Steps Forwards in Diagnosing and Controlling Influenza*, D. M. Baddour, Ed., InTech, 2016.

[14] H. Gao, H. Cui, X. Cui et al., "Expression of HA of HPAI H5N1 virus at US2 gene insertion site of turkey herpesvirus induced better protection than that at US10 gene insertion site," *PLoS One*, vol. 6, no. 7, article e22549, 2011.

[15] Y. Li, K. Reddy, S. M. Reid et al., "Recombinant herpesvirus of turkeys as a vector-based vaccine against highly pathogenic H7N1 avian influenza and Marek's disease," *Vaccine*, vol. 29, no. 46, pp. 8257–8266, 2011.

[16] F. Rauw, V. Palya, Y. Gardin et al., "Efficacy of rHVT-AI vector vaccine in broilers with passive immunity against challenge with two antigenically divergent Egyptian clade 2.2.1 HPAI H5N1 strains," *Avian Diseases*, vol. 56, no. 4s1, pp. 913–922, 2012.

[17] Y. Gardin, V. Palya, K. M. Dorsey et al., "Experimental and field results regarding immunity induced by a recombinant turkey herpesvirus H5 vector vaccine against H5N1 and other H5 highly pathogenic avian influenza virus challenges," *Avian Diseases*, vol. 60, no. 1s, pp. 232–237, 2016.

[18] M. Steensels, F. Rauw, T. van den Berg et al., "Protection afforded by a recombinant turkey herpesvirus-H5 vaccine against the 2014 European highly pathogenic H5N8 avian influenza strain," *Avian Diseases*, vol. 60, no. 1s, pp. 202–209, 2016.

[19] D. R. Kapczynski, M. J. Pantin-Jackwood, E. Spackman, K. Chrzastek, D. L. Suarez, and D. E. Swayne, "Homologous and heterologous antigenic matched vaccines containing different H5 hemagglutinins provide variable protection of chickens from the 2014 U.S. H5N8 and H5N2 clade 2.3.4.4 highly pathogenic avian influenza viruses," *Vaccine*, vol. 35, no. 46, article 6345, 6353 pages, 2017.

[20] K. Bertran, C. Balzli, D. H. Lee, D. L. Suarez, D. R. Kapczynski, and D. E. Swayne, "Protection of white leghorn chickens by U.S. emergency H5 vaccination against clade 2.3.4.4 H5N2 high pathogenicity avian influenza virus," *Vaccine*, vol. 35, no. 46, pp. 6336–6344, 2017.

[21] M. L. Killian and E. Spackman, "Avian influenza virus isolation, propagation, and titration in embryonated chicken eggsAnimal influenza virus," Humana Press, New York, NY, USA, 2014.

[22] M. A. Ramakrishnan, "Determination of 50% endpoint titer using a simple formula," *World Journal of Virology*, vol. 5, no. 2, pp. 85-86, 2016.

[23] M. Mueller, S. Renzullo, R. Brooks, N. Ruggli, and M. A. Hofmann, "Antigenic characterization of recombinant hemagglutinin proteins derived from different avian influenza virus subtypes," *PLoS One*, vol. 5, no. 2, article e9097, 2010.

[24] M. Ibrahim, A. F. Eladl, H. A. Sultan et al., "Antigenic analysis of H5N1 highly pathogenic avian influenza viruses circulating in Egypt (2006–2012)," *Veterinary Microbiology*, vol. 167, no. 3-4, pp. 651–661, 2013.

[25] V. R. Duvvuri, B. Duvvuri, W. R. Cuff, G. E. Wu, and J. Wu, "Role of positive selection pressure on the evolution of H5N1 hemagglutinin," *Genomics, Proteomics & Bioinformatics*, vol. 7, no. 1-2, pp. 47–56, 2009.

[26] P. A. Reche, J. P. Glutting, H. Zhang, and E. L. Reinherz, "Enhancement to the RANKPEP resource for the prediction of peptide binding to MHC molecules using profiles," *Immunogenetics*, vol. 56, no. 6, pp. 405–419, 2004.

[27] H. R. Haghighi, L. R. Read, S. M. Haeryfar, S. Behboudi, and S. Sharif, "Identification of a dual-specific T cell epitope of the hemagglutinin antigen of an h5 avian influenza virus in chickens," *PLoS One*, vol. 4, no. 11, article e7772, 2009.

[28] A. El Khantour, S. Darkaoui, T. Tatar-Kis et al., "Immunity elicited by a turkey herpesvirus-vectored Newcastle disease vaccine in Turkey against challenge with a recent genotype IV Newcastle disease virus field strain," *Avian Diseases*, vol. 61, no. 3, pp. 378–386, 2017.

[29] G. Kayali, A. Kandeil, R. El-Shesheny et al., "Do commercial avian influenza H5 vaccines induce cross-reactive antibodies against contemporary H5N1 viruses in Egypt?," *Poultry Science*, vol. 92, no. 1, pp. 114–118, 2013.

[30] E. Spackman, D. A. Senne, T. J. Myers et al., "Development of a real-time reverse transcriptase PCR assay for type A influenza virus and the avian H5 and H7 hemagglutinin subtypes," *Journal of Clinical Microbiology*, vol. 40, no. 9, pp. 3256–3260, 2002.

[31] G. Cattoli, A. Fusaro, I. Monne et al., "Evidence for differing evolutionary dynamics of A/H5N1 viruses among countries applying or not applying avian influenza vaccination in poultry," *Vaccine*, vol. 29, no. 50, pp. 9368–9375, 2011.

[32] M. S. Beato, I. Monne, M. Mancin, E. Bertoli, and I. Capua, "A proof-of-principle study to identify suitable vaccine seed candidates to combat introductions of Eurasian lineage H5 and H7 subtype avian influenza viruses," *Avian Pathology*, vol. 39, no. 5, pp. 375–382, 2010.

[33] R. A. Fouchier and D. J. Smith, "Use of antigenic cartography in vaccine seed strain selection," *Avian Diseases*, vol. 54, no. s1, pp. 220–223, 2010.

[34] D. E. Swayne and D. Kapczynski, "Strategies and challenges for eliciting immunity against avian influenza virus in birds," *Immunological Reviews*, vol. 225, no. 1, pp. 314–331, 2008.

[35] F. Rauw, V. Palya, S. Van Borm et al., "Further evidence of antigenic drift and protective efficacy afforded by a recombinant HVT-H5 vaccine against challenge with two antigenically divergent Egyptian clade 2.2.1 HPAI H5N1 strains," *Vaccine*, vol. 29, no. 14, pp. 2590–2600, 2011.

[36] M. A. Abbas, E. Spackman, R. Fouchier et al., "H7 avian influenza virus vaccines protect chickens against challenge with antigenically diverse isolates," *Vaccine*, vol. 29, no. 43, pp. 7424–7429, 2011.

[37] D. E. Swayne, M. L. Perdue, J. R. Beck, M. Garcia, and D. L. Suarez, "Vaccines protect chickens against H5 highly pathogenic avian influenza in the face of genetic changes in field viruses over multiple years," *Veterinary Microbiology*, vol. 74, no. 1-2, pp. 165–172, 2000.

[38] C. Terregino, A. Toffan, F. Cilloni et al., "Evaluation of the protection induced by avian influenza vaccines containing a 1994 Mexican H5N2 LPAI seed strain against a 2008 Egyptian H5N1 HPAI virus belonging to clade 2.2.1 by means of serological and in vivo tests," *Avian Pathology*, vol. 39, no. 3, pp. 215–222, 2010.

[39] S. J. Park, Y. J. Si, J. Kim et al., "Cross-protective efficacies of highly-pathogenic avian influenza H5N1 vaccines against a recent H5N8 virus," *Virology*, vol. 498, pp. 36–43, 2016.

[40] I. Sitaras, X. Rousou, D. Kalthoff, M. Beer, B. Peeters, and M. C. de Jong, "Role of vaccination-induced immunity and antigenic distance in the transmission dynamics of highly pathogenic avian influenza H5N1," *Journal of The Royal Society Interface*, vol. 13, no. 114, article 20150976, 2016.

[41] D. L. Suarez and M. J. Pantin-Jackwood, "Recombinant viral-vectored vaccines for the control of avian influenza in poultry," *Veterinary Microbiology*, vol. 206, pp. 144–151, 2017.

[42] Y. Furuya, J. Chan, M. Regner et al., "Cytotoxic T cells are the predominant players providing cross-protective immunity induced by γ-irradiated influenza A viruses," *Journal of Virology*, vol. 84, no. 9, article 4212, 4221 pages, 2010.

[43] M. L. Hillaire, S. E. van Trierum, J. H. Kreijtz et al., "Cross-protective immunity against influenza pH1N1 2009 viruses induced by seasonal influenza A (H3N2) virus is mediated by virus-specific T-cells," *Journal of General Virology*, vol. 92, no. 10, pp. 2339–2349, 2011.

[44] J. H. Kreijtz, G. de Mutsert, C. A. van Baalen, R. A. Fouchier, A. D. Osterhaus, and G. F. Rimmelzwaan, "Cross-recognition of avian H5N1 influenza virus by human cytotoxic T-lymphocyte populations directed to human influenza A virus," *Journal of Virology*, vol. 82, no. 11, pp. 5161–5166, 2008.

[45] J. H. Kreijtz, R. Bodewes, J. M. van den Brand et al., "Infection of mice with a human influenza A/H3N2 virus induces protective immunity against lethal infection with influenza A/H5N1 virus," *Vaccine*, vol. 27, no. 36, pp. 4983–4989, 2009.

[46] V. R. Duvvuri, S. M. Moghadas, H. Guo et al., "Highly conserved cross-reactive CD4+ T-cell HA-epitopes of seasonal and the 2009 pandemic influenza viruses," *Influenza Other Respir Viruses*, vol. 4, no. 5, pp. 249–258, 2010.

[47] M. Terajima, J. A. Babon, M. D. Co, and F. A. Ennis, "Cross-reactive human B cell and T cell epitopes between influenza A and B viruses," *Virology Journal*, vol. 10, no. 1, pp. 244–244, 2013.

[48] S. Pillet, E. Aubin, S. Trepanier et al., "A plant-derived quadrivalent virus like particle influenza vaccine induces cross-reactive antibody and T cell response in healthy adults," *Clinical Immunology*, vol. 168, pp. 72–87, 2016.

[49] K. D. Zens and D. L. FarberM. Oldstone and R. Compans, "Memory CD4 T cells in influenza," in *Influenza Pathogenesis and Control - Volume II*, vol. 386 of Current Topics in Microbiology and Immunology, pp. 399–421, Springer, Cham, 2015.

[50] J. R. Teijaro, D. Turner, Q. Pham, E. J. Wherry, L. Lefrancois, and D. L. Farber, "Cutting edge: tissue-retentive lung memory CD4 T cells mediate optimal protection to respiratory virus infection," *The Journal of Immunology*, vol. 187, no. 11, pp. 5510–5514, 2011.

[51] S. H. Seo, M. Peiris, and R. G. Webster, "Protective cross-reactive cellular immunity to lethal A/Goose/Guangdong/1/96-like H5N1 influenza virus is correlated with the proportion of pulmonary $CD8^+$ T cells expressing gamma interferon," *Journal of Virology*, vol. 76, no. 10, pp. 4886–4890, 2002.

[52] M. B. Mazanec, C. L. Coudret, and D. R. Fletcher, "Intracellular neutralization of influenza virus by immunoglobulin A anti-hemagglutinin monoclonal antibodies," *Journal of Virology*, vol. 69, no. 2, pp. 1339–1343, 1995.

[53] D. R. Kapczynski, M. Esaki, K. M. Dorsey et al., "Vaccine protection of chickens against antigenically diverse H5 highly

pathogenic avian influenza isolates with a live HVT vector vaccine expressing the influenza hemagglutinin gene derived from a clade 2.2 avian influenza virus," *Vaccine*, vol. 33, no. 9, pp. 1197–1205, 2015.

[54] A. Bouma, I. Claassen, K. Natih et al., "Estimation of transmission parameters of H5N1 avian influenza virus in chickens," *PLoS Pathogens*, vol. 5, no. 1, article e1000281, 2009.

[55] O. N. Poetri, A. Bouma, S. Murtini et al., "An inactivated H5N2 vaccine reduces transmission of highly pathogenic H5N1 avian influenza virus among native chickens," *Vaccine*, vol. 27, no. 21, pp. 2864–2869, 2009.

[56] J. A. van der Goot, M. van Boven, A. Stegeman, S. G. van de Water, M. C. de Jong, and G. Koch, "Transmission of highly pathogenic avian influenza H5N1 virus in Pekin ducks is significantly reduced by a genetically distant H5N2 vaccine," *Virology*, vol. 382, no. 1, pp. 91–97, 2008.

Hindawi
Journal of Immunology Research
Volume 2018, Article ID 9262631, 12 pages
https://doi.org/10.1155/2018/9262631

Research Article

Analysis of Immune Responses in Mice Orally Immunized with Recombinant pMG36e-SP-TSOL18/*Lactococcus lactis* and pMG36e-TSOL18/*Lactococcus lactis* Vaccines of *Taenia solium*

Bi Ying Zhou, Jun Chao Sun, Xiang Li, Yue Zhang, Bo Luo, Nan Jiang, and Mei Chen Liu

Department of Parasitology, School of Basic Medical Sciences, Zunyi Medical University, Zunyi, China

Correspondence should be addressed to Bi Ying Zhou; 1458030871@qq.com

Received 12 April 2018; Revised 10 July 2018; Accepted 26 August 2018; Published 18 November 2018

Academic Editor: Elena Criscuolo

Cysticercosis is a cosmopolitan zoonotic parasitic disease infected by larval of *Taenia solium* (*T. solium*). Several drugs for the treatment of cysticercosis, such as praziquantel, albendazole, and mebendazole, have certain toxicity and side effects. Considering that there is no vaccine available, we studied a new vaccine for cysticercosis in this study. The complete *TSOL18* gene and the optimized *SP-TSOL18* gene fragments were obtained using PCR-based accurate synthesis method. The secretory and intracellular recombinant pMG36e-SP-TSOL18/*Lactococcus lactis* (*L. lactis*) and pMG36e-TSOL18/*L. lactis* vaccines of *T. solium* were prepared. Immune responses in mice orally immunized with these two recombinant *L. lactis* vaccines were analyzed by the determination of specific antibodies (IgG, IgG1, IgG2a, and sIgA) in serum, spleen lymphocyte proliferation, and cytokines (IL-2, IFN-γ, IL-4, and IL-10) in spleen lymphocyte culture supernatant. Our results showed that, after the first immunization, in these two recombinant *L. lactis* vaccine groups, the levels of serum specific IgG, IgG2a, and IgG1 increased on 14–56 d and reached the highest level on days 42, 42, and 28, respectively. The level of specific sIgA of intestinal mucosa also increased on 14–56 d and reached the highest level on day 42. The level of spleen lymphocyte proliferation increased on 14–56 d and reached the highest level on day 42. The levels of IL-2, IFN-γ, IL-4, and IL-10 in spleen lymphocyte culture supernatant increased on 14–56 d and reached the highest level on days 42, 42, 28, and 28, respectively. These results indicated that the recombinant pMG36e-SP-TSOL18/*L. lactis* and pMG36e-TSOL18/*L. lactis* vaccines can induce specific cellular, humoral, and mucosal immune responses in mice with oral vaccination. More importantly, the recombinant pMG36e-SP-TSOL18/*L. lactis* vaccine has a better immune effect. In summary, these results demonstrated the possibility of using *L. lactis* strain as a vector to deliver protective antigens of *T. solium*.

1. Introduction

Cysticercosis is a zoonotic parasitic disease that seriously harms human health and is distributed in many developing countries or areas in Latin America, Africa, and Asia [1–3]. A large number of sporadic cases with cysticercosis have been reported in the Southeast and Southern of Guizhou province, such as Kaili, Congjiang, Duyun, and Luodian [4–8]. Surgery and chemotherapy treatment of the disease have several problems, including the limited efficacy, serious side effects, and drug resistance. It is very necessary to develop a safe and effective vaccine against cysticercosis, which can be used in China and other cysticercosis endemic countries [9–12].

TSOL18 is a specific antigen of *Taenia solium* (*T. solium*) oncosphere, which has good immunogenicity and immunoprotection. The *TSOL18* gene is considered to be the most promising candidate vaccine gene and has been studied extensively [13, 14]. *Lactococcus lactis* (*L. lactis*) is an important probiotic in intestine of human and animal. It is generally recognized as safe (GRAS) food grade microorganism and naturally present in milk foods, which has functions of regulating microecological balances, inhibiting tumor growth, reducing cholesterol, delaying aging, and improving

immunity [15]. With the development of genetic engineering technology, it has been recently used as a new foreign antigen delivery system and applied to the field of food, vaccines, medicines, health products, and domestic animal breeding industries [16–21]. The objective of this study was to prepare the recombinant pMG36e-SP-TSOL18/*L. lactis* and pMG36e-TSOL18/*L. lactis* vaccines and investigate their induced immune responses in mice. Kunming mice were immunized orally with these two recombinant *L. lactis* vaccines, and then antibodies of serum and intestinal mucosa, proliferation and cytokines of spleen lymphocytes were determined at different time points of postvaccination.

2. Materials and Methods

2.1. Construction and Identification of Recombinant Plasmids pMG36e-TSOL18 and pMG36e-SP-TSOL18. According to the *TSOL18* gene sequence (Accession No. AF017788), using the *L. lactics* as a host system for gene optimization, the *TSOL18* gene was synthesized using a PAS (PCR-based accurate synthesis) method. The signal secretion protein SP_{USP45} was added at its N-terminus to synthesize the *SP-TSOL18* target gene. Restriction enzyme digestion was performed using *Sac*I and *Hind*III for the *TSOL18* gene fragment and plasmid pMG36e to construct recombinant plasmids pMG36e-TSOL18 and pMG36e-SP-TSOL18. And then transferred them into Top10 competent cells, respectively. Positive clones were selected to perform restriction enzyme digestion and sequencing identification.

2.2. Activation of L. lactis and Preparation of Competent Cells. L. lactis. MG1363 bacteria solution was inoculated in 1 mLG/L-SGM17 (M17 medium + 0.5 M sucrose + 2.5% glycine + 0.5% glucose) liquid culture medium and cultured at 30°C for 72 hours. After obvious turbidity appeared, this culture was inoculated into 5 mLG/L-SGM17 liquid culture medium, incubated at 30°C for 24 hours, and 5 mL of this culture was diluted into 50 mLG/L-SGM17 culture medium and cultivated for 24 hours. Then, 50 mL of the culture was diluted in 400 mL of G/L-SGM17 medium and continually cultured for 3 to 5 hours until the optical density (OD_{600}) value of the bacteria solution reached 0.2 to 0.3.

The culture was transferred into a 50 mL centrifuge tube and centrifuged at 4000 rpm at 4°C for 20 minutes, and the supernatant was discarded. The pellet was resuspended in 400 mL of 4°C precooled 0.5 M sucrose containing 10% glycerol, thoroughly shaked, centrifuged, and then discarded the supernatant. Then, the pellet was resuspended in 200 mL of 4°C precooled 0.5 M sucrose containing 10% glycerol and 0.05 M ethylenediaminetetraacetic acid (EDTA), placed in ice water for 15 minutes. The cooled culture was centrifuged again at 4000 rpm at 4°C for 20 minutes, and the supernatant was discarded. The pellet was resuspended by adding 100 mL of 4°C precooled 0.5 M sucrose containing 10% glycerol and shaken well. The culture was centrifuged again, and the supernatant was discarded. The pellet was resuspended in 4 mL of 0.5 M sucrose containing 10% glycerol. After shaking, the final culture was separated into 100 tubes (each containing 40 μL) and placed in an −80°C freezer.

2.3. Electrotransformation of L. lactis MG1363. The previously obtained plasmids pMG36e-TSOL18 and pMG36e-SP-TSOL18 were separately mixed with competent *L. lactis* MG1363. Both were bathed in ice for 10 minutes and treated with an electronic current. The following electrotransformation parameters were used: a voltage of 2000 V, capacitance of 25 μF, and resistance of 200 Ω. After an initial first pulse, 900 μL of low-temperature GMMC recovery medium (M17 medium + 0.5% glucose + 20 mM $MgCl_2$ + 2 mM $CaCl_2$) was immediately added. The cultures were placed on ice untouched for 10 minutes, then allowed to resuscitate at 30°C for 2–3 hours. The bacteria solution were centrifuged at 4000 rpm and the supernatant was discarded, and the pellet was concentrated in 100 μL GMMC recovery medium. The solution was then spreaded on 10 μg/mL Erythromycin GM17 agar plates, cultured at 30°C for 2–3 days. Plates were kept in a relatively closed environment, observed for colony growth, and small circular white opaque colonies formed in about one week.

Positive single colony was picked and placed into 1 mL of G/L-SGM17+ 5 μg/mL Erythromycin liquid culture medium, which was then incubated at 30°C for 72 hours until the solution appeared cloudy.

2.4. Identification of Recombinant pMG36e-SP-TSOL18/L. lactis and pMG36e-TSOL18/L. lactis Vaccines. The above-mentioned cultured bacteria solution was centrifuged at 10000 rpm for 10 minutes, and the supernatant fluid was discarded. The bacteria solution was centrifuged and washed three times with double-distilled water, and the supernatant fluid was discarded each time. The pellets were resuspended in 30 μL of double-distilled water, placed in a boiling water bath for 10 minutes, then placed in an ice bath for 2 minutes, centrifuging again, and the supernatant was retained for extracting genomic DNA. A 579 bp region of the *T. solium* activated oncosphere *TSOL18* gene, based on the sequence reported by Gauci et al. (1998), was amplified using the forward primer 5′-ATGGTTTGTCGTTTTGCTT-3′ and the reverse primer 5′-TTATGAACGACGAACCTTTTTA-3′. After a positive clone was confirmed, it was prepared for use as an expression strain.

2.5. Expression and Identification of TSOL18 Protein. Untransformed *L. lactis* MG1363 bacteria were cultured in GM17 liquid medium. Colonies that were identified as positive were separately selected and inoculated in GM17 liquid medium containing Erythromycin. After stationary culturing at 30°C for 72 hours, the culture was centrifuged at 6000 rpm and 4°C for 15 minutes together with the transformed bacterial solution. The precipitate and supernatant were collected separately for later use. Precooled phosphate-buffered saline solution (PBS) was used to resuspend the precipitate. This culture was then placed in an ice bath and ultrasonicated (300 watts) for 20 minutes, alternating 4 s of ultrasonication with 8 s wait intervals. An equal volume of 2x SDS loading buffer (0.1 mol/L Tris-Cl, pH 6.8, 10% dithiothreitol, 4% SDS, 0.2% bromophenol blue, 20% glycerol) was added, and the culture was then placed in a boiling water bath for 4–8 minutes. The total 20 μL samples were prepared after

cooling and then were loaded in SDS-PAGE and Western blot gel electrophoresis plates to separately detect the expression of supernatant and intracellular components.

2.6. Animals and Immunity. Eighty specific-pathogen-free (SPF) Kunming mice (40 males and 40 females) were purchased from Experimental Animal Center, Daping Hospital, Third Military Medical University, China (number of animal license SCXK(YU)2012-0005). All mice were 6–8 weeks old, each weighed about 20 g. All experimental procedures involving the mice were performed in accordance with the Regulations for the Administration of Affairs Concerning Experimental Animals approved by the State Council of People's Republic of China.

The Kunming mice were randomly divided into four groups with each group containing twenty mice. The mice in group 1 were immunized with recombinant pMG36e-SP-TSOL18/*L. lactis* vaccine. In group 2, the mice were immunized with recombinant pMG36e-TSOL18/*L. lactis* vaccine. In group 3 and 4, the mice were immunized only with *L. lactis* bacteria and PBS as control groups, respectively. The immunization doses were 3×10^9 CFU [22] and given orally three times with two-week intervals.

2.7. Antibody Detection. Four mice were taken from each group on days 0, 14, 28, 42, and 56 after the first immunization. Blood was collected from the orbital vein and let stand for 12 hours at 4°C, then centrifuged at 2000 rpm for 10 minutes to separate the serum. At the same time, mice colons were aseptically removed, cut into pieces, and placed in ice saline solution then ground to homogenate and centrifuged at 3500 rpm and 4°C for 10 minutes. The supernatant was collected and frozen at −20°C for future investigation. The serum specific IgG, IgG1, IgG2a, and intestinal mucosa sIgA [23] were evaluated using the enzyme-linked immunosorbent assay (ELISA) method. The 96-well ELISA plate was coated with 10 μg/mL recombinant TSOL18 antigen. The horseradish peroxidase (HRP) conjugated goat anti-mouse IgG (1 : 100000 dilution), IgG1 (1 : 10000 dilution), IgG2a (1 : 10000 dilution), IgA (1 : 10000 dilution). A diaminobenzidine (DAB) chromogenic substrate was used for staining, and absorbance (OD_{450}) values were measured by a microplate reader. Each assay was performed in duplicate.

2.8. Preparation of Spleen Lymphocytes. Spleens were also aseptically removed from the four mice per group on days 0, 14, 28, 42, and 56 after the first immunization. The spleen lymphocytes were isolated according to the instructions of the mouse spleen lymphocyte separation kit. Spleen lymphocyte suspension was prepared and adjusted to 5×10^6 cells/mL in RPMI 1640 containing 10% fetal bovine serum. After the number of viable cells was above 90%, penicillin (100 U/mL) and streptomycin (100 U/mL) were added.

2.9. Spleen Lymphocyte Proliferation Assay. The cell counting kit CCK-8 detection method was used. Spleen lymphocytes (2×10^6 cells/mL) were dispensed in 24-well culture plates. Three wells were set for each specimen and contained 1 mL stock solution, 1 mL stock solution combining recombinant TSOL18 antigen (10 μg/mL), and 1 mL stock solution combining ConA (10 μg/mL). The cells were incubated in a 5% CO_2 incubator at 37°C for 48 hours. Two hours before the end of the incubation period, 100 μL of CCK-8 solution was added to each well. Then, absorbance values (OD_{450}) were measured for each well with a microplate reader. Each assay was performed in duplicate.

2.10. Detection of Spleen Lymphocyte Culture Supernatant IL-2, INF-γ, IL-4, and IL-10. Spleen lymphocytes (5×10^6 cells/mL) were dispensed in 24-well culture plates using the method as described in Section 2.9. After the 48-hour incubation, the samples were centrifuged in 4000 rpm for 5 minutes. The supernatant was then collected and assessed for IL-2, INF-γ, IL-4, and IL-10 cytokines using a commercial ELISA kit according to the manufacturer's manual. Each assay was performed in duplicate.

2.11. Statistical Analysis. Measured data were shown as the mean ± standard deviation (SD). ANOVA models were used for multigroup comparisons, and comparison between groups was performed using the least significant difference method (LSD). Values of $p < 0.05$ were considered to represent statistically significant differences.

3. Results

3.1. Construction of Recombinant Plasmids pMG36e-TSOL18 and pMG36e-SP-TSOL18. Recombinant plasmids pMG36e-TSOL18 and pMG36e-SP-TSOL18 were constructed following Figures 1(a) and 1(b).

3.2. Identification of Recombinant Plasmids pMG36e-TSOL18 and pMG36e-SP-TSOL18. The amplified *TSOL18* gene fragment and pMG36e vector fragment were digested by restriction enzymes *Sac*I and *Hind*III. The results of 1% agarose gel electrophoresis were shown in Figures 2(a) and 2(b), which were conformed to be the theoretical length. Gene sequencing was performed for recombinant plasmids pMG36e-TSOL18 and pMG36e-SP-TSOL18, which were proved to contain the complete sequences of *TSOL18* gene and pMG36e vector.

3.3. Identification of Recombinant pMG36e-TSOL18/L. lactis and pMG36e-SP-TSOL18/L. lactis Vaccines. The culture supernatant of *L. lactis* MG1363 bacteria containing pMG36e-TSOL18 and pMG36e-SP-TSOL18 was used to perform PCR identification. The results showed that lanes 1–6 were the PCR products of *L. lactis* MG1363-positive bacteria containing pMG36e-TSOL18 and pMG36e-SP-TSOL18. Both are consistent with the expected results (see Figures 3(a) and 3(b)).

3.4. SDS-PAGE Analysis. Positive colonies were selected and inoculated into GM17 liquid medium containing Erythromycin. The colony was cultured for 72 hours at 30°C, then supernatant and precipitation were collected for SDS-PAGE electrophoresis. The results showed that the target protein expression of recombinant pMG36e-TSOL18/*L. lactis* can be observed in around 15 KD of intracellular precipitation. However, no expression has yet

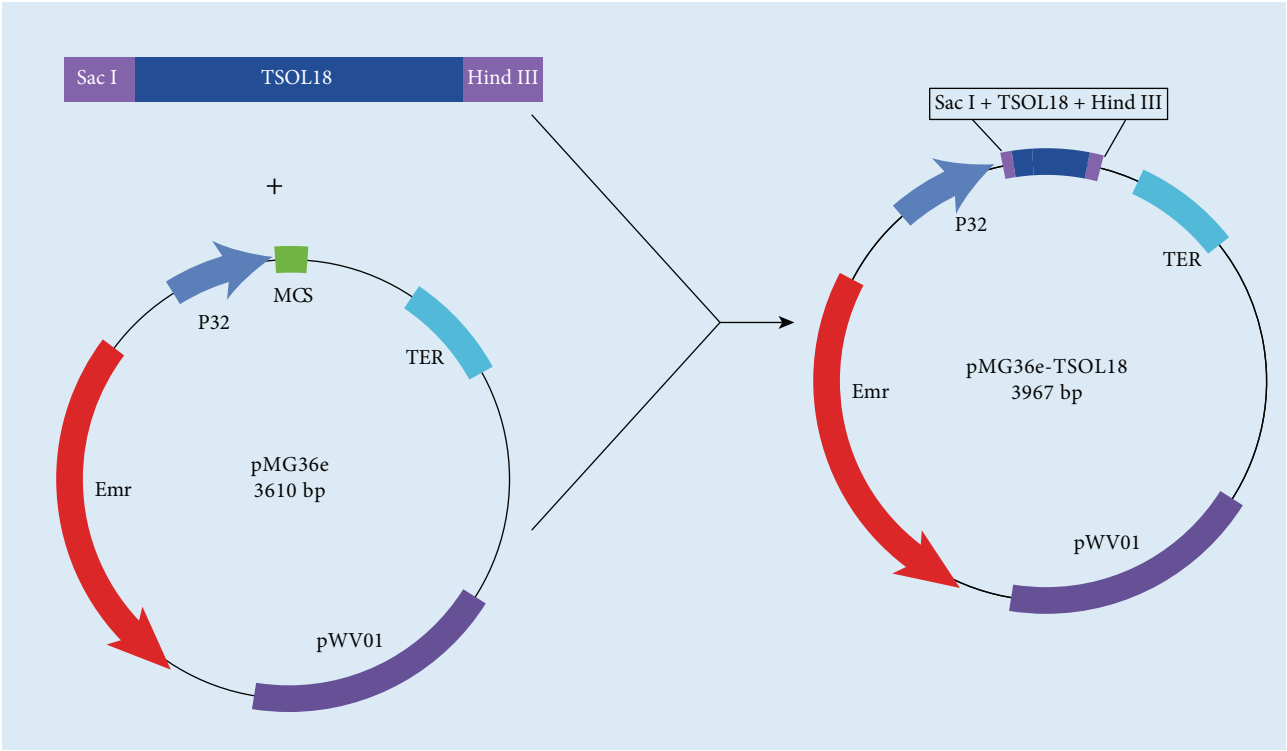

(a) pMG36e-TSOL18

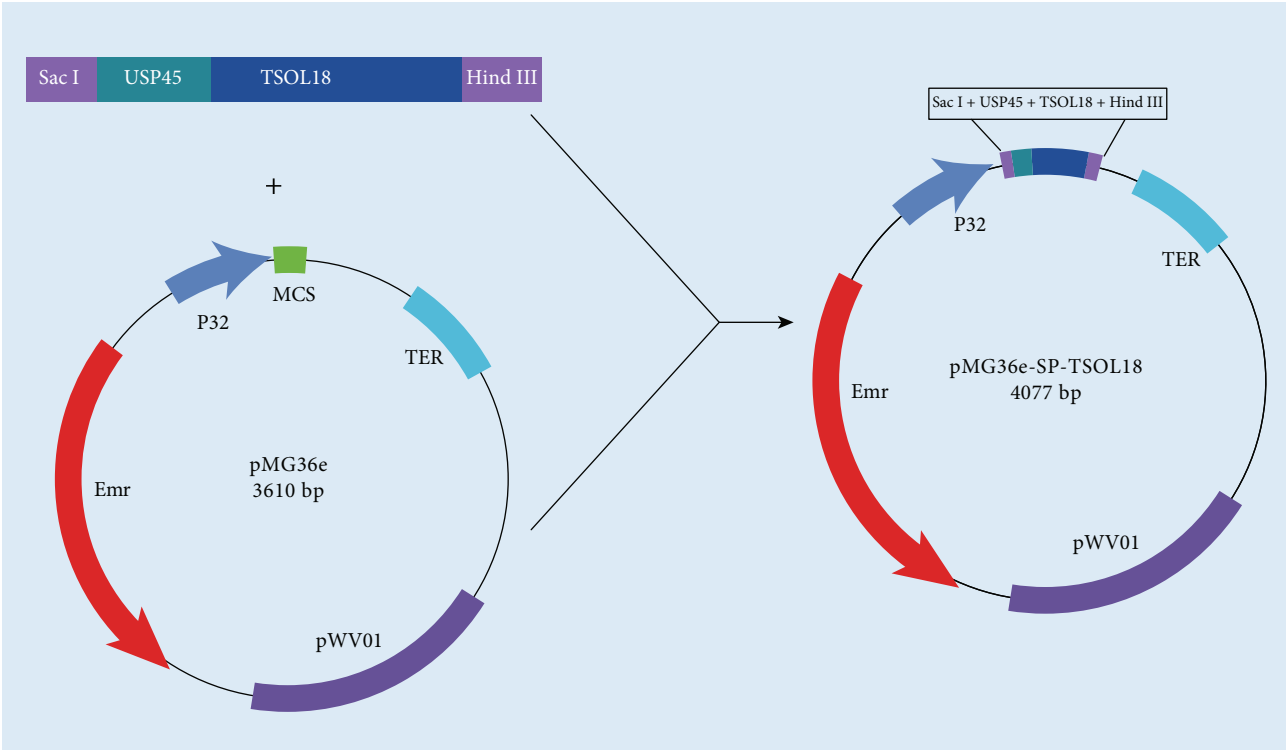

(b) pMG36e-SP-TSOL18

Figure 1: Construction of recombinant plasmids pMG36e-TSOL18 (a) and pMG36e-SP-TSOL18 (b).

been observed in the extracellular supernatant. Recombinant pMG36e-SP-TSOL18/*L. lactis* showed the corresponding target protein expression in both extracellular supernatant and intracellular precipitation (see Figures 4(a) and 4(b)).

3.5. Western Blot Identification. After expression of TSOL18 recombinant protein combined with TSOL18 recombinant rabbit antiserum protein, only the recombinant pMG36e-TSOL18/*L. lactis* appeared around 15 KD reflection band in

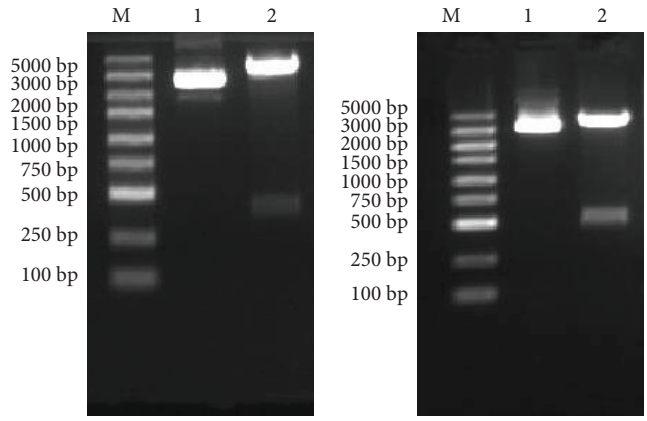

(a) pMG36e-TSOL18 (b) pMG36e-SP-TSOL18

Figure 2: Identification of recombinant plasmid (pMG36e-TSOL18 and pMG36e-SP-TSOL18) by restriction enzyme digestion (*Sac*I and *Hind*III). Lane M, DNA marker; lane 1, plasmid pMG36e; lane 2, production of restriction enzyme of recombinant plasmid pMG36e-TSOL18 (a) and pMG36e-SP-TSOL18 (b).

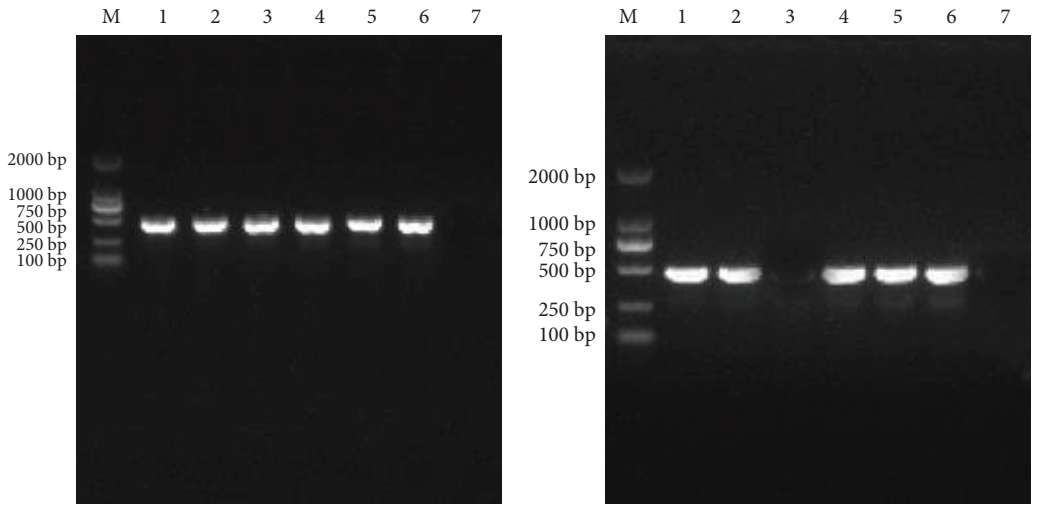

(a) pMG36e-TSOL18/*L. lactis* (b) pMG36e-SP-TSOL18/*L. lactis*

Figure 3: PCR identification of recombinant pMG36e-TSOL18/*L. lactis* and pMG36e-SP-TSOL18/*L. lactis* vaccines. Lane M, DNA marker; Lanes 1–6, PCR products of *L. lactis* MG1363-positive bacteria containing pMG36e-TSOL18 (a) and pMG36e-SP-TSOL18 (b); lane 7, PCR products of *L. lactis* MG1363-negative bacteria.

intracellular precipitation. The recombinant pMG36e-SP-TSOL18/*L. lactis* showed corresponding reaction bands in both extracellular supernatant and intracellular precipitation (see Figures 5(a) and 5(b)).

3.6. Serum Specific IgG, IgG1, and IgG2a Levels in Immunized Mice. As compared to the level on day 0, in both recombinant pMG36e-TSOL18/*L. lactis* and pMG36e-SP-TSOL18/*L. lactis* groups, the serum specific IgG, IgG1, and IgG2a levels in mice were increased from 14 to 56 days after the first immunization. Each antibody reached the highest level on days 42, 28, and 42, respectively, which was significantly higher than *L. lactis* and PBS control group ($p < 0.05$). The level of each antibody in recombinant pMG36e-SP-TSOL18/*L. lactis* group was significantly higher than that of recombinant pMG36e-TSOL18/*L. lactis* group ($p < 0.05$) (see Figures 6(a)–6(c)).

3.7. Intestinal Mucosa-Specific sIgA Levels in Immunized Mice. As compared to the level on day 0, in both recombinant pMG36e-TSOL18/*L. lactis* and pMG36e-SP-TSOL18/*L. lactis* groups, the intestinal mucosa-specific secretory IgA (sIgA) levels in mice were increased from 14 to 56 days after the first immunization. sIgA reached the highest level on day 42 which was significantly higher than *L. lactis* and PBS control group ($p < 0.05$). The level of sIgA in recombinant pMG36e-

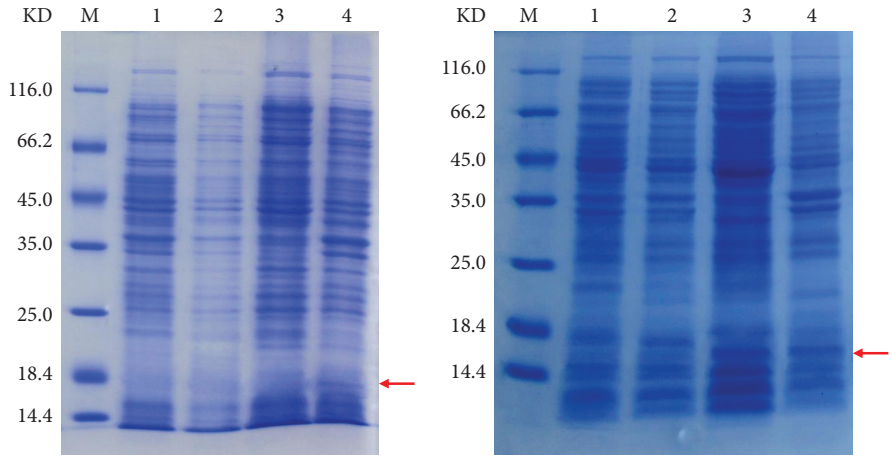

(a) pMG36e-TSOL18/*L. lactis* (b) pMG36e-SP-TSOL18/*L. lactis*

Figure 4: SDS-PAGE analysis of recombinant pMG36e-TSOL18/*L. lactis* and pMG36e-SP-TSOL18/*L. lactis* vaccines. Lane M, protein marker; lane 1, supernatant of MG1363 strain cultured for 72 h; lane 2, precipitation of MG1363 strain cultured for 72 h; lane 3, supernatant of transformation bacteria pMG36e-TSOL18/*L. lactis* (a) and pMG36e-SP-TSOL18/*L. lactis* (b) cultured for 72 h; lane 4, precipitation of transformation bacteria pMG36e-TSOL18/*L. lactis* (a) and pMG36e-SP-TSOL18/*L. lactis* (b) cultured for 72 h.

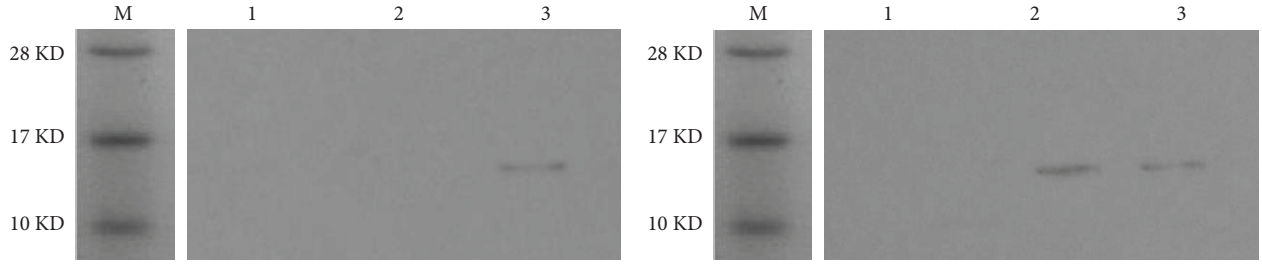

(a) pMG36e-TSOL18/*L. lactis* (b) pMG36e-SP-TSOL18/*L. lactis*

Figure 5: Western blot identification of TSOL18 and SP-TSOL18 protein expression in *L. lactis*. Lane M, protein marker; lane 1, *L. lactis* MG1363-negative bacteria; lane 2, TSOL18 (a) and SP-TSOL18 (b) protein in extracellular supernatant reacted with rabbit-anti-TSOL18; lane 3, TSOL18 (a) and SP-TSOL18 (b) protein in intracellular precipitation reacted with rabbit-anti-TSOL18.

SP-TSOL18/*L. lactis* group was significantly higher than that of recombinant pMG36e-TSOL18/*L. lactis* group ($p < 0.05$) (see Figure 7).

3.8. Spleen Lymphocyte Proliferation Levels in Immunized Mice. As compared to the level on day 0, in both recombinant pMG36e-TSOL18/*L. lactis* and pMG36e-SP-TSOL18/*L. lactis* groups, the spleen lymphocyte proliferation levels in mice were increased from 14 to 56 days after the first immunization. Spleen lymphocyte proliferation reached the highest level on day 42, which was significantly higher than *L. lactis* and PBS control group ($p < 0.05$). The level of spleen lymphocyte proliferation in recombinant pMG36e-SP-TSOL18/*L. lactis* group was significantly higher than that of recombinant pMG36e-TSOL18/*L. lactis* group ($p < 0.05$) (see Figure 8).

3.9. Spleen Lymphocyte Culture Supernatant IFN-γ, IL-2, IL-4, and IL-10 Levels in Immunized Mice. As compared to the level on day 0, in both recombinant pMG36e-TSOL18/*L. lactis* and pMG36e-SP-TSOL18/*L. lactis* groups, the levels of IFN-γ, IL-2, IL-4, and IL-10 in spleen lymphocyte culture supernatant were increased from 14 to 56 days after the first immunization. Each cytokine reached the highest level on days 42, 42, 28, and 28, respectively, which was significantly higher than *L. lactis* and PBS control group ($p < 0.05$). The level of each cytokine in recombinant pMG36e-SP-TSOL18/*L. lactis* group was significantly higher than that of recombinant pMG36e-TSOL18/*L. lactis* group ($p < 0.05$) (see Figures 9(a)–9(d)).

4. Discussion

Cysticercosis is a zoonotic parasitic disease caused by the larvae of *T. solium* in the humans and pigs and led to serious health and economic consequences [24, 25]. There were limitations to medication and surgical treatment [12]. Therefore, it was the best way to eliminate this disease by developing an effective vaccine against *T. solium* infection [26, 27]. Because the eggs of *T. solium* primarily infect hosts through ingestion, *L. lactis* as an oral vaccine for *T. solium* infection may be a more effective as well as practical new vaccine for the

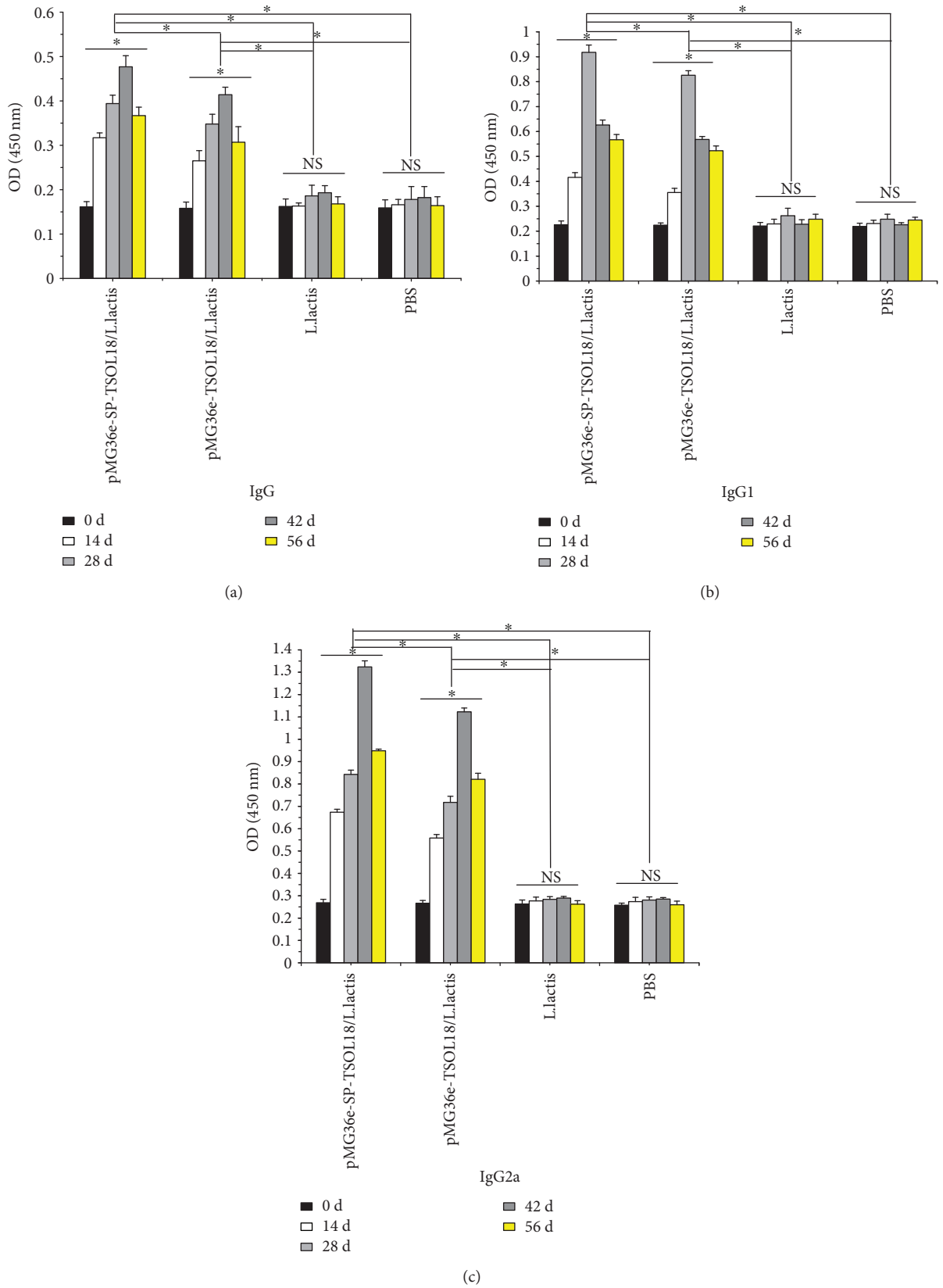

Figure 6: The level of serum specific IgG (a), IgG1 (b), and IgG2a (c) in immunized mice as measured by ELISA, respectively. Serum was obtained on days 0, 14, 28, 42, and 56 after the first immunization. Inset shows the absorbance values of four groups at different time points. *Represents the difference between groups. $p < 0.05$. NS = nonsignificant.

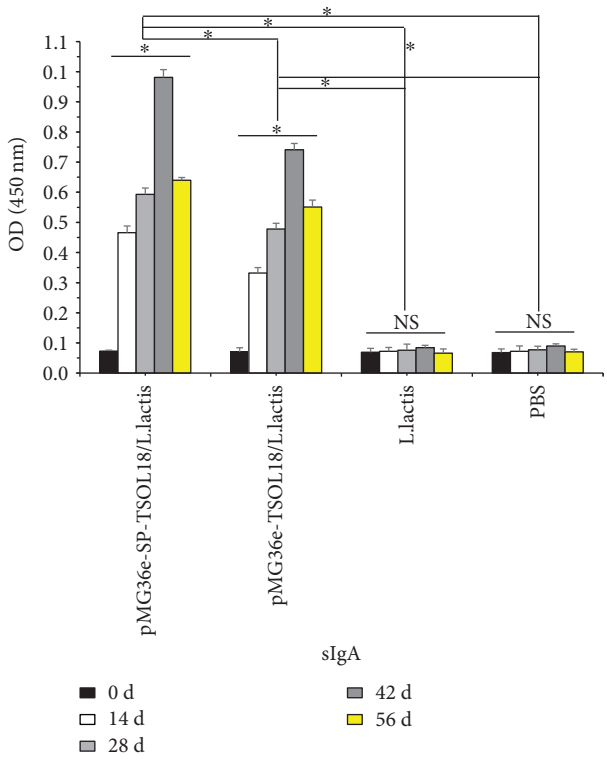

Figure 7: The level of intestinal mucosa-specific sIgA in immunized mice as measured by ELISA. Intestinal mucosa was obtained on days 0, 14, 28, 42, and 56 after the first immunization. Inset shows the absorbance values of four groups at different time points. *Represents the difference between groups. $p < 0.05$. NS = nonsignificant.

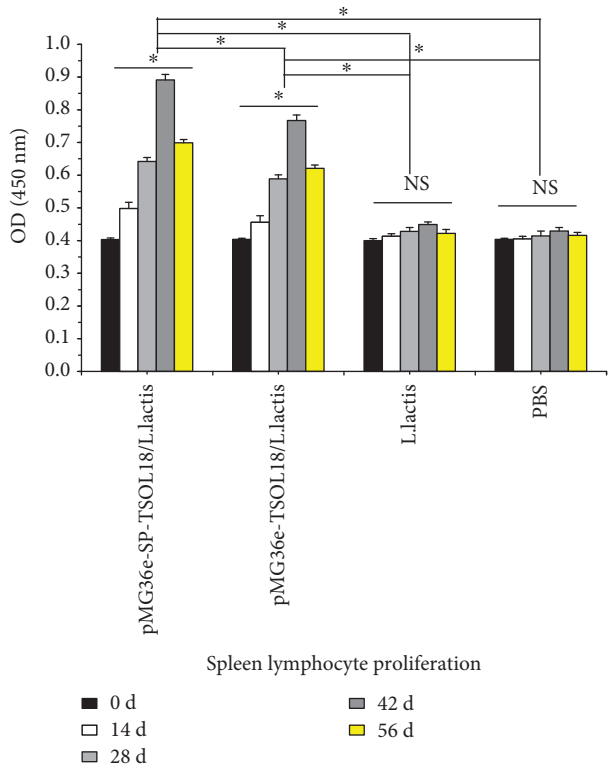

Figure 8: The level of spleen lymphocyte proliferation in immunized mice as measured by CCK-8. Spleen lymphocytes were obtained on days 0, 14, 28, 42, and 56 after the first immunization. Inset shows the absorbance values of four groups at different time points. *Represents the difference between groups. $p < 0.05$. NS = nonsignificant.

prevention and control of cysticercosis [28]. Cysticercosis is caused by *T. solium* eggs or gravid proglottid contamination, and oncospheres are hatched and developed into cysticerci, which would bring great harm to the host. Oncosphere was the key stage in the invasion of host, thus, developing an effective candidate vaccine from oncosphere antigens may be an economic and effective means.

Several recombinant antigens have been expressed and evaluated as potential vaccine candidates such as 45 W, 18 ku, and 16 ku [29–31]. Among these, TSOL18 was the primary vaccine candidate [13, 32], and the *TSOL18* gene was successfully cloned from the *T. solium* oncosphere for the first time. Its coding sequence was highly homologous to other corresponding protective antigens in the tapeworm family, and it was highly conserved among different strains and between different clones [33, 34]. Subsequently, the Chinese researchers Luo et al. successfully cloned the *TSO18* gene of *T. solium*, and the TSO18-GST protein was successfully expressed in *E. coli* [35]. There have been numerous studies on its vaccine potentialities as a recombinant protein, a DNA vaccine, a recombinant yeast vaccine, a recombinant Bacillus Calmette-Guerin vaccine, and a recombinant Bifidobacterium vaccine [36–40], but none of these vaccines has been successfully developed into available ones. *L. lactis* is a good candidate for the delivery of heterologous proteins in foods, which have many advantages such as safety, simplicity, affordability, easiness to prepare, and practicality [41]. As far as the field of parasite is concerned, there has been no report of a recombinant *L. lactis* vaccine of *T. solium*.

The data showed that the signal peptide SPUSP45 derived from *L. lactis* was a major secretory protein and was currently a signal peptide which improved the efficiency of exogenous protein secretion [42, 43]. The secretory expression scheme of this study introduced the fusion of signal peptide SP and the fusion of propeptide fusion LEISSTCDA into the TSOL18 gene to obtain the SP-TSOL18. The intracellular and extracellular (secretory) expressions were designed and expressed in full length, respectively. All of the expected TSOL18 proteins were obtained, and the specific binding to the rabbit antiserum of the recombinant protein of TSOL18 was found. The above results indicate that recombinant pMG36e-SP-TSOL18/*L. lactis* and pMG36e-TSOL18/*L. lactis* were successfully prepared and the TSOL18 protein expressed in extracellular supernatant and intracellular precipitation has specific antigenicity. It is proved that the signal peptide SP and propeptide fusion sequence LEISSTCDA can effectively realize the extracellular expression of TSOL18 and increase the success rate of protein secretion [44, 45]. This lays the experiment foundation for further research on immune responses induced in mice immunized with these two vaccines.

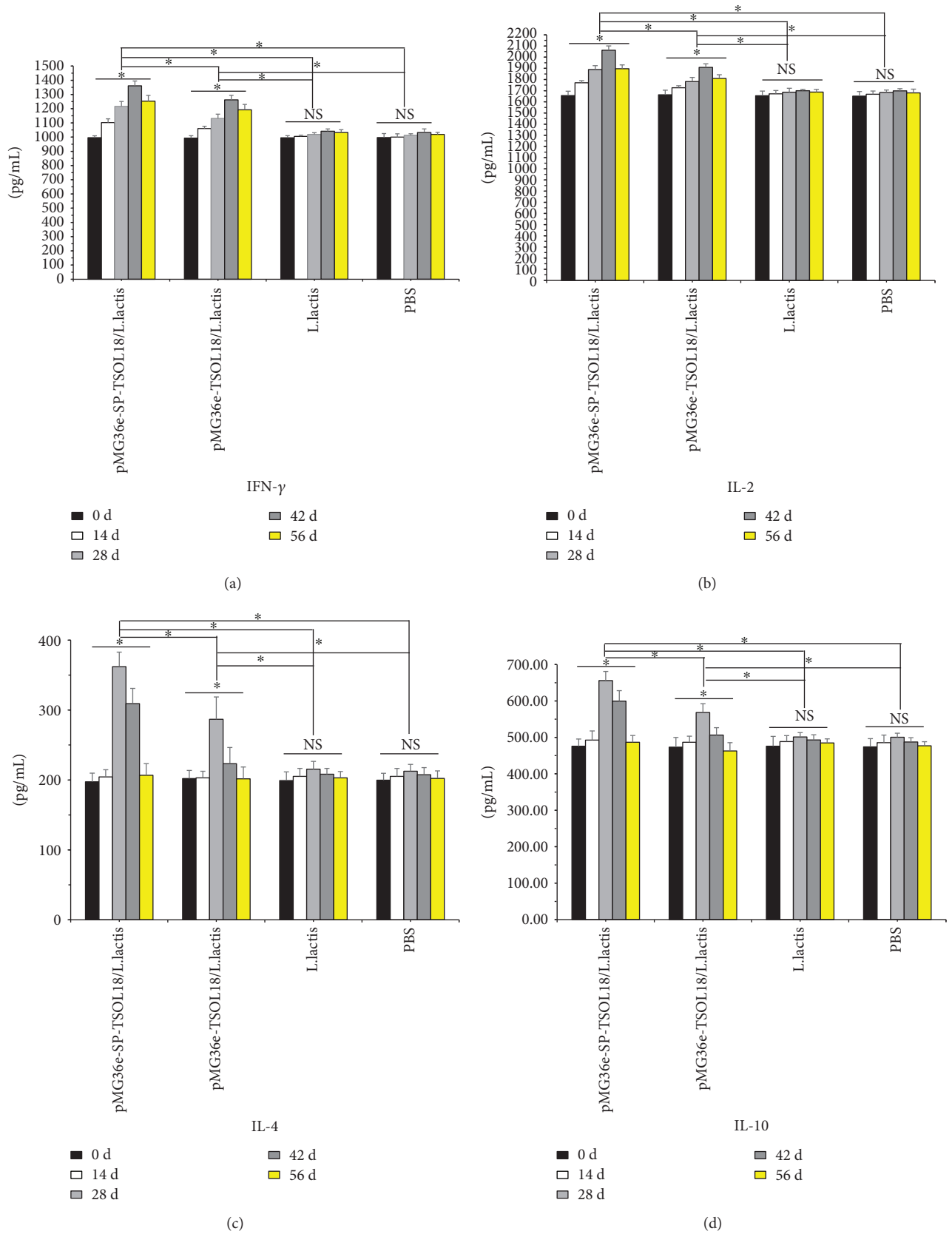

Figure 9: The level of spleen lymphocyte culture supernatant IFN-γ (a), IL-2 (b), IL-4 (c), and IL-10 (d) in immunized mice as measured by ELISA. Spleen lymphocytes were obtained on days 0, 14, 28, 42, and 56 after the first immunization. Inset shows the concentration of four groups at different time points. *Represents the difference between groups. $p < 0.05$. NS = nonsignificant.

It is important to investigate the immune responses generated in mice by recombinant pMG36e-TSOL18/*L. lactis* and pMG36e-SP-TSOL18/*L. lactis* vaccines. Our results demonstrate that these two recombinant vaccines can induce significant immune responses compared to the levels at the time of nonvaccination at day 0, including antibody isotypes, cytokines associated with activation of both $CD4^+$ Th 1 and Th 2 cells, and $CD4^+$ T-cell proliferation.

The lymphocyte proliferation test is an important indicator of cellular immunity. As our results showed, spleen lymphocytes showed a strong proliferative response upon stimulation with antigen or mitogen, and the responsiveness in orally immunized mice peaked at day 42, suggesting that recombinant pMG36e-SP-TSOL18/*L. lactis* and pMG36e-TSOL18/*L. lactis* might induce a MHC classII restricted $CD4^+$ T cell response. The $CD4^+$ T cell may play a role in B-cell differentiation, proliferation, and isotype regulation [46]. Activated $CD4^+$ T cells proliferate and differentiate into effector Th cells. This is consistent with the generation of specific cellular immune responses we observed by recombinant *L. lactis* vaccination [47–49]. In addition, lymphocyte proliferation in response to ConA was enhanced substantially. This may be attributed to the fact that ConA produces polyclonal activation of T lymphocytes. Therefore, it is possible that lymphocytes by ConA stimulation showed stronger proliferation response than that for antigen stimulation.

Cytokines and expression of specific isotypes have important role besides regulating the balance between Th1 and Th2 responses [50]. It is known that IL-2, IFN-γ, and TNF-α are indicators of Th1 response, which promote the production of IgG2a and IgG2b [51, 52], whereas IL-4, IL-5, and IL-10 are indicators of Th2 response, which promote the generation of IgG1, IgG3, and IgE [53–55]. As shown in Figure 9, the stimulation with TSOL18 produced high levels of IFN-γ, IL-2, IL-4, and IL-10 in spleen lymphocytes from all immunized groups. As shown in Figure 6, the antibody responses showed a significantly great increase in IgG, IgG1, and IgG2a in orally vaccinated mice than those in nonvaccinated mice. These results demonstrated that cytokines in spleen lymphocytes and antibody isotype in serum from all immunized mice showed that immunization with these two recombinant *L. lactis* vaccines resulted in stimulation of both Th1 and Th2 immune responses. Data showed that the intestinal mucosa is a site that induces an effective mucosal immune response, and the immunization method is simple and easy to operate [56]. sIgA is the main effector molecule of the mucosal immune system, which has a higher content in intestinal mucosa [57]. Our results showed that the specific sIgA level was significantly increased in the intestinal mucosa and these two recombinant *L. lactis* vaccines could induce a mucosal immune response in all immunized mice.

In conclusion, we have demonstrated that an oral live vaccine prepared in this study is capable of inducing specific humoral immune responses, cellular immune responses, and mucosal immune responses in mice and that *L. lactis* is a potential vaccine vehicle to deliver *T. solium* antigens.

Data Availability

The data used to support the findings of this study are available from the corresponding author upon request.

Conflicts of Interest

There are no conflicts of interest.

Acknowledgments

This study was supported by Outstanding Youth Science and Technology Talent Cultivation Support Project of Guizhou Province Grant no. Qian Sci Con Platform Talent [2017] 5629, Health and Family Planning Commission Research Project of Guizhou Province Grant no. Gzwjkj 2016-1-048 and Science and Technology Cooperation Special Fund Project of Province and City, Grant no. Prov City Sci Con [2015]52.

References

[1] C. Trevisan, B. Devleesschauwer, V. Schmidt, A. S. Winkler, W. Harrison, and M. V. Johansen, "The societal cost of *Taenia solium* cysticercosis in Tanzania," *Acta Tropica*, vol. 165, pp. 141–154, 2017.

[2] K. X. da Guarda, J. M. Costa-Cruz, and I. S. da Costa Barcelos, "Seroprevalence of human cysticercosis in Jataí, Goiás State, Brazil," *The Brazilian Journal of Infectious Diseases*, vol. 22, no. 2, pp. 146–149, 2018.

[3] M. V. Johansen, C. Trevisan, S. Gabriël, P. Magnussen, and U. C. Braae, "Are we ready for *Taenia solium* cysticercosis elimination in sub-Saharan Africa," *Parasitology*, vol. 144, no. 1, pp. 59–64, 2017.

[4] J. Sotelo, "Clinical manifestations, diagnosis, and treatment of neurocysticercosis," *Current Neurology and Neuroscience Reports*, vol. 11, no. 6, pp. 529–535, 2011.

[5] E. Sciutto, G. Fragoso, A. Fleury et al., "*Taenia solium* disease in humans and pigs: an ancient parasitosis disease rooted in developing countries and emerging as a major health problem of global dimensions," *Microbes and Infection*, vol. 2, no. 15, pp. 1875–1890, 2000.

[6] A. J. Xu and J. C. Gu, "The current situation and the prevalent trend of cysticercosis in China," *China Tropical Medicine*, vol. 10, no. 2, pp. 239-240, 2010.

[7] T. Li, P. S. Craig, A. Ito et al., "Taeniasis/cysticercosis in a Tibetan population in Sichuan Province, China," *Acta Tropica*, vol. 100, no. 3, pp. 223–231, 2006.

[8] G. Liu, Y. Li, Y. Cui et al., "Cysticercosis in Shandong Province, Eastern China," *Emerging Infectious Diseases*, vol. 24, no. 2, pp. 384-385, 2018.

[9] T. L. I. Diseases, "Treatment of neurocysticercosis," *The Lancet Infectious Diseases*, vol. 14, no. 8, p. 657, 2014.

[10] E. Sciutto, G. Fragoso, A. de Aluja, M. Hernandez, G. Rosas, and C. Larralde, "Vaccines against cysticercosis," *Current Topics in Medicinal Chemistry*, vol. 8, no. 5, pp. 415–423, 2008.

[11] A. Flisser and M. W. Lightowlers, "Vaccination against *Taenia solium* cysticercosis," *Memórias do Instituto Oswaldo Cruz*, vol. 96, no. 3, pp. 353–356, 2001.

[12] C. X. Ma, H. W. Wang, and Y. X. Yang, "Research progress on the genomics of Taenia solium and candidate vaccines for

cysticercosis," *Chinese Journal of Parasitology and Parasitic Diseases*, vol. 34, no. 2, pp. 161–165, 2016.

[13] J. Ding, Y. Zheng, Y. Wang et al., "Immune responses to a recombinant attenuated *Salmonella typhimurium*, strain expressing a *Taenia solium*, oncosphere antigen TSOL18," *Comparative Immunology Microbiology and Infectious Diseases*, vol. 36, no. 1, pp. 17–23, 2013.

[14] B. Y. Zhou, F. J. Yang, M. C. Liu et al., "Protective immune responses induced by a recombinant BCG-TSOL18 vaccine of Taenia solium in piglets," *Current Immunology*, vol. 37, no. 5, pp. 399–403, 2017.

[15] L. Y. Kun, K. Nomoto, S. Salminen, and S. L. Gorbach, "Handbook of probioties," *International Journal of Food Science and Technology*, vol. 36, no. 2, p. 224, 2010.

[16] K. Szatraj, A. K. Szczepankowska, and M. Chmielewska-Jeznach, "Lactic acid bacteria—promising vaccine vectors: possibilities, limitations, doubts," *Journal of Applied Microbiology*, vol. 123, no. 2, pp. 325–339, 2017.

[17] H.-P. Cao, H.-N. Wang, X. Yang et al., "*Lactococcus lactis* anchoring avian infectious bronchitis virus multi-epitope peptide EpiC induced specific immune responses in chickens," *Bioscience, Biotechnology, and Biochemistry*, vol. 77, no. 7, pp. 1499–1504, 2013.

[18] P. Lee, "Biocontainment strategies for live lactic acid bacteria vaccine vectors," *Bioengineered Bugs*, vol. 1, no. 1, pp. 75–77, 2010.

[19] N. A. Parlane, K. Grage, J. W. Lee, B. M. Buddle, M. Denis, and B. H. A. Rehm, "Production of a particulate hepatitis C vaccine candidate by an engineered *Lactococcus lactis* strain," *Applied and Environmental Microbiology*, vol. 77, no. 24, pp. 8516–8522, 2011.

[20] Y.-B. Yao, W.-T. Yang, G.-L. Yang, and C.-F. Wang, "Progress in application of recombinant genetic engineering LAB," *Chinese Journal of Microecology*, vol. 24, no. 9, pp. 850–852, 2012.

[21] S. Tarahomjoo, "Development of vaccine delivery vehicles based on lactic acid bacteria," *Molecular Biotechnology*, vol. 51, no. 2, pp. 183–199, 2012.

[22] J. Chen, X. Z. Zhong, and W. S. Li, "Evaluation of the optimum immune dose for recombinant Lactococcus lactis expressing P30 of Toxoplasma gondii orally immunized to mice," *Journal of Wenzhou Medical College*, vol. 37, no. 4, pp. 350–353, 2007.

[23] V. B. Pereira, T. D. L. Saraiva, B. M. Souza et al., "Development of a new DNA vaccine based on mycobacterial ESAT-6 antigen delivered by recombinant invasive *Lactococcus lactis* FnBPA+," *Applied Microbiology and Biotechnology*, vol. 99, no. 4, pp. 1817–1826, 2015.

[24] W. Wu, F. Jia, W. Wang, Y. Huang, and Y. Huang, "Antiparasitic treatment of cerebral cysticercosis: lessons and experiences from China," *Parasitology Research*, vol. 112, no. 8, pp. 2879–2890, 2013.

[25] O. H. Del Brutto, T. E. Nash, A. C. White Jr et al., "Revised set of diagnostic criteria for neurocysticercosis (in reply to Garg and Malhotra)," *Journal of the Neurological Sciences*, vol. 373, pp. 350-351, 2017.

[26] M. C. Liu, L. F. He, and B. Y. Zhou, "Progress in genetic engineering vaccine research of Taenia solium," *Chinese Journal of Endemiology*, vol. 33, no. 2, pp. 233–236, 2014.

[27] M. W. Lightowlers, "Vaccines for prevention of cysticercosis," *Acta Tropica*, vol. 87, no. 1, pp. 129–135, 2003.

[28] W. G. Li and Y. T. Chen, "Current condition of researches in recombinant bacteria mediated by lactococcus," *Foreign Medical Science Section of Medgeography*, vol. 37, no. 1, pp. 1–12, 2016.

[29] Agustín Plancarte, A. Flisser, C. G. Gauci, and M. W. Lightowlers, "Vaccination against *Taenia solium* cysticercosis in pigs using native and recombinant oncosphere antigens," *International Journal for Parasitology*, vol. 29, no. 4, pp. 643–647, 1999.

[30] B. Y. Zhou, "Research progress on recombinant antigens of Taenia solium," *Chinese Journal of Zoonoses*, vol. 30, no. 4, pp. 418–422, 2014.

[31] M. Russel, N. A. Linderoth, and A. Sali, "Filamentous phage assembly: variation on a protein export theme," *Gene*, vol. 192, no. 1, pp. 23–32, 1997.

[32] A.-J. Guo, X.-P. Cai, Y.-X. Fang, W.-Z. Jia, X.-N. Luo, and H.-X. Liu, "Construction of gene vaccine vector carrying TSOL18 gene of Taenia solium oncosphere and its immunogenicity," *Acta Veterinaria et Zootechnica Sinica*, vol. 39, no. 7, pp. 945–949, 2008.

[33] C. G. P. Gauci, A. Flisser, and M. W. Lightowlers, "Research note a Taenia solium oncosphere protein homologous to host-protective Taenia ovis and Taenia saginata 18 kDa antigens," *International Journal for Parasitology*, vol. 28, no. 5, pp. 757–760, 1998.

[34] C. G. Gauci, A. Ito, and M. W. Lightowlers, "Conservation of the vaccine antigen gene, *TSOL18*, among genetically variant isolates of *Taenia solium*," *Molecular and Biochemical Parasitology*, vol. 146, no. 1, pp. 101–104, 2006.

[35] X. N. Luo, Y. D. Zheng, X. G. Wu, Y. X. Dou, Z. Z. Jing, and X. P. Cai, "Cloning and expression of TSO18 gene of Taenia solium oncosphere," *Chinese Journal of Zoonoses*, vol. 21, no. 3, pp. 262–264, 2005.

[36] A. Flisser, C. G. Gauci, A. Zoli et al., "Induction of protection against porcine cysticercosis by vaccination with recombinant oncosphere antigens," *Infection and Immunity*, vol. 72, no. 9, pp. 5292–5297, 2004.

[37] Y.-Y. Wang, X.-L. Chang, Z.-Y. Tao et al., "Optimized codon usage enhances the expression and immunogenicity of DNA vaccine encoding Taenia solium oncosphere TSOL18 gene," *Molecular Medicine Reports*, vol. 12, no. 1, pp. 281–288, 2015.

[38] X. Cai, G. Yuan, Y. Zheng et al., "Effective production and purification of the glycosylated TSOL18 antigen, which is protective against pig cysticercosis," *Infection and Immunity*, vol. 76, no. 2, pp. 767–770, 2008.

[39] F. Yang, N. Jiang, L. Zhou, H. Liu, L. Wang, and B. Zhou, "Dynamic observation of immune responses induced in mice by immunization with a recombinant BCG-TSOL18 vaccine of Taenia solium," *Chinese Journal of Endemiology*, vol. 34, no. 12, pp. 878–883, 2015.

[40] B. Zhou, M. Liu, L. Zhou et al., "Protective effect of a mixed recombinant Bifidobacterium vaccine of Taenia solium in piglets," *Chinese Journal of Endemiology*, vol. 36, no. 8, pp. 552–556, 2017.

[41] A. Wyszyńska, P. Kobierecka, J. Bardowski, and E. K. Jagusztyn-Krynicka, "Lactic acid bacteria—20 years exploring their potential as live vectors for mucosal vaccination," *Applied Microbiology and Biotechnology*, vol. 99, no. 7, pp. 2967–2977, 2015.

[42] Y. Le Loir, S. Nouaille, J. Commissaire, L. Bretigny, A. Gruss, and P. Langella, "Signal peptide and propeptide optimization

for heterologous protein secretion in *Lactococcus lactis*," *Applied and Environmental Microbiology*, vol. 67, no. 9, pp. 4119–4127, 2001.

[43] Y. Le Loir, V. Azevedo, S. C. Oliveira et al., "Protein secretion in *Lactococcus lactis*: an efficient way to increase the overall heterologous protein production," *Microbial Cell Factories*, vol. 4, no. 1, p. 2, 2005.

[44] P. Y. Lim, L. L. Tan, D. S. W. Ow, and F. T. Wong, "A propeptide toolbox for secretion optimization of *Flavobacterium meningosepticum* endopeptidase in *Lactococcus lactis*," *Microbial Cell Factories*, vol. 16, no. 1, p. 221, 2017.

[45] Z. Dong, J. Zhang, H. Li, G. du, J. Chen, and B. Lee, "Codon and propeptide optimizations to improve the food-grade expression of bile salt hydrolase in Lactococcus lactis," *Protein and Peptide Letters*, vol. 22, no. 8, pp. 727–735, 2015.

[46] R. M. Horton, H. D. Hunt, S. N. Ho, J. K. Pullen, and L. R. Pease, "Engineering hybrid genes without the use of restriction enzymes: gene splicing by overlap extension," *Gene*, vol. 77, no. 1, pp. 61–68, 1989.

[47] G. F. Asensi, N. F. F. de Sales, F. F. Dutra et al., "Oral immunization with *Lactococcus lactis* secreting attenuated recombinant staphylococcal enterotoxin B induces a protective immune response in a murine model," *Microbial Cell Factories*, vol. 12, no. 1, pp. 32–38, 2013.

[48] L. G. Bermúdez-Humarán, P. Langella, N. G. Cortes-Perez et al., "Intranasal immunization with recombinant *Lactococcus lactis* secreting murine interleukin-12 enhances antigen-specific Th1 cytokine production," *Infection and Immunity*, vol. 71, no. 4, pp. 1887–1896, 2003.

[49] L. Steidler, K. Robinson, L. Chamberlain et al., "Mucosal delivery of murine interleukin-2 (IL-2) and IL-6 by recombinant strains of Lactococcus lactis coexpressing antigen and cytokine," *Infection and Immunity*, vol. 66, no. 7, pp. 3183–3189, 1998.

[50] F. D. Finkelman, J. Holmes, I. M. Katona et al., "Lymphokine control of in vivo immunoglobulin isotype selection," *Annual Review of Immunology*, vol. 8, no. 1, pp. 303–333, 1990.

[51] K. Kuribayashi, M. Tsukiyama, and T. Takenaka, "Secretion patterns of Th1- and Th2-type cytokines in immune deviation caused by dendritic cells," *International Archives of Allergy and Immunology*, vol. 114, no. 1, pp. 30–37, 1997.

[52] T. L. Stevens, A. Bossie, V. M. Sanders et al., "Regulation of antibody isotype secretion by subsets of antigen-specific helper T cells," *Nature*, vol. 334, no. 6179, pp. 255–258, 1988.

[53] F. Brière, C. Servet-Delprat, J. M. Bridon, J. M. Saint-Remy, and J. Banchereau, "Human interleukin 10 induces naive surface immunoglobulin D+ (sIgD+) B cells to secrete IgG1 and IgG3," *Journal of Experimental Medicine*, vol. 179, no. 2, pp. 757–762, 1994.

[54] T. R. Mosmann, H. Cherwinski, M. W. Bond, M. A. Giedlin, and R. L. Coffman, "Two types of murine helper T cell clone. I. Definition according to profiles of lymphokine activities and secreted proteins," *Journal of Immunology*, vol. 136, no. 7, pp. 2348–2357, 1986.

[55] E. Ortona, R. Riganò, B. Buttari et al., "An update on immunodiagnosis of cystic echinococcosis," *Acta Tropica*, vol. 85, no. 2, pp. 165–171, 2003.

[56] B. M. Wittig and M. Zeitz, "The gut as an organ of immunology," *International Journal of Colorectal Disease*, vol. 18, no. 3, pp. 181–187, 2003.

[57] R. D. Newberry and R. G. Lorenz, "Organizing a mucosal defense," *Immunological Reviews*, vol. 206, no. 1, pp. 6–21, 2005.

Hindawi
Journal of Immunology Research
Volume 2018, Article ID 8521060, 15 pages
https://doi.org/10.1155/2018/8521060

Research Article

A Multiagent Alphavirus DNA Vaccine Delivered by Intramuscular Electroporation Elicits Robust and Durable Virus-Specific Immune Responses in Mice and Rabbits and Completely Protects Mice against Lethal Venezuelan, Western, and Eastern Equine Encephalitis Virus Aerosol Challenges

Lesley C. Dupuy[1], **Michelle J. Richards**[1], **Brian D. Livingston**[2], **Drew Hannaman**[2] and **Connie S. Schmaljohn**[1]

[1]*United States Army Medical Research Institute of Infectious Diseases, Fort Detrick, Frederick, MD 21702-5011, USA*
[2]*Ichor Medical Systems, Inc., San Diego, CA 92121-3209, USA*

Correspondence should be addressed to Lesley C. Dupuy; lesley.c.dupuy.ctr@mail.mil

Received 1 February 2018; Accepted 26 April 2018; Published 3 June 2018

Academic Editor: Greg Kirchenbaum

There remains a need for vaccines that can safely and effectively protect against the biological threat agents Venezuelan (VEEV), western (WEEV), and eastern (EEEV) equine encephalitis virus. Previously, we demonstrated that a VEEV DNA vaccine that was optimized for increased antigen expression and delivered by intramuscular (IM) electroporation (EP) elicited robust and durable virus-specific antibody responses in multiple animal species and provided complete protection against VEEV aerosol challenge in mice and nonhuman primates. Here, we performed a comparative evaluation of the immunogenicity and protective efficacy of individual optimized VEEV, WEEV, and EEEV DNA vaccines with that of a 1 : 1 : 1 mixture of these vaccines, which we have termed the 3-EEV DNA vaccine, when delivered by IM EP. The individual DNA vaccines and the 3-EEV DNA vaccine elicited robust and durable virus-specific antibody responses in mice and rabbits and completely protected mice from homologous VEEV, WEEV, and EEEV aerosol challenges. Taken together, the results from these studies demonstrate that the individual VEEV, WEEV, and EEEV DNA vaccines and the 3-EEV DNA vaccine delivered by IM EP provide an effective means of eliciting protection against lethal encephalitic alphavirus infections in a murine model and represent viable next-generation vaccine candidates that warrant further development.

1. Introduction

Venezuelan equine encephalitis virus (VEEV), western equine encephalitis virus (WEEV), and eastern equine encephalitis virus (EEEV) are nonsegmented, positive-sense RNA viruses of the genus *Alphavirus* in the family *Togaviridae* [1]. Naturally transmitted by mosquitoes through rodent or bird hosts, VEEV, WEEV, and EEEV are highly pathogenic for equines and humans and have caused periodic epizootics throughout North, Central, and South America [2]. Human infection with these New World alphaviruses typically results in an acute, incapacitating disease characterized by fever, headache, nausea, myalgia, and malaise [3]. Severe neurological disease, including fatal encephalitis, can also result from VEEV, WEEV, and EEEV infection of humans. Although the human case-fatality rates associated with natural infection are estimated to be low for VEEV (≤1%) and intermediate for WEEV (3–15%), EEEV is the most severe of the arboviral encephalitides with a human case-fatality rate estimated to be from 33% to as high as

75% [4–7]. Moreover, numerous documented laboratory accidents and the results of animal studies have demonstrated that VEEV, WEEV, and EEEV are also highly infectious in aerosols, and infection with aerosolized virus could potentially result in higher human mortality than that observed with natural infection [8–10]. In addition to producing incapacitating or lethal infections and being infectious in aerosols, these encephalitic alphaviruses are also easily grown to high titers in inexpensive and unsophisticated cell culture systems and are considerably stable [4]. Consequently, VEEV, WEEV, and EEEV represent significant biological defense threats and are classified as Category B priority pathogens by both the Centers for Disease Control and Prevention and the National Institute of Allergy and Infectious Diseases.

Although there are no licensed human vaccines for the encephalitic alphaviruses, live-attenuated and formalin-inactivated vaccines are currently utilized under US Food and Drug Administration Investigational New Drug (IND) status to protect laboratory workers and other at-risk personnel. The live-attenuated VEEV IND vaccine, TC-83, provides long-lasting immunity and protection from both subcutaneous and aerosol VEEV challenges; however, it causes significant adverse reactions in approximately 25% of recipients, and approximately 20% of recipients fail to develop a detectable neutralizing antibody response [11, 12]. The formalin-inactivated VEEV IND vaccine derived from TC-83, C-84, and the formalin-inactivated WEEV and EEEV IND vaccines are well tolerated, but they require frequent boosting to elicit and maintain detectable neutralizing antibody responses in humans and have exhibited suboptimal protection against aerosol viral challenge in animal studies [13–15]. In addition, immune interference has been documented when the VEEV, WEEV, and EEEV IND vaccines are administered simultaneously or sequentially in humans [16–18]. Due to the significant limitations associated with these existing vaccine candidates, they are not being pursued for licensure. As a result, development of improved vaccines that can safely and effectively protect humans against encephalitic alphavirus infections is needed [19]. Toward this goal, next-generation encephalitic alphavirus vaccine candidates, including live-attenuated, inactivated, Sindbis virus-based chimeric, virus replicon particle, virus-like particle, DNA, and virus-vectored vaccines, are all currently at various stages of development [20–22].

Vaccination with DNA plasmids that express protein antigens has numerous inherent advantages as a platform for the development of next-generation vaccines. Foremost among the benefits of this approach is that the endogenous expression of target antigens achieved with DNA vaccination can elicit both cellular and humoral immune responses [23–26]. Due to the lack of a host immune response to the vector backbone, DNA vaccines also circumvent issues of preexisting or vaccine-induced vector-based immunity that can deleteriously affect vaccine immunogenicity and safety [27, 28]. From a logistical standpoint, DNA vaccines can be rapidly developed and produced using well-established manufacturing procedures and without the need to propagate a pathogen or inactivate an infectious organism. DNA vaccines can also be readily formulated to generate multiagent vaccines [29]. Importantly, DNA vaccines have also exhibited a favorable safety profile in numerous human clinical trials [30]. Despite these promising characteristics, the primary limitation of this approach has been suboptimal immunogenicity in humans when administered by conventional injection. To address this, we have pursued a range of strategies for enhancing the potency of encephalitic alphavirus DNA vaccines to include investigation of alternative delivery methods and refinement of the coding sequences for the target antigens.

In our previous studies, a DNA vaccine expressing the structural proteins (C-E3-E2-6K-E1) of VEEV subtype IAB (strain Trinidad donkey) from the wild-type genes administered by particle-mediated epidermal delivery (PMED) or "gene gun" elicited strong virus-specific antibody responses in multiple animal species; however, the virus-neutralizing antibody responses were low and only partial protection against homologous VEEV aerosol challenge was observed in mice and nonhuman primates (NHPs) [31–33]. We subsequently employed directed molecular evolution or "gene shuffling" of VEEV, WEEV, and EEEV envelope glycoprotein genes in an attempt to improve the neutralizing antibody response to VEEV, WEEV, and EEEV DNA vaccines. Although DNA vaccines expressing certain variant envelope glycoproteins elicited increased VEEV IAB-neutralizing antibody titers compared to the wild-type parental VEEV DNA vaccine and provided improved protection against VEEV IAB aerosol challenge in mice when delivered by PMED, these studies failed to identify variant envelope glycoprotein DNA vaccines exhibiting increased immunogenicity against WEEV and EEEV as compared to the wild-type parental WEEV and EEEV DNA vaccines [32]. More recently, we optimized the VEEV DNA vaccine for increased mammalian expression of the structural proteins by adapting the gene sequence to reflect the codon bias of highly expressed *Homo sapiens* genes, adjusting regions of very high (>80%) or very low (<30%) guanine-cytosine content, and avoiding *cis*-acting motifs that can negatively impact mRNA expression or stability. Because earlier studies by others indicated that the capsid protein of VEEV and EEEV can be cytotoxic and can inhibit cellular transcription and nuclear import and export in vertebrate cells [34–37], we also eliminated the capsid gene from this construct. When delivered by intramuscular (IM) electroporation (EP), the optimized VEEV DNA vaccine elicited significantly improved virus-specific antibody responses, including increased levels of virus-neutralizing antibodies, in multiple animal species and provided complete protective immunity against homologous VEEV aerosol challenge in mice and NHPs [38]. Subsequently, this VEEV DNA vaccine candidate delivered by IM or intradermal (ID) EP proved to be safe, tolerable, and immunogenic in humans in a recently completed Phase 1 clinical trial [39].

The primary objective of the studies reported here was to apply this approach in an attempt to develop fully protective DNA vaccines for WEEV and EEEV. However, our ultimate goal is to develop a single multiagent vaccine formulation capable of eliciting protective immunity against VEEV,

WEEV, and EEEV. Therefore, we performed a comparative evaluation of the immunogenicity and protective efficacy of the individual optimized VEEV, WEEV, and EEEV DNA vaccines with that of a 1 : 1 : 1 mixture of these vaccines, which we have termed the 3-EEV DNA vaccine, when delivered by IM EP in mice. To directly compare the results obtained for the DNA vaccines with those achieved with the vaccines currently used to protect at-risk personnel, mice vaccinated with the live-attenuated VEEV IND vaccine TC-83 or the formalin-inactivated WEEV or EEEV IND vaccines were also included in these studies. We also assessed the virus-neutralizing antibody responses elicited by the individual VEEV, WEEV, and EEEV and 3-EEV DNA vaccines delivered by IM EP in rabbits.

2. Materials and Methods

2.1. Ethics Statement. All animal research was conducted in compliance with the Animal Welfare Act and other federal statutes and regulations relating to animals and experiments involving animals and adheres to principles stated in the "Guide for the Care and Use of Laboratory Animals," Institute for Laboratory Animal Research, Division of Earth and Life Studies, National Research Council, National Academies Press, Washington, DC, 2011. The United States Army Medical Research Institute of Infectious Diseases (USAMRIID) facility where this animal research was conducted is fully accredited by the Association for the Assessment and Accreditation of Laboratory Animal Care International.

2.2. Vaccines. Codon-optimized WEEV and EEEV structural genes were generated by subjecting the wild-type 26S structural gene sequences minus the capsid protein coding region (E3-E2-6K-E1) of WEEV strain CBA87 (GenBank accession number DQ432026) and EEEV strain FL91-4679 (GenBank accession number AY705241) to the GeneOptimizer™ bioinformatic algorithm for optimized expression in *Homo sapiens* followed by synthesis of the codon-optimized genes (Geneart, Regensburg, Germany) as done previously for VEEV IAB strain Trinidad donkey (GenBank accession number L01442) [38]. As done previously for VEEV [38], WEEV and EEEV DNA vaccine plasmids were then constructed by inserting the synthesized codon-optimized genes into the *Not*I and *Bgl*II restriction sites of the eukaryotic expression vector pWRG7077 (PowderJect, Madison, WI), which has been described previously [40]. Endotoxin-free, research-grade plasmids used in these studies were manufactured by Aldevron (Fargo, ND). The live-attenuated VEEV vaccine TC-83 (NDBR 102, Lot 4 Run 3) used in these studies was manufactured by the National Drug Company (Swiftwater, PA). The inactivated WEEV (TSI-GSD-210, Lot 2-1-91) and EEEV (TSI-GSD-104, Lot 2-1-89) vaccines used in these studies were manufactured by the Government Services Division of the Salk Institute (Swiftwater, PA).

2.3. Animals, Vaccinations, and Blood Collections. Female BALB/c mice (6–8 weeks old, Charles River Laboratories, Wilmington, MA) and New Zealand White rabbits (3–3.5 kg, Charles River Laboratories) were vaccinated with plasmid DNA diluted to the appropriate concentration as described in the text and shown in the figures in calcium- and magnesium-free phosphate-buffered saline (Invitrogen, Carlsbad, CA) by IM EP using the TriGrid™ Delivery System (Ichor Medical Systems, San Diego, CA) as described previously [41]. Briefly, mice anesthetized with IM injection of a diluted acepromazine/ketamine/xylazine mixture or with isoflurane gas were injected into one tibialis anterior muscle with 20 μl of DNA solution using a 3/10 ml U-100 insulin syringe (Becton-Dickinson, Franklin Lakes, NJ) inserted into the center of a TriGrid electrode array with 2.5 mm electrode spacing. Rabbits anesthetized with isoflurane gas were injected into one quadriceps muscle with 0.5 ml of DNA solution using a 1 ml syringe (Becton-Dickinson) inserted into the center of a TriGrid electrode array with 6.0 mm electrode spacing. Injection of DNA was followed immediately by electrical stimulation at amplitude of 250 V/cm, and the total duration was 40 ms over a 400 ms interval. The live-attenuated VEEV vaccine TC-83 and inactivated WEEV and EEEV vaccines were delivered to mice as 0.5 ml doses by subcutaneous injection. At various times after vaccination as described in the text and shown in the figures, blood samples were collected from anesthetized mice by retroorbital or submandibular vein bleed and from anesthetized rabbits by central auricular artery bleed, and serum was recovered by centrifugation.

2.4. ELISA Assays. Total IgG anti-VEEV, WEEV, or EEEV antibody titers were determined for serum samples by indirect enzyme-linked immunosorbent assay (ELISA) using sucrose-purified, irradiated whole VEEV IAB strain Trinidad donkey, WEEV strain CBA87, or EEEV strain FL91-4679 antigen as described previously [42]. Briefly, twofold serial dilutions of sera starting at 1 : 100 were incubated with 250 ng per well of antigen in 96-well plates (Corning, Corning, NY). Horseradish peroxidase- (HRP-) conjugated anti-mouse IgG antibodies (Sigma-Aldrich, St. Louis, MO) and ABTS peroxidase substrate (KPL, Gaithersburg, MD) were used for detection. The optical density at 405 nm was determined using a SpectraMax M2e microplate reader (Molecular Devices, Sunnyvale, CA), and the endpoint titers were calculated in SoftMax Pro v5 (Molecular Devices) using a 4-parameter logistic curve fit and a cutoff value equal to the mean optical density of the negative control samples plus three standard deviations.

2.5. PRNT Assays. Virus-neutralizing antibody titers against VEEV subtypes IAB (strain Trinidad donkey), IC (strain 6119), ID (strain 3880), and IE (strain 68U201) as well as Mucambo virus (MUCV, formerly VEEV subtype IIIA, strain BeAn8), WEEV (strain CBA87), and EEEV (strain FL91-4679) were determined for serum samples by the plaque reduction neutralization test (PRNT) as described previously [42]. Briefly, twofold serial dilutions of sera starting at 1 : 20 were mixed with equal volumes of medium containing ~200 PFU of virus and incubated for 24 h at 4°C. The virus/antibody mixtures were then used to infect confluent monolayers of Vero cells contained in six-well plates (Corning) for 1 h at 37°C after which an overlay

consisting of 0.6% agar (GeneMate, Kaysville, UT) in complete Eagle's basal medium with Earle's salts (EBME) without phenol red (Invitrogen) was added. The plates were stained 24 h later by the addition of an overlay containing 5% neutral red (Gibco, Gaithersburg, MD) and 0.6% agar in complete EBME without phenol red, and the plaques were counted 24 h after staining. The neutralizing antibody titers were then calculated as a reciprocal of the highest dilution resulting in an 80% reduction of the plaque number as compared to virus-only control wells.

2.6. ELISpot Assays. Anti-VEEV cellular immune responses were analyzed by interferon- (IFN-) γ enzyme-linked immunospot (ELISpot) assay using standard methods as described previously [43]. Briefly, splenocytes isolated from individual spleens obtained from vaccinated mice using 100 μM nylon cell strainers (Corning) were resuspended in complete RPMI 1640 medium (Mediatech, Manassas, VA). The resuspended splenocytes from each spleen were then added at a concentration of 2×10^5 cells per well to triplicate wells of MultiScreen$_{HTS}$ IP 0.45 μm PVDF filter 96-well plates (Millipore, Billerica, MA) previously coated with mouse IFN-γ ELISpot capture antibody (Becton-Dickinson). The splenocytes were then cultured with no peptide, 10 μg/ml of concanavalin A (Sigma-Aldrich), 20 μg/ml of β-galactosidase peptide TPHPARIGL (New England Peptide, Gardner, MA), or 10 μg/ml of pooled 15-mer peptides with an 11-base overlap spanning the VEEV IAB E2 or E1 envelope glycoprotein (Pepscan, Lelystad, Netherlands) for 24 h at 37°C with 5% CO_2. Secreted IFN-γ was detected by aspirating the cell suspension and successively incubating the plate for 2 h at room temperature with mouse IFN-γ ELISpot detection antibody (Becton-Dickinson), for 1 h at room temperature with streptavidin-HRP (Becton-Dickinson), and for 20 min at room temperature with 3-amino-9-ethylcarbazole (AEC) substrate (Becton-Dickinson). The substrate reaction was then stopped by washing the plates with deionized H_2O, the plates were dried for 2 h at room temperature, and the spots were enumerated.

2.7. Aerosol Challenge of Mice. Mice were placed into a class III biological safety cabinet located inside a biosafety level 3 containment suite and exposed in a whole-body aerosol chamber to a VEEV, WEEV, or EEEV aerosol created by a Collison nebulizer for 10 min as previously described [44]. Sucrose-purified VEEV IAB strain Trinidad donkey, WEEV strain CBA87, or EEEV strain FL91-4679 was diluted to an appropriate starting concentration in Hank's Balanced Salt Solution (Gibco) containing 1% fetal bovine serum (Thermo Fisher Scientific, Waltham, MA) for use in aerosol generation. Samples collected from the all-glass impinger attached to the aerosol chamber were analyzed by plaque assay on Vero cells using standard methods as previously described to determine the inhaled dose of VEEV, WEEV, or EEEV [45]. The mice were monitored at least twice daily for clinical signs of disease and survival for 28 days postchallenge, and any animals found to meet early endpoint criteria were euthanized.

2.8. Statistical Methods. Log_{10} transformations were applied to whole-virus ELISA titers and $PRNT_{80}$ titers for analyses. Mixed model analysis of variance (ANOVA) with post hoc Tukey's tests was used for pairwise comparisons of ELISA and $PRNT_{80}$ titers and ELISpot counts with the same stimulation condition between groups at each time point. Paired t-tests were used to compare ELISA and $PRNT_{80}$ titers and ELISpot counts for different stimulation conditions within groups. Kaplan-Meier survival analysis and log-rank tests with stepdown Sidak adjustment was used for comparison of survival curves between groups. Fisher's exact tests with stepdown bootstrap adjustment were used to compare survival rates between groups. t-tests with stepdown bootstrap adjustment were used to compare mean times-to-death between groups. The effects of ELISA and $PRNT_{80}$ titers on the probability of survival were assessed using a backwards-selection logistic regression model. Analyses were conducted using SAS v9.2 (SAS Institute, Cary, NC). Statistical significance was defined as $p < 0.05$ in all tests.

3. Results

3.1. VEEV-Specific Antibody Responses of Vaccinated Mice. To first compare the immunogenicity and protective efficacy of the individual optimized VEEV DNA vaccine to that of a 1 : 1 : 1 mixture of the optimized VEEV, WEEV, and EEEV DNA vaccines (3-EEV DNA vaccine), female BALB/c mice ($n = 10$ per group) were vaccinated on days 0 and 21 with 5 μg of the VEEV plasmid or with 5 μg of each of the VEEV, WEEV, and EEEV plasmids (15 μg total) by IM EP. Negative control mice ($n = 10$) were vaccinated on days 0 and 21 with 5 μg of the empty vector plasmid by IM EP. To allow comparison to the live-attenuated VEEV IND vaccine, mice ($n = 10$) received a single administration of the human dose of 0.5 ml of TC-83 (1×10^4 PFU) by subcutaneous injection on day 0. Serum samples obtained on days 21 and 42 were assayed for total IgG anti-VEEV antibodies by ELISA and for VEEV-neutralizing antibodies by PRNT.

Mice vaccinated with either the VEEV DNA or the 3-EEV DNA developed a mean ELISA titer that was significantly above background after a single vaccination ($p < 0.0001$) and that was significantly boosted with a second vaccination ($p < 0.0001$) (Figure 1(a)). In addition, the mean titers of mice vaccinated with the VEEV DNA or the 3-EEV DNA were not significantly different from one another on day 21 ($p = 0.7702$) or 42 ($p = 0.7328$). Although the day 21 mean titer of mice that received TC-83 trended higher than that of mice that received the VEEV DNA vaccine, the difference was not significant ($p = 0.1258$). By day 42, the mean titer of mice that received a second dose of the VEEV DNA was significantly higher than that of mice that received the single dose of TC-83 ($p = 0.0112$). Although the day 21 mean titer of mice vaccinated with the 3-EEV DNA was significantly lower than that of mice vaccinated with TC-83 ($p < 0.0111$), there was no significant difference between the day 42 mean titers of these groups ($p = 0.1456$).

Mice vaccinated with the VEEV DNA developed a mean $PRNT_{80}$ titer that was significantly above background on day 21 ($p = 0.0260$) (Figure 1(b)). In contrast, the day 21 mean

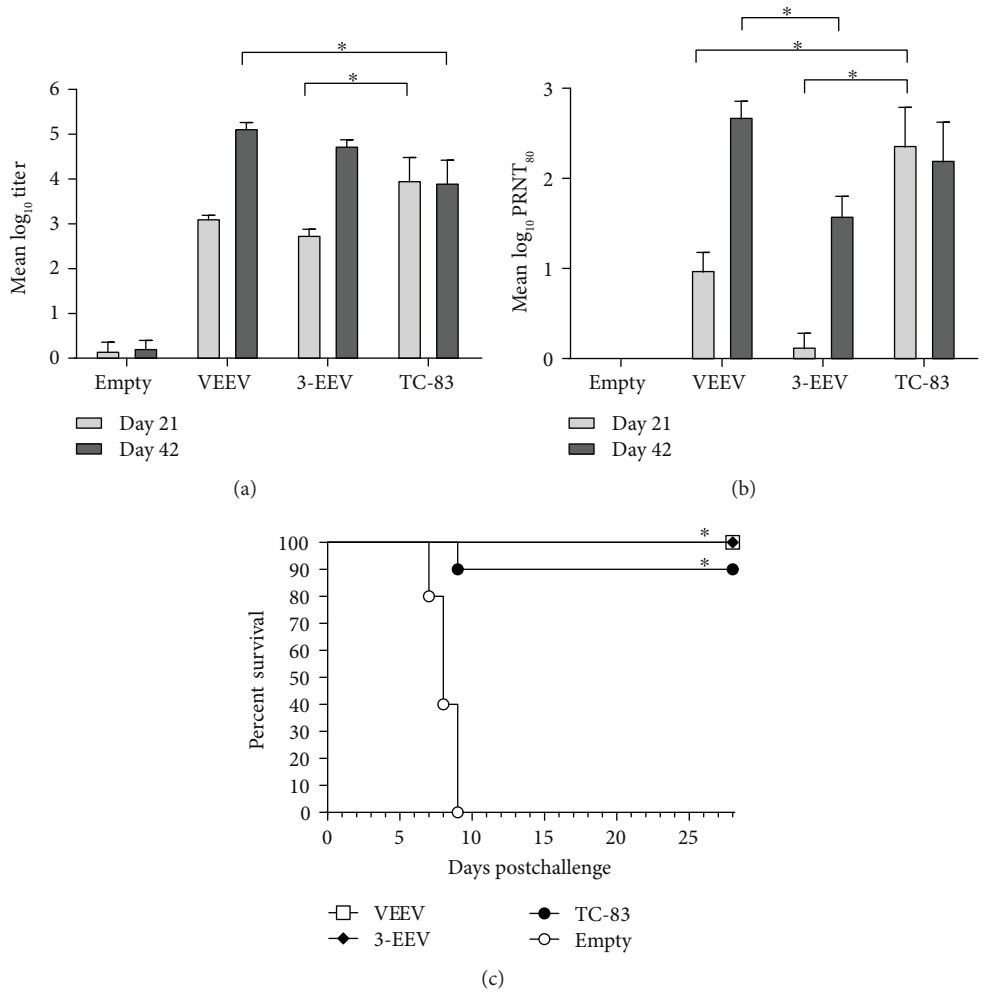

Figure 1: VEEV-specific antibody responses and survival of vaccinated mice. Female BALB/c mice ($n = 10$ per group) were vaccinated on days 0 and 21 with 5 μg of empty vector DNA, 5 μg of the VEEV DNA vaccine, or 5 μg each of the VEEV, WEEV, and EEEV DNA vaccines (3-EEV DNA vaccine) delivered by IM EP or on day 0 with 0.5 ml of the live-attenuated VEEV IND vaccine TC-83 (1×10^4 PFU) delivered by subcutaneous injection. Serum samples obtained on days 21 and 42 were assayed for total IgG anti-VEEV antibodies by ELISA and for VEEV-neutralizing antibodies by PRNT. The group mean $\log_{10}$ ELISA (a) and $PRNT_{80}$ (b) titers along with the standard error of the mean (SEM) are shown. $^*p < 0.05$ for comparison of titers between groups. Four weeks after the final vaccination, the mice were challenged with 1×10^4 PFU (~10,000 LD_{50}) of VEEV IAB strain Trinidad donkey by the aerosol route. Kaplan-Meier survival curves indicating the percentage of surviving mice at each day of the 28-day postchallenge observation period are shown (c). $^*p < 0.05$ for survival rate and survival curve as compared to negative control group.

titers of mice that received the 3-EEV DNA vaccine were low and not significantly different from those that received the empty vector DNA ($p = 0.9768$). Within groups vaccinated with either the VEEV DNA or 3-EEV DNA, the mean titer was significantly higher on day 42 as compared to that on day 21 ($p < 0.0001$). Although the mean titers of mice that received the VEEV DNA or 3-EEV DNA were not significantly different from one another on day 21 ($p = 0.0723$), the day 42 mean titer of mice that received the VEEV DNA was significantly higher than that of mice that received the 3-EEV DNA ($p = 0.0106$). In addition, although the mean titer of mice vaccinated with TC-83 was significantly higher than that of mice vaccinated with the VEEV DNA ($p < 0.0007$) or the 3-EEV DNA ($p < 0.0001$) on day 21, there was no significant difference between the day 42 mean titer of mice vaccinated with TC-83 as compared to that of mice vaccinated with the VEEV DNA ($p = 0.5403$) or 3-EEV DNA ($p = 0.2782$).

3.2. VEEV Aerosol Challenge of Vaccinated Mice. The mice from all groups were challenged on day 49 with 1×10^4 PFU (~10,000 median lethal doses [LD_{50}]) of VEEV IAB strain Trinidad donkey by the aerosol route. Negative control mice that received the empty vector DNA all displayed clinical signs of disease including ruffled fur, weight loss, inactivity, hunched posture, ataxia, and hind limb paralysis, and all succumbed to infection or were euthanized in accordance with early endpoint criteria by day 9 postchallenge (Figure 1(c)). In contrast, mice vaccinated with the VEEV DNA or 3-EEV DNA displayed no clinical signs of disease postchallenge and all survived. Consistent with our previous results [32, 38], 90% of mice vaccinated with TC-83 displayed

no clinical signs of disease postchallenge and survived, and the single mouse from this group that did not survive the challenge had no detectable VEEV-specific antibody response after vaccination. The survival of the VEEV DNA, 3-EEV DNA, and TC-83 groups was significantly higher than that of the empty vector DNA group with respect to survival rate ($p < 0.0001$) and the survival curve ($p = 0.0003$).

3.3. VEEV-Specific Cellular Immune Responses of Vaccinated Mice. Previously, we showed that delivery of the optimized VEEV DNA vaccine by IM EP resulted in cellular immune responses directed against the VEEV E2 and E1 proteins as detected by INFγ-ELISpot assay [38]. To compare the cellular responses elicited by the VEEV DNA vaccine and the 3-EEV DNA vaccine, female BALB/c mice ($n = 6$ per group) were vaccinated on days 0 and 21 with 5 μg of the empty vector plasmid, 5 μg of the VEEV plasmid, or 5 μg of each of the VEEV, WEEV, and EEEV plasmids (15 μg total) delivered by IM EP. On day 35, splenocytes isolated from the vaccinated mice were restimulated with concanavalin A, no peptide, an irrelevant β-galactosidase peptide, or pools of overlapping peptides spanning the VEEV IAB strain Trinidad donkey E2 or E1 envelope glycoproteins and analyzed by IFN-γ ELISpot. After restimulation with concanavalin A, splenocytes from mice from all groups produced spots that were too numerous to count (data not shown). Splenocytes restimulated with no peptide ($p \geq 0.5964$) or with the β-galactosidase peptide ($p \geq 0.1515$) failed to produce significant responses in this assay. After restimulation with the VEEV E2 or E1 peptide pools, splenocytes obtained from mice vaccinated with the VEEV DNA ($p < 0.0001$) or 3-EEV DNA ($p \leq 0.0010$) produced mean IFN-γ responses that were significantly above background (Figure 2). However, the mean IFN-γ responses of mice receiving the VEEV DNA were significantly higher than those of mice receiving the 3-EEV DNA against the E2 ($p = 0.0218$) and E1 ($p = 0.0180$) peptide pools. Consistent with our previous results, the mean IFN-γ responses of splenocytes restimulated with the E2 peptides were significantly higher than those restimulated with the E1 peptides for both the VEEV DNA ($p = 0.0142$) and 3-EEV DNA ($p = 0.0010$) groups.

3.4. WEEV-Specific Antibody Responses of Vaccinated Mice. To perform a comparative evaluation of the immunogenicity and protective efficacy of the individual optimized WEEV DNA and 3-EEV DNA vaccines, female BALB/c mice ($n = 10$ per group) were vaccinated on days 0 and 21 with 5 μg of the WEEV plasmid or with 5 μg of each of the VEEV, WEEV, and EEEV plasmids (15 μg total) by IM EP. Negative control mice ($n = 10$) were vaccinated on days 0 and 21 with 5 μg of the empty vector plasmid by IM EP. To allow comparison to the formalin-inactivated WEEV IND vaccine, mice ($n = 10$) were vaccinated on days 0 and 21 with the human dose of 0.5 ml of this vaccine by subcutaneous injection. Serum samples obtained on days 21 and 42 were assayed for total IgG anti-WEEV antibodies by ELISA and for WEEV-neutralizing antibodies by PRNT.

Mice that received the WEEV DNA vaccine, 3-EEV DNA vaccine, or WEEV IND vaccine developed mean ELISA titers

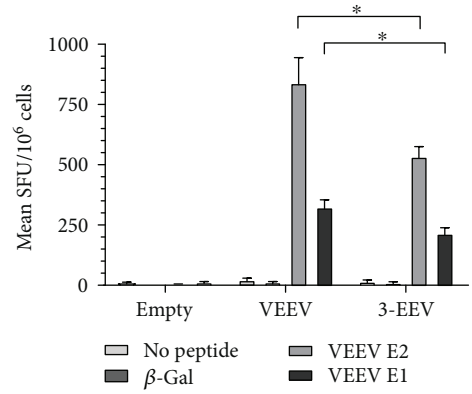

Figure 2: VEEV-specific cellular immune responses of vaccinated mice. Female BALB/c mice ($n = 6$ per group) were vaccinated twice at a 3-week interval with 5 μg of empty vector DNA, 5 μg of the VEEV DNA vaccine, or 5 μg each of the VEEV, WEEV, and EEEV DNA vaccines (3-EEV DNA vaccine) delivered by IM EP. Two weeks after the second vaccination, splenocytes were isolated and restimulated with no peptide, a peptide from the unrelated β-galactosidase protein, or pools of overlapping peptides spanning the VEEV IAB E2 or E1 envelope glycoproteins and analyzed by IFN-γ ELISpot assay. The mean spot forming units (SFU) per 10^6 cells along with the SEM are shown for each group. $^*p < 0.05$ for comparison of spot counts between groups.

that were significantly above background after a single vaccination ($p < 0.0001$) and that were significantly boosted with a second vaccination ($p \leq 0.0007$) (Figure 3(a)). The mean titers of mice vaccinated with the WEEV DNA or 3-EEV DNA were not significantly different from one another on day 21 ($p = 0.1435$) or 42 ($p = 0.4116$). In addition, the mean titers of mice vaccinated with the WEEV DNA or 3-EEV DNA were statistically higher than that of mice receiving the WEEV IND vaccine at day 21 ($p \leq 0.0004$) and 42 ($p < 0.0001$).

Mice vaccinated with the WEEV DNA developed a mean $PRNT_{80}$ titer that was significantly above background after a single vaccination ($p < 0.0001$) and that was significantly boosted with a second vaccination ($p = 0.0011$) (Figure 3(b)). In contrast, although mice that received a single vaccination with the 3-EEV DNA did not develop a mean titer that was significantly above background ($p = 0.4304$), the mean titer of these mice was significantly boosted ($p = 0.0004$) and was significantly above background after a second vaccination ($p < 0.0001$). Although the mean titer of mice that received the WEEV IND vaccine was significantly above background after a single vaccination ($p < 0.0001$), the mean titer was not significantly boosted with a second vaccination ($p = 0.0596$). In comparing the mean titers between groups, the titers of mice that received the WEEV DNA or WEEV IND vaccine were not significantly different on day 21 ($p = 0.8361$) or 42 ($p = 0.1557$). However, the mean titer of mice that received the 3-EEV DNA vaccine was significantly lower than those of mice that received the WEEV DNA or WEEV IND vaccine at day 21 ($p < 0.0001$) and 42 ($p \leq 0.0004$).

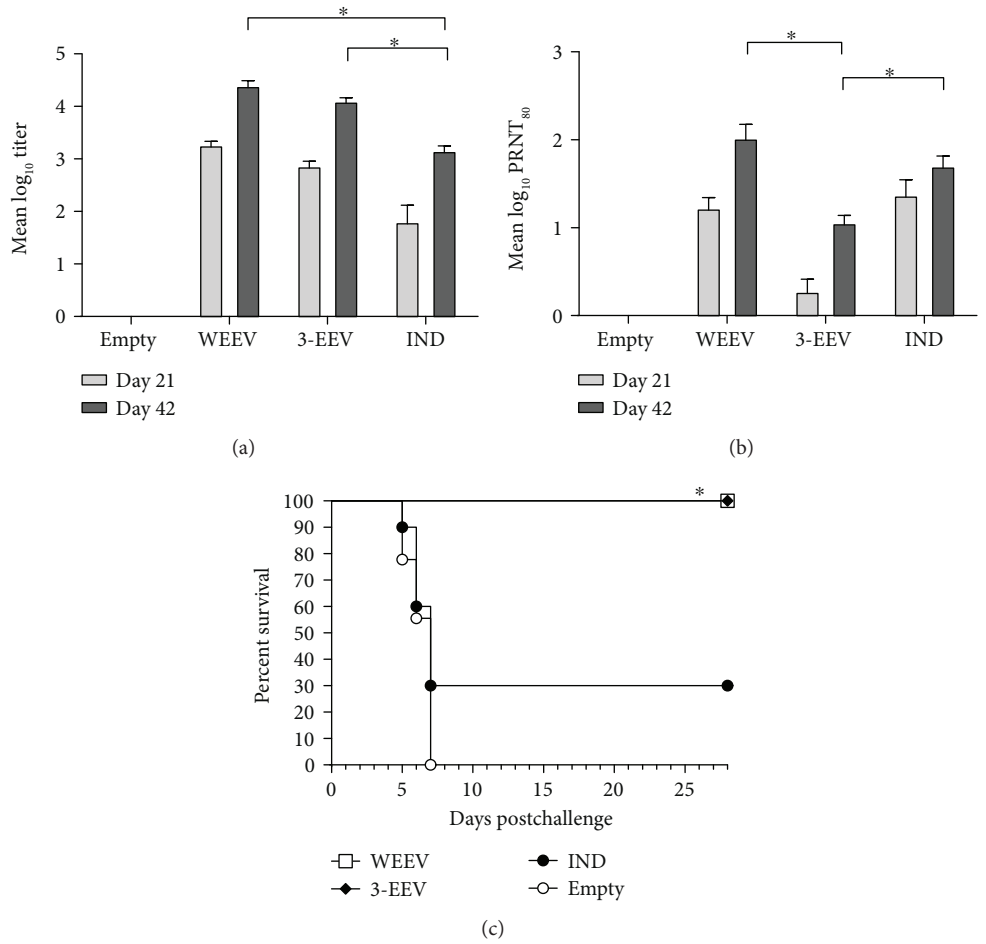

Figure 3: WEEV-specific antibody responses and survival of vaccinated mice. Female BALB/c mice ($n = 10$ per group) were vaccinated on days 0 and 21 with 5 μg of empty vector DNA, 5 μg of the WEEV DNA vaccine, or 5 μg each of the VEEV, WEEV, and EEEV DNA vaccines (3-EEV DNA vaccine) delivered by IM EP or 0.5 ml of the formalin-inactivated WEEV IND vaccine delivered by subcutaneous injection. Serum samples obtained on days 21 and 42 were assayed for total IgG anti-WEEV antibodies by ELISA and for WEEV-neutralizing antibodies by PRNT. The group mean $\log_{10}$ ELISA (a) and $PRNT_{80}$ (b) titers along with the SEM are shown. $^*p < 0.05$ for comparison of titers between groups. Four weeks after the final vaccination, the mice were challenged with 2×10^4 PFU (~500 LD_{50}) of WEEV strain CBA87 by the aerosol route. Kaplan-Meier survival curves indicating the percentage of surviving mice at each day of the 28-day postchallenge observation period are shown (c). $^*p < 0.05$ for survival rate as compared to negative control group.

3.5. WEEV Aerosol Challenge of Vaccinated Mice. The mice from all groups were challenged on day 49 with 2×10^4 PFU (~500 LD_{50}) of WEEV strain CBA87 by the aerosol route. Negative control mice that received the empty vector DNA all displayed clinical signs of disease including ruffled fur, weight loss, inactivity, hunched posture, ataxia, and hind limb paralysis, and all succumbed to infection or were euthanized in accordance with early endpoint criteria by day 7 postchallenge (Figure 3(c)). In contrast, mice vaccinated with the WEEV DNA or 3-EEV DNA displayed no clinical signs of disease postchallenge and all survived. Consistent with our previous unpublished results, only 30% of the mice that received the WEEV IND vaccine survived the challenge. The survival of the WEEV DNA and 3-EEV DNA groups was significantly higher than that of the WEEV IND group with respect to the survival rate ($p = 0.0030$) and survival curve ($p = 0.0056$). In addition, the survival of the empty vector DNA and WEEV IND groups were not significantly different with respect to the survival rate ($p = 0.2101$), mean time-to-death ($p = 0.8420$), and survival curve ($p = 0.2856$).

3.6. EEEV-Specific Antibody Responses of Vaccinated Mice. We also completed a comparative evaluation of the immunogenicity and protective efficacy of the individual optimized EEEV DNA and 3-EEV DNA vaccines delivered by IM EP in mice. In our unpublished studies, it has proven difficult to elicit protective immunity in mice against EEEV aerosol challenge. Consequently, for this study, we vaccinated female BALB/c mice ($n = 10$ per group) three times, instead of twice, on days 0, 21, and 42 with 5 μg of the EEEV plasmid or with 5 μg of each of the VEEV, WEEV, and EEEV plasmids (15 μg total) by IM EP. Negative control mice ($n = 10$) were vaccinated on days 0, 21, and 42 with 5 μg of the empty vector plasmid by IM EP. To allow comparison to the formalin-inactivated EEEV IND vaccine, mice ($n = 10$) were vaccinated on days 0, 21, and 42 with the human dose of 0.5 ml

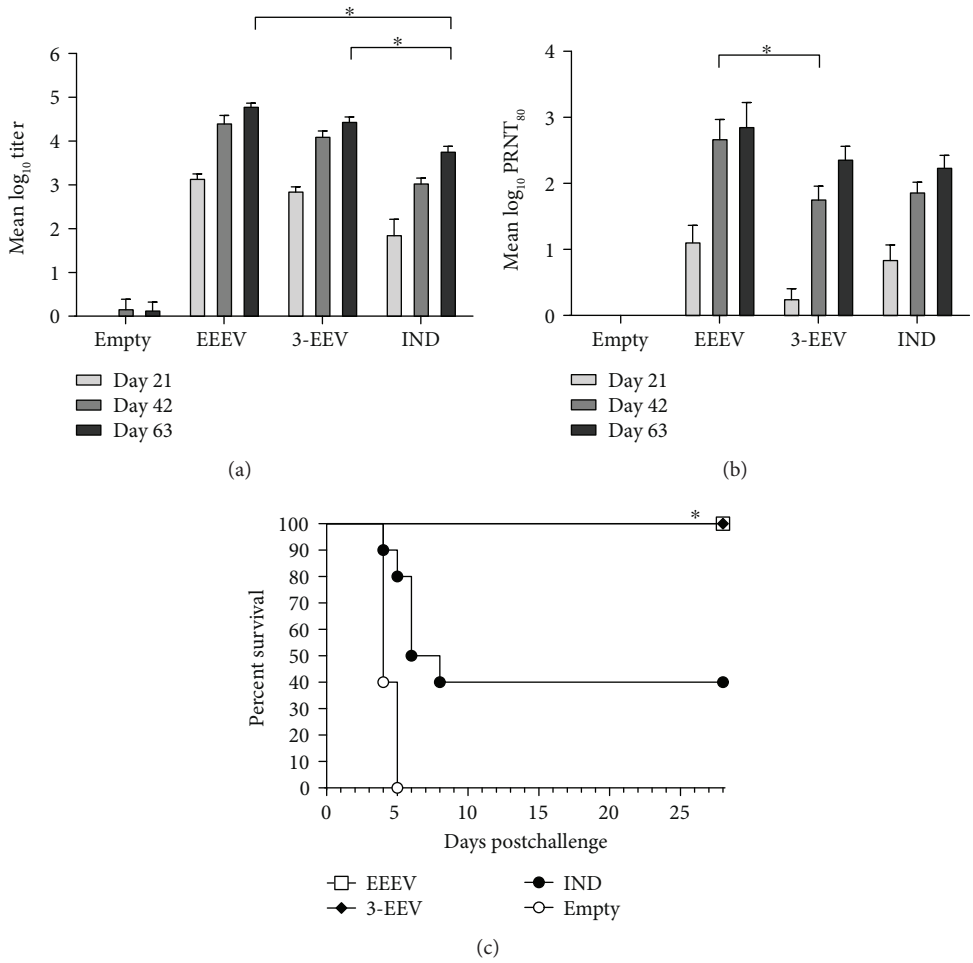

Figure 4: EEEV-specific antibody responses and survival of vaccinated mice. Female BALB/c mice ($n = 10$ per group) were vaccinated on days 0, 21, and 42 with 5 μg of empty vector DNA, 5 μg of the EEEV DNA vaccine, or 5 μg each of the VEEV, WEEV, and EEEV DNA vaccines (3-EEV DNA vaccine) delivered by IM EP or 0.5 ml of the formalin-inactivated EEEV IND vaccine delivered by subcutaneous injection. Serum samples obtained on days 21, 42, and 63 were assayed for total IgG anti-EEEV antibodies by ELISA and for EEEV-neutralizing antibodies by PRNT. The group mean $\log_{10}$ ELISA (a) and $PRNT_{80}$ (b) titers along with the SEM are shown. $^*p < 0.05$ for comparison of titers between groups. Four weeks after the final vaccination, the mice were challenged with 1×10^5 PFU (~3000 LD_{50}) of EEEV strain FL91-4679 by the aerosol route. Kaplan-Meier survival curves indicating the percentage of surviving mice at each day of the 28-day postchallenge observation period are shown (c). $^*p < 0.05$ for survival rate as compared to negative control group.

of this vaccine by subcutaneous injection. Serum samples obtained on days 21, 42, and 63 were assayed for total IgG anti-EEEV antibodies by ELISA and for EEEV-neutralizing antibodies by PRNT.

Mice that received the EEEV DNA vaccine, 3-EEV DNA vaccine, or EEEV IND vaccine developed mean ELISA titers that were significantly above background after a single vaccination ($p < 0.0001$) and that were significantly boosted with a second vaccination ($p \leq 0.0040$) (Figure 4(a)). While the mean titer of mice vaccinated with the EEEV DNA was not significantly boosted with a third vaccination ($p = 0.0508$), those of mice that received the 3-EEV DNA or EEEV IND vaccine were significantly higher on day 63 as compared to day 42 ($p \leq 0.0432$). In comparing the mean titers between groups, the titers of mice vaccinated with the EEEV DNA or 3-EEV DNA were not significantly different from one another on day 21 ($p = 0.9280$), 42 ($p = 0.7396$), or 63 ($p = 0.1267$). In addition, the mean titers of mice vaccinated with the EEEV DNA or 3-EEV DNA were significantly higher than those of mice receiving the EEEV IND vaccine on day 21 ($p \leq 0.0021$), 42 ($p < 0.0001$), and 63 ($p < 0.0001$).

Mice that received the EEEV DNA vaccine developed a mean $PRNT_{80}$ titer that was significantly above background after a single vaccination ($p = 0.0030$) and significantly boosted with a second vaccination ($p < 0.0001$), but not significantly boosted with a third vaccination ($p = 0.4473$) (Figure 4(b)). Although the mean titers of mice that received the 3-EEV DNA or EEEV IND vaccine were not significantly above background after a single vaccination ($p \geq 0.0538$), they were significantly boosted ($p \leq 0.0002$) and significantly above background after a second vaccination ($p < 0.0001$). The mean titers of the 3-EEV DNA or EEEV IND vaccine groups were also significantly boosted with a third vaccination ($p \leq 0.0310$). In comparing the mean titers between

groups, the titers of mice vaccinated with the EEEV DNA or 3-EEV DNA were not significantly different from one another on day 21 ($p = 0.0533$) and 63 ($p = 0.5463$), while the day 42 titer of the EEEV DNA group was significantly higher than that of the 3-EEV DNA group ($p = 0.0346$). In addition, the mean titer of mice that received the EEEV IND vaccine was not significantly different from those of mice vaccinated with the EEEV DNA or 3-EEV DNA at day 21 ($p \geq 0.4041$), 42 ($p \geq 0.0927$), or 63 ($p \geq 0.2960$).

3.7. EEEV Aerosol Challenge of Vaccinated Mice. The mice from all groups were challenged on day 70 with 1×10^5 PFU (~3000 LD_{50}) of EEEV strain FL91-4679 by the aerosol route. Negative control mice that received the empty vector DNA all displayed clinical signs of disease including ruffled fur, weight loss, inactivity, hunched posture, ataxia, and hind limb paralysis, and all succumbed to infection or were euthanized in accordance with early endpoint criteria by day 5 postchallenge (Figure 4(c)). In contrast, mice vaccinated with the EEEV DNA or 3-EEV DNA displayed no clinical signs of disease postchallenge and all survived. Consistent with our previous unpublished results, only 40% of the mice that received the EEEV IND vaccine survived the challenge. The survival rates of the EEEV DNA and 3-EEV DNA groups were significantly higher than that of the EEEV IND group ($p = 0.0329$). Although the survival rates of mice receiving the EEEV IND group and the empty vector DNA group were not statistically different ($p = 0.3025$), the survival of the EEEV IND group was significantly enhanced relative to that of the empty vector DNA group with respect to the mean time-to-death ($p = 0.0452$) and the survival curve ($p = 0.0066$). Of note, mice that received only two vaccinations with the EEEV DNA vaccine were also completely protected from challenge (data not shown).

3.8. Virus-Specific Antibody Responses of Vaccinated Rabbits. To perform a comparative evaluation of the immunogenicity of the individual optimized VEEV, WEEV, and EEEV DNA vaccines and the 3-EEV DNA vaccine in an additional animal model that permits administration of higher DNA doses that are more similar to those expected to be delivered to humans and is better suited to assessment of antibody durability, we also completed a study in rabbits. New Zealand White rabbits ($n = 5$ per group) were vaccinated on days 0, 28, and 230 with 0.5 mg of the VEEV, WEEV, or EEEV plasmid or with 0.5 mg each of the VEEV, WEEV, and EEEV DNA plasmids (1.5 mg total) delivered by IM EP. Serum samples obtained on days 27, 42, 230, 266, and 349 were assayed for neutralizing antibodies against VEEV, WEEV, or EEEV by PRNT.

Rabbits that received the VEEV DNA vaccine or 3-EEV DNA vaccine developed mean $PRNT_{80}$ titers against VEEV that were significantly above background after a single vaccination ($p < 0.0001$) and significantly boosted with a second vaccination ($p < 0.0001$) (Figure 5(a)). While the day 230 mean titer of rabbits vaccinated with the VEEV DNA was significantly lower than that on day 42 ($p = 0.0004$), there was no significant difference in the day 42 and day 230 mean titers for rabbits vaccinated with the 3-EEV DNA ($p = 0.2827$). The mean titer of rabbits that received the VEEV DNA was also significantly boosted with the long-range boosting vaccination performed on day 230 ($p = 0.0133$). Although the long-range boosting vaccination increased the mean $\log_{10}$ titer of rabbits that received the 3-EEV DNA from 2.80 on day 230 to 2.97 on day 266, this increase was not statistically significant ($p > 0.9999$). In addition, there was no significant difference in the day 266 and day 349 mean titers of rabbits vaccinated with the VEEV DNA or 3-EEV DNA within these groups ($p > 0.9999$). In comparing the mean titers between groups, there was no significant difference in the titers of rabbits vaccinated with the VEEV DNA or 3-EEV DNA at day 27 ($p = 0.523$), 42 ($p = 0.3935$), and 230 ($p > 0.9999$). However, after the long-range boosting vaccination, the mean titers of rabbits that received the VEEV DNA vaccine were significantly higher than those of rabbits that received the 3-EEV DNA vaccine at day 266 ($p = 0.0252$) and 349 ($p = 0.0464$).

To assess the potential for the subtype IAB-based VEEV DNA vaccine to provide protection against heterologous VEEV strains, we measured the neutralizing activity of the day 42 samples from rabbits vaccinated with the VEEV DNA or 3-EEV DNA against VEEV subtypes IC, ID, and IE and MUCV (formerly VEEV IIIA). Within groups receiving the VEEV DNA or 3-EEV DNA, there was no significant difference in the mean $PRNT_{80}$ titers against VEEV subtypes IAB, IC, ID, or IE or MUCV ($p \geq 0.0587$) (Figure 5(b)). In comparing the mean titers between groups, there was no significant difference in the titers of rabbits vaccinated with the VEEV DNA or 3-EEV DNA against VEEV subtypes IAB, IC, ID, or IE or MUCV ($p \geq 0.2802$).

Rabbits that received the WEEV DNA vaccine or 3-EEV DNA vaccine developed mean $PRNT_{80}$ titers against WEEV that were significantly above background after a single vaccination ($p < 0.0001$) (Figure 5(c)). Although the mean titer of rabbits vaccinated with the WEEV DNA was significantly boosted with a second vaccination ($p = 0.005$), there was no significant difference in the day 27 and day 42 mean titers of rabbits vaccinated with the 3-EEV DNA ($p = 0.394$). There was also no significant difference in the day 42 and day 230 mean titers for rabbits vaccinated with the WEEV DNA ($p = 0.7824$) or 3-EEV DNA ($p = 0.9976$). Although the long-range boosting vaccination increased the mean $\log_{10}$ titer from 3.10 on day 230 to 3.93 on day 266 for rabbits receiving the WEEV DNA and from 2.53 on day 230 to 3.50 on day 266 for rabbits receiving the 3-EEV DNA, these increases were not statistically significant ($p \geq 0.1551$). In addition, there was no significant difference in the day 266 and day 349 mean titers of rabbits vaccinated with the WEEV DNA or 3-EEV DNA within these groups ($p \geq 0.9917$). In comparing the mean titers between groups, there was no significant difference in the titers of rabbits vaccinated with the WEEV DNA or 3-EEV DNA at any of the time points ($p \geq 0.3404$).

Rabbits that received the EEEV DNA vaccine or 3-EEV DNA vaccine developed mean $PRNT_{80}$ titers against EEEV that were significantly above background after a single vaccination ($p \leq 0.0013$) (Figure 5(d)). Although the mean titer of rabbits vaccinated with the EEEV DNA was significantly

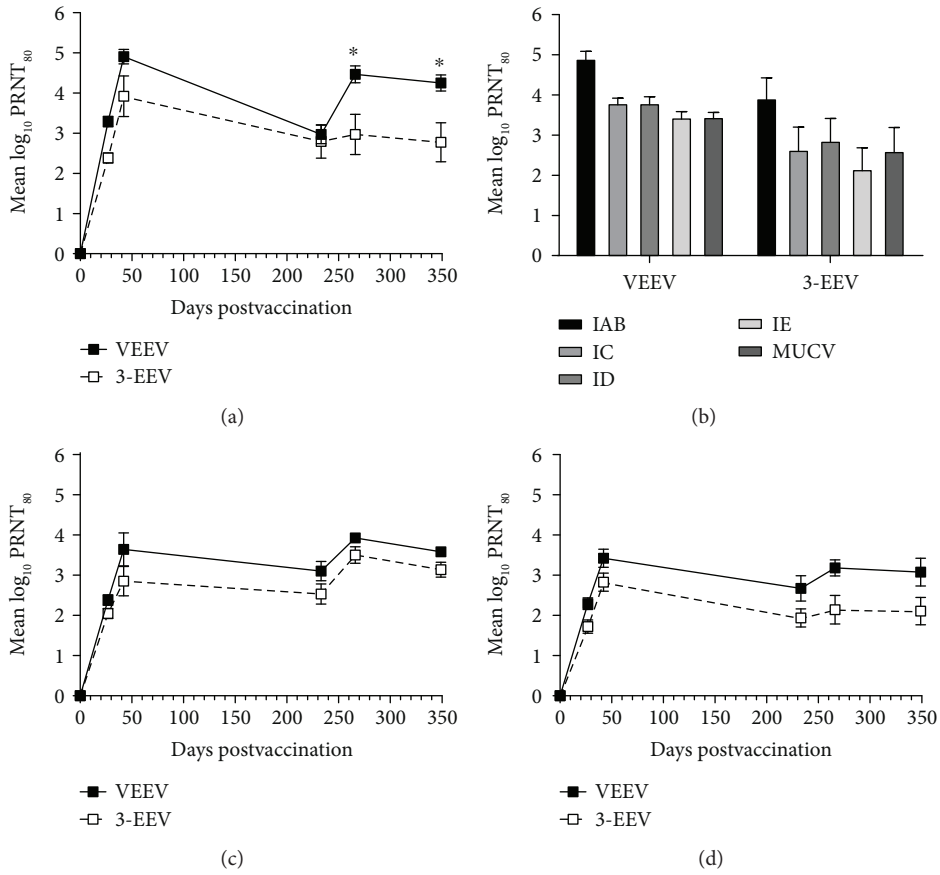

Figure 5: Virus-neutralizing antibody responses of vaccinated rabbits. New Zealand White rabbits ($n = 5$ per group) were vaccinated on days 0, 28, and 230 with 0.5 mg of the VEEV, WEEV, or EEEV DNA vaccine or with 0.5 mg each of the VEEV, WEEV, and EEEV DNA vaccines (3-EEV DNA vaccine) delivered by IM EP. Serum samples obtained on days 27, 42, 230, 266, and 349 were assayed for neutralizing antibodies against VEEV IAB (a), WEEV (c), or EEEV (d) by PRNT. The day 42 serum samples from rabbits vaccinated with the VEEV DNA or 3-EEV DNA were also assayed for neutralizing activity against heterologous VEEV subtypes IC, ID, and IE and MUCV (b) by PRNT. The group mean $\log_{10}$ $PRNT_{80}$ titers along with the SEM are shown. $^{*}p < 0.05$ for comparison of titers between groups.

boosted with a second vaccination ($p = 0.048$), there was no significant difference in the mean titers at day 27 and day 42 for rabbits vaccinated with the 3-EEV DNA ($p = 0.135$). There was also no significant difference in the day 42 and day 230 mean titers for rabbits vaccinated with the EEEV DNA ($p = 0.4883$) or 3-EEV DNA ($p = 0.3987$). Although the long-range boosting vaccination increased the mean $\log_{10}$ titer from 2.67 on day 230 to 3.18 on day 266 for rabbits receiving the EEEV DNA and from 1.94 on day 230 to 2.14 on day 266 for rabbits receiving the 3-EEV DNA, these increases were not statistically significant ($p \geq 0.9108$). In addition, there was no significant difference in the day 266 and day 349 mean titers of rabbits vaccinated with the EEEV DNA or 3-EEV DNA within these groups ($p > 0.9999$). In comparing the mean titers between groups, there was no significant difference in the titers of rabbits vaccinated with the EEEV DNA or 3-EEV DNA at any of the time points ($p \geq 0.1383$).

4. Discussion

The results of our previous studies demonstrated that a strategy that encompassed optimization of the construct for increased antigen expression and EP-based delivery successfully improved the immunogenicity and protective efficacy of a VEEV DNA vaccine [38]. Consistent with those results, mice that received two doses of the optimized VEEV DNA vaccine delivered by IM EP in the present studies developed robust virus-specific total IgG and virus-neutralizing antibody responses. Comparison against mice that received a single vaccination with a human dose of the live-attenuated VEEV IND vaccine TC-83 revealed that the virus-specific total IgG titers elicited by the VEEV DNA vaccine were significantly higher than those observed for TC-83, while the virus-neutralizing antibody responses were similar between these two vaccination regimens. Also consistent with our previous results, mice that received the VEEV DNA vaccine were completely protected against lethal VEEV aerosol challenge, whereas 90% of mice receiving TC-83 were protected. In a similar manner, mice that received the optimized WEEV or EEEV DNA vaccine delivered by IM EP developed robust virus-specific total IgG and virus-neutralizing antibody responses. Comparison against mice that received the same number of vaccinations with human doses of the formalin-inactivated WEEV or EEEV IND vaccine revealed that the virus-specific total IgG titers elicited

by the WEEV or EEEV DNA vaccine were significantly higher than those observed for the respective WEEV or EEEV IND vaccine, while the virus-neutralizing antibody responses were similar between these vaccination regimens. Mice that received the WEEV or EEEV DNA vaccine were also completely protected from lethal homologous WEEV or EEEV aerosol challenge and exhibited significantly higher survival rates than were mice that received the WEEV or EEEV IND vaccine, which only protected 30% and 40% of vaccinated mice, respectively. These results demonstrate that this vaccination strategy was also successful in developing protective DNA vaccines for WEEV and EEEV that provide significantly increased protection against lethal viral aerosol challenge in mice compared to the formalin-inactivated IND vaccines.

In the present studies, we also evaluated whether the optimized VEEV, WEEV, and EEEV DNA vaccines could elicit immune responses adequate for protection when administered in a multiagent formulation. While the virus-specific total IgG antibody titers of mice that received the individual VEEV, WEEV, or EEEV DNA vaccine were similar to those of mice that received the 3-EEV DNA vaccine, the virus-neutralizing antibody titers were significantly lower in mice that received the 3-EEV DNA vaccine compared to those that received the individual VEEV or WEEV DNA vaccine. Therefore, it is possible that some level of interference occurs when the three different but related vaccine antigens are expressed in the same target tissue. However, this may also be a function of competition for antigen production based on the larger amount of DNA delivered to the same tissue for the 3-EEV DNA as compared to the individual DNA vaccines. Despite these observed differences, all of the mice that received the 3-EEV DNA vaccine had detectable neutralizing antibody responses against VEEV, WEEV, and EEEV and were completely protected against lethal VEEV, WEEV, and EEEV aerosol challenge. As observed for the individual VEEV, WEEV, and EEEV DNA vaccines, the 3-EEV DNA vaccine also provided similar levels of protection against lethal VEEV aerosol challenge as compared to TC-83 and significantly increased protection against lethal WEEV and EEEV aerosol challenge as compared to the formalin-inactivated WEEV and EEEV IND vaccines in mice. Furthermore, there was no significant difference in the neutralizing antibody responses against VEEV, WEEV, and EEEV elicited by the individual DNA vaccines or 3-EEV DNA vaccine after the initial vaccination series in rabbits. These results provide important preliminary evidence to support the potential use of the 3-EEV DNA as a single multiagent vaccine formulation capable of eliciting protective immunity against VEEV, WEEV, and EEEV.

Of note, there have been previous published reports on the evaluation of WEEV DNA vaccines in mice. In one report, a DNA vaccine expressing the structural proteins (C-E3-E2-6K-E1) of WEEV strain 71V-1658 from the wild-type genes administered in four 5 μg doses by PMED provided complete protection against homologous intranasal challenge with 1.5×10^3 PFU (25 LD_{50}) of virus [46]. However, this vaccine provided only partial protection against similar challenges with the heterologous WEEV strains CBA87 and Fleming. Although cell-mediated immune responses against the E2 and E1 antigens were elicited by this DNA vaccine as measured by lymphocyte proliferation assays, no virus-specific antibody responses were detected by ELISA. In a subsequent report by this group, DNA vaccines expressing the C-E3-E2-6K-E1, E3-E2-6K-E1, or 6K-E1 proteins of WEEV strain 71V-1658 from the wild-type genes administered in three 2 μg doses by PMED provided complete protection against homologous intranasal challenge with the same 1.5×10^3 PFU (25 LD_{50}) dose of virus, while a DNA vaccine expressing the E3-E2 proteins did not provide any protection [47]. Although the DNA vaccines expressing the C-E3-E2-6K-E1, E3-E2-6K-E1, or 6K-E1 proteins provided significant protection against a similar challenge with the CBA87 strain, only the DNA vaccines expressing the C-E3-E2-6K-E1 and E3-E2-6K-E1 proteins provided significant protection against the Fleming strain. In addition, the DNA vaccine expressing the E3-E2-6K-E1 proteins provided better protection against this strain than the DNA vaccine expressing C-E3-E2-6K-E1. In our studies, we showed that two administrations of a 5 μg dose of a DNA vaccine expressing E3-E2-6K-E1 proteins of WEEV CBA87 from codon-optimized genes delivered by IM EP provided complete protection against aerosol challenge with 2×10^4 PFU (~500 LD_{50}) of homologous virus. Taken together, the described results of the studies previously performed by others and of those reported here support the use of E3-E2-6K-E1 as the most appropriate target antigens for a successful DNA vaccination strategy against encephalitic alphaviruses. However, our results indicate that it is likely that codon optimization of the structural genes in the construct along with the efficiency of EP-based delivery contributed to the ability of the DNA vaccine evaluated here to protect against the higher challenge dose with fewer DNA administrations. Because no immunogenicity results were provided in the report by Gauci et al., it is not possible to make an indirect comparison of the immunogenicity of the previously tested WEEV DNA vaccines with that of the one we evaluated here.

It should also be noted that evaluation of individual and combined VEEV, WEEV, and EEEV virus replicon particle (VRP) vaccines in mice and NHPs has also been recently reported. In these experiments, the individual VRP vaccines delivered twice at a dose of 1×10^7 infectious units elicited strong and durable virus-specific antibody responses in mice as measured by ELISA and PRNT and provided complete protection against homologous lethal VEEV, WEEV, and EEEV aerosol challenges [48]. The VEEV VRP vaccine based on the IAB strain was also shown to elicit durable protective immunity in mice against lethal aerosol challenge with the heterologous VEEV strain IE and MUCV. In the murine studies, there were also no significant differences in the antibody or protection levels when the VRP vaccines were administered in combination. While the individual VEEV and EEEV and combination VRP vaccines protected NHPs against homologous VEEV and EEEV aerosol challenge, the protection elicited by the WEEV or combination VRP vaccines against WEEV aerosol challenge was not significantly different from that of mock-vaccinated controls. The DNA vaccines evaluated in our studies reported here compare

favorably to the VRP vaccines in that complete protection in mice against the same challenge doses of aerosolized VEEV, WEEV, and EEEV was also afforded by the individual and 3-EEV DNA vaccines. Although we did not directly assess the duration of protective immunity elicited by the individual and 3-EEV DNA vaccines in the mouse studies reported here, our results in rabbits demonstrated that virus-neutralizing antibody titers elicited by these vaccines remained significantly above background out to 349 days after the initial vaccination. We also showed that sera from rabbits that received the subtype IAB-based VEEV DNA vaccine administered individually or in the 3-EEV DNA formulation had high levels of neutralizing activity against heterologous VEEV subtypes IC, ID, and IE and MUCV. While these results are indicative of the potential for the individual and 3-EEV DNA vaccines to elicit durable protective immunity and for the VEEV DNA and 3-EEV DNA vaccines to protect against heterologous VEEV subtypes, we are currently completing studies to directly evaluate these possibilities. We are also currently completing studies to evaluate the immunogenicity and protective efficacy of the individual and 3-EEV DNA vaccines delivered by EP against VEEV, WEEV, and EEEV aerosol challenge in NHPs. The results of these studies will be important for further comparisons to the VRP and other next-generation alphavirus vaccine candidates.

The most widely accepted correlate of protection against the encephalitic alphaviruses is neutralizing antibodies directed against the envelope glycoproteins [49–53]. However, neutralizing antibody titers are not always significantly associated with protection against encephalitic alphavirus challenge by the aerosol route [54–56]. In the studies reported here, the VEEV, WEEV, and EEEV DNA vaccines elicited robust virus-specific antibody responses, to include detectable levels of virus-neutralizing antibodies, when delivered individually or in a multiagent formulation. Although we observed that mice that received the individual WEEV DNA or WEEV IND vaccine had similar virus-neutralizing antibody titers, those that received the WEEV DNA vaccine were completely protected from WEEV aerosol challenge and had significantly improved protection as compared to mice that received the WEEV IND vaccine. More strikingly, mice that received the 3-EEV DNA vaccine were also completely protected from WEEV aerosol challenge and had significantly improved protection as compared to mice that received the WEEV IND vaccine despite having significantly lower virus-neutralizing antibody titers. Similarly, although mice that received the individual EEEV DNA, the 3-EEV DNA, or the EEEV IND vaccine had similar virus-neutralizing antibody titers, those that received the EEEV DNA or 3-EEV DNA vaccine were completely protected from EEEV aerosol challenge and had significantly improved protection as compared to mice that received the EEEV IND vaccine. The ability of non-neutralizing antibodies to also mediate protection against encephalitis caused by alphaviruses has been previously documented [57, 58]. Therefore, it is likely that nonneutralizing antibody responses elicited by the individual VEEV, WEEV, and EEEV DNA vaccines and 3-EEV DNA vaccine also contributed to the protection levels observed in the present studies. This is supported by our observation that mice that received the individual WEEV, individual EEEV, or 3-EEV DNA vaccine had significantly higher virus-specific total IgG antibody titers than mice receiving the respective IND vaccine. Roles for mucosal antibody responses and antibody-dependent cellular cytotoxicity in protection against aerosol VEEV challenge in mice have also been documented [59–61]. Therefore, we are currently performing a more thorough characterization of the antibody responses elicited by the individual VEEV, WEEV, and EEEV DNA vaccines and 3-EEV DNA vaccine to further elucidate the contributing role of these responses in the protection observed for these vaccines against VEEV, WEEV, and EEEV aerosol challenge.

Although cytotoxic T cell activity was not observed in previous studies with TC-83, more recent studies have also demonstrated an importance for certain populations of T cells in protection against lethal encephalitis caused by VEEV in mice [62–65]. In our previous studies, we demonstrated that the optimized VEEV DNA vaccine delivered by IM EP elicited significant cell-mediated immune responses against the VEEV E2 and E1 glycoproteins as measured by IFN-γ ELISpot assay [38]. The ELISpot assay results obtained for the individual VEEV DNA vaccine in our current studies were consistent with those previous results. Although the 3-EEV DNA vaccine elicited significantly lower responses against the VEEV E2 and E1 proteins as compared to the individual VEEV DNA vaccine in this assay, they remained at significant levels. Therefore, it is possible that cell-mediated immune responses elicited by the 3-EEV DNA vaccine also contributed to the protection against VEEV aerosol challenge observed here. IFN-γ ELISpot assays required to directly measure cell-mediated immune responses against WEEV and EEEV are currently under development in our laboratory, and the results from these assays will be helpful in determining the potential for virus-specific cell-mediated immune responses elicited by the individual WEEV, individual EEEV, and 3-EEV DNA vaccines to contribute to the protection observed for these vaccines against WEEV and EEEV aerosol challenge.

5. Conclusions

Taken together, the results of our studies described here clearly demonstrate that the individual VEEV, WEEV, and EEEV DNA vaccines and 3-EEV DNA vaccine delivered by IM EP are capable of eliciting robust and protective immune responses against the encephalitic alphaviruses with relatively low DNA doses and with few vaccinations. To our knowledge, this is the first report of a single nucleic acid-based multiagent vaccine formulation that can provide complete protection against VEEV, WEEV, and EEEV aerosol challenge in mice. Consequently, these DNA vaccines appear to represent a viable next-generation alternative to the current alphavirus IND vaccines. The DNA vaccine platform used here also avoids issues with manufacturing, boosting potential, stability, and safety that can be problematic for other approaches to develop next-generation vaccines. In

addition, the results from our completed Phase 1 clinical trial demonstrated the safety, tolerability, and immunogenicity of the VEEV DNA vaccine candidate delivered by IM or ID EP in humans. Therefore, we are currently completing studies to evaluate and compare the immunogenicity and protective efficacy of the individual VEEV, WEEV, and EEEV and 3-EEV DNA vaccines delivered by IM or ID EP in NHPs. Should protective efficacy be successfully demonstrated in these studies, then the individual EEEV, individual WEEV, and 3-EEV DNA vaccines will also be well poised for clinical evaluation.

Data Availability

The data used to support the findings of these studies were generated under funding from the Joint Science and Technology Office for Chemical and Biological Defense of the Defense Threat and Reduction Agency to USAMRIID and Ichor Medical Systems, and so cannot be made freely available. Access to these data will be considered by the corresponding author upon request, with permission of the Joint Science and Technology Office for Chemical and Biological Defense of the Defense Threat and Reduction Agency, USAMRIID, and Ichor Medical Systems.

Disclosure

Drew Hannaman is Vice President, Research and Development of Ichor Medical Systems Inc. The funding agency had no role in study design, data collection and interpretation, or the decision to submit the work for publication. The opinions, interpretations, conclusions, and recommendations contained herein are those of the authors and are not necessarily endorsed by the US Army. Brian D. Livingston present address is Gilead Sciences, Inc., Foster City, CA 94404-1147, USA.

Conflicts of Interest

The other authors declare that they have no conflicts of interest.

Acknowledgments

The authors thank Diana Fisher for performing the statistical analyses, Lillian Chau and Juwan Song for performing the ELISpot assays, the USAMRIID Veterinary Medicine Division for performing the mouse anesthetizations and blood collections, and the USAMRIID Center for Aerobiological Sciences for performing the aerosol exposures. The studies described herein were supported by Grant CBM.VAXV.03.10.RD.006 to USAMRIID and Contract HDTRA1-07-C-0029 to Ich or Medical Systems from the Joint Science and Technology Office for Chemical and Biological Defense of the Defense Threat and Reduction Agency. This research was performed under US Army Medical Research and Material Command Cooperative Research and Development Agreement W81XWH-07-0029 between USAMRIID and Ichor Medical Systems.

References

[1] D. E. Griffin, *Alphaviruses*, F. Virology, D. Knipe, and P. M. Howley, Eds., Lippincott, Williams, and Wilkins, Philadelphia, PA, USA, 2001.

[2] T. F. Tsai, "Arboviral infections in the United States," *Infectious Disease Clinics of North America*, vol. 5, no. 1, pp. 73–102, 1991.

[3] J. F. Bale Jr., "Viral encephalitis," *Medical Clinics of North America*, vol. 77, no. 1, pp. 25–42, 1993.

[4] K. Steele, D. S. Reed, P. J. Glass et al., "Alphavirus Encephalitides," in *Medical Aspects of Biological Warfare*, Z. F. Dembek, Ed., pp. 241–270, Borden Institute (U.S. Army Walter Reed), Washington, DC, USA, 2007.

[5] P. T. Franck and K. M. Johnson, "An outbreak of Venezuelan encephalitis in man in the Panamá Canal zone," *The American Journal of Tropical Medicine and Hygiene*, vol. 19, no. 5, pp. 860–865, 1970.

[6] C. H. Calisher, "Medically important arboviruses of the United States and Canada," *Clinical Microbiology Reviews*, vol. 7, no. 1, pp. 89–116, 1994.

[7] B. Rozdilsky, H. E. Robertson, and J. Chorney, "Western encephalitis: report of eight fatal cases. Saskatchewan epidemic, 1965," *Canadian Medical Association Journal*, vol. 98, no. 2, pp. 79–86, 1968.

[8] D. R. Franz, P. B. Jahrling, D. McClain et al., "Clinical recognition and management of patients exposed to biological warfare agents," *Clinics in Laboratory Medicine*, vol. 21, no. 3, pp. 435–473, 2001.

[9] R. P. Hanson, S. E. Sulkin, E. L. Buescher, W. M. D. Hammon, R. W. McKinney, and T. H. Work, "Arbovirus infections of laboratory workers. Extent of problem emphasizes the need for more effective measures to reduce hazards," *Science*, vol. 158, no. 3806, pp. 1283–1286, 1967.

[10] M. G. Kortepeter, T. J. Cieslak, and E. M. Eitzen, "Bioterrorism," *Journal of Environmental Health*, vol. 63, no. 6, pp. 21–24, 2001.

[11] R. W. Mckinney, T. O. Berge, W. D. Sawyer, W. D. Tigertt, and D. Crozier, "Use of an attenuated strain of Venezuelan equine encephalo-myelitis virus for immunization in man," *The American Journal of Tropical Medicine and Hygiene*, vol. 12, no. 4, pp. 597–603, 1963.

[12] P. R. Pittman, R. S. Makuch, J. A. Mangiafico, T. L. Cannon, P. H. Gibbs, and C. J. Peters, "Long-term duration of detectable neutralizing antibodies after administration of live-attenuated VEE vaccine and following booster vaccination with inactivated VEE vaccine," *Vaccine*, vol. 14, no. 4, pp. 337–343, 1996.

[13] F. E. Cole Jr., S. W. May, and D. M. Robinson, "Formalin-inactivated Venezuelan equine encephalomyelitis (Trinidad strain) vaccine produced in rolling-bottle cultures of chicken embryo cells," *Applied and Environmental Microbiology*, vol. 25, no. 2, pp. 262–265, 1973.

[14] P. J. Bartelloni, R. W. McKinney, F. E. Cole, and T. P. Duffy, "An inactivated eastern equine encephalomyelitis vaccine propagated in chick-embryo cell culture. II. Clinical and serologic responses in man," *The American Journal of Tropical Medicine and Hygiene*, vol. 19, no. 1, pp. 123–126, 1970.

[15] P. J. Bartelloni, R. W. McKinney, H. H. Ramsburg, F. M. Calia, and F. E. Cole, "Inactivated western equine encephalomyelitis vaccine propagated in chick embryo cell culture. Clinical and serological evaluation in man," *The American Journal*

of Tropical Medicine and Hygiene, vol. 20, no. 1, pp. 146–149, 1971.

[16] D. J. McClain, P. R. Pittman, H. H. Ramsburg et al., "Immunologic interference from sequential administration of live attenuated alphavirus vaccines," *The Journal of Infectious Diseases*, vol. 177, no. 3, pp. 634–641, 1998.

[17] P. R. Pittman, C. T. Liu, T. L. Cannon, J. A. Mangiafico, and P. H. Gibbs, "Immune interference after sequential alphavirus vaccine vaccinations," *Vaccine*, vol. 27, no. 36, pp. 4879–4882, 2009.

[18] R. B. Reisler, P. H. Gibbs, D. K. Danner, and E. F. Boudreau, "Immune interference in the setting of same-day administration of two similar inactivated alphavirus vaccines: eastern equine and western equine encephalitis," *Vaccine*, vol. 30, no. 50, pp. 7271–7277, 2012.

[19] D. N. Wolfe, D. G. Heppner, S. N. Gardner et al., "Current strategic thinking for the development of a trivalent alphavirus vaccine for human use," *The American Journal of Tropical Medicine and Hygiene*, vol. 91, no. 3, pp. 442–450, 2014.

[20] S. Paessler and S. C. Weaver, "Vaccines for Venezuelan equine encephalitis," *Vaccine*, vol. 27, Supplement 4, pp. D80–D85, 2009.

[21] F. Nasar, D. Matassov, R. L. Seymour et al., "Recombinant Isfahan virus and vesicular stomatitis virus vaccine vectors provide durable, multivalent, single-dose protection against lethal alphavirus challenge," *Journal of Virology*, vol. 91, no. 8, pp. e01729–e01716, 2017.

[22] J. H. Erasmus, R. L. Seymour, J. T. Kaelber et al., "Novel insect-specific eilat virus-based chimeric vaccine candidates provide durable, mono- and multivalent, single-dose protection against lethal alphavirus challenge," *Journal of Virology*, vol. 92, no. 4, pp. e01274–e01217, 2018.

[23] J. J. Donnelly, J. B. Ulmer, J. W. Shiver, and M. A. Liu, "DNA vaccines," *Annual Review of Immunology*, vol. 15, no. 1, pp. 617–648, 1997.

[24] H. L. Robinson and T. M. Pertmer, "DNA vaccines for viral infections: basic studies and applications," *Advances in Virus Research*, vol. 55, pp. 1–74, 2000.

[25] S. Gurunathan, D. M. Klinman, and R. A. Seder, "DNA vaccines: immunology, application, and optimization," *Annual Review of Immunology*, vol. 18, no. 1, pp. 927–974, 2000.

[26] D. H. Barouch, "Rational design of gene-based vaccines," *The Journal of Pathology*, vol. 208, no. 2, pp. 283–289, 2006.

[27] S. P. Buchbinder, D. V. Mehrotra, A. Duerr et al., "Efficacy assessment of a cell-mediated immunity HIV-1 vaccine (the Step Study): a double-blind, randomised, placebo-controlled, test-of-concept trial," *The Lancet*, vol. 372, no. 9653, pp. 1881–1893, 2008.

[28] C. D. Harro, M. N. Robertson, M. A. Lally et al., "Safety and immunogenicity of adenovirus-vectored near-consensus HIV type 1 clade B *gag* vaccines in healthy adults," *AIDS Research and Human Retroviruses*, vol. 25, no. 1, pp. 103–114, 2009.

[29] L. C. Dupuy and C. S. Schmaljohn, "DNA vaccines for biodefense," *Expert Review of Vaccines*, vol. 8, no. 12, pp. 1739–1754, 2009.

[30] J. A. C. Schalk, F. R. Mooi, G. A. M. Berbers, L. A. G. J. M. van Aerts, H. Ovelgönne, and T. G. Kimman, "Preclinical and clinical safety studies on DNA vaccines," *Human Vaccines*, vol. 2, no. 2, pp. 45–53, 2006.

[31] J. Riemenschneider, A. Garrison, J. Geisbert et al., "Comparison of individual and combination DNA vaccines for *B. Anthracis*, Ebola virus, Marburg virus and Venezuelan equine encephalitis virus," *Vaccine*, vol. 21, no. 25-26, pp. 4071–4080, 2003.

[32] L. C. Dupuy, C. P. Locher, M. Paidhungat et al., "Directed molecular evolution improves the immunogenicity and protective efficacy of a Venezuelan equine encephalitis virus DNA vaccine," *Vaccine*, vol. 27, no. 31, pp. 4152–4160, 2009.

[33] L. C. Dupuy, M. J. Richards, D. S. Reed, and C. S. Schmaljohn, "Immunogenicity and protective efficacy of a DNA vaccine against Venezuelan equine encephalitis virus aerosol challenge in nonhuman primates," *Vaccine*, vol. 28, no. 46, pp. 7345–7350, 2010.

[34] N. Garmashova, R. Gorchakov, E. Volkova, S. Paessler, E. Frolova, and I. Frolov, "The Old World and New World alphaviruses use different virus-specific proteins for induction of transcriptional shutoff," *Journal of Virology*, vol. 81, no. 5, pp. 2472–2484, 2007.

[35] N. Garmashova, S. Atasheva, W. Kang, S. C. Weaver, E. Frolova, and I. Frolov, "Analysis of Venezuelan equine encephalitis virus capsid protein function in the inhibition of cellular transcription," *Journal of Virology*, vol. 81, no. 24, pp. 13552–13565, 2007.

[36] P. V. Aguilar, S. C. Weaver, and C. F. Basler, "Capsid protein of eastern equine encephalitis virus inhibits host cell gene expression," *Journal of Virology*, vol. 81, no. 8, pp. 3866–3876, 2007.

[37] S. Atasheva, A. Fish, M. Fornerod, and E. I. Frolova, "Venezuelan equine Encephalitis virus capsid protein forms a tetrameric complex with CRM1 and importin α/β that obstructs nuclear pore complex function," *Journal of Virology*, vol. 84, no. 9, pp. 4158–4171, 2010.

[38] L. C. Dupuy, M. J. Richards, B. Ellefsen et al., "A DNA vaccine for venezuelan equine encephalitis virus delivered by intramuscular electroporation elicits high levels of neutralizing antibodies in multiple animal models and provides protective immunity to mice and nonhuman primates," *Clinical and Vaccine Immunology*, vol. 18, no. 5, pp. 707–716, 2011.

[39] D. Hannaman, L. C. Dupuy, B. Ellefsen, and C. S. Schmaljohn, "A phase 1 clinical trial of a DNA vaccine for Venezuelan equine encephalitis delivered by intramuscular or intradermal electroporation," *Vaccine*, vol. 34, no. 31, pp. 3607–3612, 2016.

[40] C. Schmaljohn, L. Vanderzanden, M. Bray et al., "Naked DNA vaccines expressing the prM and E genes of Russian spring summer encephalitis virus and Central European encephalitis virus protect mice from homologous and heterologous challenge," *Journal of Virology*, vol. 71, no. 12, pp. 9563–9569, 1997.

[41] A. Luxembourg, D. Hannaman, K. Wills et al., "Immunogenicity in mice and rabbits of DNA vaccines expressing woodchuck hepatitis virus antigens," *Vaccine*, vol. 26, no. 32, pp. 4025–4033, 2008.

[42] L. A. Hodgson, G. V. Ludwig, and J. F. Smith, "Expression, processing, and immunogenicity of the structural proteins of Venezuelan equine encephalitis virus from recombinant baculovirus vectors," *Vaccine*, vol. 17, no. 9-10, pp. 1151–1160, 1999.

[43] T. Taguchi, J. R. McGhee, R. L. Coffman et al., "Detection of individual mouse splenic T cells producing IFN-γ and IL-5 using the enzyme-linked immunospot (ELISPOT) assay," *Journal of Immunological Methods*, vol. 128, no. 1, pp. 65–73, 1990.

[44] M. K. Hart, W. Pratt, F. Panelo, R. Tammariello, and M. Dertzbaugh, "Venezuelan equine encephalitis virus vaccines induce mucosal IgA responses and protection from airborne infection in BALB/c, but not C3H/HeN mice," *Vaccine*, vol. 15, no. 4, pp. 363–369, 1997.

[45] W. D. Pratt, P. Gibbs, M. L. Pitt, and A. L. Schmaljohn, "Use of telemetry to assess vaccine-induced protection against parenteral and aerosol infections of Venezuelan equine encephalitis virus in non-human primates," *Vaccine*, vol. 16, no. 9-10, pp. 1056–1064, 1998.

[46] L. P. Nagata, W. G. Hu, S. A. Masri et al., "Efficacy of DNA vaccination against western equine encephalitis virus infection," *Vaccine*, vol. 23, no. 17-18, pp. 2280–2283, 2005.

[47] P. J. Gauci, J. Q. H. Wu, G. A. Rayner, N. D. Barabe, L. P. Nagata, and D. F. Proll, "Identification of Western equine encephalitis virus structural proteins that confer protection after DNA vaccination," *Clinical and Vaccine Immunology*, vol. 17, no. 1, pp. 176–179, 2010.

[48] D. S. Reed, P. J. Glass, R. R. Bakken et al., "Combined alphavirus replicon particle vaccine induces durable and cross-protective immune responses against equine encephalitis viruses," *Journal of Virology*, vol. 88, no. 20, pp. 12077–12086, 2014.

[49] J. H. Mathews and J. T. Roehrig, "Determination of the protective epitopes on the glycoproteins of Venezuelan equine encephalomyelitis virus by passive transfer of monoclonal antibodies," *The Journal of Immunology*, vol. 129, no. 6, pp. 2763–2767, 1982.

[50] J. T. Roehrig and J. H. Mathews, "The neutralization site on the E2 glycoprotein of Venezuelan equine encephalomyelitis (TC-83) virus is composed of multiple conformationally stable epitopes," *Virology*, vol. 142, no. 2, pp. 347–356, 1985.

[51] A. R. Hunt and J. T. Roehrig, "Localization of a protective epitope on a Venezuelan equine encephalomyelitis (VEE) virus peptide that protects mice from both epizootic and enzootic VEE virus challenge and is immunogenic in horses," *Vaccine*, vol. 13, no. 3, pp. 281–288, 1995.

[52] R. J. Phillpotts, L. D. Jones, and S. C. Howard, "Monoclonal antibody protects mice against infection and disease when given either before or up to 24 h after airborne challenge with virulent Venezuelan equine encephalitis virus," *Vaccine*, vol. 20, no. 11-12, pp. 1497–1504, 2002.

[53] A. R. Hunt, S. Frederickson, C. Hinkel, K. S. Bowdish, and J. T. Roehrig, "A humanized murine monoclonal antibody protects mice either before or after challenge with virulent Venezuelan equine encephalomyelitis virus," *Journal of General Virology*, vol. 87, no. 9, pp. 2467–2476, 2006.

[54] A. M. Bennett, S. J. Elvin, A. J. Wright, S. M. Jones, and R. J. Phillpotts, "An immunological profile of Balb/c mice protected from airborne challenge following vaccination with a live attenuated Venezuelan equine encephalitis virus vaccine," *Vaccine*, vol. 19, no. 2-3, pp. 337–347, 2000.

[55] D. S. Reed, C. M. Lind, M. G. Lackemeyer, L. J. Sullivan, W. D. Pratt, and M. D. Parker, "Genetically engineered, live, attenuated vaccines protect nonhuman primates against aerosol challenge with a virulent IE strain of Venezuelan equine encephalitis virus," *Vaccine*, vol. 23, no. 24, pp. 3139–3147, 2005.

[56] C. J. Roy, A. P. Adams, E. Wang et al., "A chimeric Sindbis-based vaccine protects cynomolgus macaques against a lethal aerosol challenge of eastern equine encephalitis virus," *Vaccine*, vol. 31, no. 11, pp. 1464–1470, 2013.

[57] A. L. Schmaljohn, E. D. Johnson, J. M. Dalrymple, and G. A. Cole, "Non-neutralizing monoclonal antibodies can prevent lethal alphavirus encephalitis," *Nature*, vol. 297, no. 5861, pp. 70–72, 1982.

[58] M. D. Parker, M. J. Buckley, V. R. Melanson, P. J. Glass, D. Norwood, and M. K. Hart, "Antibody to the E3 glycoprotein protects mice against lethal venezuelan equine encephalitis virus infection," *Journal of Virology*, vol. 84, no. 24, pp. 12683–12690, 2010.

[59] J. H. Mathews, J. T. Roehrig, and D. W. Trent, "Role of complement and the Fc portion of immunoglobulin G in immunity to Venezuelan equine encephalomyelitis virus infection with glycoprotein-specific monoclonal antibodies," *Journal of Virology*, vol. 55, no. 3, pp. 594–600, 1985.

[60] S. J. Elvin, A. M. Bennett, and R. J. Phillpotts, "Role for mucosal immune responses and cell-mediated immune functions in protection from airborne challenge with Venezuelan equine encephalitis virus," *Journal of Medical Virology*, vol. 67, no. 3, pp. 384–393, 2002.

[61] C. B. Brooke, A. Schafer, G. K. Matsushima, L. J. White, and R. E. Johnston, "Early activation of the host complement system is required to restrict central nervous system invasion and limit neuropathology during Venezuelan equine encephalitis virus infection," *Journal of General Virology*, vol. 93, no. 4, pp. 797–806, 2012.

[62] L. D. Jones, A. M. Bennett, S. R. Moss, E. A. Gould, and R. J. Phillpotts, "Cytotoxic T-cell activity is not detectable in Venezuelan equine encephalitis virus-infected mice," *Virus Research*, vol. 91, no. 2, pp. 255–259, 2003.

[63] S. Paessler, N. E. Yun, B. M. Judy et al., "Alpha-beta T cells provide protection against lethal encephalitis in the murine model of VEEV infection," *Virology*, vol. 367, no. 2, pp. 307–323, 2007.

[64] N. E. Yun, B. H. Peng, A. S. Bertke et al., "$CD4^+$ T cells provide protection against acute lethal encephalitis caused by Venezuelan equine encephalitis virus," *Vaccine*, vol. 27, no. 30, pp. 4064–4073, 2009.

[65] C. B. Brooke, D. J. Deming, A. C. Whitmore, L. J. White, and R. E. Johnston, "T cells facilitate recovery from Venezuelan equine encephalitis virus-induced encephalomyelitis in the absence of antibody," *Journal of Virology*, vol. 84, no. 9, pp. 4556–4568, 2010.

Hindawi
Journal of Immunology Research
Volume 2018, Article ID 8964085, 14 pages
https://doi.org/10.1155/2018/8964085

Research Article

Recombinant Enolase of *Trypanosoma cruzi* as a Novel Vaccine Candidate against Chagas Disease in a Mouse Model of Acute Infection

Minerva Arce-Fonseca,[1] María Cristina González-Vázquez,[2] Olivia Rodríguez-Morales,[1] Verónica Graullera-Rivera,[3] Alberto Aranda-Fraustro,[3] Pedro A. Reyes,[1] Alejandro Carabarin-Lima,[1,4] and José Luis Rosales-Encina[4]

[1]*Departamento de Biología Molecular, Juan Badiano No. 1, Col. Sección XVI, Delegación Tlalpan, Instituto Nacional de Cardiología "Ignacio Chávez", 14080 Mexico City, Mexico*
[2]*Departamento de Biología Celular, Avenida Instituto Politecnico Nacional No. 2508, Col. San Pedro Zacatenco, Centro de Investigación y de Estudios Avanzados del Instituto Politecnico Nacional, 07360 Mexico City, Mexico*
[3]*Departamento de Anatomía Patológica, Juan Badiano No. 1, Col. Sección XVI, Delegación Tlalpan, Instituto Nacional de Cardiología "Ignacio Chávez", 14080 Mexico City, Mexico*
[4]*Departamento de Infectómica y Patogénesis Molecular, Avenida Instituto Politecnico Nacional No. 2508, Col. San Pedro Zacatenco, Centro de Investigación y de Estudios Avanzados del Instituto Politecnico Nacional, 07360 Mexico City, Mexico*

Correspondence should be addressed to Alejandro Carabarin-Lima; ecoli_75@hotmail.com

Received 7 February 2018; Accepted 3 April 2018; Published 7 May 2018

Academic Editor: Giuseppe A. Sautto

Trypanosoma cruzi is the protozoan parasite that causes Chagas disease, which is considered by the World Health Organization to be a neglected tropical disease. Two drugs exist for the treatment of Chagas disease, nifurtimox and benznidazole; they are only effective in the acute phase, and a vaccine is currently not available. In this study, we used the recombinant enolase from *T. cruzi* H8 strain (MHOM/MX/1992/H8 Yucatán) (rTcENO) and its encoding DNA (pBKTcENO) to immunize mice and evaluate their protective effects in an experimental murine model of acute phase infection. Our results showed that mice vaccinated with rTcENO or its encoding DNA were able to generate typical specific antibodies (IgG1, IgG2a, and IgG2b), suggesting that a mixed Th1/Th2 immune response was induced. The parasite burden in the blood was reduced to 69.8% and 71% in mice vaccinated with rTcENO and pBKTcENO, respectively. The group vaccinated with rTcENO achieved 75% survival, in contrast to the group vaccinated with pBKTcENO that showed no survival in comparison to the control groups. Moreover, rTcENO immunization elevated the production of IFN-γ and IL-2 after the parasite challenge, suggesting that the Th1-type immune response was polarized. These results indicated that rTcENO could be used as a vaccine against Chagas disease.

1. Introduction

The intracellular protozoan parasite *Trypanosoma cruzi* is the etiologic agent of Chagas disease, considered as a neglected tropical disease [1]. Currently, approximately 5.7 million people are infected worldwide, more than 70.2 million people are at risk of contracting the disease [2], and 50,000 patients die each year as a result of the disease [3].

Because of its natural life cycle, involving mitotic division in reduviid insects, which then transmit the infection by feeding on the blood of different vertebrates, *T. cruzi* is considered to be a severe health problem in rural areas of Mexico and Central and South America, where these insects are endemic. Chagas disease is also a health problem in nonendemic countries, such as the United States of America (USA), Canada, Australia, Japan, France, Spain,

and Switzerland [4–8]. In Mexico, as well as in other endemic countries, cases are becoming more common in urban areas. This shift in the epidemiology of Chagas disease is connected to the migration of people infected with *T. cruzi*, blood transfusion, vertical transmission (mother to child), and organ transplantation [9].

Chagas disease has two different phases: acute and chronic. The acute phase is usually subclinical. Most acute cases are asymptomatic, last for 6–12 weeks, and typically occur in childhood [10]. Two major forms of the disease are observed during the chronic phase: indeterminate or latent and symptomatic. A high percentage of chagasic patients remain in the indeterminate phase for 10 or 30 years or even for life. These patients usually have no clinical or physical signs of disease but display positive serology. Approximately 30–40% of infected individuals develop clinical symptoms, involving severe cardiomyopathy or gastrointestinal pathology, several years after the infection.

Nifurtimox and benznidazole are currently the only licensed drugs with proven efficacy specifically against Chagas disease. Both drugs have significant activity during the acute phase of the disease, causing parasitological cure in up to 80% of patients who were treated early [11, 12]. In addition to chemotherapy, a vaccine may provide a suitable preventive measure to control the spread of the disease. Different parasite antigens have been tested for their effectiveness in controlling the infection. These immunizations, which were carried out at the level of DNA or recombinant proteins, showed different degrees of protection (e.g., reduced parasitemia and survival). In most immunization cases, a Th1-type immune response was observed. These genes and proteins were tested for vaccine trials in experimental models of infection, including cruzipain [13, 14], *trans*-sialidase [15, 16], amastigote surface protein-2 [17], LYT-1 [18], and paraflagellar rod protein [19] among others.

In recent years, several studies have shown that the "moonlighting" protein enolase is capable of generating a protective immune response against *Plasmodium falciparum* [20], *Candida albicans* [21], and *Ascaris suum* [22].

Enolase (2-phospho-D-glycerate hydrolase, EC 4.2.1.11) is a metalloenzyme that catalyzes the reversible dehydration of D-2-phosphoglycerate (PGA) to phosphoenolpyruvate (PEP) in both glycolysis and gluconeogenesis. Enolases, ranging from bacteria to higher vertebrates, show highly conserved amino acid sequences, particularly at the catalytic site. Consequently, enzymes from diverse species share similar kinetic properties. Enolase requires magnesium for both catalysis and dimer stabilization [23]. Furthermore, enolase that acts as a plasminogen receptor on the cell surface of certain pathogens [24, 25] has been implicated in nuclear functions, such as transcriptional regulation (as a repressor or activator) in protozoa [26–28], plants [29], and animal cells [30, 31]. Enolase is also involved in the stress response [32], vacuolar fusion processes [33], and alternative molecular chaperone functions [34, 35].

Previously, we cloned and sequenced the gene encoding enolase from *T. cruzi* and performed immunological in silico assays. Our data showed that the resulting sequence had several predicted peptides for B cells and cytotoxic T lymphocytes (CTL), which suggested that enolase could be a good immunogen [36].

In the present study, we immunized mice with the recombinant protein rTcENO or the recombinant pBKTcENO DNA plasmid. We then challenged the immunized mice with a lethal dose of *T. cruzi*. The mice immunized with rTcENO showed typical immunoglobulins for Th1/Th2 immune responses, a significant reduction in the level of parasite burden in the blood, and 75% survival rate in comparison to the control groups. Moreover, the detection of IFN-γ, TNF (alpha and beta), and IL-2, but not IL-4, showed a polarized Th1 immune response when mice were challenged with *T. cruzi*. Conversely, mice immunized with pBKTcENO did not survive after challenge with a high inoculum of *T. cruzi*, despite a significant reduction in the level of parasitemia. We found that immunization with rTcENO, but not with pBKTcENO, induced substantial protection in mice, indicating that rTcENO could be a good candidate to develop a vaccine against Chagas disease.

2. Materials and Methods

2.1. Immunization and Trypanosoma cruzi Challenge. All mice (female BALB/c mice 6–8 weeks old) were randomly assigned into control or vaccinated groups of eight mice each in two independent experiments. The mice were immunized by intraperitoneal (i.p.) injection with 10 μg of the recombinant protein (rTcENO) emulsified in Freund's complete adjuvant (CFA) (Sigma) and boosted twice with 10 μg of the rTcENO in Freund's incomplete adjuvant (IFA) every 2 weeks. The control, nonvaccinated animals were mock immunized with PBS/adjuvant in the same schedule as the immunized mice (they received one injection with CFA and two with IFA). This i.p. route has been used in the mouse model for immunization of vaccines based on recombinant proteins, epitopes, or microvesicles, demonstrating its protective efficacy [37–41].

For DNA-based immunizations, 100 μg of recombinant plasmid (pBKTcENO) or vector DNA (pBK-CMV) (Stratagene) was dissolved in 50 μL of sterile PBS, injected intramuscularly (i.m.) in the *tibialis anterioris* muscle and boosted twice every 2 weeks [42].

Both vaccinated (rTcENO or pBKTcENO) and control mice (PBS or pBK-CMV) had access to food and water ad libitum, and two weeks after the last immunization, they received an i.p. injection of 8×10^4 bloodstream trypomastigotes of *T. cruzi*. The *T. cruzi* H8 strain (MHOM/MX/1992/H8 Yucatán (*T. cruzi*)) used in this work was a kind gift from Dr. Jorge E. Zavala Castro from the Centro de Investigaciones Regionales "Dr. Hideyo Noguchi", Universidad Autónoma de Yucatán, Mérida, Yucatán, Mexico. Blood samples were collected from the tail vein to determine parasite burden every three days in the peripheral blood; in another similar experiment, survival rates were monitored daily. Mice were housed in a controlled environment and managed according to the National Institutes of Health Guide for Care and Use of Experimental Animals [43], with the approval of the CINVESTAV-IPN Animal Care and Use Committee.

2.2. rTcENO Polyclonal Antibodies. The recombinant protein rTcENO was obtained as previously described [36] and the purified rTcENO did not contain detectable levels of endotoxin contamination as measured by the E-Toxate assay (Sigma, St. Louis, MO, USA). Female BALB/c mice (6–8 weeks old) were immunized with10 μg/mouse. Each animal received three i.p. doses of antigen every seven days; the first immunization dose was administered in complete Freund's adjuvant, and the following immunizations were administered in incomplete Freund's adjuvant. Before and at the end of the immunization scheme, animals were bled to collect serum.

2.3. Plasmid DNA Construction and Purification. The gene encoding TcENO (GenBank access number: KC862322) was obtained from the pRSETB-TcENO plasmid [36] as a 1.1 kb Kpn I/Hind III (New England Biolabs) fragment. This fragment was subcloned into the prokaryotic/eukaryotic expression vector pBK-CMV (InvitrogenTM by Life Technologies) to generate the pBKTcENO plasmid. The correct subcloning of the TcENO gene was confirmed by restriction enzyme analysis and sequencing.

Plasmid DNA was purified by anion-exchange chromatography using a Qiagen Plasmid Maxi Kit. DNA used for immunizations was sterilized by ethanol precipitation and resuspended in lipopolysaccharide-free PBS (Gibco).

Enolase was identified in *T. cruzi* total protein extracts or purified rTcENO by western blot.

Briefly, *T. cruzi* epimastigotes were harvested from cultures and resuspended in lysis buffer (10 mM Tris-HCl, pH 7.5; 5 mM EDTA; 1% Nonidet P-40; 1 mM phenylmethanesulfonyl fluoride; 10 mg/mL aprotinin; 50 U/L trasylol; and 10 mg/mL leupeptin) by repeated freezing and thawing cycles. Lysates were cleared by centrifugation (30 min, 4°C at 14,000 ×g), and the supernatants were collected and resolved by 12% sodium dodecyl-sulfate polyacrylamide gel electrophoresis (SDS-PAGE, 10 μg and 20 μg per lane) or purified rTcENO (10 μg per lane). Proteins were electrotransferred onto nitrocellulose membranes at 70 V for 1 h. The membranes were blocked with 5% (*w*/*v*) skim milk in phosphate-buffered saline (PBS, pH 7.4) for 1 h at 37°C, washed three times with PBS containing 0.05% Tween 20 (PBS-T), 10 min/per time, and then incubated overnight at 4°C with anti-rTcENO polyclonal antibodies (1 : 500 dilution in 2% skim milk-PBS) or anti-pBKTcENO polyclonal antibodies (1 : 500 dilution in 2% skim milk-PBS). The negative control consisted of a pool of serum from different healthy mice diluted 1 : 500 in PBS with 2% nonfat milk. After washing, the membranes were incubated with secondary antibody conjugated with alkaline phosphatase (Zymed Lab) for 1 h at 37° C at 1 : 5000 dilution in 2% skim milk-PBS. The blots were visualized with nitro-blue tetrazolium chloride (NBT) and 5-bromo-4-chloro-3′-indolyphosphate p-toluidine salt (BCIP) (Sigma).

2.4. Indirect Immunofluorescence Assays. T. cruzi epimastigotes were washed three times in PBS supplemented with 0.1% glucose (PBSG), pH 7.4, and fixed in 2% paraformaldehyde in PBS (*v*/*v*) for 2 h at 4°C. After that, 1×10^6 parasites/mL were placed on glass slides for 45 min at 37°C. These preparations were divided into two sets; one remained nonpermeabilized, and the other was permeabilized with 0.2% Triton X-100 in PBS. Both preparations were incubated with antibodies against either TcENO or *T. cruzi* total protein extract from mice serum (diluted 1 : 100 in PBS-5% BSA) for 1 h at room temperature using an FITC-labelled IgG (Pierce) as a secondary antibody diluted 1 : 3000 in PBS. After 1 h at room temperature, we rinsed the slides in PBS, stained the nuclear and kinetoplast DNA with DAPI, and mounted them with Vecta-Shield medium (Vector Laboratories). The results were observed with a Carl Zeiss LSM 700 confocal microscope.

2.5. Immunoglobulin Determination. Total IgG immunoglobulin and isotypes IgG1, IgG2a, IgG2b, IgG3, IgA, and IgM were evaluated by the ELISA method according to the manufacturer's instructions (Zymed Labs). Briefly, plates were coated with rTcENO (2 μg/mL) in carbonate buffer (pH 9.6) and incubated overnight at 4°C. Plates were washed with PBS-0.1% Tween (PBST), incubated for 2 h at 37°C with blocking solution (PBS containing 5% skim milk), washed with PBST and PBS, and then incubated with 50 μL of either mouse anti-rTcENO or anti-pBKTcENO (1 : 500 dilutions). As a negative control, a pool of preimmune sera was used in all experiments. After washing, the peroxidase-labeled rabbit anti-mouse IgG antibodies were added at 1 : 1000 dilution in PBST and incubated for 1 h at room temperature. Plates were incubated with 100 μL of ABTS substrate (2,2,-azinobis[3-ethylbenzthiazoline]-6-sulphonic acid) (Zymed Labs) for 10 min and read at 405 nm in an ELISA microplate reader (MultisKan MS).

2.6. Cytokine Determination by Flow Cytometry. The levels of serum Th1- (INF-γ, IL-2, and TNF) and Th2- (IL-4) type cytokines were analyzed in duplicate using a fluorescent bead immunoassay for quantitative detection by flow cytometry (Mouse Th1/Th2 Cytokine Kit, BD™ Cytometric Bead Array (CBA); BD Biosciences) according to the manufacturer's instructions. Briefly, serum samples (50 μL) and phycoerythrin- (PE-) conjugated antibodies were incubated with capture bead reagent for 2 h in the dark at room temperature. Unbound antibodies were washed (1.0 mL wash buffer) and resuspended in 300 mL of PBS. Samples were analyzed in a FACScalibur Flow Cytometer (BD Biosciences), and fluorescence intensity was calculated using FCAP Array v3 Software (BD Biosciences). All four cytokines exhibited single well-separated peaks. Four individual cytokine standard curves (range 20–5000 pg/mL) were run in each assay. Cytokine concentrations were determined by reference to standard curves and expressed in pg/mL.

2.7. Histology. Heart and skeletal muscle samples were aseptically isolated, rinsed with sterile PBS, and fixed in 4% paraformaldehyde in PBS (pH 7.4) for 24 h. Fixed samples were embedded in paraffin, sectioned (5 μm), stained with hematoxylin and eosin or Masson trichrome, and examined by light microscopy (Nikon Eclipse E600). To examine inflammatory infiltrate/myocarditis or myositis and amastigote

nets, each tissue section was analyzed for >10 microscopic fields (40x magnifications) by two investigators who were blinded to identity of the experimental groups. Myocarditis or myositis (presence of inflammatory cells) from H&E-stained sections was scored as 0 (absent, without foci of inflammation), 1 (1 or less foci of inflammatory cells/field), 2 (moderate, >2 foci/field), 3 (generalized coalescing of foci of inflammation or disseminated inflammation with minimal cell necrosis and retention of tissue integrity), and 4 (diffused inflammation with severe tissue necrosis, interstitial edema, and loss of integrity).

2.8. Statistical Analysis. The results were expressed as the means ± SD. Statistical analysis was performed using one-way ANOVA followed by Tukey's test. The survival time was calculated by the Kaplan-Meier method. Data sets that were found not to be normally distributed were analyzed with the Kruskal-Wallis test followed by the Mann–Whitney test to assess the differences between pairwise comparisons. Differences were considered to be statistically significant when the p value was <0.01 or <0.05.

3. Results

3.1. Polyclonal Antibodies Anti-TcENO Are Specific. In our previous work, we cloned the enolase gene sequence into the pRSETB vector and purified the recombinant rTcENO protein [36]. In this report, we immunized mice with the recombinant rTcENO protein to produce polyclonal antibodies. The endotoxin level of rTcENO used for immunization was found to be <1 EU/mL. The serum of these immunized mice was used in western blot assays as a first antibody against *T. cruzi* total protein extract, resulting in a specific band of approximately 46 kDa. This band was also detected when anti-pBKTcENO antibodies were used (Figure 1(a)). To confirm the specificity of the antibodies generated by immunization with rTcENO and pBKTcENO, the antibodies produced were used in western blot assays against purified rTcENO. Both antibodies recognized the recombinant protein, indicating that the antibodies generated were specific (Figure 1(b)).

The antibodies against rTcENO were also used in immunofluorescence assays against permeabilized and nonpermeabilized *T. cruzi* cells. In permeabilized parasites, TcENO labeling was found in the cytoplasm, and no reaction was detected in structures such as the flagellum, whereas in nonpermeabilized parasites, labeling was found in the membrane. This localization might facilitate its recognition by the host's immune system, suggesting that TcENO could have strong antigenic properties (Figure 1(c)).

3.2. Humoral Response in Mice Immunized with rTcENO or pBKTcENO. To characterize the immune response induced by *T. cruzi* enolase, we immunized BALB/c mice intraperitoneally with rTcENO or intramuscularly with pBKTcENO as described in Materials and Methods. The immunizations with either rTcENO or pBKTcENO induced a significant production of IgGs against the rTcENO antigen (Figure 2) seven days after the last immunization. Moreover, antigen-specific isotypes of immunoglobulins in the sera of immunized animals with rTcENO revealed high levels of IgG1>IgG2b>IgG2a (Figure 3(a)), indicating that this antigen induced a mixed Th1-/Th2-like immune response. In contrast, the mice immunized with pBKTcENO showed IgG2a>IgG2b>IgG1 with an IgG2b/IgG1 ratio > 1, suggesting that a predominantly Th1-like immune response was induced (Figure 3(b)). As expected, the mice immunized with rTcENO or pBKTcENO exhibited high titers of antibodies compared to the control groups inoculated with PBS or pBK-CMV ($p < 0.01$). In contrast, the isotyping mice immunized with pBKTcENO did not show any significant difference from those in the pBK-CMV group.

3.3. rTcENO or pBKTcENO Immunizations Reduce the Parasitemia, but Only Mice Immunized with rTcENO Survive after Challenge with T. cruzi. To determine if immunizations with either rTcENO or pBKTcENO reduce parasitic burden in the blood and confer protection to experimentally infected mice with *T. cruzi*, we recorded parasitemia profiles and mortality rates. The parasitemia profile showed a 69.8% decrease when the mice were immunized with rTcENO compared to the control group (PBS) ($p < 0.01$) (Figure 4(a)). The pBKTcENO plasmid also reduced the parasite load in the mice at 70% and 42% during the parasitemia peak (day 24 after challenge) compared to the PBS and pBK-CMV controls, respectively ($p < 0.01$).

The mice immunized with rTcENO showed 75% survival rate compared to the control group (PBS) ($p < 0.01$) at the end of the experiment. Nevertheless, all mice immunized with pBKTcENO eventually died, not exceeding day 33 post-infection (Figure 4(b)).

3.4. Th1-Type Immune Response Is Polarized in rTcENO-Immunized Mice after Parasite Challenge. To determine the type of immunological response induced after parasite challenge, the mice were bled after the peak of parasitemia (day 30 after challenge), and serum IFN-γ, IL-2, TNF, and IL-4 cytokines were determined (Figure 5). The mice vaccinated with rTcENO showed increased levels of the Th1-related cytokines IFN-γ and IL-2 but low levels of TNF compared with the nonvaccinated control group ($p < 0.01$). In contrast, the mice vaccinated with pBKTcENO showed significantly higher levels of TNF and IFN-γ and lower levels of IL-2, but these latter levels were significantly higher than those found in nonvaccinated mice. The levels of TNF in the control mice vaccinated with the plasmid pBK-CMV were higher than those in the mice vaccinated with pBKTcENO ($p < 0.01$).

3.5. Immunization with rTcENO Confers Protection to the Heart and Skeletal Muscle. Histological analysis of the heart of nonvaccinated mice and that of mice immunized with pBK-CMV revealed histopathological features compatible with acute chagasic myocarditis. We observed numerous nests of *T. cruzi* amastigotes accompanied by inflammatory infiltrates and few affected myocardial fibers that showed regeneration. In contrast, histological analysis of the heart of mice immunized with rTcENO revealed

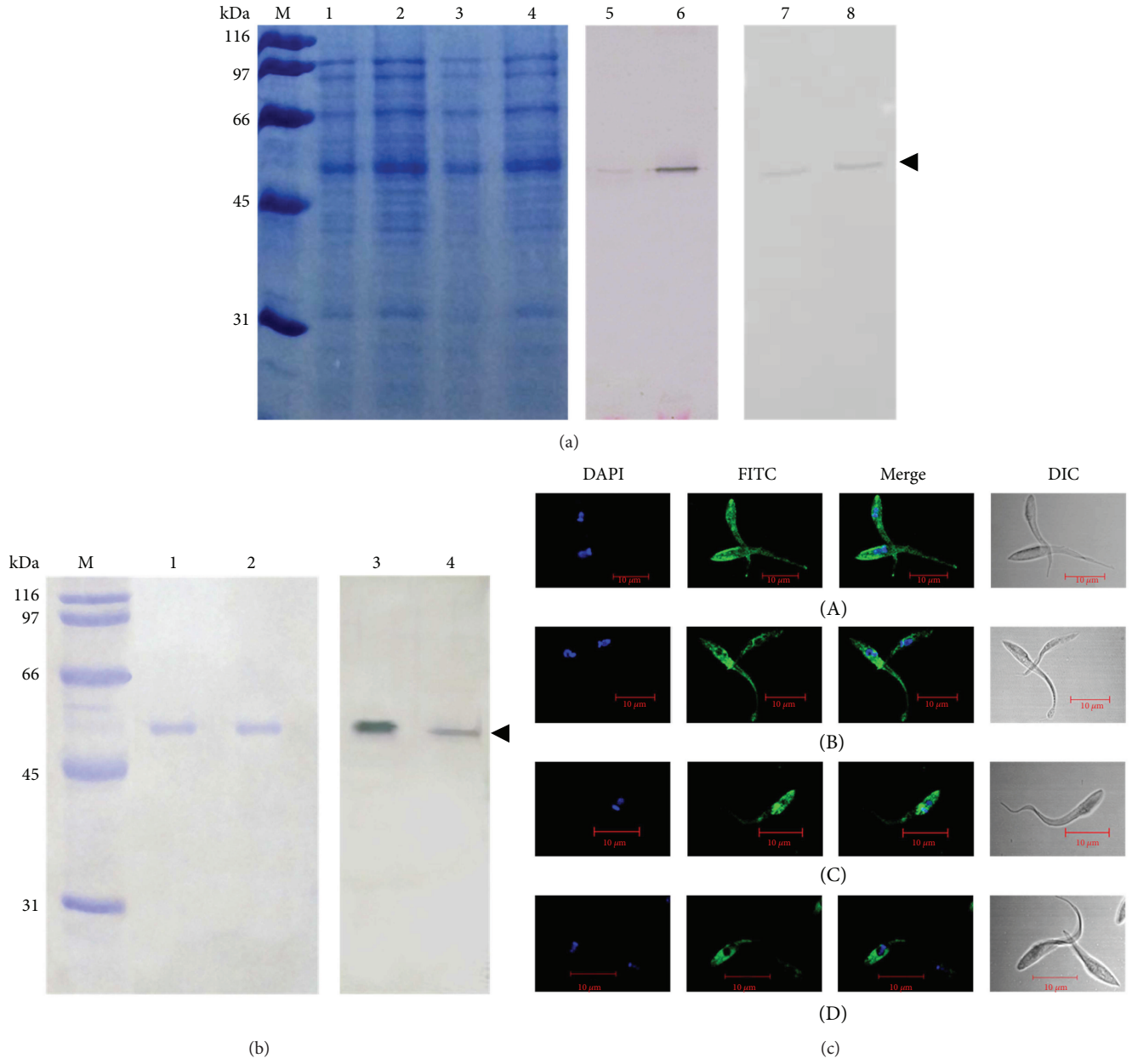

Figure 1: *T. cruzi* enolase immunodetection. (a) Total extract of *T. cruzi* soluble proteins and its respective replica for western blotting. Lane M: molecular weight marker; lanes 1 and 3: total soluble proteins (10 μg); lanes 2 and 4: total soluble proteins (20 μg); lanes 5 and 6: western blot of immobilized proteins with polyclonal antibodies anti-rTcENO; lanes 7 and 8: western blot of immobilized proteins with polyclonal antibodies anti-pBKTcENO. (b) Purified rTcENO and its respective replica for western blotting. Lane M: molecular weight marker; lanes 1 and 2: rTcENO (10 μg); lane 3: western blot with pool of polyclonal antibodies anti-rTcENO; lane 4: western blot with pool of polyclonal antibodies anti-pBKTcENO. The arrowhead indicates the signal for a band of approximately 46 kDa (the TcENO estimated weight). (c) Indirect immunofluorescence assay. The secondary antibody that recognized the anti-rTcEno was FITC labeled (green fluorescence). Nuclear and kinetoplast DNA were stained with DAPI and shown by blue fluorescence. Each image is a representative of at least two independent experiments and captured by confocal microscope. (A) Nonpermeabilized parasite with anti-*T. cruzi* polyclonal antibodies; (B) nonpermeabilized parasite with anti-rTcENO polyclonal antibodies; (C) permeabilized parasite with anti-*T. cruzi* polyclonal antibodies; (D) permeabilized parasite with anti-rTcENO polyclonal antibodies.

diffuse myocarditis with a mild mononuclear inflammatory infiltrate composed mainly of lymphocytes and a few plasma cells, while amastigote nests were absent. In mice immunized with pBKTcENO, severe myocarditis, with the presence of amastigote nest associated with necrosis of the myocardial fibers, and intense inflammatory infiltrates, composed of lymphocytes, plasma cells, and a few polymorphonuclear leukocytes, were observed (Figure 6).

Skeletal muscle samples of the control mice exhibited disorganization of tissue architecture, necrosis, and large nests of *T. cruzi* amastigotes, while in the vaccinated mice, the skeletal muscle showed inflammatory infiltrates that consisted

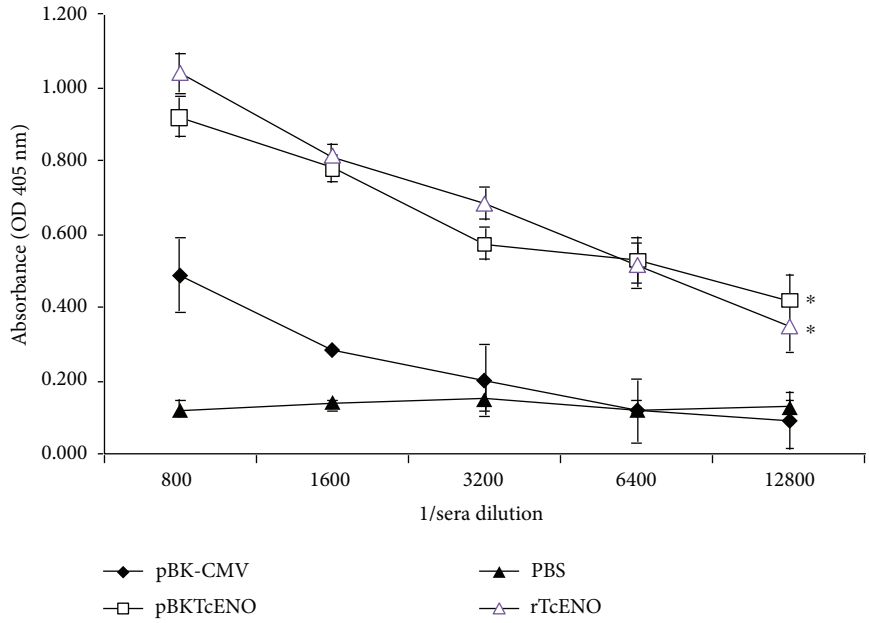

Figure 2: Antibody titers in immunized mice. ELISA was performed seven days after the last immunization to evaluate the serum levels (absorbance in optical density at 405 nm) of rTcENO-specific antibodies at different dilutions. The values represent the average of triplicate assays ± S.D. A significant difference was detected by comparing rTcENO or pBKTcENO versus PBS or pBK-CMV ($^*p < 0.01$).

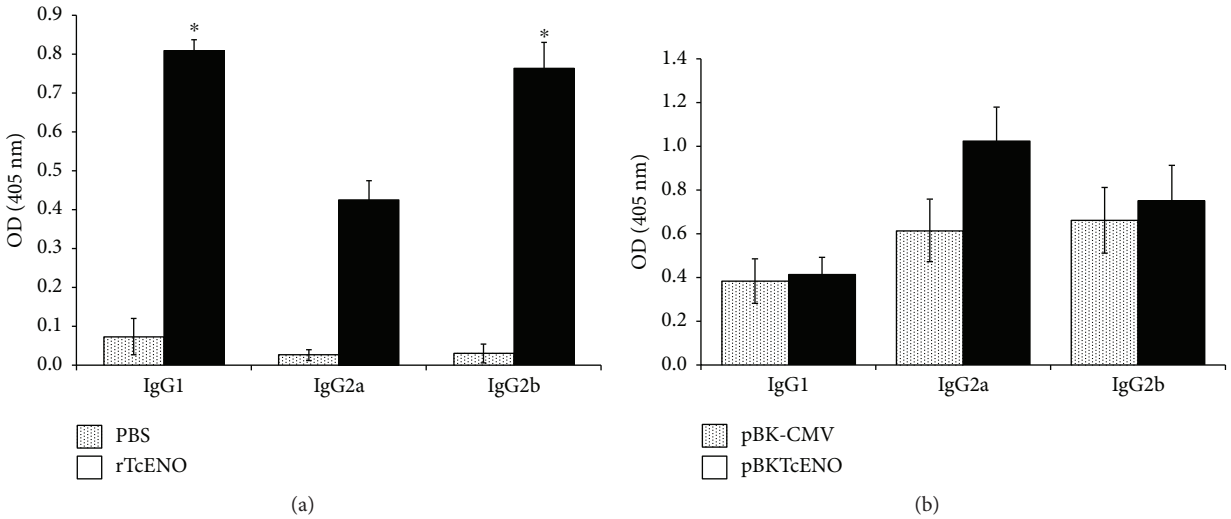

Figure 3: Antibody isotypes in immunized mice. Seven days after the last immunization with rTcENO (a) or pBKTcENO (b), generated antibody isotypes were evaluated by ELISA. The plotted data show optical density (OD) values for eight mice per group representing the mean ± SD of at least three independent experiments. A significant difference was detected in immunized mice with rTcENO by comparing IgG1 and IgG2b versus IgG2a ($^*p < 0.01$).

mainly of mononuclear cells. We did not detect any amastigote nests in the mice vaccinated with rTcENO (Figure 7).

4. Discussion

Chagas disease is a neglected tropical disease that affects the poorest population in endemic areas. Recently, several forms of transmission have reemerged and affected the population in nonendemic countries [9, 44]. Specific treatment of this disease consists of two drugs, nifurtimox and benznidazole. The efficacy of both drugs in the acute phase has been shown; however, their use in the chronic phase is currently the subject of discussion. Unfortunately, a vaccine for Chagas disease is not available to date [11, 45].

DNA vaccination has been shown to generate both humoral and cell-mediated immune responses [46] and has been shown to be an effective means of generating protective responses against *T. cruzi* infection in murine models [15, 42, 47]. Moreover, immunization with recombinant proteins has also generated promising results [16, 19, 48, 49]. Several membrane proteins have been proposed as good options to develop vaccines against different diseases.

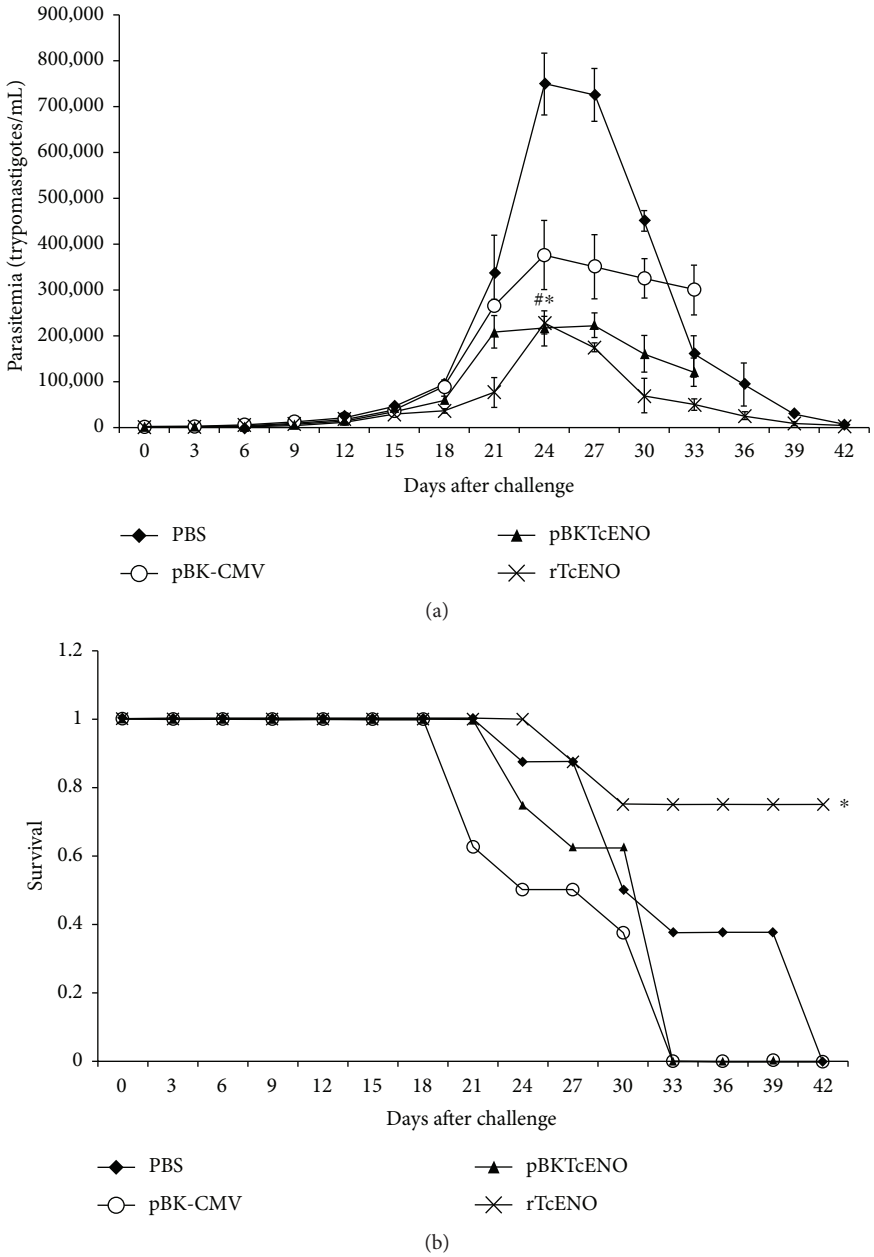

Figure 4: Evaluation of protection generated by vaccination with rTcENO or pBKTcENO. (a) Parasitemia in immunized mice after challenge with *T. cruzi*. BALB/c mice were immunized as described in Materials and Methods. Values plotted show the mean ± standard deviation of eight mice per group and are representative of two independent experiments. At the peak of infection, parasitemia levels were compared using one-way analysis of variance and post hoc Tukey's tests. A significant difference was detected by comparing rTcENO versus PBS ($^{*}p < 0.01$), pBKTcENO versus PBS ($^{\#}p < 0.01$) and pBKTcENO versus pBK-CMV ($^{*}p < 0.01$). (b) Survival of immunized and infected mice. Values plotted show the mean ± SD of eight mice per group and are representative of two independent experiments with similar results. A statistically significant difference ($^{*}p < 0.01$) between rTcENO versus PBS is indicated.

Among these membrane proteins, enolase has been demonstrated to be immunogenic [20–22] suggesting that a vaccine with this protein is possible. In our previous work, we evaluated the immunogenic characteristics of *T. cruzi* enolase using in silico assays. Our study showed that the recombinant protein was recognized by serum from both mice and humans infected with *T. cruzi* [36]. To support these data, in this study, we used rTcEno polyclonal antibodies against total protein extracts of *T. cruzi* in western blot and immunofluorescence assays to determine the specificity of these antibodies. These results demonstrated that enolase was located in both the cytoplasm and the cell membrane, in agreement with studies carried out in parasites such as *Echinococcus granulosus*, *Trichomonas vaginalis*, and *Plasmodium falciparum* [20, 50, 51].

Antibodies against both rTcENO and pBKTcENO were bound to intact epimastigotes, indicating that enolase protein was antigenic and exposed on the parasite surface.

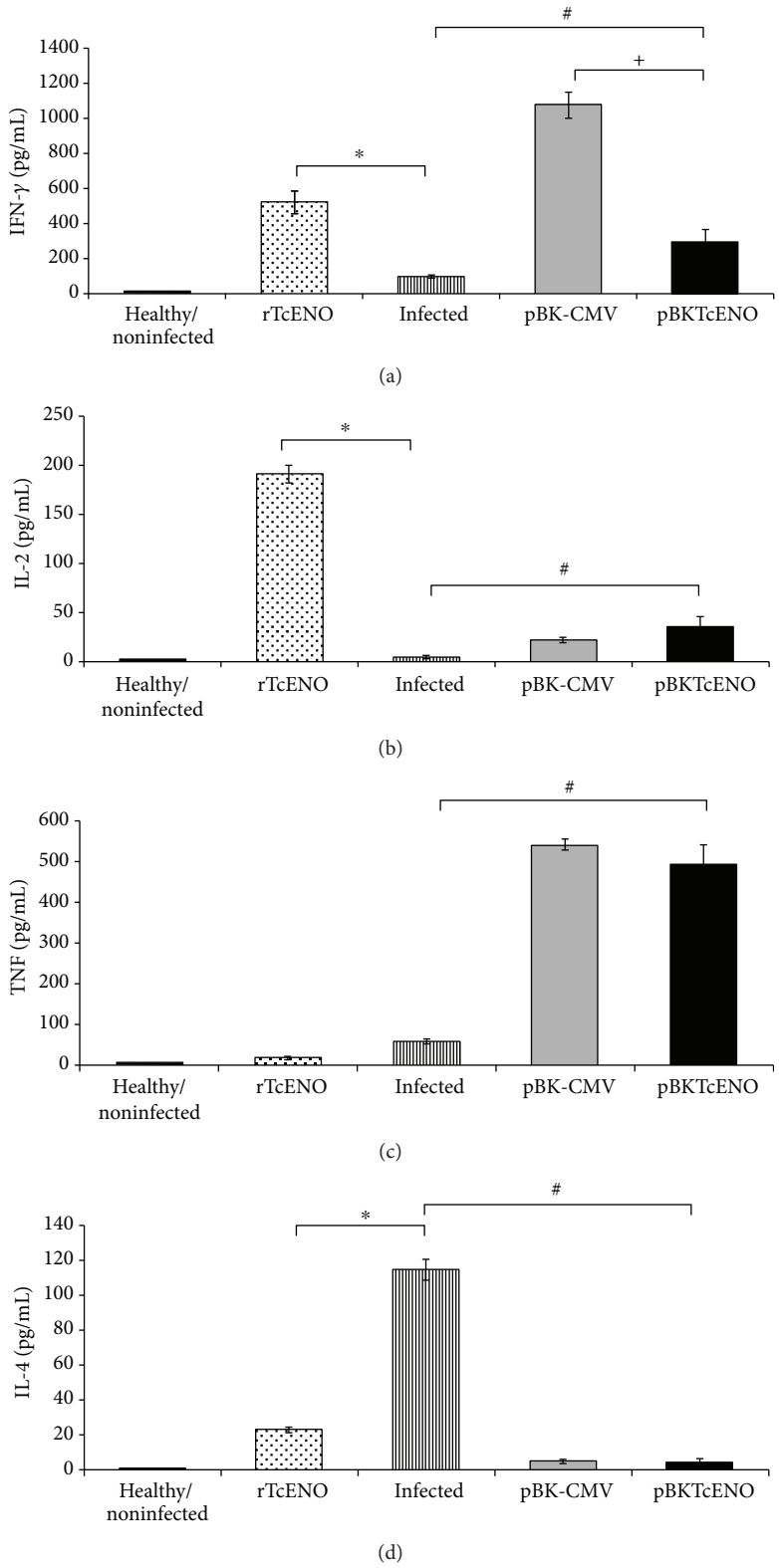

Figure 5: Serum cytokine levels in immunized and nonimmunized mice after challenge. Serum levels of (a) IFN-γ, (b) IL-2, (c) TNF, and (d) IL-4 were determined by flow cytometry. The concentration of a particular cytokine was established by comparing the obtained data with a standard curve for each experiment. The data are represented as the mean ± SD. All measurements were performed in duplicate, with serum from eight mice per group. Sera from healthy mice (noninfected and nonimmunized) were used as controls. Significant differences were detected as follows: rTcENO versus infected ($^{*}p < 0.01$), pBKTcENO versus infected ($^{\#}p < 0.01$), and pBKTcENO versus pBK-CMV ($^{+}p < 0.01$).

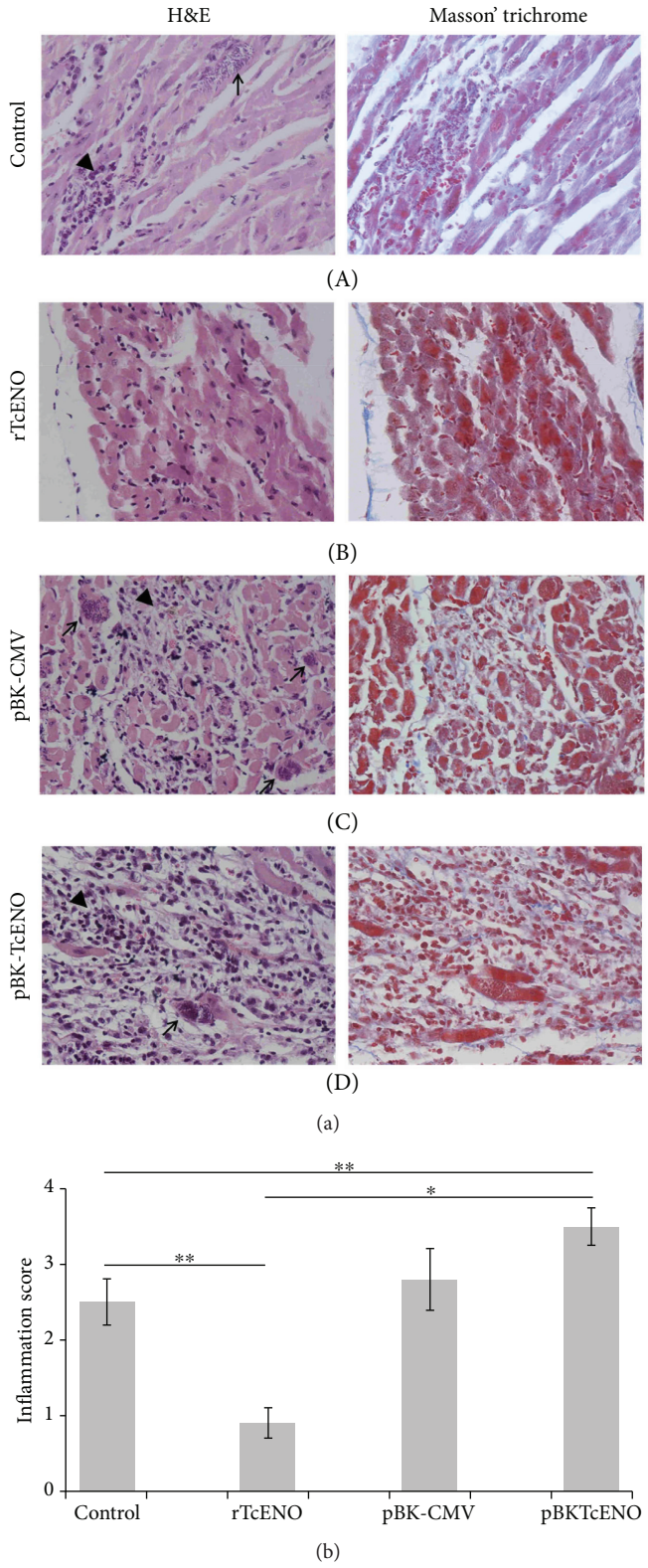

Figure 6: Vaccination effects on the cardiac muscle sections. (a) Tissue sections were stained with hematoxylin and eosin or Masson's trichrome and visualized by light microscopy (original magnification: 40x). Representative micrographs of the heart tissue from control-infected mice and mock-immunized with PBS (A), rTcENO (B), pBK-CMV empty plasmid vector (C), and pBK-TcENO (D) are shown. Black arrows show amastigote nests. Black arrowheads show inflammatory infiltrates. (b) Inflammatory lesion (lymphocyte infiltrates) scores. The inflammatory score was derived from two different experiments as described in Materials and Methods. The data are expressed as mean ± SD, and significance is presented as $^{*}p < 0.01$ and $^{**}p < 0.05$ (**control group nonimmunized and infected versus vaccinated and infected groups, rTcENO and pBK-TcENO; *rTcENO versus pBK-TcENO).

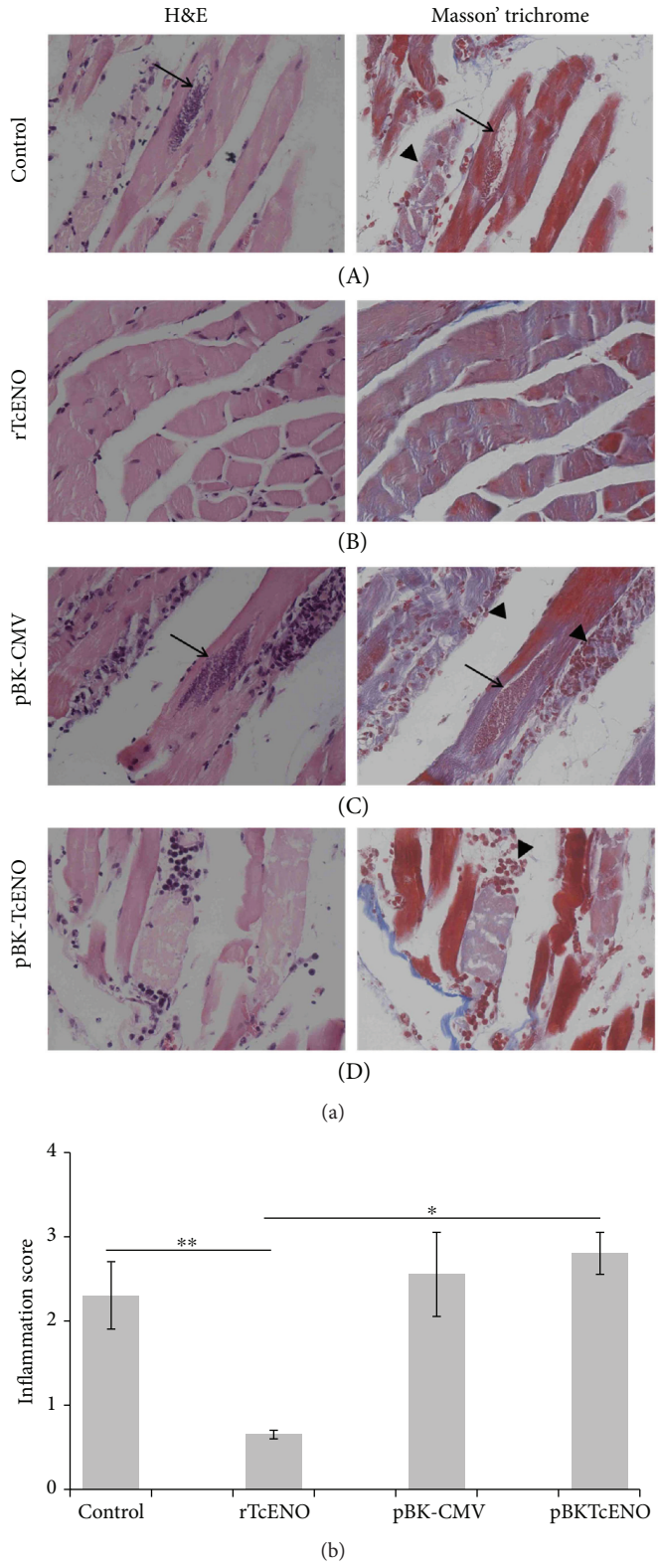

Figure 7: Vaccination effects on the skeletal muscle sections. (a) Tissue sections were stained with hematoxylin and eosin or Masson's trichrome and visualized by light microscopy (original magnification: 40x). Representative micrographs of skeletal tissue from control-infected mice and mock-immunized with PBS (A), rTcENO (B), pBK-CMV empty plasmid vector (C), and pBK-TcENO (D) are shown. Black arrows show amastigote nests. Black arrowheads show inflammatory infiltrates. (b) Inflammatory lesion (lymphocyte infiltrates) scores. The inflammatory score was derived from two different experiments as described in Materials and Methods. The data are expressed as mean ± SD, and significance is presented as $^{*}p < 0.01$ and $^{**}p < 0.05$ (**control group nonimmunized and infected versus vaccinated and infected groups, rTcENO and pBK-TcENO; *rTcENO versus pBK-TcENO).

Nevertheless, the exact mechanism by which enolase is secreted and translocated to the parasite surface is still unknown. However, it is known that the amino acid sequence lacks a conventional N-terminal signal sequence. It has been suggested that enolases could be secreted in exosomes and other vesicles [52] and that secreted enolases could reassociate with the cell membrane [24].

Enolase has been analyzed as a vaccine in several parasites and bacteria, demonstrating that it may be an important immunogenic protein and a protective antigen [20–22, 53–55]. In this study, analysis of the humoral immune response showed that the generated antibodies in the mice vaccinated with rTcENO were a mixture of Th1- and Th2-type immune responses (IgG1>IgG2b>IgG2a). Moreover, the mice vaccinated with pBKTcENO showed an increase in IgG2a immune response and the rate of IgG2b/IgG1 being >1, which suggested the dominance of Th1-type immune response. Previous studies showed that Th1-type immune response was required for clearing the parasite from infected mice [56, 57].

We found that the mice immunized with rTcENO were capable of significantly inducing IL-2 and IFN-γ in comparison to the control group, showing that in the immune response after challenge, there was a polarization towards Th1-type immune response. In the mice vaccinated with pBKTcENO, there was induction of IFN-γ and TNF but not IL-2. IFN-γ was required to activate macrophages and indirectly constitutes an important source of protective proinflammatory cytokines, which could effectively kill intracellular parasites such as *T. cruzi* by nitric oxide-(NO-) dependent mechanisms [58]. In this experimental group, discrete levels of IFN-γ were detected, and animals showed reduction in parasitemia profile. However, no mice survived at day 33 postchallenge. Interestingly, the pBK-CMV-immunized animals were able to induce high levels of IFN-γ and decrease parasitemia significantly compared to the PBS control group. Despite its low parasitemia, this group also showed reduced survival. These results might be due to the induced response by immunostimulatory sequences in the plasmid that trigger innate immunity in the host [59] but could not confer a specific response that favors the survival of the animals against parasitic challenge.

Therefore, other factors that did not prevent mortality might be involved in the reduction of parasitemia. One of these factors could be the IL-10 cytokine because it acted as an immunoregulatory cytokine in the Th1-type response [60]. In turn, IL-10 would prevent the collateral damage generated by a strong immune response against the parasite and suppress the development of inflammatory cell infiltrates that otherwise would be exacerbated. A previous study proposed that an exacerbated response to infections could result in harmful injuries [61].

To determine whether vaccination conferred protection in the cardiac and skeletal muscle, histological sections were prepared and stained. The results showed that animals immunized with rTcENO were able to prevent the establishment of parasites in the heart tissue, as shown by the absence of amastigote nests and low amount of inflammatory infiltrates in the heart sections (Figures 6 and 7). Furthermore, the low amount of inflammatory cells indicated that the immune response was adequate to eliminate the parasites.

Although the pBKTcENO vaccine reduced the parasitemia in the immunized/infected mice, these animals showed exacerbated damage in the heart and skeletal tissues (Figures 5 and 6), with many amastigote nests and inflammatory cells. The tissue injured by *T. cruzi* typically shows mononuclear cells and progression from multifocal to diffuse lesions. Activated neutrophils and eosinophils are efficient cells to destroy *T. cruzi*, and indirectly their activity causes severe damage to other host cells. Although neutrophils and eosinophils are not as abundant as mononuclear cells, their presence correlates with the severity of lesions observed in the cardiac tissue [62, 63].

Several researchers have demonstrated that DNA immunization is effective in protecting animals against *T. cruzi*, particularly with *TSA-1* [64], *Tc2* [65], and *SSP4* [66] genes, where immunizations generated high levels of cytokines which modulate the Th1-type immune response such as IFN-γ, and in the case of *SSP4*, the immunization also favored the increase of IL-10.

The exact mechanism by which pBKTcENO-immunized/infected or pBK-CMV-mock-immunized/infected mice died after challenge with *T. cruzi* even after producing antibodies related to Th1-type immune response is not known. It is possible that these antibodies were not opsonic, failing to induce *T. cruzi* killing by mouse phagocytes, as it was reported by Esgleas et al. [67], who found that the immunization with SsEno of *Streptococcus suis* failed to protect mice after experimental infection with bacteria. Another possible explanation is that the immune response was exacerbated enough in the cardiac tissue to induce death of the immunized animals. In this case, IL-10 is an important pleiotropic immunoregulatory cytokine that can participate during the Th1 immune response [60] to prevent collateral damage generated by a strong immune response against the parasites and suppress the development of inflammatory cell infiltrates that otherwise would be exacerbated. However, IL-10 can suppress immune responses [68] thus favoring the observed increased levels of parasites after acute infection. Therefore, we will conduct experiments using anti-IL-10 mAbs or IL-10 KO mice to determine the role of IL-10 in the protection against death of vaccinated mice with pBKTcENO.

In summary, we have shown that the immunization with rTcENO effectively controlled acute *T. cruzi* infection in a murine model by reducing parasite burden in the blood, preventing the establishment of inflammatory infiltrates in the heart and skeletal muscle and increasing the survival of immunized mice. Our data support further studies to improve the efficacy of rTcENO and examine its potential as a good candidate for the development of a vaccine against *T. cruzi*.

Data Availability

The data used to support the findings of this study are available from the corresponding author upon request.

Disclosure

María Cristina González-Vázquez's and Alejandro Carabarin-Lima's current address is Instituto de Ciencias, Benemérita Universidad Autónoma de Puebla, Edificio IC10, Ciudad Universitaria, Col. San Manuel, 72570 Puebla, PUE, Mexico.

Conflicts of Interest

No potential conflicts of interest were disclosed.

Acknowledgments

The authors are grateful to Sandra Aguilar Pérez and Benito Salvador Chávez Rentería for their help with tissue processing. The authors thank Lidia Baylón Pacheco and Enrique Martínez de Luna for their technical help. Alejandro Carabarin-Lima was a recipient of a postdoctoral fellowship from the ICyTDF, Mexico. This work was supported by a grant from the Consejo Nacional de Ciencia y Tecnología (CONACyT), Mexico (Grant no. 69081FONSECSSA/IMSS/ISSSTE).

References

[1] WHO, "World Health Organization," 2017, March 2018, http://www.who.int/chagas/en/.

[2] J. A. Perez-Molina and I. Molina, "Chagas disease," *Lancet*, vol. 391, no. 10115, pp. 82–94, 2018.

[3] World Health Organization, *Chagas Disease (American Trypanosomiasis)*, World Health Organization, Geneva, 2015, March 2018, http://www.who.int/mediacentre/factsheets/fs340/en/.

[4] C. Bern, S. Kjos, M. J. Yabsley, and S. P. Montgomery, "Trypanosoma cruzi and Chagas' disease in the United States," *Clinical Microbiology Reviews*, vol. 24, no. 4, pp. 655–681, 2011.

[5] Y. Jackson, L. Gétaz, H. Wolff et al., "Prevalence, clinical staging and risk for blood-borne transmission of Chagas disease among Latin American migrants in Geneva, Switzerland," *PLoS Neglected Tropical Diseases*, vol. 4, no. 2, article e592, 2010.

[6] F. X. Lescure, A. Canestri, H. Melliez et al., "Chagas disease, France," *Emerging Infectious Diseases*, vol. 14, no. 4, pp. 644–646, 2008.

[7] J. Muñoz, O. Coll, T. Juncosa et al., "Prevalence and vertical transmission of Trypanosoma cruzi infection among pregnant Latin American women attending 2 maternity clinics in Barcelona, Spain," *Clinical Infectious Diseases*, vol. 48, no. 12, pp. 1736–1740, 2009.

[8] G. A. Schmunis, "Epidemiology of Chagas disease in non endemic countries: the role of international migration," *Memórias do Instituto Oswaldo Cruz*, vol. 102, Supplement 1, pp. 75–86, 2007.

[9] A. Carabarin-Lima, M. C. González-Vázquez, O. Rodríguez-Morales et al., "Chagas disease (American trypanosomiasis) in Mexico: an update," *Acta Tropica*, vol. 127, no. 2, pp. 126–135, 2013.

[10] F. J. Carod-Artal and J. Gascon, "Chagas disease and stroke," *Lancet Neurology*, vol. 9, no. 5, pp. 533–542, 2010.

[11] L. M. G. Bahia-Oliveira, J. A. S. Gomes, J. R. Cançado et al., "Immunological and clinical evaluation of chagasic patients subjected to chemotherapy during the acute phase of Trypanosoma cruzi infection 14-30 years ago," *The Journal of Infectious Diseases*, vol. 182, no. 2, pp. 634–638, 2000.

[12] J. R. Cancado, "Criteria of Chagas disease cure," *Memórias do Instituto Oswaldo Cruz*, vol. 94, Supplement 1, pp. 331–335, 1999.

[13] S. I. Cazorla, P. D. Becker, F. M. Frank et al., "Oral vaccination with Salmonella enterica as a cruzipain-DNA delivery system confers protective immunity against Trypanosoma cruzi," *Infection and Immunity*, vol. 76, no. 1, pp. 324–333, 2008.

[14] F. M. Frank, S. I. Cazorla, M. J. Sartori, and R. S. Corral, "Elicitation of specific, Th1-biased immune response precludes skeletal muscle damage in cruzipain-vaccinated mice," *Experimental and Molecular Pathology*, vol. 84, no. 1, pp. 64–70, 2008.

[15] F. Costa, G. Franchin, V. L. Pereira-Chioccola, M. Ribeirao, S. Schenkman, and M. M. Rodrigues, "Immunization with a plasmid DNA containing the gene of trans-sialidase reduces Trypanosoma cruzi infection in mice," *Vaccine*, vol. 16, no. 8, pp. 768–774, 1998.

[16] D. F. Hoft, C. S. Eickhoff, O. K. Giddings, J. R. C. Vasconcelos, and M. M. Rodrigues, "Trans-sialidase recombinant protein mixed with CpG motif-containing oligodeoxynucleotide induces protective mucosal and systemic Trypanosoma cruzi immunity involving CD8+ CTL and B cell-mediated cross-priming," *Journal of Immunology*, vol. 179, no. 10, pp. 6889–6900, 2007.

[17] E. L. V. Silveira, C. Claser, F. A. B. Haolla, L. G. Zanella, and M. M. Rodrigues, "Novel protective antigens expressed by Trypanosoma cruzi amastigotes provide immunity to mice highly susceptible to Chagas' disease," *Clinical and Vaccine Immunology*, vol. 15, no. 8, pp. 1292–1300, 2008.

[18] B. H. Fralish and R. L. Tarleton, "Genetic immunization with LYT1 or a pool of trans-sialidase genes protects mice from lethal Trypanosoma cruzi infection," *Vaccine*, vol. 21, no. 21-22, pp. 3070–3080, 2003.

[19] K. A. Luhrs, D. L. Fouts, and J. E. Manning, "Immunization with recombinant paraflagellar rod protein induces protective immunity against Trypanosoma cruzi infection," *Vaccine*, vol. 21, no. 21-22, pp. 3058–3069, 2003.

[20] I. Pal-Bhowmick, M. Mehta, I. Coppens, S. Sharma, and G. K. Jarori, "Protective properties and surface localization of Plasmodium falciparum enolase," *Infection and Immunity*, vol. 75, no. 11, pp. 5500–5508, 2007.

[21] W. Q. Li, X. C. Hu, X. Zhang et al., "Immunisation with the glycolytic enzyme enolase confers effective protection against Candida albicans infection in mice," *Vaccine*, vol. 29, no. 33, pp. 5526–5533, 2011.

[22] N. Chen, Z. G. Yuan, M. J. Xu et al., "Ascaris suum enolase is a potential vaccine candidate against ascariasis," *Vaccine*, vol. 30, no. 23, pp. 3478–3482, 2012.

[23] V. Pancholi, "Multifunctional alpha-enolase: its role in diseases," *Cellular and Molecular Life Sciences*, vol. 58, no. 7, pp. 902–920, 2001.

[24] S. Bergmann, M. Rohde, G. S. Chhatwal, and S. Hammerschmidt, "alpha-Enolase of Streptococcus pneumoniae is a plasmin(ogen)-binding protein displayed on the bacterial cell surface," *Molecular Microbiology*, vol. 40, no. 6, pp. 1273–1287, 2001.

[25] V. Pancholi and V. A. Fischetti, "alpha-enolase, a novel strong plasmin(ogen) binding protein on the surface of pathogenic streptococci," *Journal of Biological Chemistry*, vol. 273, no. 23, pp. 14503–14515, 1998.

[26] D. J. P. Ferguson, S. F. Parmley, and S. Tomavo, "Evidence for nuclear localisation of two stage-specific isoenzymes of enolase in Toxoplasma gondii correlates with active parasite replication," *International Journal for Parasitology*, vol. 32, no. 11, pp. 1399–1410, 2002.

[27] M. Labbe, M. Peroval, C. Bourdieu, F. Girard-Misguich, and P. Pery, "Eimeria tenella enolase and pyruvate kinase: a likely role in glycolysis and in others functions," *International Journal for Parasitology*, vol. 36, no. 14, pp. 1443–1452, 2006.

[28] T. Mouveaux, G. Oria, E. Werkmeister et al., "Nuclear glycolytic enzyme enolase of Toxoplasma gondii functions as a transcriptional regulator," *PLoS One*, vol. 9, no. 8, article e105820, 2014.

[29] H. Lee, Y. Guo, M. Ohta, L. Xiong, B. Stevenson, and J. K. Zhu, "LOS2, a genetic locus required for cold-responsive gene transcription encodes a bi-functional enolase," *EMBO Journal*, vol. 21, no. 11, pp. 2692–2702, 2002.

[30] S. Feo, D. Arcuri, E. Piddini, R. Passantino, and A. Giallongo, "ENO1 gene product binds to the c-myc promoter and acts as a transcriptional repressor: relationship with Myc promoter-binding protein 1 (MBP-1)," *FEBS Letters*, vol. 473, no. 1, pp. 47–52, 2000.

[31] A. Subramanian and D. M. Miller, "Structural analysis of alpha-enolase. Mapping the functional domains involved in down-regulation of the c-myc protooncogene," *The Journal of Biological Chemistry*, vol. 275, no. 8, pp. 5958–5965, 2000.

[32] J. C. Wilkins, K. A. Homer, and D. Beighton, "Analysis of Streptococcus mutans proteins modulated by culture under acidic conditions," *Applied and Environmental Microbiology*, vol. 68, no. 5, pp. 2382–2390, 2002.

[33] B. L. Decker and W. T. Wickner, "Enolase activates homotypic vacuole fusion and protein transport to the vacuole in yeast," *The Journal of Biological Chemistry*, vol. 281, no. 20, pp. 14523–14528, 2006.

[34] I. Brandina, J. Graham, C. Lemaitre-Guillier et al., "Enolase takes part in a macromolecular complex associated to mitochondria in yeast," *Biochimica et Biophysica Acta (BBA) - Bioenergetics*, vol. 1757, no. 9-10, pp. 1217–1228, 2006.

[35] N. Entelis, I. Brandina, P. Kamenski, I. A. Krasheninnikov, R. P. Martin, and I. Tarassov, "A glycolytic enzyme, enolase, is recruited as a cofactor of tRNA targeting toward mitochondria in Saccharomyces cerevisiae," *Genes and Development*, vol. 20, no. 12, pp. 1609–1620, 2006.

[36] A. Carabarín-Lima, O. Rodríguez-Morales, M. C. González-Vázquez et al., "In silico approach for the identification of immunological properties of enolase from Trypanosoma cruzi and its possible usefulness as vaccine in Chagas disease," *Parasitology Research*, vol. 113, no. 3, pp. 1029–1039, 2014.

[37] W. H. Lee, H. I. Choi, S. W. Hong, K. S. Kim, Y. S. Gho, and S. G. Jeon, "Vaccination with Klebsiella pneumoniae-derived extracellular vesicles protects against bacteria-induced lethality via both humoral and cellular immunity," *Experimental and Molecular Medicine*, vol. 47, no. 9, article e183, 2015.

[38] K. A. Pasquevich, S. M. Estein, C. G. Samartino et al., "Immunization with recombinant Brucella species outer membrane protein Omp16 or Omp19 in adjuvant induces specific CD4 + and CD8+ T cells as well as systemic and oral protection against Brucella abortus infection," *Infection and Immunity*, vol. 77, no. 1, pp. 436–445, 2009.

[39] C. N. Pollak, M. M. Wanke, S. M. Estein et al., "Immunization with Brucella VirB proteins reduces organ colonization in mice through a Th1-type immune response and elicits a similar immune response in dogs," *Clinical and Vaccine Immunology*, vol. 22, no. 3, pp. 274–281, 2015.

[40] C. Serna, J. A. Lara, S. P. Rodrigues, A. F. Marques, I. C. Almeida, and R. A. Maldonado, "A synthetic peptide from Trypanosoma cruzi mucin-like associated surface protein as candidate for a vaccine against Chagas disease," *Vaccine*, vol. 32, no. 28, pp. 3525–3532, 2014.

[41] Y. Shimizu, H. Takagi, T. Nakayama et al., "Intraperitoneal immunization with oligomannose-coated liposome-entrapped soluble leishmanial antigen induces antigen-specific T-helper type immune response in BALB/c mice through uptake by peritoneal macrophages," *Parasite Immunology*, vol. 29, no. 5, pp. 229–239, 2007.

[42] M. Arce-Fonseca, A. Ramos-Ligonio, A. Lopez-Monteon, B. Salgado-Jimenez, P. Talamas-Rohana, and J. L. Rosales-Encina, "A DNA vaccine encoding for TcSSP4 induces protection against acute and chronic infection in experimental Chagas disease," *International Journal of Biological Sciences*, vol. 7, no. 9, pp. 1230–1238, 2011.

[43] National Research Council (US) Committee for the Update of the Guide for the Care and Use of Laboratory Animals, *Guide for the Care and Use of Laboratory Animals*, National Academies Press (US), Washington (DC), 8th edition, 2011.

[44] P. Hotez, E. Ottesen, A. Fenwick, and D. Molyneux, "The neglected tropical diseases: the ancient afflictions of stigma and poverty and the prospects for their control and elimination," *Advances in Experimental Medicine and Biology*, vol. 582, pp. 23–33, 2006.

[45] C. Bern, "Antitrypanosomal therapy for chronic Chagas' disease," *The New England Journal of Medicine*, vol. 364, no. 26, pp. 2527–2534, 2011.

[46] J. J. Donnelly, B. Wahren, and M. A. Liu, "DNA vaccines: progress and challenges," *Journal of Immunology*, vol. 175, no. 2, pp. 633–639, 2005.

[47] N. Garg and R. L. Tarleton, "Genetic immunization elicits antigen-specific protective immune responses and decreases disease severity in Trypanosoma cruzi infection," *Infection and Immunity*, vol. 70, no. 10, pp. 5547–5555, 2002.

[48] A. Carabarin-Lima, M. C. González-Vázquez, B.-P. Lidia, P.-T. Rohana, and R.-E. J. Luis, "Immunization with the recombinant surface protein rTcSP2 alone or fused to the CHP or ATPase domain of TcHSP70 induces protection against acute Trypanosoma cruzi infection," *Journal of Vaccines & Vaccination*, vol. 1, no. 3, 2010.

[49] R. A. Wrightsman and J. E. Manning, "Paraflagellar rod proteins administered with alum and IL-12 or recombinant adenovirus expressing IL-12 generates antigen-specific responses and protective immunity in mice against Trypanosoma cruzi," *Vaccine*, vol. 18, no. 14, pp. 1419–1427, 2000.

[50] W. Gan, G. Zhao, H. Xu et al., "Reverse vaccinology approach identify an Echinococcus granulosus tegumental membrane protein enolase as vaccine candidate," *Parasitology Research*, vol. 106, no. 4, pp. 873–882, 2010.

[51] V. Mundodi, A. S. Kucknoor, and J. F. Alderete, "Immunogenic and plasminogen-binding surface-associated α-enolase of Trichomonas vaginalis," *Infection and Immunity*, vol. 76, no. 2, pp. 523–531, 2008.

[52] C. Olver and M. Vidal, "Proteomic analysis of secreted exosomes," *Subcellular Biochemistry*, vol. 43, pp. 99–131, 2007.

[53] Y. Feng, X. Pan, W. Sun et al., "Streptococcus suis enolase functions as a protective antigen displayed on the bacterial cell surface," *The Journal of Infectious Diseases*, vol. 200, no. 10, pp. 1583–1592, 2009.

[54] J. Sha, T. E. Erova, R. A. Alyea et al., "Surface-expressed enolase contributes to the pathogenesis of clinical isolate SSU of Aeromonas hydrophila," *Journal of Bacteriology*, vol. 191, no. 9, pp. 3095–3107, 2009.

[55] A. Zhang, B. Chen, X. Mu et al., "Identification and characterization of a novel protective antigen, enolase of Streptococcus suis serotype 2," *Vaccine*, vol. 27, no. 9, pp. 1348–1353, 2009.

[56] D. F. Hoft and C. S. Eickhoff, "Type 1 immunity provides optimal protection against both mucosal and systemic Trypanosoma cruzi challenges," *Infection and Immunity*, vol. 70, no. 12, pp. 6715–6725, 2002.

[57] C. N. Paiva, M. T. L. Castelo-Branco, J. Lannes-Vieira, and C. R. Gattass, "Trypanosoma cruzi: protective response of vaccinated mice is mediated by CD8+ cells, prevents signs of polyclonal T lymphocyte activation, and allows restoration of a resting immune state after challenge," *Experimental Parasitology*, vol. 91, no. 1, pp. 7–19, 1999.

[58] R. T. Gazzinelli, I. P. Oswald, S. Hieny, S. L. James, and A. Sher, "The microbicidal activity of interferon-γ-treated macrophages againstTrypanosoma cruzi involves an L-arginine-dependent, nitrogen oxide-mediated mechanism inhibitable by interleukin-10 and transforming growth factor-β," *European Journal of Immunology*, vol. 22, no. 10, pp. 2501–2506, 1992.

[59] A. M. Abdelnoor, "Plasmid DNA vaccines," *Current Drug Targets - Immune, Endocrine & Metabolic Disorders*, vol. 1, no. 1, pp. 79–92, 2001.

[60] G. Trinchieri, "Interleukin-10 production by effector T cells: Th1 cells show self control," *Journal of Experimental Medicine*, vol. 204, no. 2, pp. 239–243, 2007.

[61] J. L. Mege, S. Meghari, A. Honstettre, C. Capo, and D. Raoult, "The two faces of interleukin 10 in human infectious diseases," *The Lancet Infectious Diseases*, vol. 6, no. 9, pp. 557–569, 2006.

[62] Z. A. Andrade, S. G. Andrade, R. Correa, M. Sadigursky, and V. J. Ferrans, "Myocardial changes in acute Trypanosoma cruzi infection. Ultrastructural evidence of immune damage and the role of microangiopathy," *American Journal of Pathology*, vol. 144, no. 6, pp. 1403–1411, 1994.

[63] J. A. Marin-Neto, E. Cunha-Neto, B. C. Maciel, and M. V. Simoes, "Pathogenesis of chronic Chagas heart disease," *Circulation*, vol. 115, no. 9, pp. 1109–1123, 2007.

[64] H. Zapataestrella, C. Hummelnewell, G. Sanchezburgos et al., "Control of Trypanosoma cruzi infection and changes in T-cell populations induced by a therapeutic DNA vaccine in mice," *Immunology Letters*, vol. 103, no. 2, pp. 186–191, 2006.

[65] V. Tekiel, C. D. Alba-Soto, S. M. Gonzalez Cappa, M. Postan, and D. O. Sanchez, "Identification of novel vaccine candidates for Chagas' disease by immunization with sequential fractions of a trypomastigote cDNA expression library," *Vaccine*, vol. 27, no. 9, pp. 1323–1332, 2009.

[66] M. Arce-Fonseca, M. A. Ballinas-Verdugo, E. R. A. Zenteno et al., "Specific humoral and cellular immunity induced by Trypanosoma cruzi DNA immunization in a canine model," *Veterinary Research*, vol. 44, no. 1, p. 15, 2013.

[67] M. Esgleas, M. de la Cruz Dominguez-Punaro, Y. Li, J Ã.©e. Harel, J. Daniel Dubreuil, and M. Gottschalk, "Immunization with SsEno fails to protect mice against challenge with Streptococcus suis serotype 2," *FEMS Microbiology Letters*, vol. 294, no. 1, pp. 82–88, 2009.

[68] A. O'Garra and P. Vieira, "TH1 cells control themselves by producing interleukin-10," *Nature Reviews Immunology*, vol. 7, no. 6, pp. 425–428, 2007.